# SYNTHESIS AND BIOCHEMICAL EVALUATION OF AMINOBORANEPHOSPHONATE PHOSPHORAMIDIMIDATE AND PHOSPHORAMIDATE DNA

by

**AYMAN GHALIB ALAWNEH**

B.A., University of Jordan, 2005

M.A., University of Jordan, 2009

A thesis submitted to the

Faculty of the Graduate School of the

University of Colorado in partial fulfillment

of the requirement for the degree of

Doctor of Philosophy

Department of Chemistry and

Biochemistry

2018

This thesis entitled:
Synthesis and Biochemical Evaluation of Aminoboranephosphonate Phosphoramidimidate and Phosphoramidate DNA

written by Ayman Ghalib Alawneh
has been approved for the Department of Chemistry and Biochemistry

_____
Marvin H. Caruthers

_____
Robert D. Kuchta

Date_____

The final copy of this thesis has been examined by the signatories, and we find that both the content and the form meet acceptable presentation standards of scholarly work in the above-mentioned discipline.

## ABSTRACT

**Alawneh, Ayman Ghalib (Ph.D., Chemistry)**

**Synthesis and Biochemical Evaluation of Aminoboranephosphonate Phosphoramidimidate and Phosphoramidate DNA**

**Thesis directed by Distinguished Professor Marvin H. Caruthers**

Antisense oligonucleotides are synthetic DNAs that bind to RNA and alter or reduce the biological activity of the target RNA. Studies performed in recent years have demonstrated that an antisense strategy can be utilized to address various issues in fundamental biomedical research and have additionally shown that this approach can be used to create novel therapeutic drugs. For example, IONIS Pharmaceuticals has so far commercialized three drugs using antisense oligonucleotides. These drugs target spinal muscular atrophy, homozygous familial hypercholesterolemia, and pouchitis. Antisense oligonucleotides targeting several other diseases are in various stages of clinical study at IONIS and elsewhere.

My research focuses on synthesizing a new DNA analogue called phosphoramidimidate DNA that has nitrogen joined covalently to phosphorus at both nonlinking internucleotide positions. The analogue was prepared using phosphoramidite chemistry that has been modified to facilitate the synthesis. The resulting phosphoramidimidate DNA is positively charged, nuclease resistant, forms duplexes with complementary, unmodified oligonucleotides and is stable to neutral and basic conditions. Most importantly, this new analogue is RNase H1 active and can be transfected into cells in culture where it is located in the cytoplasm. These attributes are essential for any analogue that has antisense activity. Additionally, a very unique attribute of this analogue is that the phosphoramidimidate linkage is tolerated in the RNase H1 cleavage domain. Moreover,

phosphoramidimidate antisense oligonucleotides are expected to be more stable toward cellular nucleases and consequently have significantly longer half-lives when used as therapeutic drugs.

The synthesis of phosphoramidate DNA using a similar chemistry generates this analogue by a new methodology that is far superior to previously developed chemistries. This analogue is also efficiently transfected, via passive transfection, into the cytoplasm of HeLa cells.

## ACKNOWLEDGMENTS

I want to express my deepest appreciation and sincere gratitude to Dr Marven Caruthers for his strong mentorships and amazing guidance toward research during my entire years of Ph.D. program. He has given me many opportunities not limited to learning technical skills, constructing research plans and presenting works in conferences to share and communicate with other individual researchers; but also I learned from him to have responsibility and leadership on the research project.

Special thanks to Dr. Robert Kuchta for his professional guidance, encouragement and personal support throughout graduate school. I will greatly miss our discussions about science. Thanks, are also due to the members of the examining committee Dr. Natalie Ahn, Dr. David Walba and Dr. Doug Dellinger for their valuable discussions and fruitful suggestions.

Thanks to all my teachers throughout all my stages, my friends, colleagues, lab mates and chemistry department. It was an unforgettable experience sharing and interacting with a large number of group members in a daily basis. I am thankful to everyone who spares their time for me. Especially, I am gratefully thankful to Richard N. Threlfall, whom I worked closely at the beginning, for providing mentorships and guidance on my research. I also want to thank to other lab members who helped my research in many different aspects.

All my thanks and love to my father, mother, brothers and sisters who gave me light of hope to accomplish my goal by their encouragement and endless support; without their existence, I would have never been courageous to start and continue the journey. And Finally, special thanks to my wife and son Nancy and Yousef for their support and every great moment we spent together through out these years.

## CONTENTS

# LIST OF TABLES

## LIST OF FIGURES

Figure

## LIST OF ABBREVIATIONS

| | |
|---|---|
| CPG | Controlled Pore Glass |
| DBU | 1,8-Diazabicyclo[5.4.0]undec-7-ene |
| DCM | Dichloromethane |
| DMEM | Dulbecco's Modified Eagle Medium |
| DMT | Dimethoxytrityl |
| DNA | Deoxyribonucleic Acid |
| DPBP | Diisopropyl Boranephosphonate |
| EDTA | Ethylenediaminetetraacetic Acid |
| ESI | Electron Spray Ionization |
| ETT | 5-(Ethylthio)tetrazole |
| FBS | Fetal Bovine Serum |
| Fmoc | Fluorenylmethyloxycarbonyl |
| LC-MS | Liquid Chromatography Mass Spectrometry |
| LNA | Locked Nucleic Acids |
| ODN | Oligodeoxynucleotide |
| ODT | Oligodeoxythymidine |
| Opti-MEM | Gibco Reduced Serum Medium |
| PAGE | Polyacrylamide Gel Electrophoresis |
| PBS | Phosphate Buffered Saline |
| RP-HPLC | Reverse Phase High Performance Liquid Chromatography |
| RNA | Ribonucleic Acid |
| SVPDE | Snake Venom Phosphodiesterase Exonuclease |
| TIC | Total Ion Chromatogram |
| TCA | Trichloroacetic Acid |
| TEA | Triethyl Amine |
| TFA | Trifluoroacetic Acid |
| THF | Tetrahydrofuran |
| TLC | Thin Layer Chromatography |
| TMPB | Trimethylphosphite-Borane |
| TMT | Trimethoxytrityl |
| NMR | Nuclear Magnetic Resonance Spectroscopy |

# CHAPTER 1

# INTRODUCTION TO SOLID PHASE SYNTHESIS OF OLIGONUCLEOTIDES

## 1.1 Introduction

Oswald Avery's discovery that deoxyribonucleic acid (DNA) carries the genetic information in humans and almost all other organisms[1] followed by Watson and Crick solving in 1953 the structure of DNA,[2] provided a compelling target for organic chemists. Over the years, many highly motivated scientists came up with different methods to synthesize the DNA. Multiple solution- and solid-phase methods have been developed including for example, the H-phosphonate, phosphodiester, phosphotriester and phosphoramidite methods. Each method has its advantages and disadvantages. Ultimately however the phosphoramidite method, which was developed in the 1980's in our lab,[3] became the method of choice largely due to its ease and ready conversion to automated solid-phase technology.

### Solid Phase Phosphoramidite Chemistry

Solid phase phosphoramidite DNA synthesis (Figure 1) is a repetitive four-step cycle that typically proceeds in the 3' to 5'-direction and adds one nucleotide per synthesis cycle. Initially, the first nucleoside (that will become the 3'-end of the DNA) is covalently attached to a solid phase support. The cycle initiates with deprotection of the 5'-hydroxy, typically a dimethoxytrityl (DMT), by 3% trichloroacetic acid (TCA) in dichloromethane (DCM). This is followed by coupling to a 2'-deoxyribonucleoside-3'-phosphoramidite that will become the next nucleoside (step 1). A weak acid activates the phosphoramidite that then reacts with the 5' hydroxyl of the support-linked 2'-deoxyribonucleoside to form a phosphite triester. Any unreacted 5'-hydroxyls are then capped by acetylation (step 2) and the phosphite triester is oxidized (step 3) to a phosphate

triester. The 5'-protecting group of the newly attached 2'-deoxynucleotide is then removed (step 4) and the chain extended with further repetitions of the cycle.

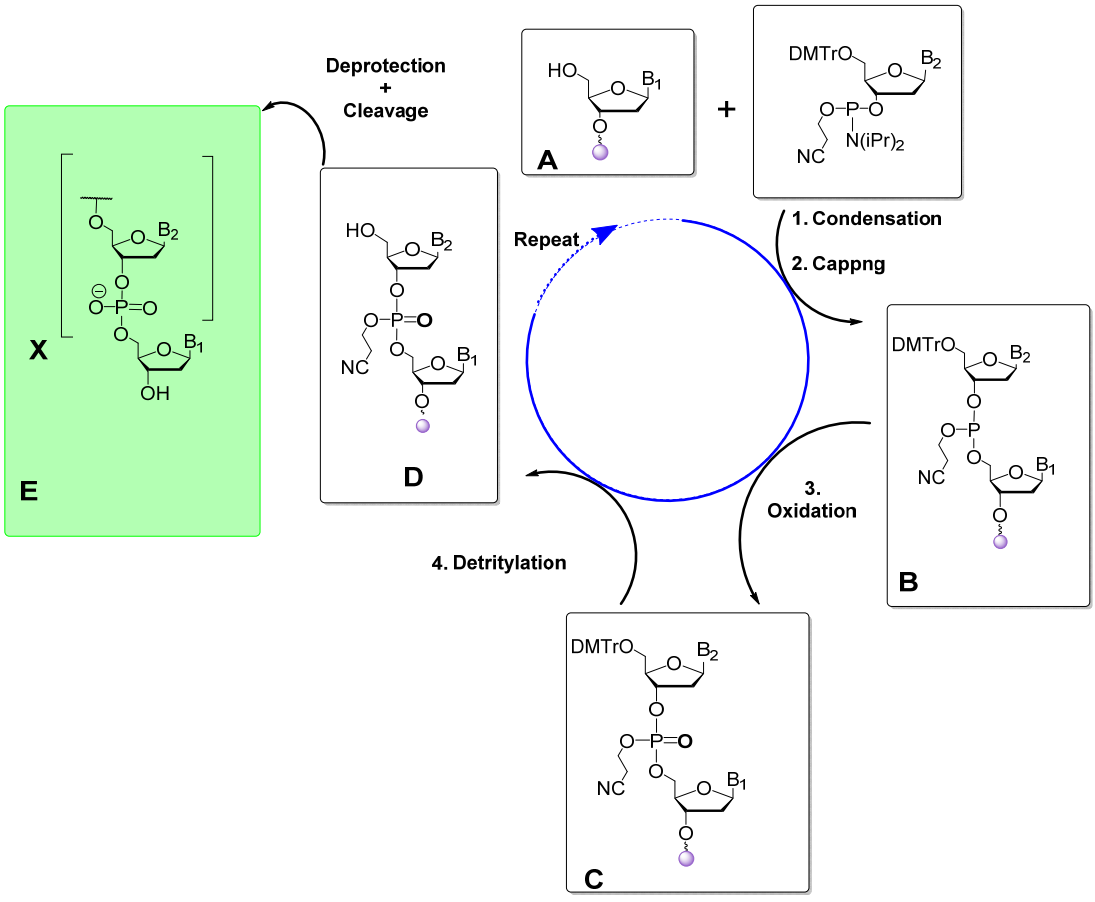


**Figure 1.1**: Solid-phase DNA synthesis cycle using phosphoramidite chemistry.

The final product is cleaved from the solid phase and obtained free of base and phosphate protecting groups, typically by treatment of the support with concentrated ammonium hydroxide. The outstanding yields of each step in the cycle allows synthesis of DNA up to around 150 nucleotides long. This general approach has also been used for solid-phase RNA synthesis,

although very different protecting group chemistry must be used due to the 2' hydroxyl on the ribose sugar.

### 1.2 Application of Phosphoramidite Chemistry in Synthesizing Several DNA Modifications

The ready availability of synthetic DNA of any sequence has been essential to molecular biology. Uses include, for example, detection of specific RNA/DNA sequences via hybridization, DNA and RNA sequencing and DNA/RNA amplification via PCR. More recently, therapeutic approaches using modified synthetic DNA (or RNA) have been considered, most prominently antisense therapy. Antisense therapy is the inhibition of translation by using a single-stranded oligonucleotide (antisense oligonucleotide) that binds to a target RNA. This can result in direct inhibition of translation by blocking binding of a transcription factor to the RNA. Alternatively, the DNA:RNA hybrid can become a target for RNase H such that the RNA is cleaved. If the therapeutic oligonucleotide is an RNA mimic, therapeutic effects can be obtained via the activation of the DICER/RISC proteins and subsequent destruction of the target RNA. Thus high-throughput DNA,RNA synthesis and an increased demand for synthesizing natural and modified DNA (which is normally done by the application of the automated solid-phase phosphoramidite chemistry) especially for therapeutics processes has led to the development of numerous DNA/RNA analogues.

To be useful as a therapeutic, the synthetic oligonucleotide must be stable against nucleases, have low toxicity, be readily transported across cell membranes and enter the cytosol, and retain the appropriate biological activity. Unfortunately, natural DNA lacks stability against

nucleases and is not readily transported into cells. To solve these major problems, a wide range of backbone oligonucleotide modifications have been developed.[4]

**Methylphosphonate**

The first chemically modified oligonucleotides were the methylphosphonates.[5] Methylphosphonate oligonucleotides (compound 2 figure 1.2) were developed by Miller and Ts'o in the late 1970s and have one of the nonbridging oxygen atom replaced by a methyl group forming a noncharged DNA. The absence of charge eliminates charge- charge repulsions in a duplex nucleic acid that would ordinarily occur. However, the absence of charge reduced DNA solubility and also limited cellular uptake, thereby limiting their antisense application as therapeutics. For example, even in cell culture this analogue typically required concentrations in excess of 20 μM for good activity. Furthermore, a DNA:RNA duplex where the DNA strand contains just methylphosphonate linkages cannot activate RNase H activity.

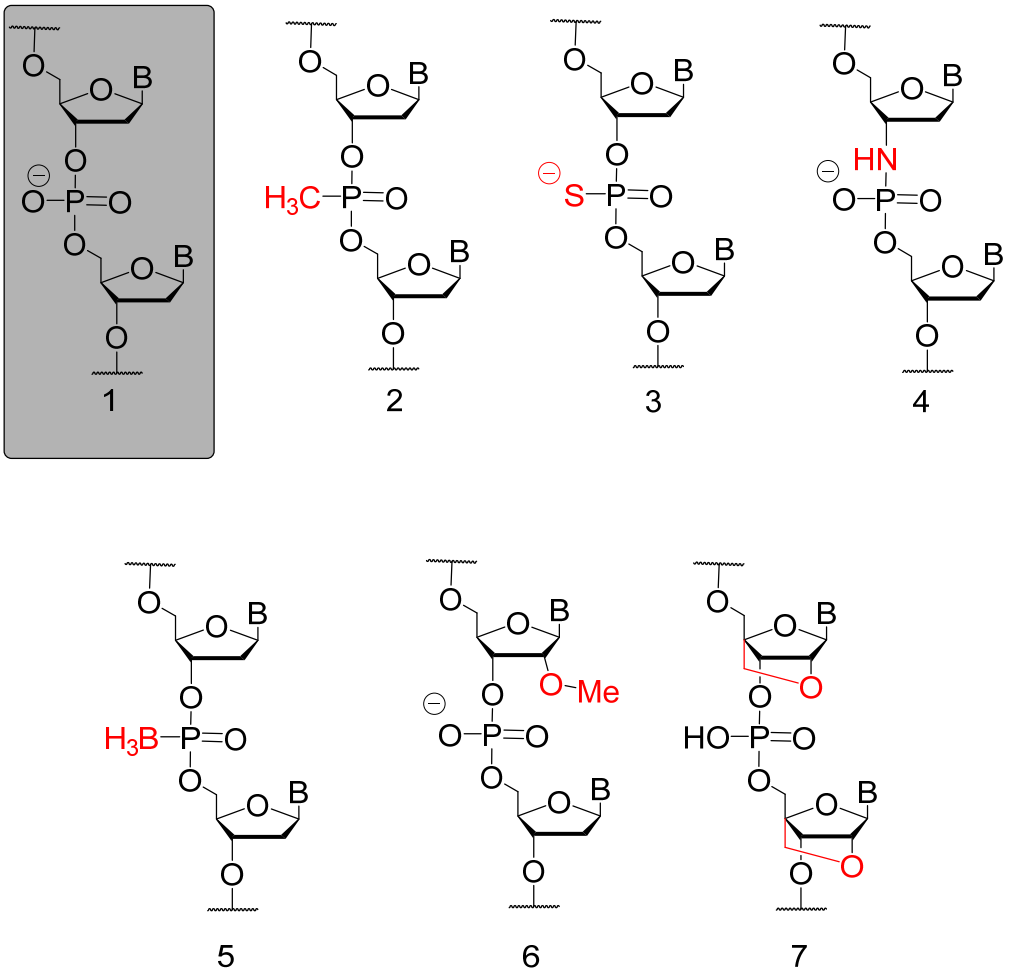


**Figure 1.2**: Figure shows the structure of natural DNA (compound 1) and some examples of modified nucleic acids; 2: Methylphosphonate; 3: Phosphorothioate; 4: N3'→P5' Phosphoramidates; 5: Boranephosphonate; 6: 2'-O-Methylribonucleotide; 7: Locked nucleic acid; B: nucleobases: adenine (A), cytosine (C), guanine (G) or thymine (T).

## Phosphorothioates

Another phosphate modification, phosphorothioate[6] (compound 3 figure 1.2), was synthesized by replacing one of the nonbridging oxygens with a sulfur atom. This replacement introduces chirality at each phosphorothioate linkage in the oligonucleotide chain (Rp diastereomer for R configuration and Sp diastereomer for S configuration). They are prepared on standard DNA synthesizers with only a small modification of the oxidation step by using a sulfurizing agent instead of the traditional $I_2$/water mixture. Phosphorothioate oligonucleotides are

highly soluble in water, have excellent antisense activity and, they are also capable of activating RNase H activity. The phosphorothioates are the most widely studied oligonucleotide analogues due to their ease of synthesis, high resistance against nucleases and good biological activity at concentrations 100-fold lower than the corresponding methylphosphonates. While the Sp phosphorothioate diastereomer is nuclease resistant, the Rp diastereomer is as nuclease sensitive as a phosphodiester linkage.[7] Generally, the introduction of thiophosphate linkages lowers the melting temperature of 2'-deoxyoligonucleotides by about 0.6 °C per linkage.[8] The first antisense drug made with a phosphorothioate backbone was Fomivirsen, approved in 1998 by the U.S. Food and Drug Administration (U.S.FDA) and by the European Agency for the Evaluation of Medicinal Products (EMEA) in 1999, for the treatment of retinitis cytomegalovirus in patients with AIDS.[9] Since then, several other phosphorothioate based drugs have been synthesized and approved.[10]

**Phosphoramidates**

The phosphoramidate, phosphoramide acid derivatives, consist of compounds that have one amino group bound directly to the phosphorus atom. It was first synthesized through H-phosphonate chemistry in 1986 (a nonbridging nitrogen introduced to the phosphorous instead of the hydrogen as a final step).[11] When a 3'- or 5'-bridging oxygen atom is replaced with an amino group, a very different type of phosphoramidate DNA modification is generated. Replacing 3'-hydroxyl nucleosides produces the N3'→P5' phosphoramidate oligonucleotides[12] (compound 4 figure 1.2) and replacing the 5'-hydroxyl nucleosides produces the P3'→N5' phosphoramidate.[13] These two linkages in addition to the nonbridging phosphoramidate have increased resistance to snake venom phosphodiesterases and higher Tms during duplex formation with complementary DNA or RNA. N3'→P5' phosphoramidates form extremely stable triple-stranded complexes with

single or double-stranded DNA targets. These 2′-deoxyoligonucleotide N3'→P5' phosphoramidates and their duplexes are also structurally and functionally similar to those formed by native RNA molecules.[14] On the other hand, the P3'→N5' phosphoramidate linkage showed more sensitivity towards acid hydrolysis than phosphodiester DNA.[15]

In the last few decades, the phosphoramidates have attracted the attention of many researchers due to their reported activities in several fields such as biological activities and their use as pharmaceuticals drugs for treating and controlling various diseases.[16] Thus phosphoramidates are promising candidates for exploring new types of modified oligonucleotides. In order to further investigate their biochemical properties and applications, a new synthetic method has been developed for the synthesis phosphoramidate analogues and a new phosphoramidimidate analogue was synthesized as described in this dissertation.

**Boranophosphate**

Boranophosphate analogues,[17] in which a $BH_3$ group replaces one of the non-bridging oxygen atoms in the normal phosphate moiety (compound 5 figure 1.2) is isosteric to the neutral methylphosphonate group but, like the phosphate and phosphorothioate groups, retains a negative charge. Despite retaining the negative charge, the polarity of the molecule changes because the negative charge is localized on the remaining non-bridging oxygen. Barbara R. Shaw et al. showed that negatively charged dithymidine boranophosphate d(TBpT) was 18 times more lipophilic than the parent dithymidine phosphate, d(TpT).[18]

DNA containing boranophosphate linkages have several appealing features. This analogue has been shown to be a promising DNA drug alternative due to its increased lipophilicity and high

nuclease resistance relative to normal nucleic acids. Most importantly, it also activates RNase H cleavage of RNA-an important component of some possible oligonucleotide therapeutic drugs.[19,20] Considering these properties, boranophosphate oligonucleotides are also promising candidates for exploring new types of modified nucleotides drug candidates. In order to further investigate their biochemical properties and explore various applications, a broad spectrum of aminoboranophosphate analogues were synthesized in research outlined in this dissertation.

**Sugar modifications**

Several sugar modifications, primarily at the 2'-position, have been synthesized where the fluoro, amino, 2'-C-allyl, methoxy and allyloxy have been introduced. These modifications show RNA–like conformation when double stranded. There has been an increased interest in oligoribonucleotides containing such modifications to generate more stable RNA aptamers and ribozymes as well as novel therapeutics. The absence of a 2'-OH stabilizes the resulting oligonucleotide against both base and RNases, and can enhance duplex stability. For example, the 2'-O-methyl modification (compound 6 figure 1.2) showed an increases target binding affinity (2°C per modification)[21] and an improved nuclease stability compared to phosphorothioate modification. Fully modified oligonucleotides at the 2'-position do not support RNase H activity. A number of oligonucleotides containing 2'-modifications are undergoing clinical trials (Ex., PRO044[22] and PRO045[23]). Another promising clinical candidate advancing in clinical trials is Drisapersen,[24] a second-generation antisense oligonucleotide containing both phosphorothioate linkages and 2'-O-Methyl sugars.

**Locked nucleic acids (LNA)**

A more radical sugar modification is locked nucleic acid (LNA) (**compound 7 figure 1.2**). This is a modified RNA analogue having a methylene bridge joining the 2'-OH to the 4'-C, thereby forming a conformationally restricted bicyclic nucleoside. LNA-DNA heteroduplexes form an A-type duplex geometry similar to that of dsRNA duplexes (based on NMR spectroscopy and X-ray). In addition, LNA modification improves nuclease resistance that is similar to 2'-O-methyl modification. LNA shows the highest affinity towards complementary RNA with an increase in duplex melting temperature (Tm) of +2 to 6°C per introduced LNA monomer against complementary RNA when compared to unmodified duplexes.[25] The strong binding properties of LNA make them particularly useful in anti-miRNA applications. However, this strong binding could reduce their specificity, and moreover, there appear to be more severe toxicological problems with these oligonucleotides in animals.

In conclusion, several DNA modifications have been synthesized and applied in therapeutic purposes, however few of them showed good results due to their limitations to cross the cell membrane, and cellular degradations. In this dissertation research, new types of modified DNAs have been synthesized and their biochemical properties have been investigated in order to further demonstrate their applications.

## 1.3 Nitrogen protecting groups

For both nucleic acid and peptide synthesis, amine protecting groups play pivotal roles due to the presence of primary amines in the nucleobases and amino acids. Amines are very good nucleophiles. Since many of the reactions in both protein and nucleic acid synthesis are the attack of a nucleophile on an electrophile (Ex., during DNA synthesis the attack of the 5'-hydroxyl on the phosphoramidite of the next nucleotide to be added), it is essential to protect these amino groups in order to prevent their unwanted reactions. Hence, amine protecting groups are a vital part of the planning for any synthesis and demand careful synthetic planning in order to achieve the required degree of orthogonality among the protective groups present in a molecule as well as the ability to remove them without damaging the target molecule.

There are a countless number of amine protecting groups that are used for DNA synthesis although most share the same principle of deactivating the nitrogen by converting it to the corresponding amide or by substituting its hydrogen by a good leaving group under specified conditions. The most common amino-protecting groups include; (1) acylated amine derivatives such as acetyl or benzoyl, both of which are base labile; (2) carbamate derivatives such the as the acid labile tert-butyloxycarbonyl (Boc) group and the base labile 9-fluorenylmethoxycarbonyl (Fmoc); (3) carboxybenzyl (Cbz (old symbol), or Z (in honor of its inventor Leonidas Zervas)) that can be deprotected by catalytic hydrogenolysis or sodium in liquid ammonia, and (4) convert the primary or secondary amine into a tertiary amine via addition of a benzyl (Bn) group that is usually removed by catalytic hydrogenolysis. This last approach is primarily used in solution phase synthesis.

In the research outlined in this dissertation, several amine protecting groups were used and intensively investigated in order to synthesize multiple aminophsphate 2'-deoxyoligonucleotides

analogues. This research on amino protection was based mainly on finding suitable amine protecting groups that can be orthogonal with the solid phase DNA synthesis cycle conditions and reagents. It also included finding the right protecting group that can be removed leaving the final products of these novel 2'-deoxyoligonucleotides intact.

# CHAPTER 2

# SYNTHESIS AND CHARACTERIZATION OF DIALKYLAMINO-BORANEPHOSPHONATE AND MORPHOLINOBORANEPHOSPHONATE DNA

## 2.1 Synthesis of Dialkylaminoboranephosphonate DNA

The first synthesis of enantiomerically pure oligodeoxynucleotide (ODN) having dialkylaminoboranephosphonate internucleotide linkage was completed by Richard Threlfall in this laboratory. Synthesis begins (**figure 2.1**) by condensing 5'-O-dimethoxytritylthymidine (**8**) with bis(diisopropylamino)chloro-phosphine using Hunig Base to quench the generated hydrochloride. The product of this reaction (**10a**) was then used to form the dinucleotide (**11a**) by reaction with 3'-O-acetylthymidine and 5-(Ethylthio)-1H-tetrazole (ETT). The reacting P(III) isomers were separated by flash chromatography. The next step was boronation of both isomers with a dimethylsulfide.$BH_3$ complex followed by removal of the 3'-O-acetyl group. As a final synthesis step, these isomers were converted to the 3'-O-diisopropylamino cyanoethyl phosphoramidites by condensation of (**12a**) with bis(diisopropylamino)cyanoethyl phosphine in the presence of ETT.

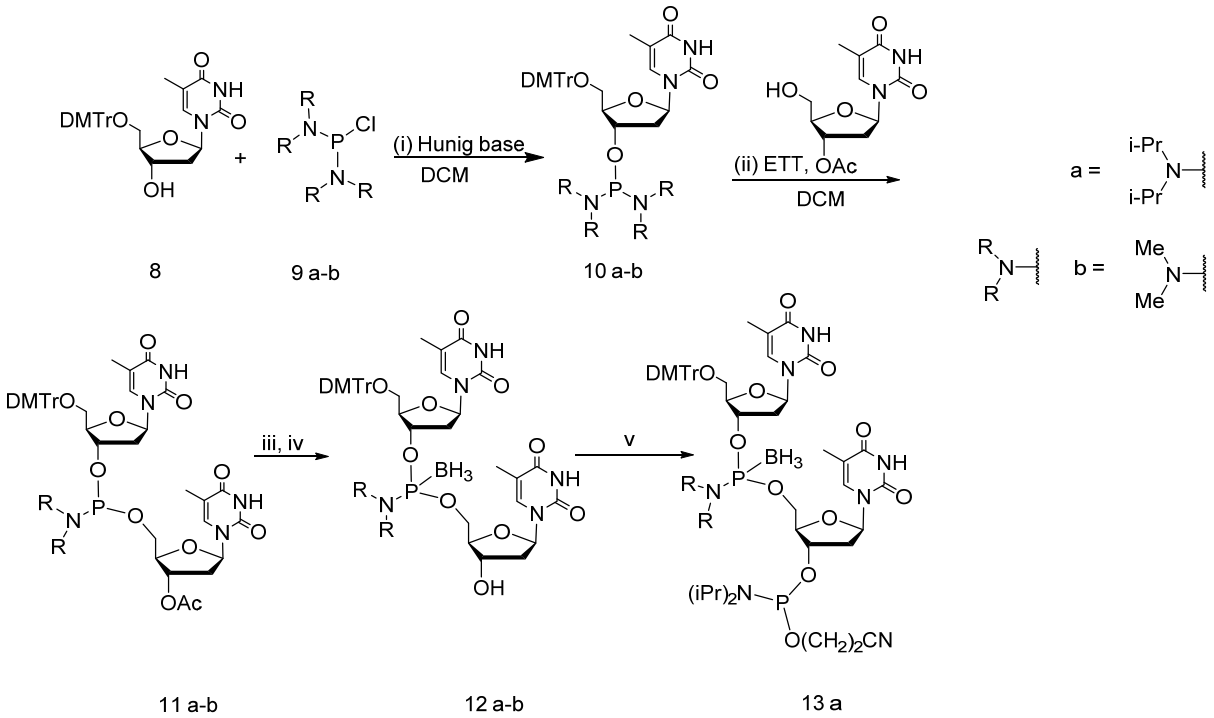


**Figure 2.1**: Synthesis scheme for chemical synthons (compounds 8–13) used to prepare 2'-deoxyoligonuclotides containing dialkylaminoboranephosphonate internucleotide linkage. (iii) $Me_2S{:}BH_3$, 2 equiv 15min; (iv) $NH_4OH$, 3 hr ; (v) 1.2 equiv of 2-cyanoethyl-N,N,N',N'-tetraisopropyl phosphane, $CH_2Cl_2$, 1 equiv 4,5-dicyanoimidazole, 1 hr; DMTr = 4,4-dimethoxytrityl; DCM: dichloromethane; ETT: 5-(ethylthio)-1H-tetrazole.

2'-Deoxyoligonuclotides containing this novel diisopropylaminoborane-phosphonate linkage were prepared using the dinucleotide isomers (**13a**) and 5'-O-dimethoxytritylthymidine-3'-O-(N,N-diisopropylamino-β-cyanoethyphosphor-amidite). The synthesis cycle as performed on controlled pore glass (CPG) is shown in figure 2.2. Relative to the standard synthesis cycle as carried out on CPG, triethylsilane was added to the acidic detritylation reagent in order to quench the dimethoxytrityl cation that is generated during the detritylation step. It is well known that this cation interacts with borane linked phosphorous derivatives which leads to degradation of the internucleotide linkage.[26]

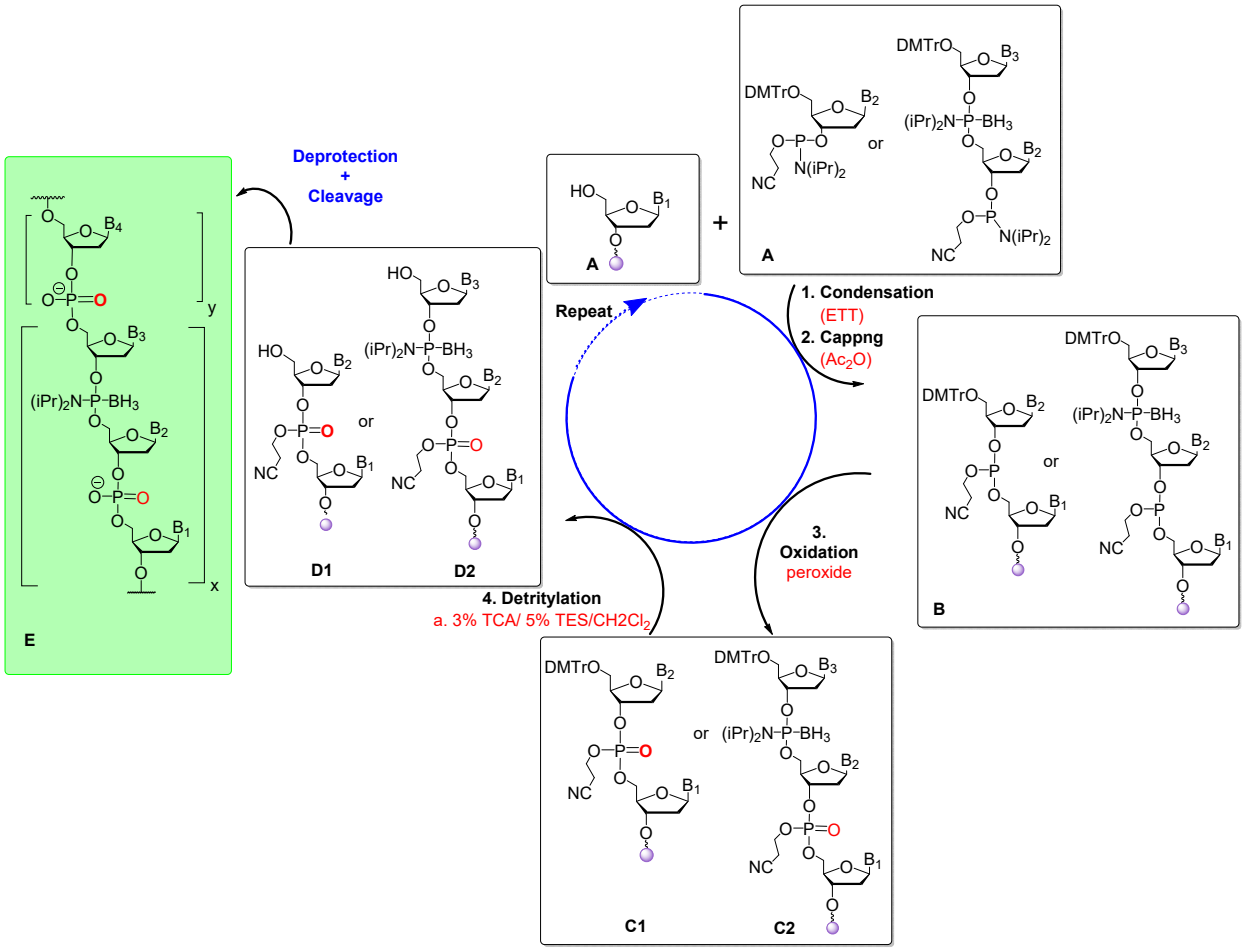


Figure 2.2: Solid-phase synthesis cycle used to synthesize diisopropylaminoboranephosphonate DNA; peroxide: tert-butyl peroxide (1.0 M in DCM); TES: triethylsilane.

As shown in figure 2.2 the four steps solid-phase DNA synthesis using the phosphoramidite have been modified to be compatible with the synthesis of diisopropylaminoboranephosphonate DNA. The dinucleotide isomers (**13a**) were introduced to the cycle when the boranephosphonate modification is needed and the condensation time was extended to 15 minutes instead of 1 minute (step 2: A to B). The oxidation (step 3: B to C) of the phosphite triester to phosphate (C1 or C2) with more commonly used iodine is replaced by with 1.0 M tert-butyl peroxide in DCM to avoid boranephosphonate linkage cleavage (C1 or C2). To the 3% trichloroacetic acid (TCA) in dichloromethane solution, which is routinely used for detritylation, triethylsilane was added to the

acidic detritylation reagent in order to quench the dimethoxytrityl cation that is generated during the detritylation step (step 4 C to D).

The successful synthesis of diisopropylaminoboranephosphonate DNA encouraged me to synthesize the dimethylaminoboranephosphonate derivative. As outlined later in this chapter, a significant depression of melting temperature (Tm) was observed with the diisopropylaminoboranephosphonate DNA derivative. This observation encouraged me to examine the dimethylamino derivative as it would be less bulky than the diisopropylamino analogue and therefore perhaps the melting temperature would not be significantly depressed.

Synthesis of the dimethylaminoboranephosphonate analogue begins by reacting 5'-O-dimethoxytritylthymidine (**8**) with bis(dimethylamino)chloro-phosphine in dichloromethane (DCM) using Hunig Base to quench the generated hydrochloride (figure 2.1). The resulting product (**10b**) was then reacted with ETT (0.9 equivalents) and 3'-O-acetyl thymidine in order to form (**11b**). The use of 0.9 equivalent of ETT minimized activation of the second dimethylamino group in compound (**10b**) which leads to formation of a trinucleotide phosphite triester. In contrast to the diisopropyl amino derivative, (**10b**) diastereomers were inseparable on the silica column chromatography under multiple solvent conditions. Boronation with $BH_3/(CH_3)_2S$ (less than 15 minutes) and ammonia treatment to deprotect the 3'-O-acetyl group leads to the final product (**12b**). However, the treatment with aqueous ammonia gave a cleavage side reaction as the major product and only small amounts of the targeted compound. This by-product was identified by mass spectrometry and resulted from bond cleavage between the phosphorous and one of the bonding oxygens as shown from $^{31}P$ NMR in

figure 2.3 where the single broad peak of the boronated phosphorous was divided into two broad peaks indicating the formation of two boronated phosphorus species.

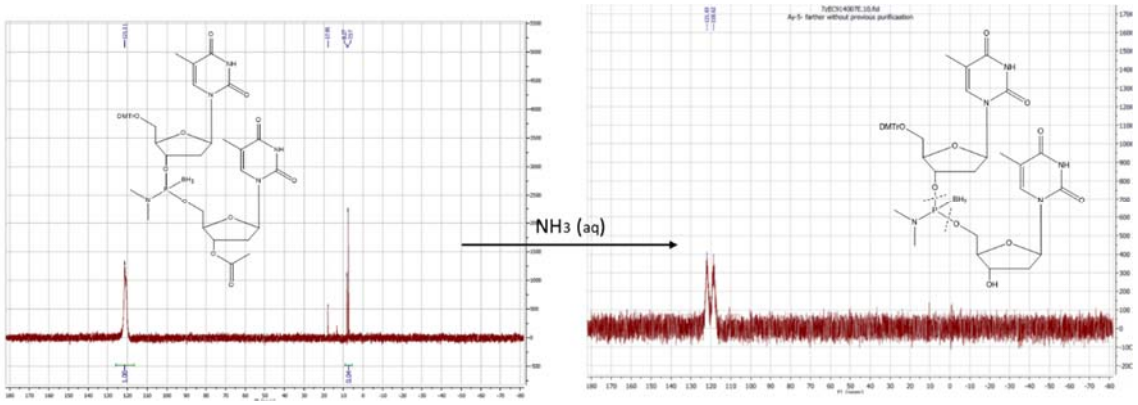


Figure 2.3: $^{31}$P NMR showing bond cleavage after aqueous ammonia treatment for compound 12b.

This cleavage side reaction was expected to create significant problems when this dimer was used in oligonucleotide synthesis. This is because ammonia, which is needed for cleaving the product oligonucleotide from the solid support and for deprotecting the nucleobases, would also degrade the oligonucleotide product.

These results suggest that the dimethyl amine derivative demonstrated improved synthesis stability relative to the isopropyl analogue and showed some satisfactory results; however, base treatment was problematic. Potentially, an amino functionality with properties somewhere between diisopropyl amine bulky alkyl group and dimethyl amine could solve the Tm suppression problem as well as the cleavage problem (instability of the dimethylamino derivative).

## 2.2: Synthesis of Morpholinoboranephosphonate DNA

To overcome the cleavage side reaction during base treatment as observed with the dimethylamine derivative and the reduction in duplex stability found with the diisopropyl analogue, the morpholinoboranephosphonate was considered a viable alternative. It is a secondary amine with less steric bulk than the diisopropylamine. Thus, this derivative should not reduce duplex stability to the same extent as the diisopropyl analog. Moreover, the morpholino diamidite should have similar reactivity towards various activators such as ETT, tetrazole and 4,5-dicyanoimidazole. A unique advantage of the morpholinophosphordiamidite (**figure 2.4 compound 15**) over other secondary amines is that, when one of the morpholino groups is activated, the other remains relatively unreactive.[27] Thus, the intermediate similar to **10b** in figure 2.1 should be stable and not reactive towards forming a phosphite triester as observed with the dimethylamino analogue.

Synthesis of the morpholinoboranephosphonate is outlined in figure 2.4. The synthesis begins by reacting $PCl_3$ with 6.2 equivalents of morpholine in order to prepare the trimorpholinophosphite. The product of this reaction (**14**) was condensed with 5'-O-dimethoxytrityl-2'-deoxythymidene in DCM using ETT as activator to generate (**15**) in 92% yield following column chromatography. Characterization by mass spectrometry and $^{31}P$ NMR confirmed the synthesis. The next step is condensation with 3'-O-acetyl-2-deoxythymidine using 0.9 equivalents of ETT as activator. The product (**16**) was purified by column chromatography and characterization by mass spectrometry and $^{31}P$ NMR was consistent with the literature. Boronation using $BH_3/(CH_3)_2S$ complex (15 min) and ammonia treatment to remove the 3'-O-acetyl group from (**16**) generated (**17**). In contrast to the dimethylamine,

analysis by mass spectrometry and $^{31}P$ NMR indicated that there was no detectable cleavage side reaction, even in a 10g synthesis. This result was very encouraging as it suggests, in contrast to the results with the dimethylamino derivative, that this analogue could be used successfully for the preparation of deoxyoligonucleotides containing the morpholinoboranephosphonate internucleotide linkage. Consequently, compound (**17**) was converted to (**18**) using 2-cyanoethyl N,N,N′,N′-tetraisopropylphosphorodiamidite in the presence of 1.2 equivalents of 4,5-dicyanoimidazole. The product of this reaction was isolated in 84% yield and characterized by $^{1}H$ NMR, $^{31}P$ NMR (**figure 2.5**) and mass spectrometry. It was used for the synthesis of 2'-deoxythymidine oligonucleotides containing the morpholinoboranephosphonate internucleotide linkage.

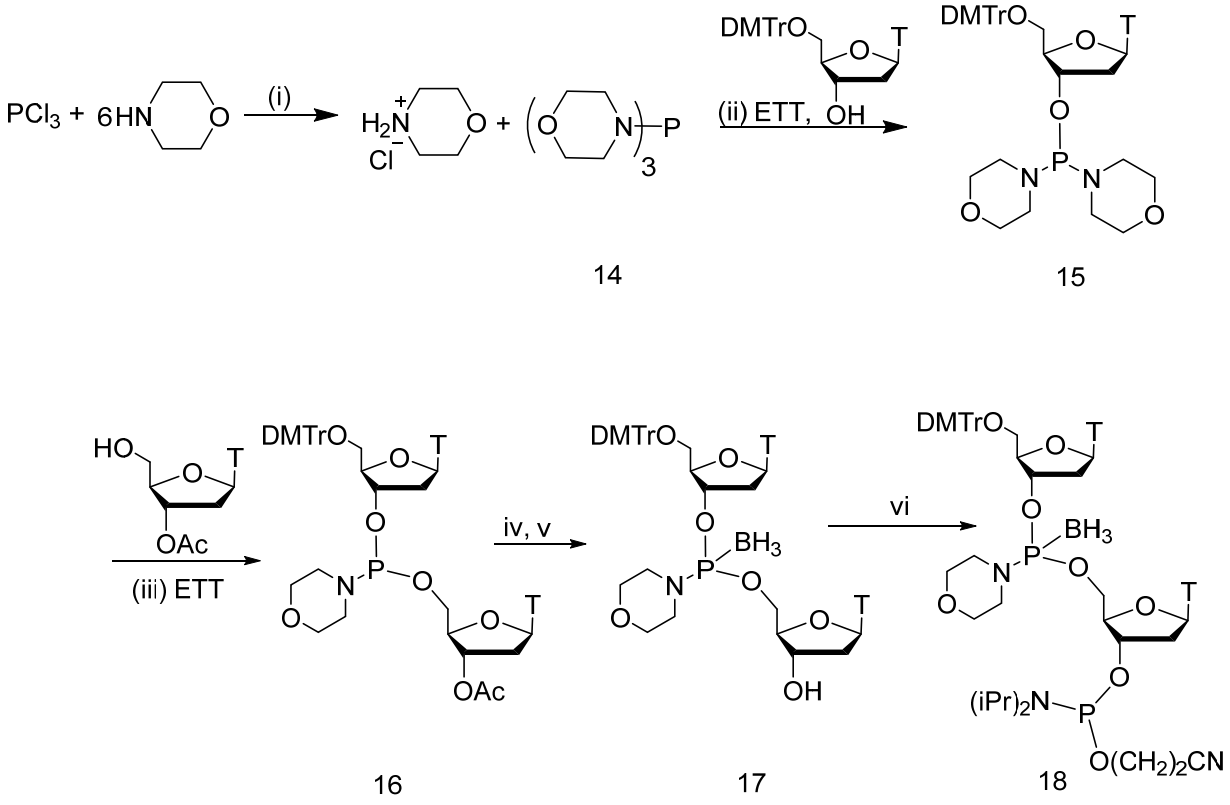

Figure 2.4: Synthesis scheme for chemical synthons (compounds 14–18) used to prepare morpholino boranephosphonate DNA. (iv) $Me_2S:BH_3$, 2 equiv 15min; (v) $NH_4OH$, 3 hr; (vi) 1.2 equiv of 2-Cyanoethyl N,N,N′,N′-tetraisopropylphosphorodiamidite, $CH_2Cl_2$, 1 equiv 4,5-dicyanoimidazole, 1 hr; DMTr = 4,4-dimethoxytrityl; T = thymin-1-yl.

In figure 2.5 the $^{31}P$ NMR confirming the synthesis of compound (**18**) showing a broad peak at 119 ppm for morpholinoboranephosphonate internucleotide linkage and triplet peak at 149 ppm corresponds to 2-cyanoethyl-N,N-diisopropyl-phosphorodiamidite part.

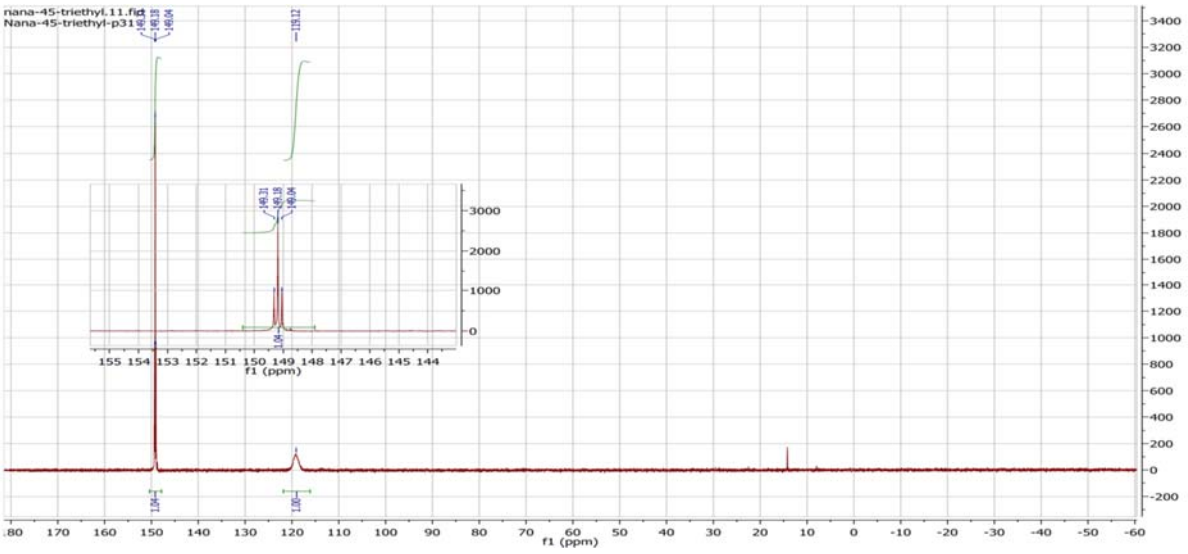


Figure 2.5: $^{31}P$ NMR for compound (18) showing a broad peak at 119 ppm for morpholinoboranephosphonate internucleotide linkage and triplet peak at 149 ppm corresponds to 2-cyanoethyl-N,N-diisopropyl-phosphorodiamidite part.

In order to develop a methodology for preparing deoxyoligonucleotides containing morpholinoboranephosphonate internucleotide linkages, several variables in the synthesis procedures had to be examined. I started by synthesizing 2'-deoxythymidine oligonucleotides where one boranephosphonate was introduced in

each 2'-deoxyoligonucleotide and one variable was studied in each synthesis. The results were analyzed relative to yield, purity and failure sequences. Initially, the modification was introduced as the last synthon in order to minimize exposure of the morpholinoboranephosphonate internucleotide linkage to the different reagents used during multiple solid phase synthesis cycles. Each synthesis was also completed so as to retain the large hydrophobic DMT group located at the 5' end of each 2'-deoxyoligonucleotide. This strategy leads to a shift of the polynucleotide product away from failure sequences when analyzed using reverse-phase HPLC. Thus the only compound bearing the terminal 5' DMT group is the full-length product 2'-deoxyoligonucleotide if all the reactions involved in synthesis have been completed properly. The retention time differences between tritylated and nontritylated oligonucleotides in the crude oligonucleotide mixture are quite large, and therefore this RP-HPLC procedure gives a clearer image of our synthesis and coupling efficiency.[28]

An initial investigation involved comparing monomer (**15**) and dimer (**18**) synthons for preparing oligonucleotides. Thus two 2'-deoxythymidine oligonucleotides were synthesized on CPG supports (**figure 2.6**). The first step in each case was preparing 2'-deoxythymidine oligonucleotides having only standard internucleotide phosphate linkages. Next the monomer synthon, compound (**15**) was added with ETT activator to one sample and the dimer synthon, compound (**18**) was condensed using ETT activator with second sample. After boronation of the morpholinophosphoramidite linkage as generated from the monomer synthon and oxidation of the phosphite triester as produced by coupling the dimer synthon, the

product mixtures were hydrolyzed from CPG using ammonium hydroxide and analyzed by RP-HPLC.

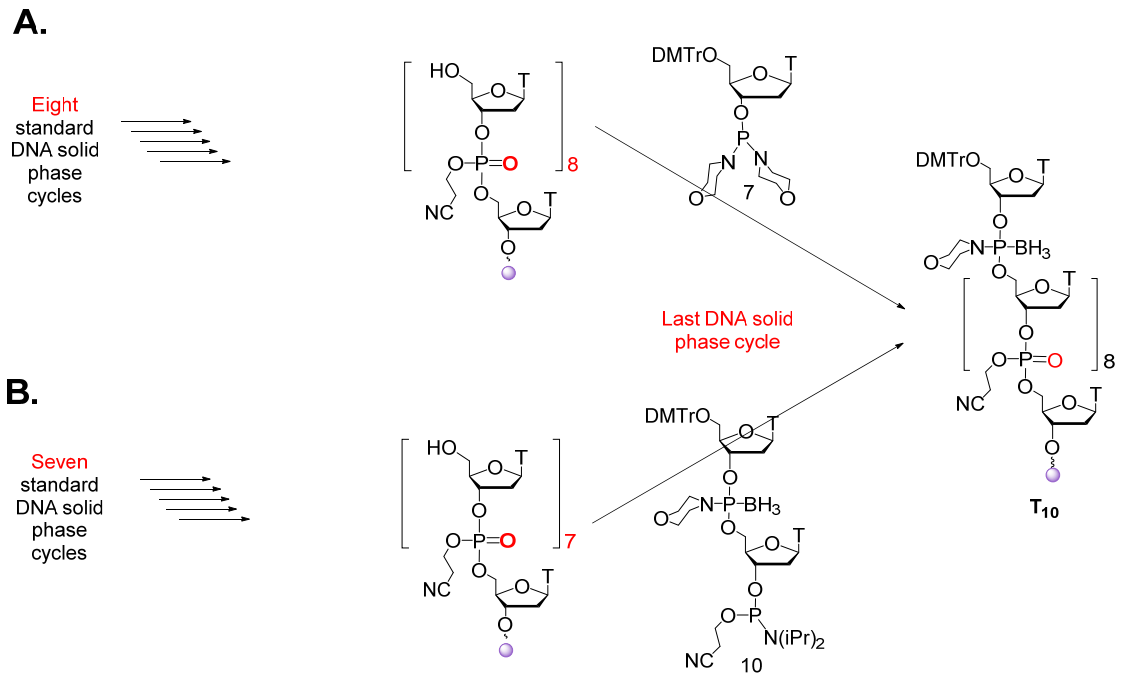


Figure 2.6: Synthesis scheme for synthesis of $T_{10}$ by adding mononucleotide at the last step using compound (15) as shown in part A or synthesis of $T_{10}$ by adding dinucleotide at the last step using compound (18) as shown in part B.

As can be seen from the results displayed in figure 2.7 the coupling reaction with the monomer synthon (part B) was essentially quantitative where the products as diastereomers dominates the RP-HPLC profile. In contrast, when the dimer synthon was tested (part A) approximately 40% yield of the product observed. The remaining material was primarily the 2'-deoxythymidine oligonucleotide that had not condensed with dimer (and hence did not contain the hydrophobic DMT group). As a result of this experiment, the monomer (**15**) was used as the synthon of choice.

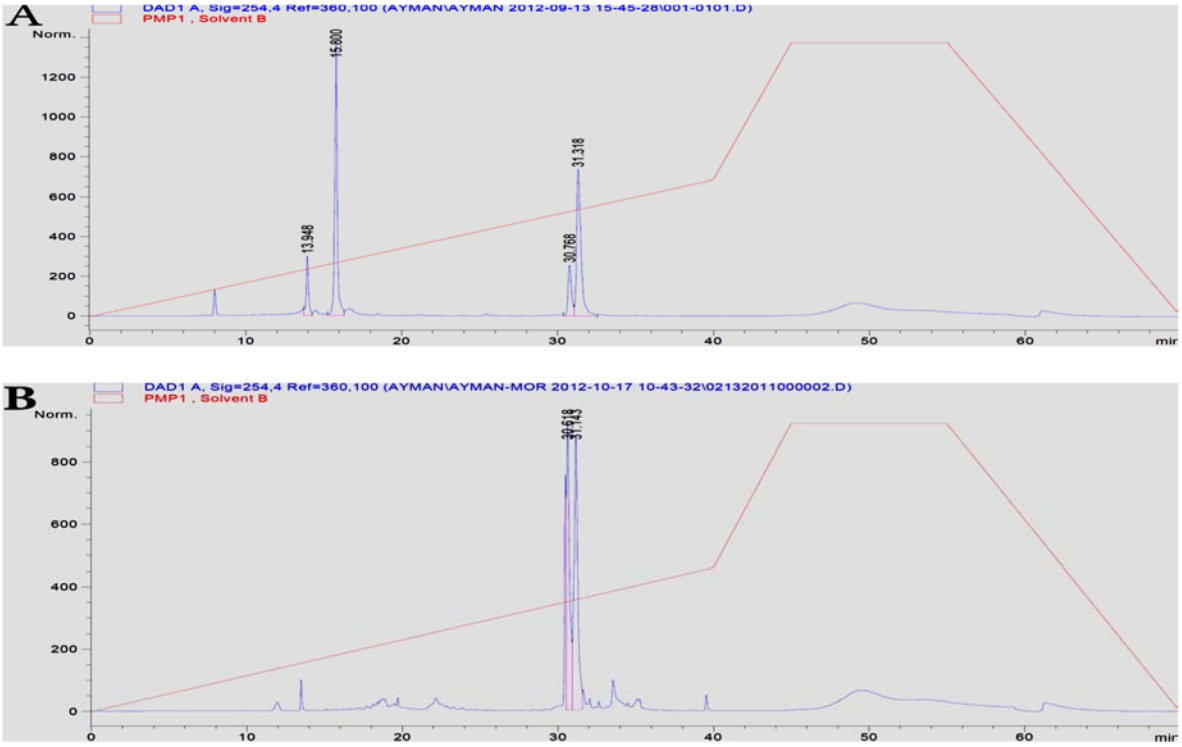


Figure 2.7: RP-HPLC profiles showing the crude $T_{10}$ product from solid phase synthesis; A) $T_{10}$ synthesis product using the dimer (18) in the last coupling step. The peaks at 15.8 minutes and 31 minutes corresponds to unreacted $T_8$ and $T_{10}$ product respectively; B) $T_{10}$ synthesis using (15) as the last coupling step. The expected $T_{10}$ at 31 minutes was only observed product.

A similar strategy was followed in order to study several additional modifications to the standard solid phase phosphoramidite synthesis cycles.

1) Condensation Step: Changing the concentration of 5'-dimethoxytrityl-2'-deoxythymidinedimorpholino phosphoramidite (**15**) from 0.1 M to 0.15 M increased the efficiency of the condensation step and decreased the amount of failure oligonucleotides. Similar results were obtained when ETT was the activator and the condensation time was extended from 1 minute to 30 minutes. However, introduction of the synthons twice during one synthesis cycle did not change the overall coupling yield.

2) Boronation: Instead of using the $BH_3/(CH_3)_2S$ complex as the boronating reagent, 0.05M $BH_3$ in THF was tested in order to avoid the production of $(CH_3)_2S$ gas inside the synthesizer during the boronation step. No difference in boronation rate or yield was observed with either reagent.

3) Peroxide oxidation: Because we are synthesizing DNA sequences having both phosphate and morpholinoboranephosphonate internucleotide linkages, an oxidizing solution reactive only with the phosphite triester was needed so as to convert the phosphite into phosphate without reacting with morpholino boranephosphonate internucleotide linkages. This was because the standard oxidizing solution, consisting of $I_2/H_2O$/ pyridine, could not be used in the presence of the borane phosphorus amine bonds. Iodine has been shown to catalyzed conversion of borane phosphite into phosphate in the presence of a nucleophile such as water.[29] In order to confirm this expectation, an NMR study was completed on a sample containing the borane morpholino dimer **17**. Thus, to a few milligrams of this dimer, the standard oxidizing solution containing aqueous iodine was added and the reaction monitored by $^{31}$P-NMR. It was found that conversion to phosphate was rapid and complete in less than 10 minutes. Therefore, 1.0 M tertbutyl peroxide dissolved in DCM was used as the oxidizing solution. This reagent was shown to convert the phosphate diester to the corresponding phosphate triester with results similar to those observed with aqueous iodine. Additionally, this reagent did not modify the morpholino boranephosphonate linkage.

4) 5' Deprotection and scavenger: During the detritylation process, a dimethoxy trityl carbocation is generated. This carbocation has been shown to degrade phosphitetriesters.[30,31] We have also previously observed that this carbocation forms side reactions that cause boron phosphite bond cleavage.[32] Although triethylsilane ($Et_3SiH$) has been described as an efficient

trityl cation scavenger,[26] we observed many degradation products with this reagent. As a result, trimethylphosphite-borane (TMPB), was developed in our laboratory and shown to quench this carbocation without damaging internucleotide boranephosphonate linkage.[32] Further studies[33] in this laboratory[32] also revealed that trichloroacetic acid (TCA) binds strongly to 2′-deoxyoligonucleotides on a solid support. This leads to a high local concentration of acid and oligonucleotide degradation. In contrast trifluoroacetic acid (TFA) does not lead to a similar degradation. For my research with DNA having morpholino boranephosphonate internucleotide linkages, degradation was not observed when a 0.5% (TFA) solution used. Thus, the detritylation step, as used in the standard synthesis cycle was modified to include 10% (v/v) TMPB and 0.5% TFA.[32]

5) Nucleobases nitrogen protection: Previous research has shown that boronating reagents lead to the reduction of N-acyl protecting groups on nucleobases having exocyclic amino groups (cytosine, guanine and adenine). The reduction leads to the corresponding N-alkyl derivatives.[34,35] Therefore, in order to avoid these side reactions a new N-acyl protecting group was developed for this project. Further details will be discussed in chapter 3.

To test the generality of the optimized conditions as described above, 2′-deoxythmidine oligonucleotides 21 nucleotides in length and containing variable numbers of morpholino boranephosphonate linkages at various positions were synthesized using the solid phase synthesis cycle shown in figure 2.8:

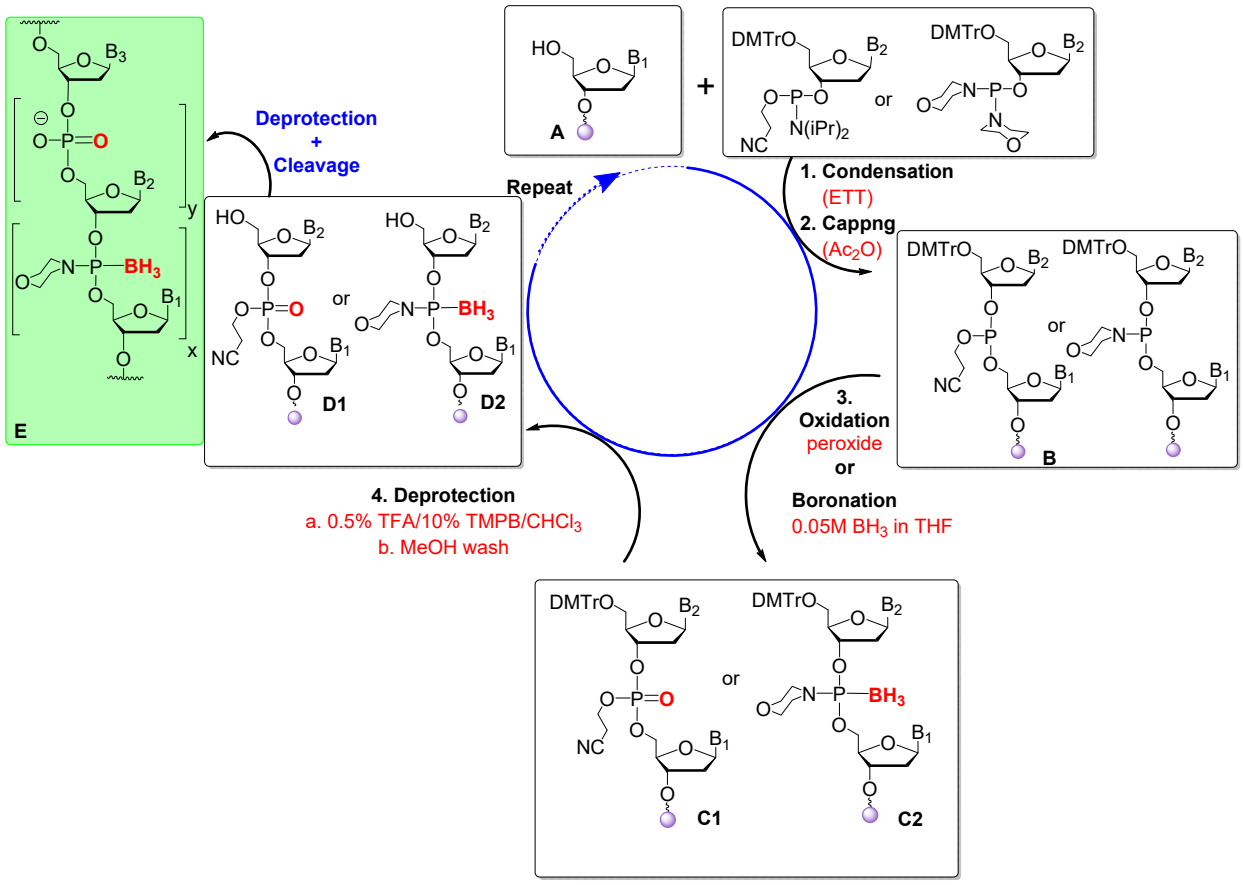


Figure 2.8 Solid-Phase Synthesis Cycle Used to Synthesize Morpholino Boranephosphonate DNA.

As shown in figure 2.2 the four steps solid-phase DNA synthesis using the phosphoramidite have been modified to be compatible with the synthesis of morpholinoboranephosphonate DNA. The dimorpholinophosphoramidite (**15**) was introduced to the cycle when the morpholinoboranephosphonate modification is needed and the condensation time was extended to 15 minutes instead of 1 minute (step A to B). The oxidation (step 3) of the phosphite triester to phosphate (C1) was carried using peroxide and boronation with 0.50 M $BH_3$ was used to yield morpholinoboranephosphonate linkage (C2). The detritylation step, as used in the standard synthesis cycle was modified to include 10% (v/v) TMPB and 0.5% TFA instead of 3% TCA.

The 2'-deoxyoligonucleotides that were synthesized are shown table 2.1. The structure of these oligonucleotides were confirmed by mass spectrometry and $^{31}P$ NMR.

**Table 2.1: ODNs Having Morpholinoboranephosphonate Modification**

| | Sequence 5' to 3' | Calculated Mass $[M-4H]^{4-}$ | Observed Mass $[M-4H]^{4-}$ | Yield (%) |
|---|---|---|---|---|
| ODN1 | T*TTTTTTTTTTTTTTTTT*TT | 1614.0380 | 1614.0025 | 83 |
| ODN2 | T*TT*TTTTTTTTTTTTT*TT*TT | 1647.4736 | 1647.3339 | 80 |
| ODN3 | 6-FAM-P(O)- T*TTTTTTTTTTTTTTTTTT*T | 1748.3678 | 1748.3173 | 74 |
| ODN4 | 6-FAM-P(O)- T*TT*TTTTTTTTTTTTTT*TT*T | 1781.8388 | 1781.9163 | 74 |

(*: Morpholinoboranephosphonate); % yield measured by UV absorbance.

Figure 2.9 shows $^{31}P$ NMR spectrum for ODN1 which has two morpholino boranephosphonate internucleotide and 18 natural DNA linkages. The broad peak at 116 ppm corresponds to the morpholino boranephosphonate internucleotide linkage and integrates for 2 units. The peak at -1 ppm integrates for 18 units and corresponds to the natural DNA linkages.

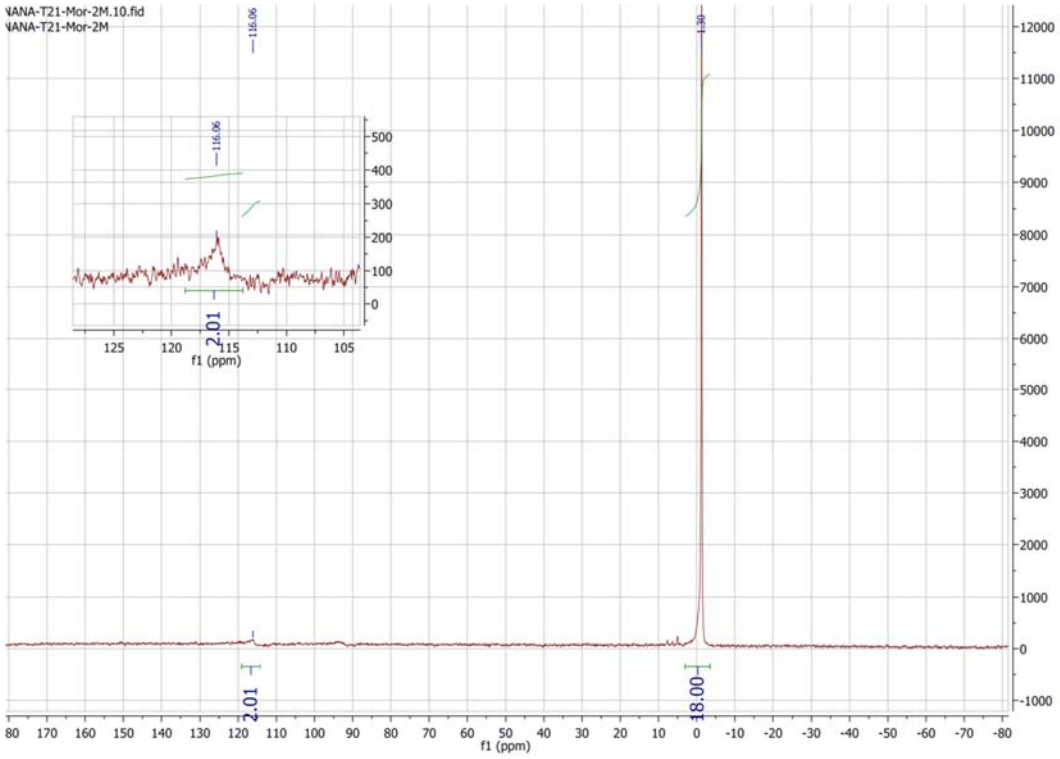


**Figure 2.9**: $^{31}P$ NMR for ODN1 which contains two morpholino boranephosphonate linkages and 18 natural phosphate linkages.

Figure 2.10 illustrates mass profile for ODN1 which consists of three parts; part B-1 shows the total ion chromatogram (TIC) using the electron spray ionization (ESI) method, part B-2 shows the UV absorption profile and part B-3 shows the ESI scan profile for the main peak from 29.4 to 31 minutes. The ion peak at 1614.0380 in B-3 corresponds to $[M-4H]^{-4}$.

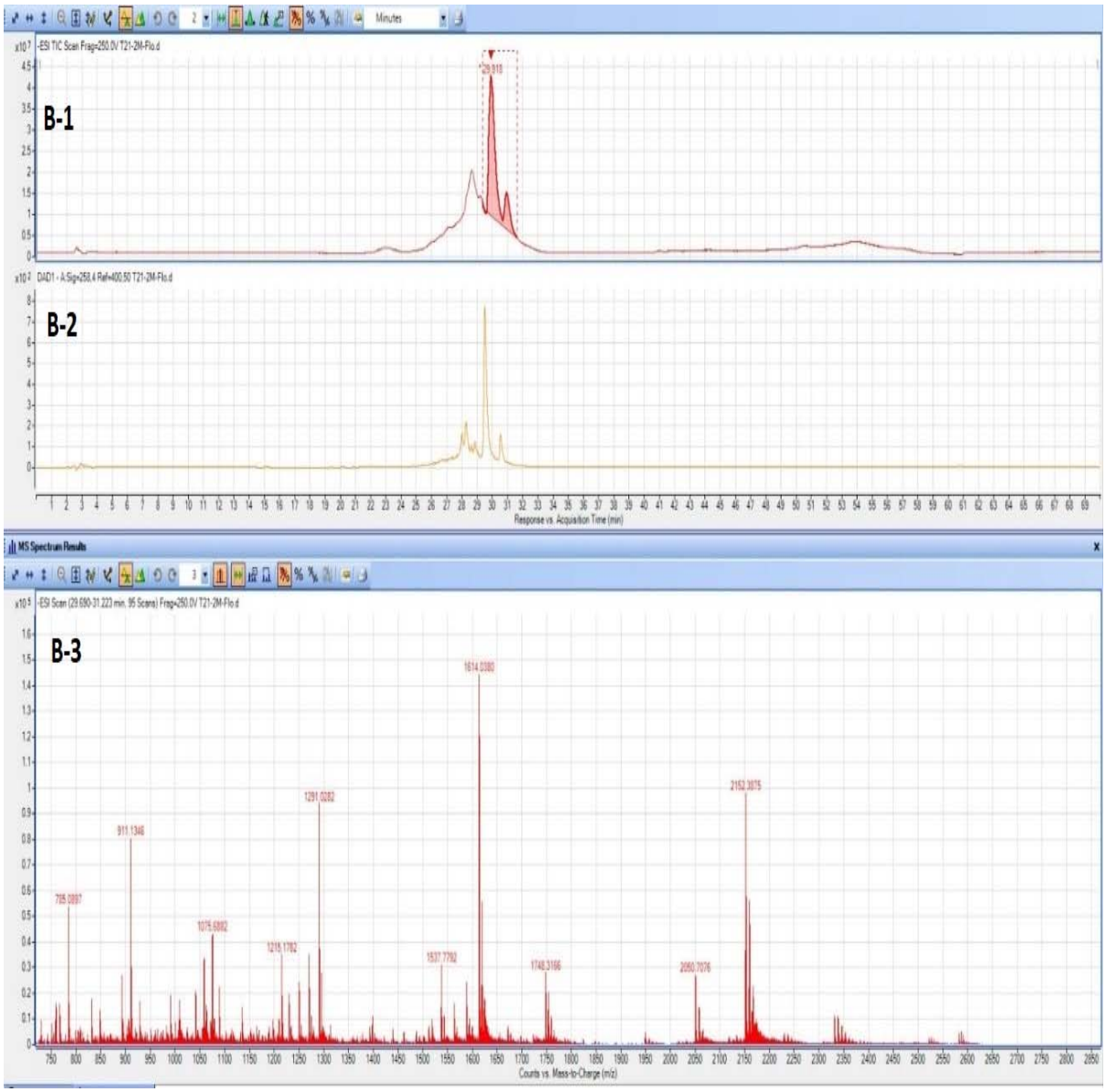


Figure 2.10 LC-UV/MS chromatogram of purified ODN1 which contains two morpholino boranephosphonate linkages and 18 natural phosphate linkages; B-1: total ion chromatogram B-2: UV absorbance chromatogram; B-3: extracted ion chromatogram for the main peak from 29.4 to 31 minutes. The ion peak at 1614.0380 in B-3 corresponds to $[M-4H]^{-4}$.

## 2.3 Duplex Stability Studies with Morpholinoboranephosphonate DNA

As shown in table 2.1, two 2'-deoxyoligonucleotides, ODN1 and ODN2, have been synthesized having two and four morpholino boranephosphonate linkages. Using these ODNs, Tm studies were then carried out with duplexes having complementary $d(A)_{21}$ and $r(A)_{21}$ oligonucleotides. Unmodified duplexes having $d(T)_{21}$ in complementation with $d(A)_{21}$ and $r(A)_{21}$ were also used as standard controls. Since the Tm of double-stranded nucleic acids depends upon the salt concentrations and pH, two salt concentrations were studied (1.0 M NaCl and 0.1 M NaCl). All measurements were performed in 10 mM sodium phosphate buffer, pH 7.3.

**Table 2.2: Melting temperature studies with ODN1 and ODN2 having morpholino boranephosphonate modification**

| Salt Concentration | Duplexes | | | | | |
|---|---|---|---|---|---|---|
| | $d(A)_{21}$ $d(T)_{21}$ | $d(A)_{21}$ ODN1 | $d(A)_{21}$ ODN2 | $r(A)_{21}$ $d(T)_{21}$ | $r(A)_{21}$ ODN1 | $r(A)_{21}$ ODN2 |
| 1.0 M NaCl | 61.2 | 59.2 | 58.2 | 54.0 | 52.12 | 51.12 |
| 0.1 M NaCl | 43.8 | 43.2 | 41.1 | 42.2 | 40.2 | 39.3 |

ODN1: 5'-d(TT*TTTTTTTTTTTTTTTTTT*T), ODN2: 5'-d(TT*TT*TTTTTTTTTTTTT*TT*T);

*: Morpholino Boranephosphonate.

These results indicate that adding morpholinoboranephosphonate linkages resulted in decreases in the Tm for all duplexes. The decrease was approximately 0.7 °C per modification which is similar to that observed with DNA containing thiophosphate.[21] In contrast, duplexes having the diisopropylamino boranephosphonate linkage generated Tm decreases of about 5 °C per modification. These results are summarized in figure 2.11.

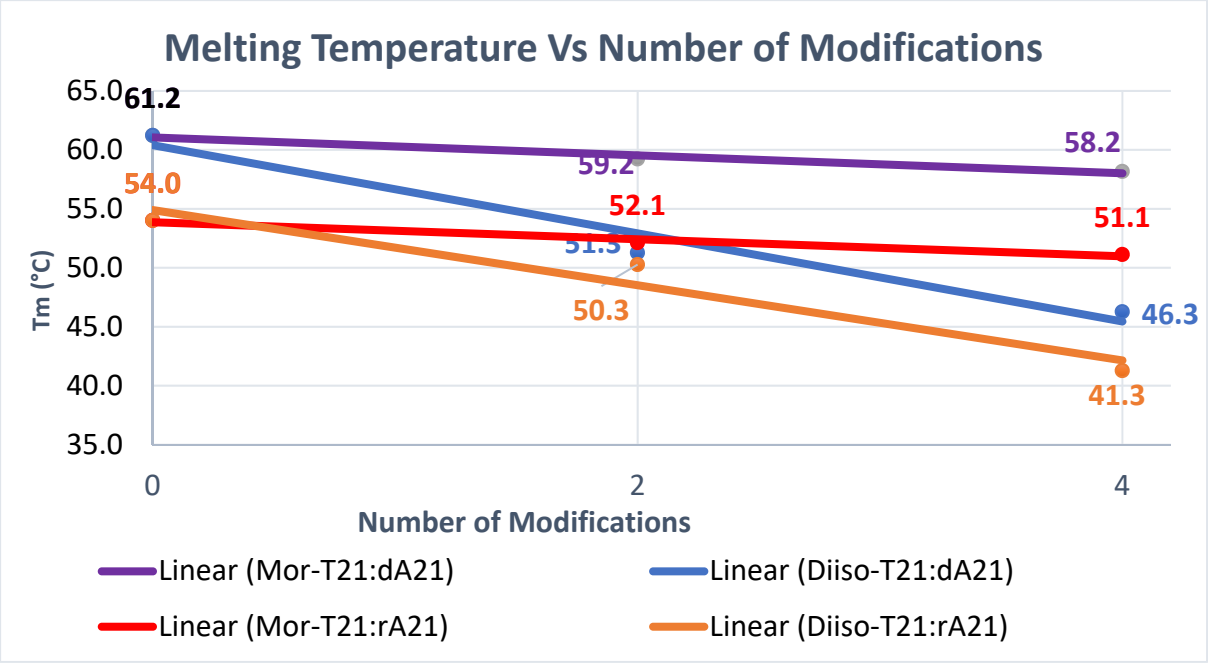


Figure 2.11 Melting temperature (Tm) versus the number of morpholinoboranephosphonate and diisopropylamino boranephosphonate modifications. The results from duplexes formed with complementary $d(A)_{21}$ and $r(A)_{21}$ are shown. Buffer: 1.0 M NaCl, 10 mM sodium phosphate, pH 7.3; Sequences: 2 modifications: 5'-T*TTTTTTTTTTTTTTTTT*TT; 4 modifications: 5'-T*TT*TTTTTTTTTTTTT*TT*TT where * represent the corresponding modification.

These results confirm that the Tm depression is significantly less for the morpholinoboranephosphonate analogue when compared to the more bulky diisopropylaminoboranephosphonate derivatives.

## 2.4 Cell Uptake Measurement of Morpholinoboranephosphonate DNA Using Fluorescence-Activated Cell Sorting (FACS)

In order to study how morpholinoboranephosphonate modifications affect DNA uptake in eukaryotic cells, passive transfection experiments were carried out using HeLa cells. 5'-Fuorescein labeled ODNs having two or four modifications were synthesized (**ODN 3 and ODN 4 table 2.1**) and cell uptake of these ODNs was measured at 3 different concentrations (0.5, 1.0 and 3.0 µM). HeLa cells were seeded for 24 hours, transfected with the appropriate ODN in DMEM buffer at the required final concentration and incubated at 37 °C for 24 hours. Increases in intracellular fluorescence due to ODN uptake were then measured by flow cytometry. The results are summarized in figure 2.12.

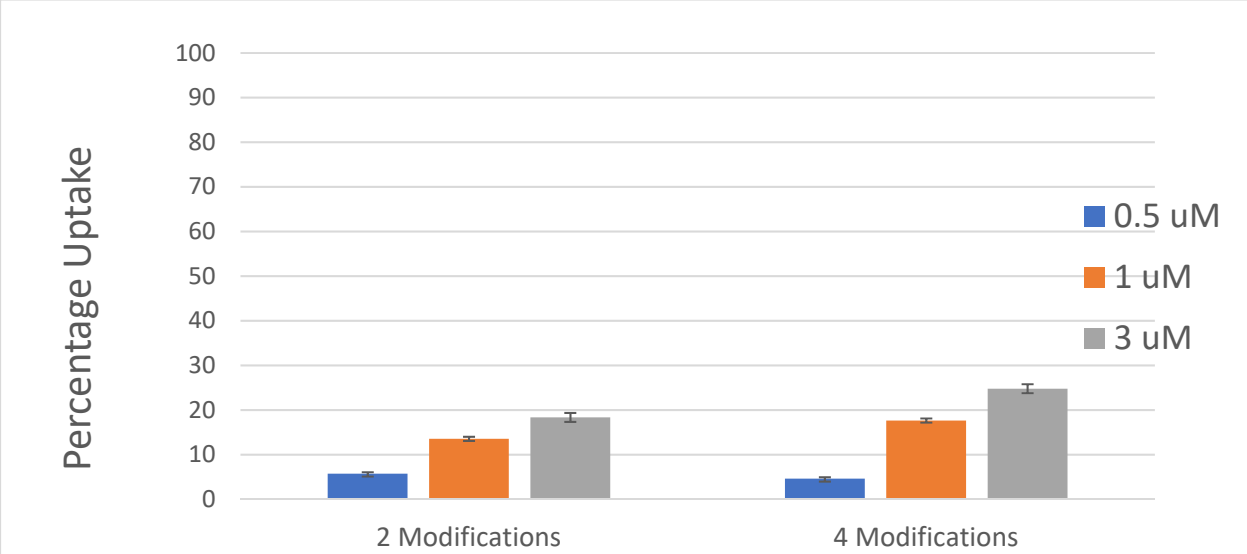


Figure 2.12 Bar diagram showing the percentage of HeLa cells with uptake, at various concentrations 0.5, 1.0 and 3.0 µM, of fluorescently labeled single-stranded DNAs ODNs 3−4 after 24h of transfection in Opti-MEM in absence of lipid transfecting agent.

Increasing the number of modification showed a slight increase (about 20%) relative to unmodified DNA in cell uptake at 3 μM for both ODN3 an dODN4. However at lower concentration (0.5 μM) the uptake was similar to unmodified DNA.

These two results, small depression in Tm per modification and a slight increase in cell uptake, encouraged us to try other amino boranephosphonate derivatives. This system looked promising and having a more basic nitrogen could affect the overall charge carried on the amino phosphate group and generate a positively charged phosphate which could affect both cell uptake and Tm.

# CHAPTER 3

# SYNTHESIS AND CHARACTERIZATION OF AMINOBORANEPHOSPHONATE DNA

## 3.1 Introduction

Having the morpholine ring attached to phosphorous showed a 20% increase in cell uptake activity when compared to standard DNA. Moreover, its effect on Tm was minor when compared to DNA having the sterically bulky diisopropylaminoboranephosphonate group. These observations led me to explore synthesizing an internucleotide linkage having borane and the primary amine attached to phosphorus. This linkage would be more electropositive than morpholine and this might lead to enhance transfection efficiency. Additionally, the minimal size of an amino group might lead to even less instability of DNA duplexes when compared to morpholine.

In order to synthesize a primary aminoboranephosphonate internucleotide linkage and due to the reactivity of amines either as a base or a nucleophile, the reactivity of the primary amine attached on the phosphorous should be suppressed (protected) during the solid phase DNA synthesis and restored by the end of the synthesis as shown in figure 3.1.

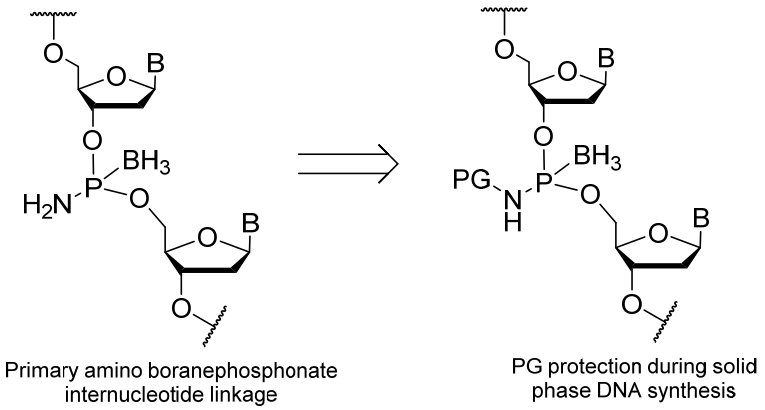


Figure 3.1: Retrosynthesis scheme for aminoboranephosphonate DNA internucleotide linkage showing the use of a protecting group during a DNA solid phase synthesis cycle. PG: protecting group; B nucleobase.

Choosing the right protecting group not only involves its compatibility with the DNA solid phase synthesis cycle, but also the ability of removing it without degrading the desired DNA

synthon. Thus, this protecting group should be resistant to acid, iodine and reduction by borane. Its removal should be by using moderate basic conditions similar to the conditions used to deprotect the exocyclic amines. As a result of these considerations pivalamide was chosen as an amine protecting group (a detailed study of pivalamide will be discussed in section 3.6).

### 3.2 Synthesis of Thymidine Aminoboranephosphonate DNA

In the condensation step of phosphoramidite DNA synthesis, a protonatable secondary amine such as pyrrolidine or the most commonly used diisopropylamine is attached on the phosphorous. This secondary amine is then activated by a weak acid (commonly known as activator) and replaced by the 5' or 3' oxygen of a nucleoside. Thus in order to use the phosphoramidite method, diisopropylamine must be attached to the precursor monomer used to synthesize the aminoboranephosphonate and, as mentioned previously, the pivalamide should be attached on the phosphorus as well. Thus, the desired monomer to synthesize aminoboranephosphonate using solid phase phosphoramidite chemistry is 5'- DMT-3'-((N-diisopropylamino)phosphanyl)-N-pivalamide) 2'-deoxythymidine ( 20 figure 3.2).

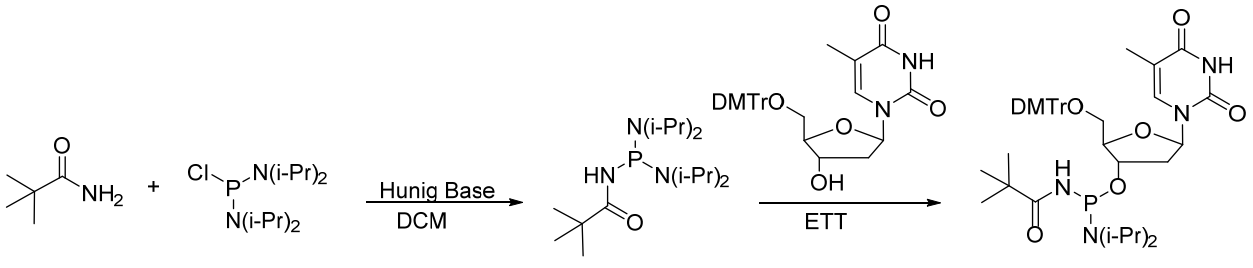


Figure 3.2: Synthesis scheme for 5'- DMT-3'-((N-diisopropylamino)phosphanyl)-N-pivalamide) 2'-deoxythymidine (20).

The synthesis begins with preparation of N- pivalamide(bis-(N,N-diisopropylamine))phosphite (**19**). Pivalamide and 1.1 equivalents of Hünig's Base were added to DCM. Hünig's Base deprotonates the amide and also forms an amine salt with the acid chloride generated during the synthesis. After stirring for 15 minutes, bis(diisopropylamino)-chlorophosphine was added and the reaction monitored by $^{31}P$ NMR. The disappearance of the 141 ppm peak on the $^{31}P$ NMR indicates complete consumption of the starting material. Appearance of a new peak around 114 ppm indicated the formation of the desired phosphoramidite (**19**). 5' DMT protected nucleoside and 0.9 equivalents of ETT were added, the reaction was monitored by TLC until the 5' DMT protected nucleoside was consumed (**figure 3.2**). The product 20 was confirmed by $^{1}H$ NMR, 2D NMR, $^{31}P$ NMR and mass spectrometry. Based on $^{31}P$ NMR and TLC the reaction generated both diastereomers. However, they proved inseparable by silica gel column chromatography under multiple solvent conditions.

In order to validate that this synthon (**20**) could be used for solid phase DNA synthesis, several 2'-deoxyoligothymidine derivatives having the pivalamide boranephosphonate internucleotide linkages at variable positions were synthesized. I first synthesized $T_{10}$ 2'-deoxyoligonucleotides where each oligomer contained one pivalamide modification. Synthesis conditions were optimized by varying condensation time, monomer concentration and oxidizing agent for each synthesis attempt. Initially, this modification was placed at the 5' -end as the last monomer unit in order to minimize its exposure to different reagents during the solid phase synthesis cycle. I also did not remove the final 5' DMT protecting group because it provides a very good hydrophobic handle for separating the product from various failure sequences that lack the DMT. As outlined previously, this is because the presence of the DMT group shifts the product polynucleotide away from failure sequences and therefore provides a clearer image of the synthesis

and coupling efficiency. The optimized solid phase synthesis cycle used to synthesize 2'-deoxyoligonucleotides that contained variable numbers of aminoboranephosphonate modification at various positions is shown in figure 3.3.

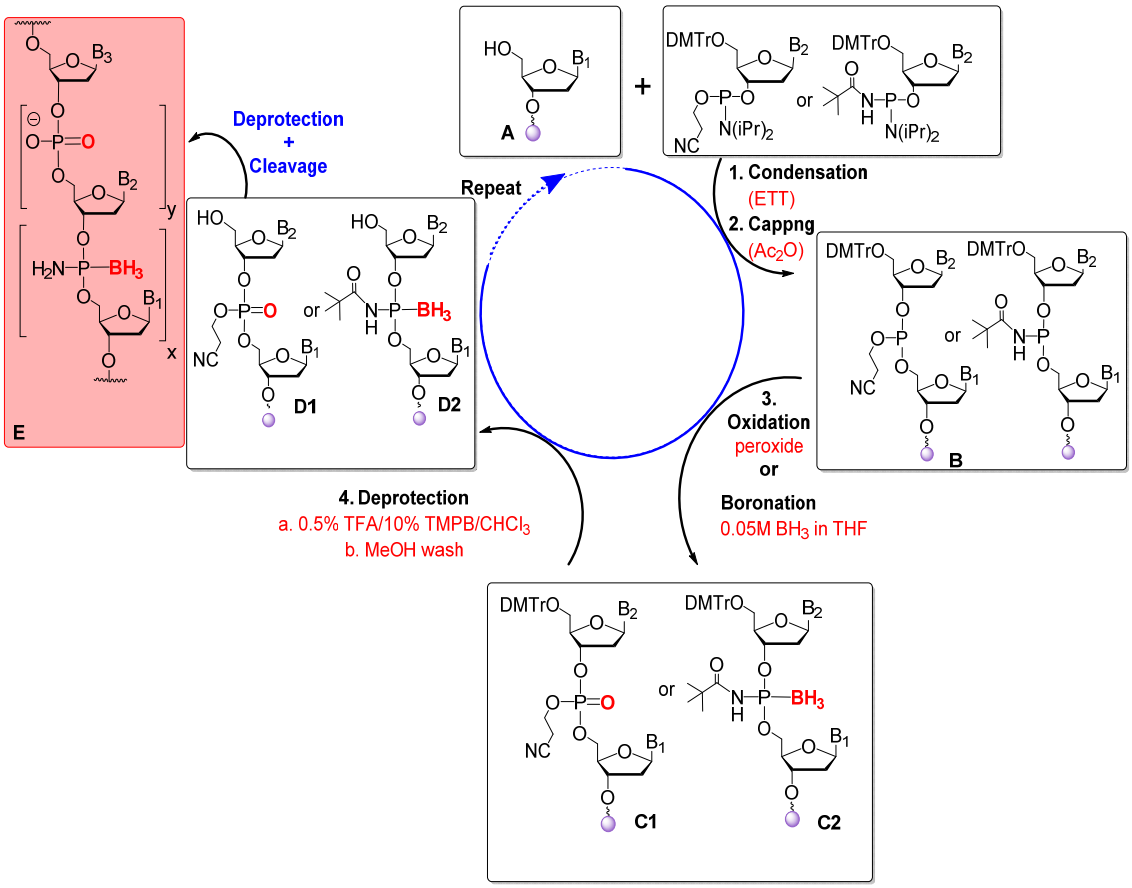


Figure 3.3 Solid-phase synthesis cycle used to synthesize amino boranephosphonate DNA. peroxide: tert-butyl peroxide (1.0 M in DCM); TMPB: trimethylphosphite-borane.

The following modifications to the standard solid phase phosphoramidite synthesis were introduced:

1) Condensation Step: The concentration of phosphoramidite (**20**) was increased from 0.1 M to 0.15 M. This increase led to a higher condensation yield and decreased the quantity of failure sequences. ETT (0.25 M) was the activator and the condensation time was extended to 30

minutes. However, introduction of the monomer **20** twice to the reaction column did not change the overall coupling yield.

2) Boronation: 0.05M $BH_3$ in THF was used as the boronating reagent. This reagent was introduced to the reaction column through 15 seconds flow and a wait time of 60 seconds.

3) Peroxide oxidation: Tertbutyl peroxide (1.0 M) dissolved in DCM was used as an oxidizing solution. This reagent was shown to convert the phosphodiester to the corresponding phosphotriester with results similar to those observed with aqueous iodine. Unlike iodine, this reagent did not modify the pivaloylaminoboranephosphonate linkage.

4) 5' Deprotection and scavenger: Previous research has determined that borane phosphonate internucleotide linkages are degraded by the dimethoxytrityl cation as generated during the acid cleavage step with TCA.[28,29] Several reagents have been used neutralize this cation. As outlined previously, we have discovered that TMPB is an efficient scavenger. Therefore, 10% TMPB was added to the detritylation solution and shown to generate superior results as scavenger.[32] In contrast, TCA binds strongly to 2′-deoxyoligonucleotides on a solid support which leads to a high local concentration of acid and 2′-deoxyoligonucleotide degradation even in the presence of 10% TMPB. Thus, the detritylation step as used in the standard synthesis was modified to include 10% (v/v) TMPB and 0.5% TFA.

After solid phase synthesis of 2'-deoxythymidine oligonucleotides, the CPG resins are incubated in aqueous ammonia for 16 hours at 55 °C (Deprotection and Cleavage step figure 4.3). These conditions were used in order to deprotect the non-bridging oxygen in the phosphate group from the cyanoethyl and to deprotect the aminoboranephosphonate from the pivaloyl. Detailed studies about the use of pivalamide protecting group on the phosphorous and the nucleobases and

its deprotection are outlined in sections 3.5 and 3.6. Using these synthesis procedures, the oligomers shown in table 3.1 were prepared.

**Table 3.1: 2'-Deoxythymidine oligonucleotide containing aminoboranephosphonate internucleotide linkage**

| | Sequence 5' to 3' | Calculated Mass $[M-4]^{4-}$ | Observed Mass $[M-4]^{4-}$ | Yield (%) |
|---|---|---|---|---|
| ODN5 | T*TTTTTTTTTTTTTTTTT*TT | 1579.4599 | 1579.4462 | 66 |
| ODN6 | T*TT*TTTTTTTTTTTTT*TT*TT | 1578.3847 | 1578.2618 | 64 |
| ODN7 | T*TT*TT*TTTTTTTTTT*TT*TT*TT | 1577.3075 | 1577.2534 | 58 |
| ODN8 | T*TT*TT*TT*TTTTTT*TT*TT*TT*TT | 1576.2325 | 1576.3584 | 51 |
| ODN9 | TT*TTT*TTT*TTT*TTT*TTT*TTT*T | 1576.7706 | 1576.6384 | 43 |
| ODN10 | T*TT*TT*TT*TT*TT*TT*TT*TT*TT | 1575.1591 | 1575.2348 | 36 |
| ODN11 | 6-FAM-P(O)- T*TTTTTTTTTTTTTTTTTT*T | 1713.8200 | 1713.773 | 54 |
| ODN12 | 6-FAM-P(O)- T*TT*TTTTTTTTTTTTTT*TT*T | 1712.7475 | 1713.0461 | 62 |
| ODN13 | 6-FAM-P(O)- T*TT*TT*TTTTTTTTTTT*TT*TT*T | 1711.6733 | 1711.5742 | 51 |
| ODN14 | 6-FAM-P(O)- T*TT*TT*TT*TTTTTTT*TT*TT*TT*T | 1710.5987 | 1710.3433 | 46 |

(*: Aminoboranephosphonate); 6-FAM-P(O); 5'-fluorescein phosphoramidate.

Figure 3.4 shows the $^{31}P$ NMR spectrum for ODN11 which has two morpholino boranephosphonate internucleotide, 18 natural DNA linkages and one 5' phosphate conjugating the 2'-deoxyoligonuclotide with the fluorescein tag. The broad peak at 93 ppm corresponds to aminoboranephosphonate internucleotide linkage and integrates for 2 units and the peak at -1 ppm and integrates for 19 units corresponds to phosphate linkages. Figure 3.5 illustrates the mass profile for ODN11 which consists of three parts; part B-1 shows the total ion chromatogram (TIC) using electron spray ionization (ESI) method, part B-2 shows the UV absorption profile and part B-3 shows the ESI scan profile at selected time.

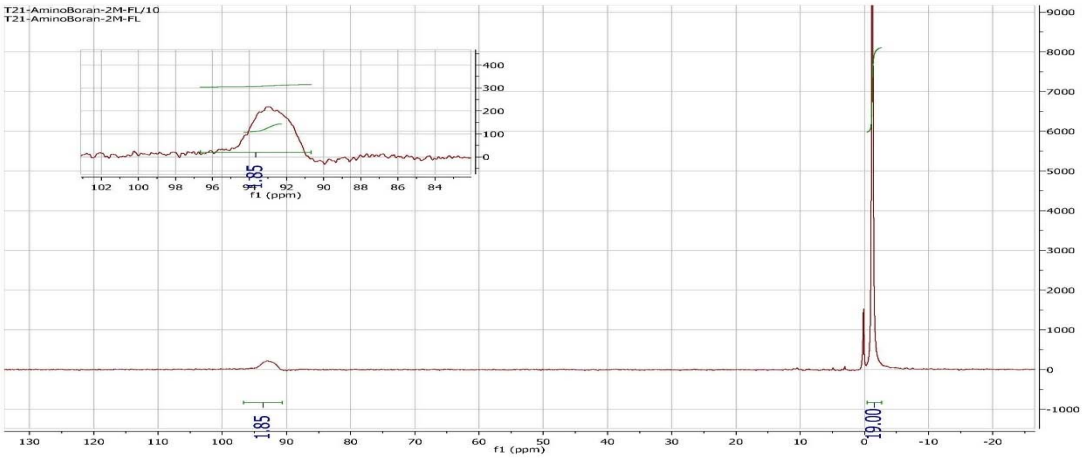


Figure 3.4 $^{31}$P NMR for ODN11 with the following sequence 6-FAM-P(O)- T*TTTTTTTTTTTTTTTTT*TT; the peaks at -1 ppm correspond to phosphate and the broad peak at 93 ppm corresponds to aminoboranephosphonate internucleotide linkage; *: Aminoboranephosphonate; 6-FAM-P(O): 5'-fluorescein phosphoramidite.

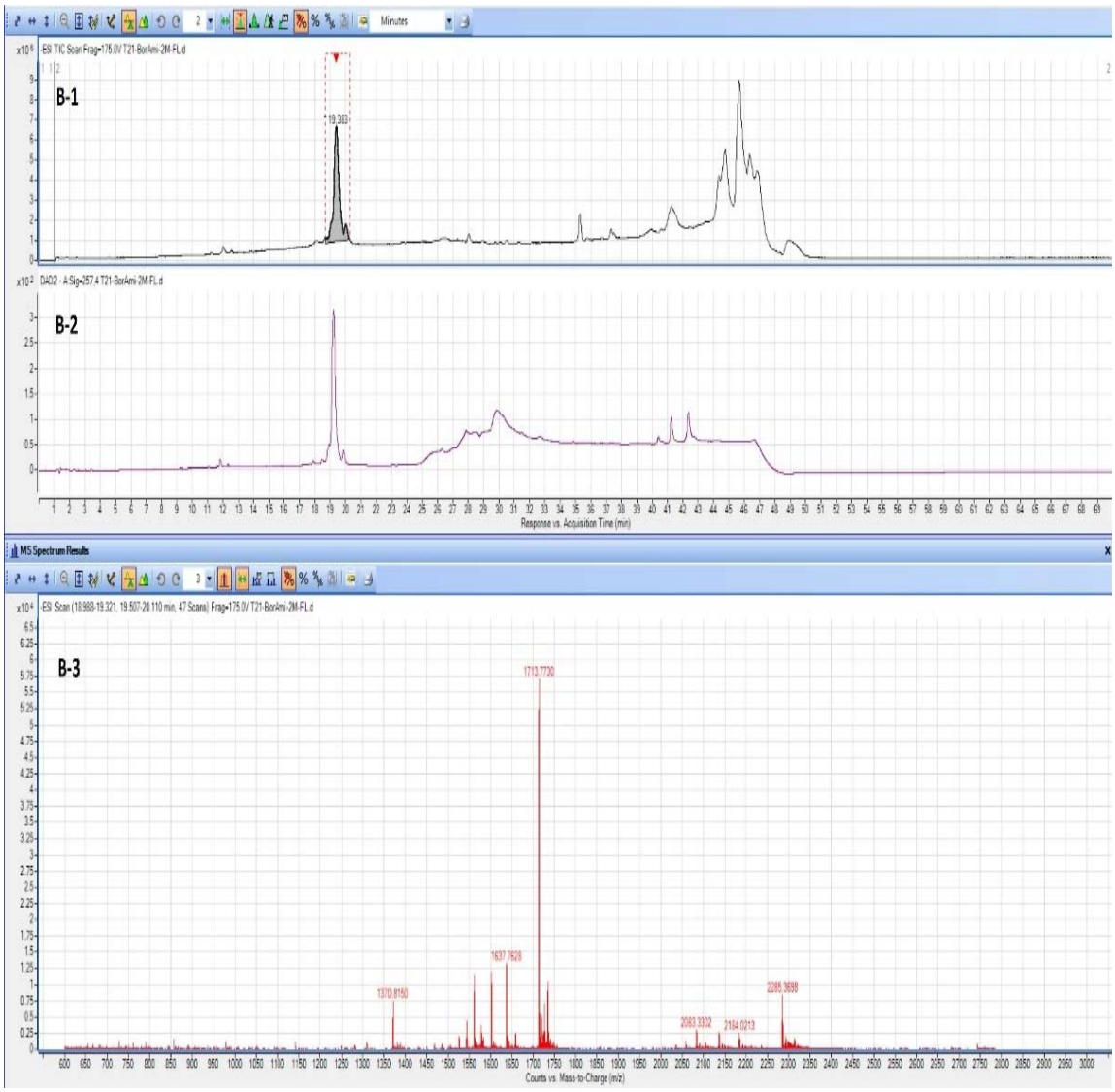


Figure 3.5: LC-UV/MS for the purified ODN11 (6-FAM-P(O)- T*TTTTTTTTTTTTTTTTT*TT, $[M-4H]^{-4}$ = 1712.7730) *: Amino Boranephosphonate; 6-FAM-P(O): 5'-fluorescein phosphoramidite. B-1: total ion chromatogram B-2: UV absorbance chromatogram; B-3: extracted ion chromatogram of the main peak in B-1 from 18.8 to 20 minutes showing the mass of ODN7 at 1712.7730 having an ionization state -4.

### 3.3 Duplex Stability Studies of Aminoboranephosphonate DNA

Four thymidine polynucleotides that contained two, four six and eight aminoboranephosphonate internucleotide linkages were synthesized. Tm studies were then completed using these oligomers with complementary $d(A)_{21}$ and $r(A)_{21}$. Since the Tm experiment depends upon the salt concentrations and pH, two salt concentrations were studied (1.0 M NaCl and 0.1 M NaCl) at pH = 7.3 using 0.01 M $Na_2HPO_4$ as the buffer. Table 3.2 summarizes results.

**Table 3.2: Melting temperature for ODNs having aminoboranephosphonate modifications**

| Salt Concentration | Duplexes | | | | | | | | | |
|---|---|---|---|---|---|---|---|---|---|---|
| | $d(A)_{21}$ $d(T)_{21}$ | $d(A)_{21}$ ODN1 | $d(A)_{21}$ ODN2 | $d(A)_{21}$ ODN3 | $d(A)_{21}$ ODN4 | $r(A)_{21}$ $d(T)_{21}$ | $r(A)_{21}$ ODN5 | $r(A)_{21}$ ODN6 | $r(A)_{21}$ ODN7 | $r(A)_{21}$ ODN8 |
| 1.0M NaCl | 61.22 | 61.17 | 58.12 | 55.07 | 51.07 | 54.02 | 54.12 | 51.22 | 48.27 | 44.22 |
| 0.1M NaCl | 43.88 | 43.12 | 41.12 | 38.07 | 34.07 | 42.2 | 40.12 | 37.21 | 34.22 | 31.22 |

ODN5: 5'-d(TT*TTTTTTTTTTTTTTTTT*T) ODN6: 5'-d(TT*TT*TTTTTTTTTTTTT*TT*T) ODN7: 5'-d(TT*TT*TT*TTTTTTTTT*TT*TT*T) ODN8: 5'-d(TT*TT*TT*TT*TTTTTT*TT*TT*TT*T); *: Amino Boranephosphonate.

Based upon these results, the depression in Tm values was about 0.7 °C per modification which is very close to the DNA containing the thiophosphate derivative. When the modifications were introduced near to the middle of the 2'-deoxyoligonuclotide, a higher depression per modification was observed (**figure 3.6**). Moreover aminoboranephosphonate showed a similar depression per modification to morpholino boranephosphonate.

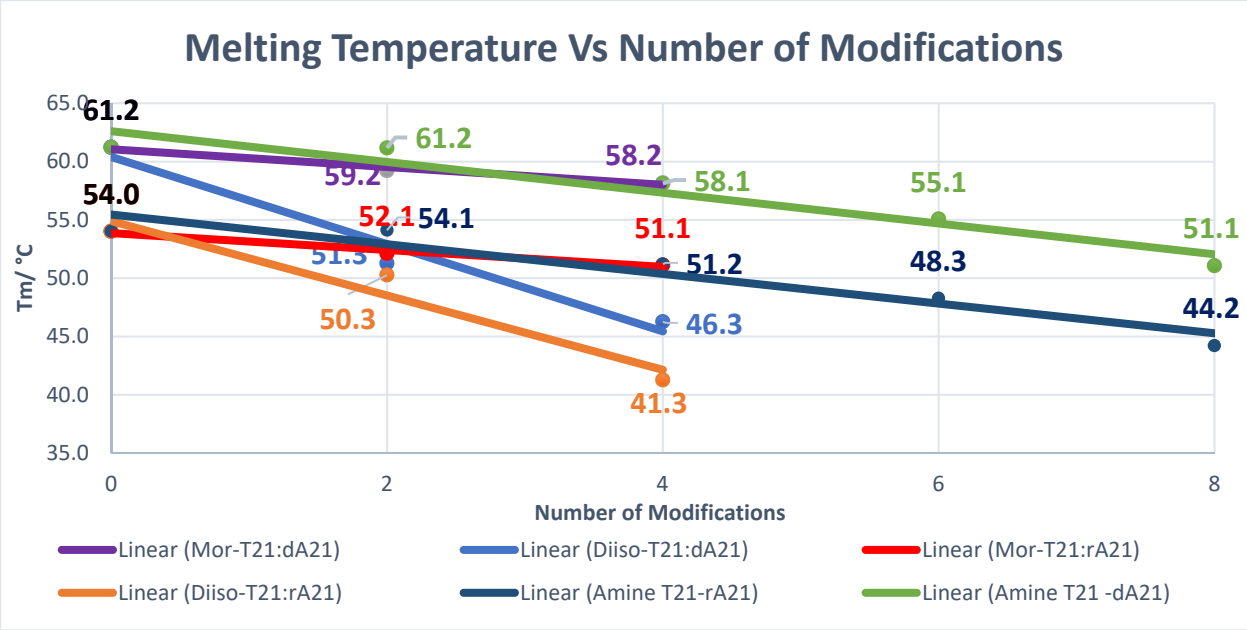


Figure 3.6 Melting temperature (Tm) versus the number of modifications of aminoboranephosphonate, morpholino boranephosphonate and diisopropylamino boranephosphonate modified oligodeoxythymidines with complementary $d(A)_{21}$ and $r(A)_{21}$. Sequences: 2 modifications: 5'-d(TT*TTTTTTTTTTTTTTTTT*T); 4 modifications: 5'-d(TT*TT*TTTTTTTTTTTTT*TT*T); 6 modifications: 5'-d(TT*TT*TT*TTTTTTTTT*TT*TT*T); 8 modifications: 5'-d(TT*TT*TT*TT*TTTTT*TT*TT*TT*T) where * represent the corresponding modification. Buffer: 1.0 M NaCl, 10 mM sodium phosphate, pH 7.3.

### 3.4 Cell Uptake Transfection Measurements Using Fluorescence-Activated Cell Sorting (FACS)

Passive transfection experiments were completed using HeLa cells. 5'-Fuorescein labeled ODNs having two, four, six and eight aminoboranephosphonate modifications were used (**ODN11, ODN12, ODN13, ODN14, Table 3.1**) at three concentrations (0.5 µM, 1.0 µM and 3.0 µM). HeLa cells were seeded for 24 hours, transfected with the appropriate ODN in DMEM buffer to give the required final concentration and incubated at 37 °C for 24 hours. Increases in intracellular fluorescence due to ODN uptake were then measured by flow cytometry.

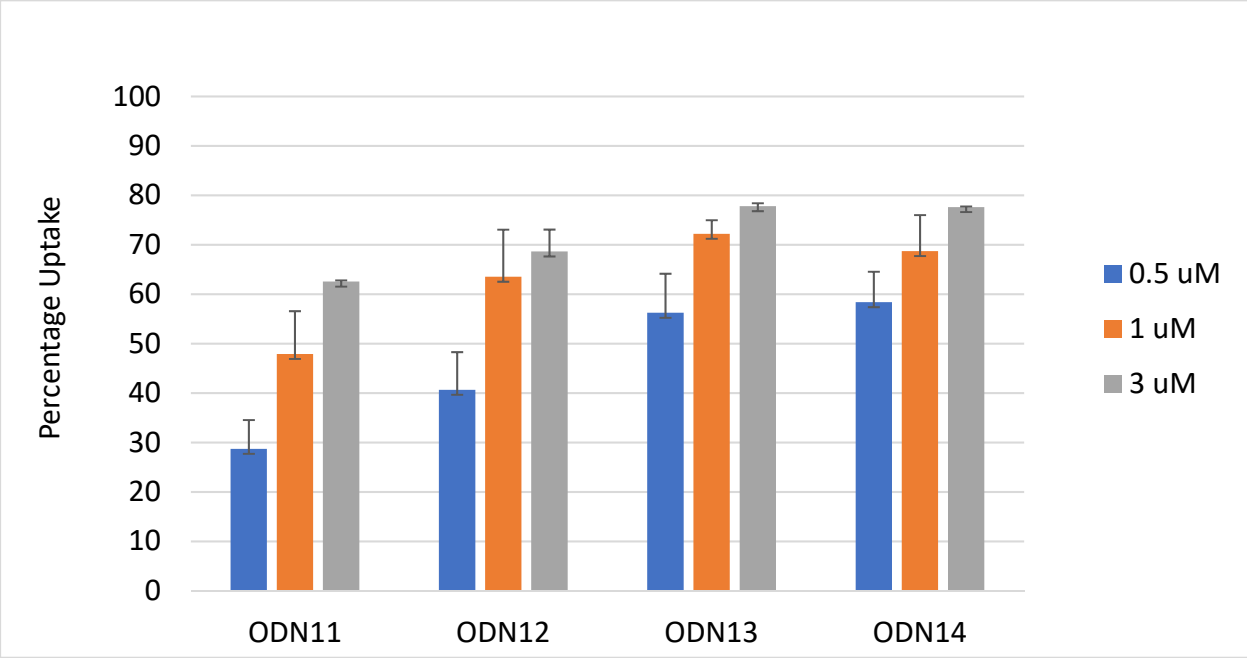


Figure 3.7 Bar diagram showing the percentage of HeLa cells with uptake, at various concentrations 0.5, 1.0 and 3.0 µM, of fluorescently labeled single-stranded DNAs ODNs 11−14 after 24h of transfection in Opti-MEM in absence of lipid transfecting agent.

As shown in figure 3.7, with 2′-deoxyoligonucleotides having 2, 4, 6 and 8 aminoboranephosphonate modifications (**ODNs 11 - 14**) increasing the number of modification

was reflected on cell uptake at the three concentrations mostly for ODN13 and ODN14 which contain 6 and 8 modifications respectively. At 3 μM both reached close to saturation. This suggests oligomers having 6 and 8 phosphoramidimidate modifications are maximally transfected at 3 μM. Additionally, even at 0.5 μM these ODNs were taken up by 55% of the HeLa cells. On the other hand, more than 25% of cells showed cell uptake when **ODN11** containing 2 modifications was used at 0.5 μM concentration. When the concentration was increased to 1.0 μM and 3.0 μM for the same ODN, the uptake increased to ~50% and 60% respectively. In general, this modification showed significantly higher uptake results than morpholinoboranephosphonate showed in chapter 3.

### 3.5 Enzymatic Studies with Snake Venom Phosphodiesterase Exonuclease

Aminoboranephosphonate is isosteric to the methylphosphonate and boranephosphonate internucleotide linkages. These two modifications were highly resistant to exonuclease activity.[38,39] In order to evaluate the relative exonuclease susceptibility of the aminoboranephosphonate internucleotide linkage, a $d(T)_{10}$ having this modification on the 3' and 5' termini was tested. A $d(T)_{10}$ unmodified oligonucleotide was used as a control. The oligomers were tested for stability against snake venom phosphodiesterase (SVPDE, 3' exonuclease). The sample of the oligomer (1 optical density unit) was incubated at 37 °C with 5 μg of the enzyme in Tris-HCl buffer (pH 9) containing 10 mM $MgCl_2$. Aliquots were removed at different time points, denatured, and analyzed by RP-HPLC. A single modification at each end generated an oligomer that was approximately 20 times more stable than native DNA toward SVPDE digestion.

When a 2'-deoxyoligonucleotide was incubated with SVPDE, it degrades the oligonucleotide from the 3' end and generates mononucleotides which appears using the reverse phase HPLC (RF-HPLC) with a retention time around 8 minutes. From figure 3.8 the degradation rate with natural phosphate DNA was at least 20 times faster than the degradation of **ODN16** having two aminoboranephosphonate internucleotide linkages.

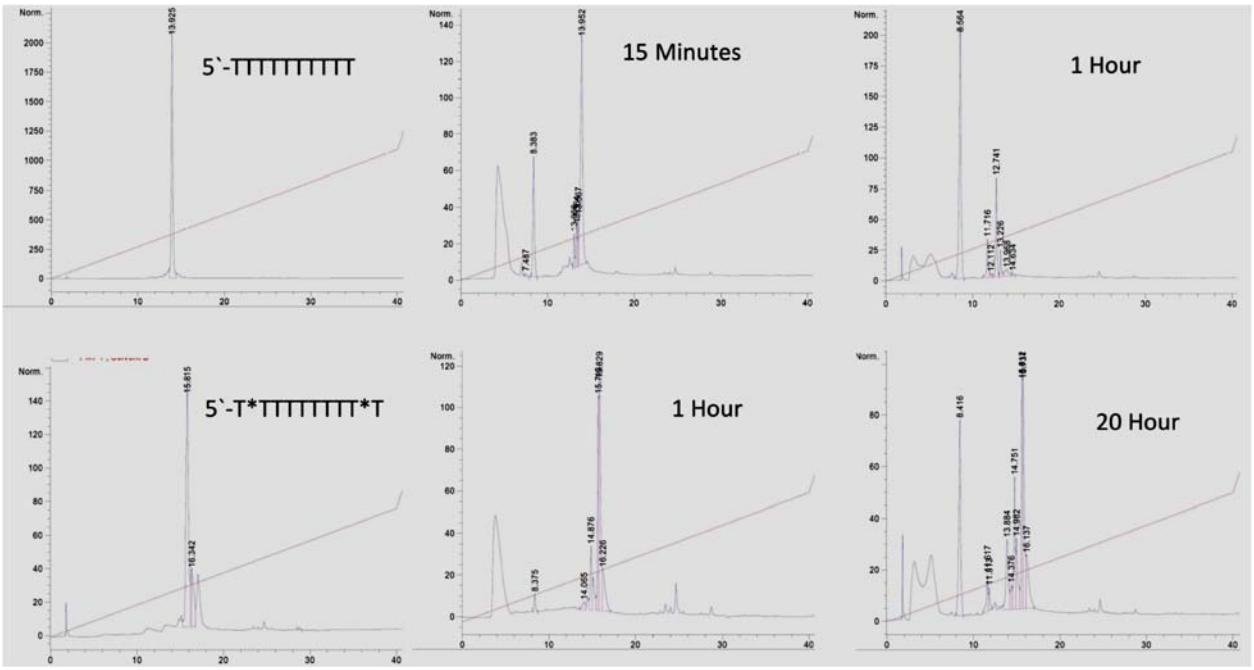


Figure 3.8: Time-dependent enzymatic exonuclease degradation of ODN15: 5'-TTTTTTTTTT and ODN16: 5'-T*TTTTTTTT*T with Snake Venom Phosphodiesterase (SVPDE). ODNs were treated with SVPDE, aliquots of reaction mixture at different time points were analyzed by RP-HPLC. Upper set time left to right 0, 15, 60 min. Lower set time left to right 0, 1, 20 hours. Oligonucleotide degradation from the 3' end is indicated by appearance of mononucleotide peaks at a retention time around 8. *: Amino boranephosphonate.

### 3.6 Pivalamide: A New Nucleobases Protecting Group

In the preceding section of this chapter, I outlined a method for synthesizing DNA having aminoboranephosphonate internucleotide linkages. The procedure utilized pivaloyl protection on the amino group linked to the phosphorous, boronation and removal of the pivaloyl protection with ammonia. This initial research was completed utilizing only thymidine nucleotides where no protection of thymine is required. However, a central problem during synthesis of 2'-deoxyoligonucleotides on solid supports is the protection and deprotection of the exocyclic amino groups on cytosine, adenine and guanine. In particular, we need protecting groups that are orthogonal with the solid phase synthesis conditions and can be removed after completion of 2'-deoxyoligonucleotide synthesis. There are several amide protecting groups that have been used to protect the exocyclic amino groups of the nucleobases. However, many of these amides are unacceptable when a boronating reagent is part of the synthesis. This is because boronation also cause the reduction of the standard N-acylamides to the corresponding N-alkyl derivatives. These N-alkyl analogues are stable towards synthesis conditions and are an undesirable side product. This side reaction was first reported by Barbara R. Shaw (**figure 3.9**)[35] and confirmed in our laboratory. Thus, it is necessary to develop a protecting group for the nucleobases that is stable towards boronating reagents as well as the other reagents that are used during 2'-deoxyoligonucleotide synthesis.

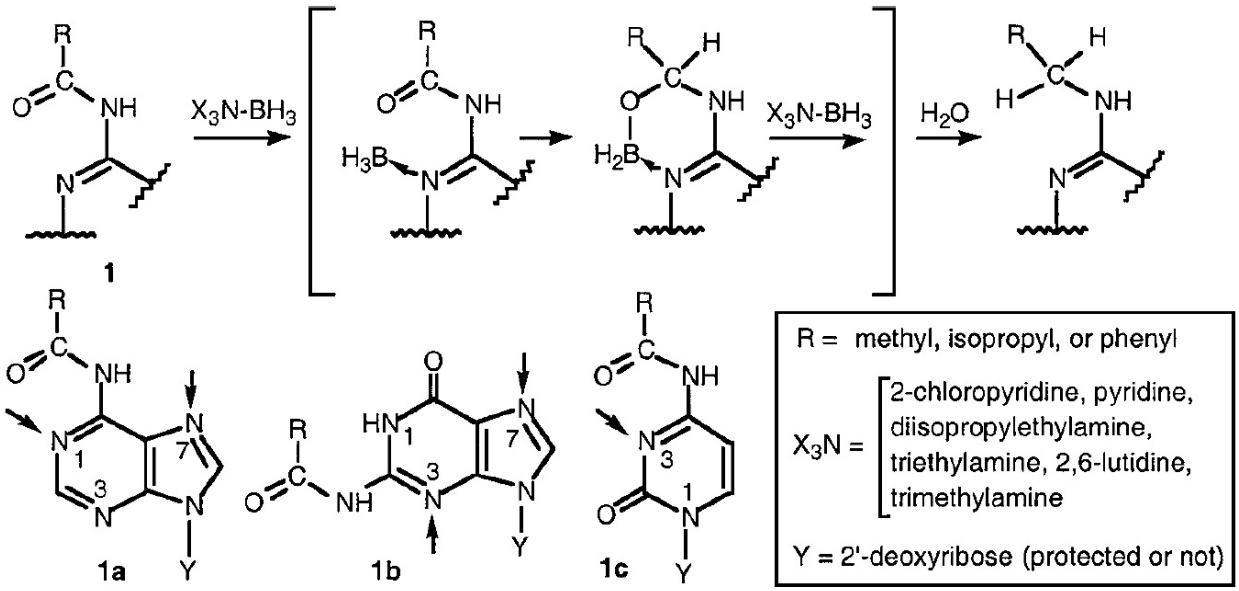


Figure 3.9 Proposed mechanism of the nucleoside N-acyl protecting group reduction. Arrows indicate possible sites of borane coordination in the acyl protected nucleosides. This figure is taken from [35]

In order to overcome this problem, the nucleobases (A, G and C) were protected with pivalamide using Jones' method[40] (**figure 3.10 for 2'-deoxadenosine**). Following protection of exocyclic amines, these 2'-deoxynucleoside were then treated with dimethoxy trityl or trimethoxy trityl chloride in order to generate the fully protected 2'-deoxynucleoside. The standard 2'-deoxycytidine and 2'-deoxyguanosine were protected using the same procedure.

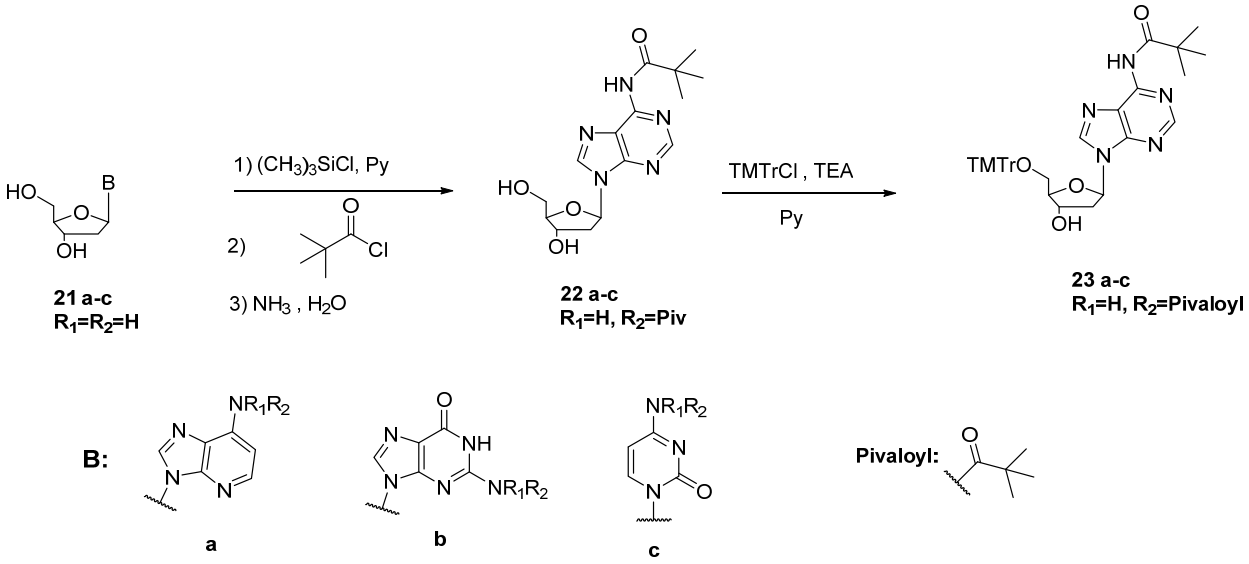


Figure 3.10: Protection of the exocyclic amines of 2'-deoxynucleosides (A, G and C) with pivaloyl and the 5'-hydroxyl with DMT using the Jones' method. TMTrCl: trimethoxytrityl chloride; TEA: triethylamine; Py: pyridine.

Due to the bulkiness of the pivaloyl group, two problems must be solved in order to validate this group for use in preparation of aminoboranephosphonate DNA. First the resistance of this group towards boronation must be evaluated and second a procedure for removal of this group from the 2'-deoxynucleosides without generating side products must be found. For example, a proposed conversion of 2'-deoxyadenosine into 2'-deoxyinosine, 2'-deoxyguanosine into 2'-deoxyxanthosine and 2'-deoxycytidine into 2'-deoxyuridine is possible with ammonium hydroxide when this reagent is used with a sterically bulky protecting group. This is because the hydroxide anion may preferentially attack the nucleobase base instead of the amide protecting group (**figure 3.11**).

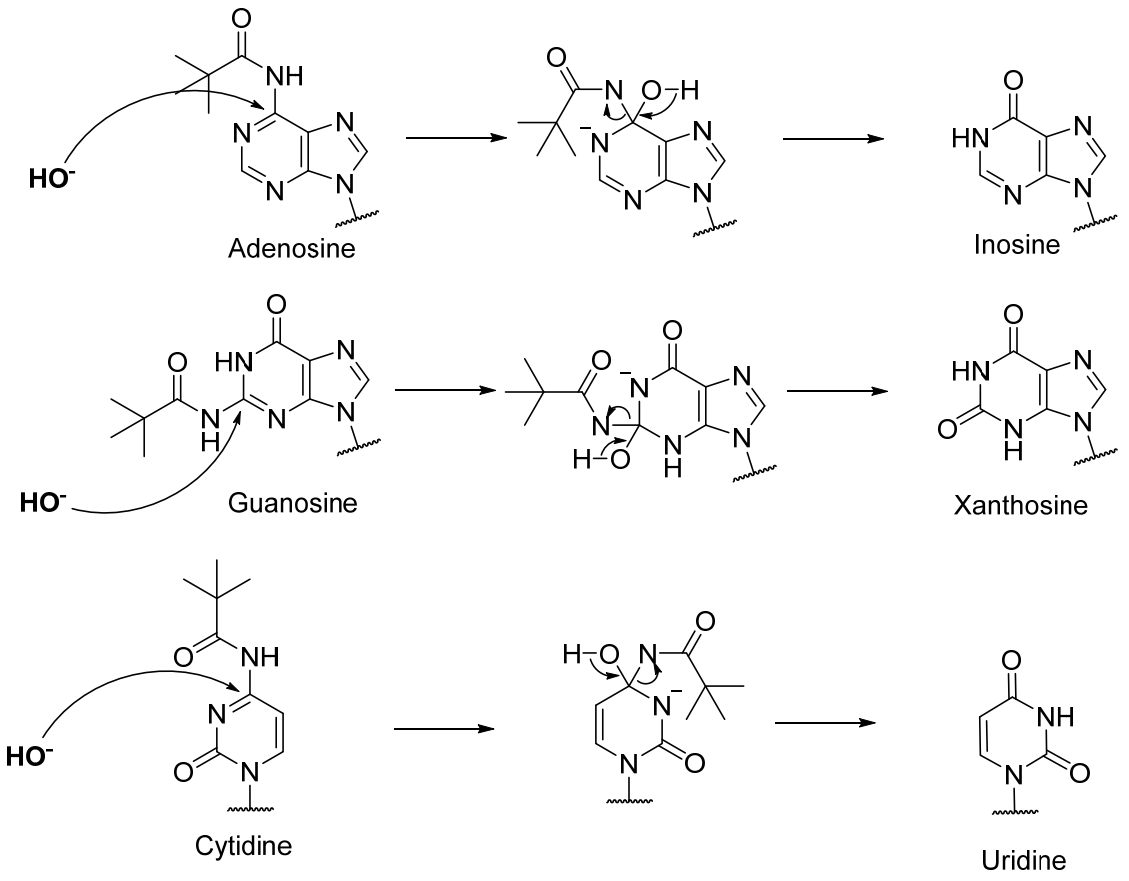


Figure 3.11: Proposed attack mechanism of hydroxide anion on the 2'-deoxynucleobase (adenosine, guanosine and cytidine) instead of the pivalamide protecting group converting them into inosine xanthosine and uridine respectively.

In order to carefully study these conversions, relative to removal of the pivaloyl group using ammonium hydroxide, a RP-HPLC method was developed for identifying the exact retention time for each product and modification. Using this system, a co-injection of 100 µL solution containing 1 mg/mL of: 2'-deoxyadenosine, 2'-deoxyinosine, 2'-deoxyguanosine, 2'-deoxycytidine and 2'-deoxyuridine was used as a standard. Elution conditions were 1 mL/min with a gradient of acetonitrile/50 mM triethylammoniumbicarbonate buffer, pH 8.5, starting with 100% buffer for the first 30 minutes, followed by increasing the acetonitrile to 100% within 10 minutes and then back to 100% buffer within 30 minutes. A 1 µg/ml detection limit was validated by co-injection

of 1 mg/ml 2'-deoxyadenosine with 1 µg/ml 2'-deoxyinosine and 1mg/ml 2'-deoxycytidine with 1µg/ml 2'-deoxyuridine (**figure 3.12**).

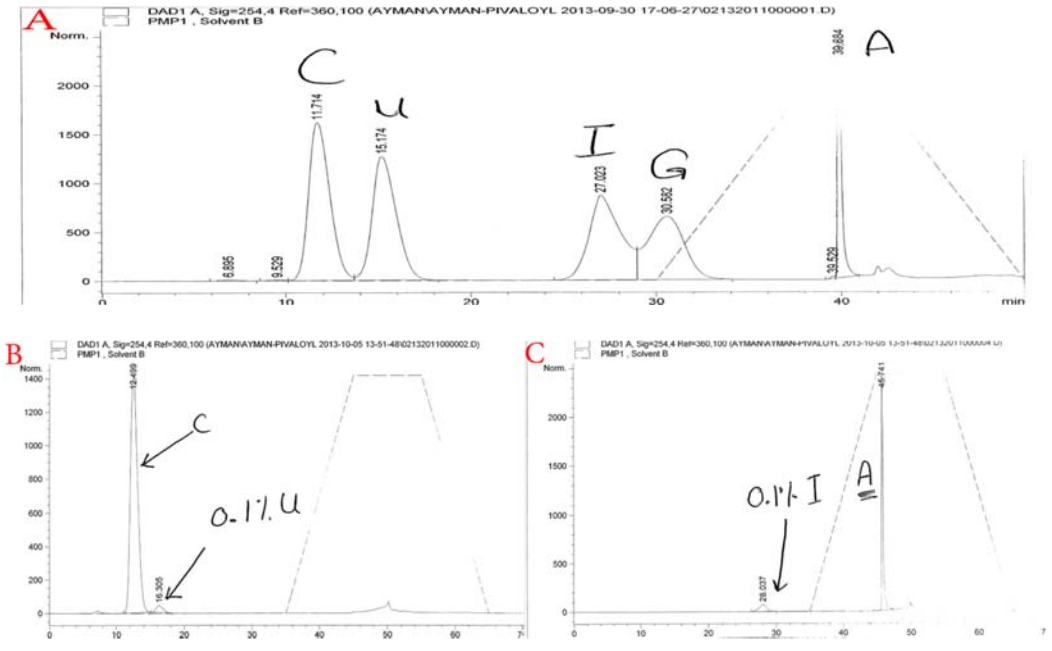


Figure 3.12: Part A: RP-HPLC profile for co-injection of 1 mg/mL of: 2' deoxyadenosine (A), 2'-deoxyinosine (I), 2'-deoxyguanosine (G), 2'-deoxycytidine (C) and 2'-deoxyuridine (U); Part B: RP-HPLC profile for co-injection of 1 mg/mL 2'-deoxycytidine (C) with 1 µg/mL 2'-deoxyuridine (U); Part C: RP-HPLC profile for co-injection of 1 mg/mL 2'-deoxyadenosine (A) with 1 µg/mL 2'-deoxyinosine (I).

The N-pivaloyl protected compounds were incubated with aqueous ammonia for 16 hours at 55 °C, the ammonia was evaporated to complete dryness. Stock solutions at concentration 5 mg/ mL of each crude reaction mixture was prepared and injected onto the HPLC. Although the analysis were carried out at 5 times the amount used for method development, the results demonstrated that the undesirable side products were observed at less than the 0.01% detection limit used during the method development (**figure 3.13**).

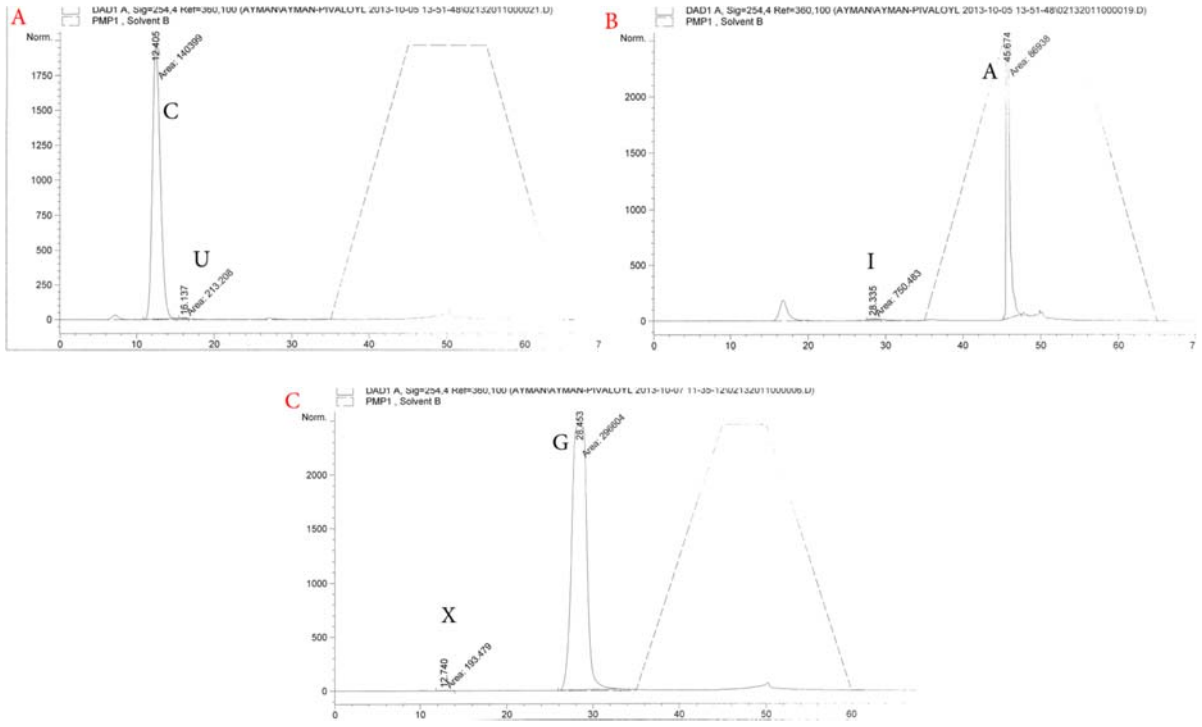


Figure 3.13: RP-HPLC profiles (A, B and C) for the crude mixtures of 2'-deoxycytidine (C), 2'-deoxyadenosine (A) and 2'-deoxyguanosine (G) respectively after incubating with aqueous ammonia for 16 hours at 55 °C inorder to detect the undesired 2'-deoxyuridine(U) 2'-deoxyinosine (I) 2'-deoxyxanthosine (X).

In order to study the resistance of the pivaloyl protected 2'-deoxynucleobases towards reduction with $BH_3$, 100 mg of each protected 2'-deoxynucleoside was stirred with 20 ml of 0.25 M $BH_3$ in THF for 15 minutes. The reaction mixtures were cooled to 0 °C, 20 ml of methanol was added dropwise to each sample and the solutions were evaporated to complete dryness using rotary evaporator. These samples were then analyzed by mass spectrometry and $^1$H-NMR in order to see if any new products had formed. Neither analysis by $^1$H-NMR nor the mass spectrometry showed any sign of the formation of reduced products.

### 3.7 Limitations on the Removal of Pivaloyl Group from Aminoboranephosphonate Protected 2'-Deoxyoligonucleotides

Following the synthesis of several 2'-deoxythymidine oligonucleotides having different numbers of modifications, we noticed an increase in the percentage of side products generated through cleavage of internucleotide linkages. Additionally, pivalamide boranephosphonate internucleotide linkages were detected by mass spectrometry even after extensive treatment with ammonium hydroxide. For example, with ODN10 (Table 3.1) where it was incubated twice with aqueous ammonia at 55 °C for 16 hours each time in order to achieve a higher percentage of deprotected product, a significant amount pivalamide boranephosphonate product was still present. Therefore, a new protecting group strategy was required in order to maintain the nucleobase nitrogens unreactive during solid phase synthesis and also capable of complete removal from the internucleotide linkages. A separate chapter will discuss the different types of protecting groups that have been used to achieve this goal.

# CHAPTER 4

# SYNTHESIS OF PHOSPHORAMIDIMIDATE DNA USING AMIDE BASED PROTECTING GROUP

## 4.1 Introduction

Natural DNA is a highly negatively charged molecule at biological pH; thus, it is repelled by negatively charged cellular membranes and subject to inefficient intracellular uptake. This prompted the development of a large number of synthetic analogs of natural DNA by changing phosphorous constituents, such as phosphorothioates, methylphosphonates, and boranephosphonates or by replacing the ribose ring, not only to enhance cellular uptake but also to decrease nuclease degradations.

Another approach to overcome the DNA negative charge is to conjugate a cationic group to either the 3' or 5' termini of oligonucleotides. My research focuses on developing an alternative approach for introducing a positive charge into a DNA oligonucleotide and therefore reduce the inherent negative charge. The objective was to prepare a novel self-neutralizing positively charged phosphoramidimidate internucleotide linkage. Previous work in our lab was able to synthesize dinucleotide compounds containing aliphatic and aromatic substituted phosphoramidimidate linkage (**compounds 24a and 24b figure 4.1**).[41,42] However, these compounds were not compatible with solid phase DNA synthesis cycles and neither our lab nor any other research group was able to synthesize longer 2'-deoxyoligonucleotides containing phosphoramidimidate internucleotide modification.

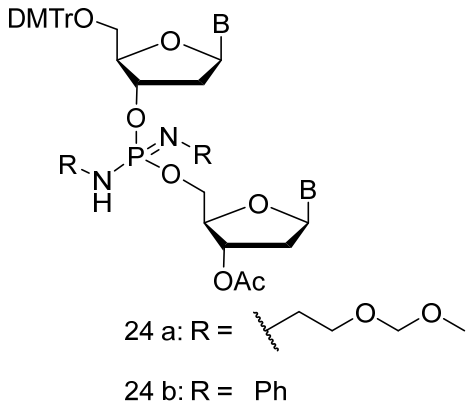


Figure 4.1: Structure of previously synthesized compounds containing phosphoramidimidate linkage; B: nucleobases: adenine (A), cytosine (C), guanine (G) or thymine (T).

This chapter will discuss several attempts to synthesize 2'-deoxyoligonucleotides containing phosphoramidimidate internucleotide linkages through different approaches.

## 4.2 Conversion of Phosphoramidimidate into Aminoboranephosphonate

Boranephosphonate showed an interesting conversion using iodine as oxidizing reagent in the presence of nucleophile, this conversion is well known in our lab and several nucleophiles have been used.[29] Thus in the approach outlined in this chapter I propose converting an aminoboranephosphonate to phosphoramidimidate using iodine in the presence of anhydrous ammonia (**figure 4.2**).

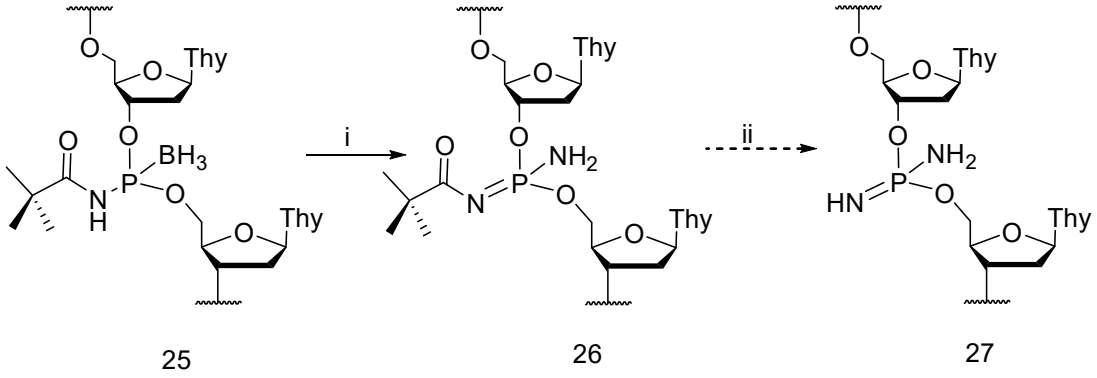


**Figure 4.2: Scheme shows the conversion of aminoboranephosphonate DNA into phosphoramidimidate DNA using iodine and anhydrous ammonia**; (i) 0.02 M iodine/ 0.5 $NH_3$ in dioxane, 6 hours; (ii) base: Several bases have been used; Thy: 1-thymidyl.

This conversion reaction was first tested on a thymidine dinucleotide with an aminoboranephosphonate linkage, then using $T_{21}$ 2'-deoxyoligonucleotides containing 4 pivaloylaminoboranephosphonate internucleotide linkage (**figure 4.3**).

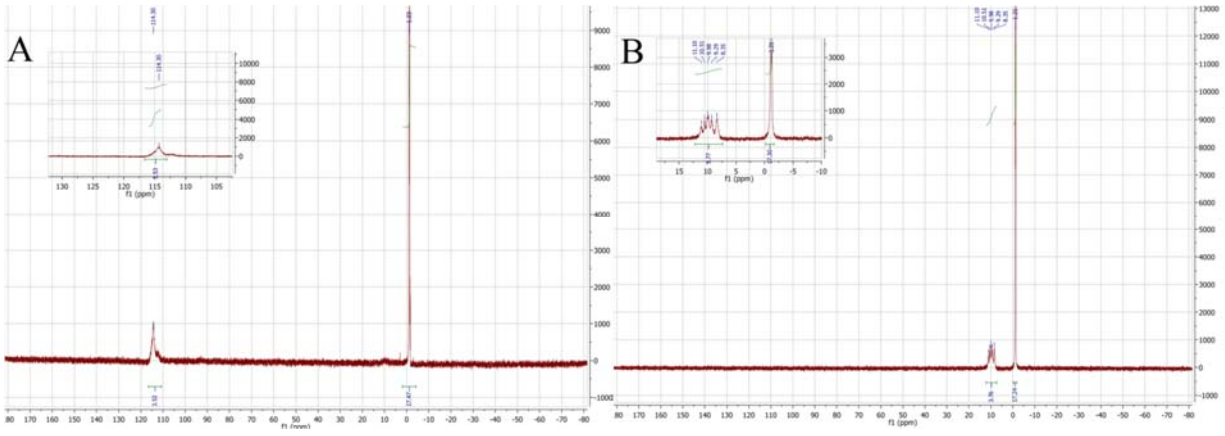


**Figure 4.3: $^{31}$P NMR spectrum for purified $T_{21}$**; A) $^{31}$P NMR spectrum for purified $T_{21}$ containing four pivaloylaminoboranephosphonate internucleotide linkages, the peaks at -1 ppm correspond to phosphate, the broad peak at 114 ppm corresponds to protected aminoboranephosphonate; B) $^{31}$P NMR spectrum for purified $T_{21}$ containing four phosphoramidimidate internucleotide linkages, the peaks at -1 ppm correspond to phosphate, the peaks at 10 ppm correspond to protected aminoboranephosphonate; ODN1 in spectrum A was converted into ODN2 shown in B using 0.02 M iodine/ 0.5 $NH_3$ in dioxane, 6 hours; Sequence : 5'-DMT-d(T*TT*TTTTTTTTTTTTT*TT*TT), *: modification.

As shown in figure 4.3, part A shows the $^{31}P$ NMR spectrum for purified $T_{21}$ containing four pivaloylaminoboranephosphonate internucleotide linkages which were converted into the 2'-deoxyoligonucleotide pivaloylphosphoramidimidate shown in part B using 0.02 M iodine/ 0.5 NH3 in dioxane (6 hours). This result was also confirmed by mass spectrometry (**figure 4.4**).

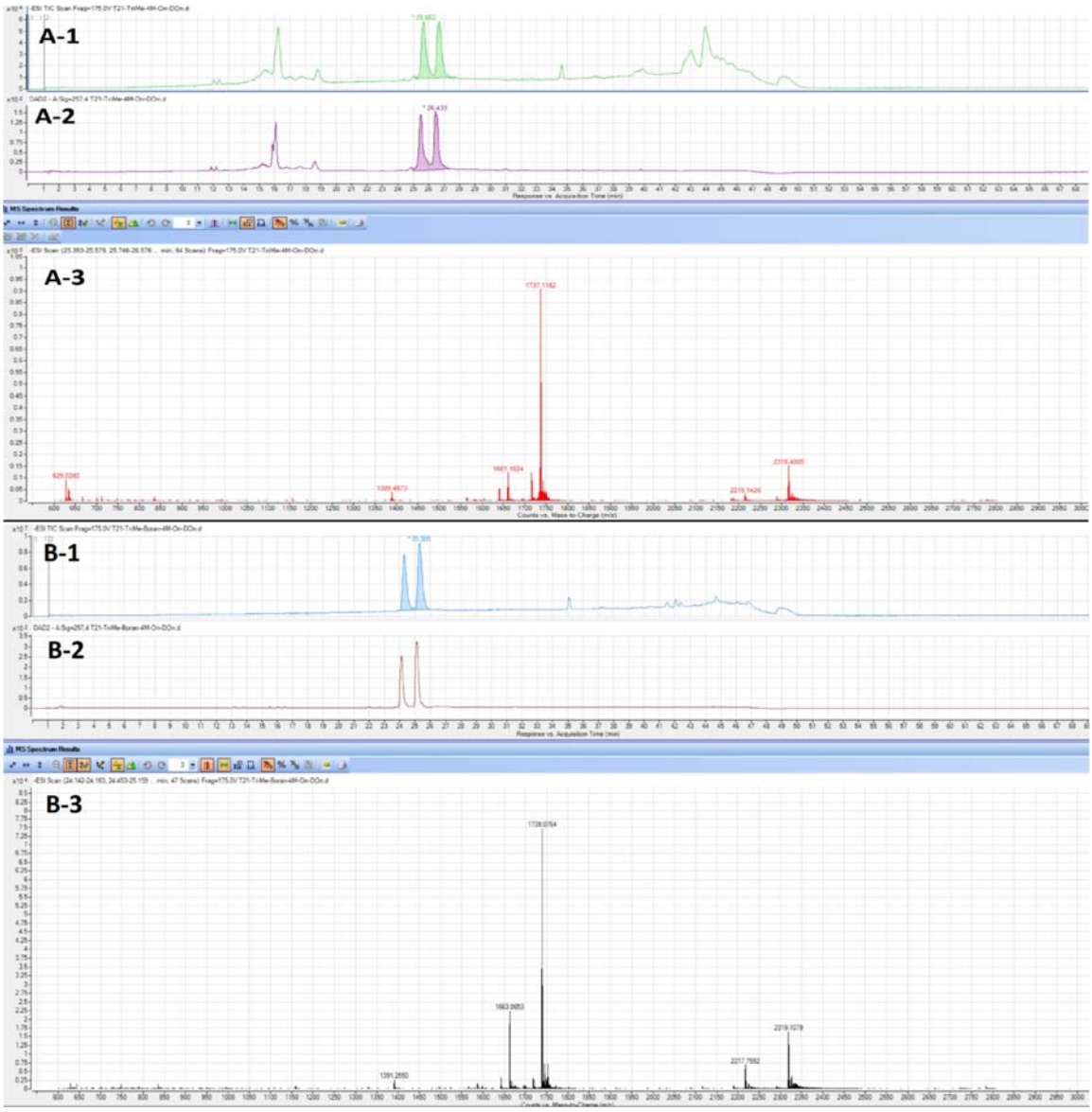


Figure 4.4: LC-UV/MS for the crude 2'-deoxyoligonucleotide 5'-DMT-d(T*TT*TTTTTTTTTTTTT*TT*TT) $[M-4H]^{-4}$: 1737.1162 (A-1, A-2, A-3) and the same purified 2'-deoxyoligonucleotide after iodine oxidation using 0.02 M iodine/ 0.5 $NH_3$ in dioxane $[M-4H]^{-4}$: 1739.0764 (B-1, B-2, B-3). A-1/B-1: total ion chromatogram. A-2/B-2: UV absorbance chromatogram. A-3/B-3: extracted ion chromatogram of the main peak in A-1/B-1 at selected time, 25-27 minutes in A-1 and 24-26 minutes in B-1.

Several deprotection procedures were evaluated for removal of the pivaloyl group from the phosphoramidimidate. These included varying the basic conditions, time, temperature and hydrous versus anhydrous conditions. The specific reagents and conditions included: aqueous ammonia, anhydrous ammonia in dioxane, 1:1 anhydrous ammonia/ toluene, 1:1 anhydrous ammonia/ ethylenediamine, 1:1 ethylenediamine/toluene, aqueous ammonia with 10% ethylene diamine, DBU, aqueous ammonia with 10% 2-pyrrolidone, aqueous ammonia with 10% pyrrolidine and aqueous ammonia with 10% ethylenediamine. Unfortunately, all these reagents were either too strong and degraded the oligonucleotide or too weak and not able to completely remove the pivaloyl group. Thus a new protecting group was proposed in order to synthesize 2-deoxyoligonucleotides containing the unprotected phosphoramidimidate.

### 4.3 (3,3′-Iminodipropionitrile) as New Amine Protecting Group

The cyanoethyl group is routinely used in DNA synthesis to protect the non-bonding oxygen of the phosphate triester intermediate during synthesis and it is removed with base at the end of the synthesis. Deprotection starts where a base removes the acidic β-proton. This initiates an elimination mechanism (**figure 4.5 A**). I chose to use the same strategy in a first attempt to synthesize the phosphoramidimidate linkage. The approach started with two β-cyanoethyl groups attached to an internucleotide nitrogen. Following synthesis, these protecting groups would be removed using base (**figure 4.5 B**).

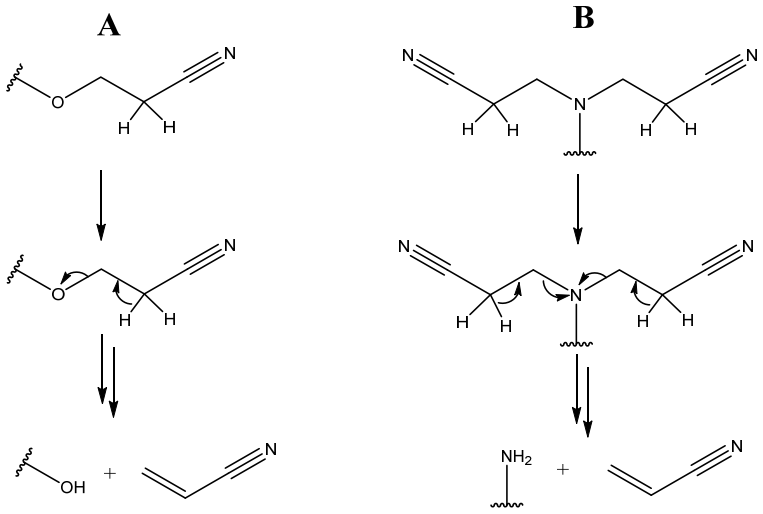


Figure 4.5: Deprotection mechanism of the cyanoethyl protecting group employed to protect phosphate triester group in phosphoramidite oligonucleotide synthesis (A) and the proposed amino deprotection mechanism (B) using the same strategy.

The same synthetic procedure previously used to prepare the morpholine derivative as outlined in chapter 3 was applied here where morpholine was replaced by 3,3′-iminodipropionitrile

(**figure 4.6**). This new compound has been confirmed by $^{1}H$, $^{31}P$ and mass spectroscopy (see experimental section).

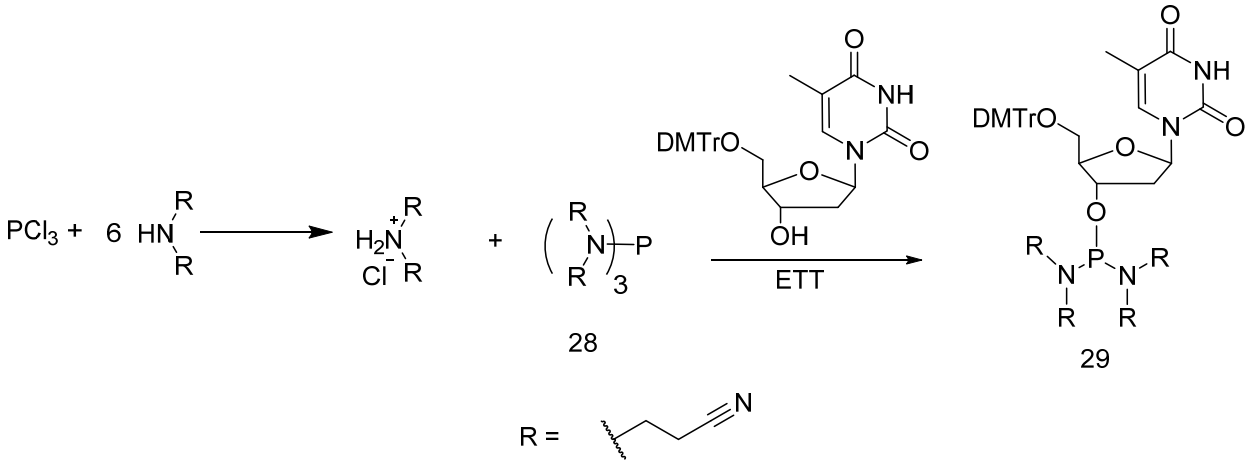


Figure 4.6: Synthesis scheme for preparing 5'- DMT-3'-(di-(N,N-3,3′-diiminodipropionitrile)phosphaneyl)-2'-deoxy thymidine (29).

The synthesis begins by reacting $PCl_3$ with 6.2 equivalents of 3,3′-diiminodipropionitrile in order to prepare tri(3,3′-diiminodipropionitrile)phosphite (**28**). The product of this reaction (**28**) was condensed with 5'-O-dimethoxytrityl-2'-deoxythymidine in DCM using ETT as activator to generate (**29**) in 72% yield following column chromatography. Characterization by mass spectrometry and $^{31}P$ NMR confirmed the synthesis.

The next step was to examine the coupling efficiency of compound (**29**). It was reacted with 3'-O-acetylthymidine in acetonitrile using 0.9 equivalents of ETT as activator. The reaction as monitored by TLC and $^{31}P$ NMR, was completed within 4 hours. The synthon (**29**) was next used in conjugation with the standard phosphoramidite synthons and the same solid phase synthesis cycle as outlined in chapter 3 figure 3-3. Unfortunately, the synthon (**29**) was quite unreactive relative to oligonucleotide synthesis and generated primarily failure sequences.

Reflections on the activation process for standard phosphoramidite chemistry suggests a possible synthesis pathway for preparing the phosphoramidimidate internucleotide linkage. The initial step in the standard process is activation by protonation of the diisopropylamino group. This process generates a good leaving group, diisopropylammonium, which is replaced by the anionic activator. This mechanism explains why we generated many failure sequences. With a diamidite compound having two strong bases, initial activation leads to the amidite dinucleotide. Further reaction of the nucleophile with the amidite leads to degradation.

In conclusion, both 3,3′-iminodipropionitrile and the dimethyl amine are stronger aliphatic bases relative to pivalamide and appeared to lead to cleavage products. Thus, I chose to move in the direction of using protected amide phosphoramidites as synthons.

## 4.4 A New Amino protected Phosphoramidite Synthon

Based on the phosphoramidite mechanism, as explained in the previous section, a new synthesis approach could involve using an amide protected diamidite. Following condensation, the amide protected internucleotide linkage is only weakly basic and therefore not easily protonated by activator. Therefore internucleotide cleavage would be less likely. However, with a bulky amide protecting group such as pivaloyl as outlined in the synthesis of aminoboranephosphonate DNA, difficulties in removal of the pivaloyl precludes its use for synthesis of the phosphoramidimidate linkage. These observations led to investigations of several amide derivatives (**Figure 4.7**). These were tested for compatibility with solid phase phosphoramidite chemistry and for relative removal of the amide with base following synthesis.

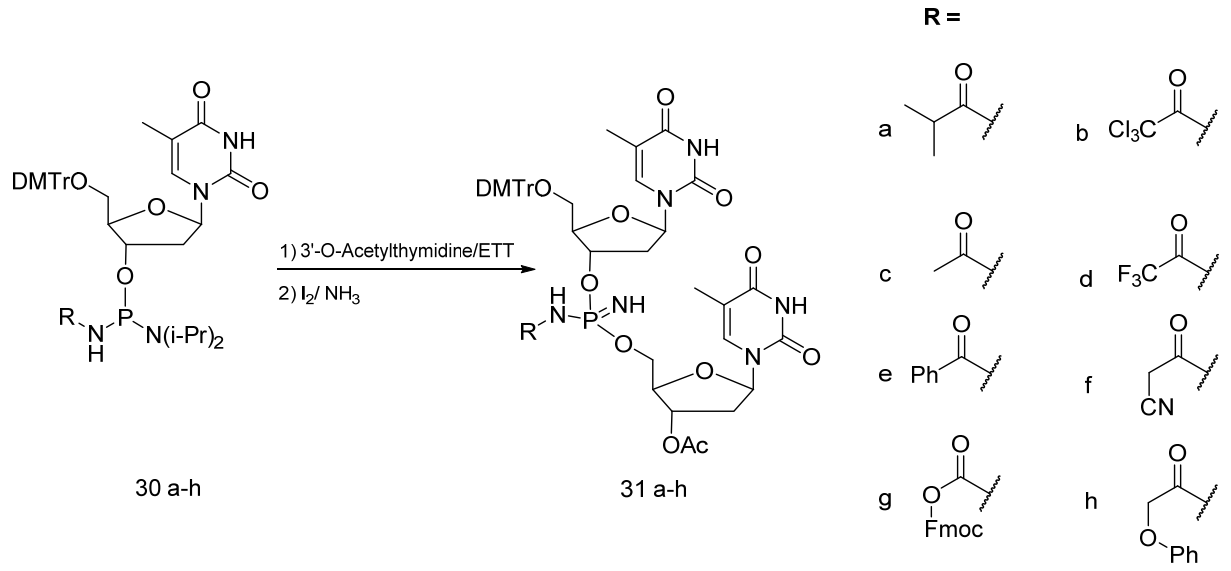


**Figure 4.7: Protecting groups used as test derivatives for synthesis of phosphoramidimidate DNA**.

Derivatives where the steric bulk of the amide was reduced from the pivaloyl to isopropyl or acetyl showed improved deprotection of the amide with base but the difference was not sufficient to completely deprotect the amide from the

phosphoramidimidate internucleotide linkage. Increasing carbonyl electrophilicity by adding α-halogen atoms to the amide protecting group decreased the stability of the phosphoramidite and caused significant decomposition of the products during silica column purification (60-80%). Similar results were obtained irrespective of the base used for deprotection such as methyl amine, 1,8-diazabicyclo[5.4.0]undec-7-ene (DBU), ethylenediamine or tert-butyl hydroperoxide.

This approach, where various amide protection strategies were examined, was next extended to include the cyanoacetamide, fluorenylmethyloxycarbonyl (fmoc) and phenoxyacetyl derivatives. Significant success was obtained with the cyanoacetamide and especially the phenoxyacetyl derivative. The results using cyanoacetamide protection follow in significant detail. Chapter 5 outlines results with the phenoxyacetyl derivative.

## 4.5 A New Cyanoacetamide Protecting Group

A new protecting group, cyanoacetamide, was investigated whereby the carbonyl electrophilicity was increased through base catalyzed α- hydrogen deprotonation (**Figure 4.8**). Two routes would produce the desired phosphoramidimidate. The first is α- hydrogen deprotonation with base followed by nucleophilic attack on the carbonyl and elimination to produce the phosphoramidimidate and cyanoacetamide. The second route involves α- hydrogen deprotonation with base followed by rearrangement which generates the unprotected phosphoramidimidate and 1-cyano ketene.

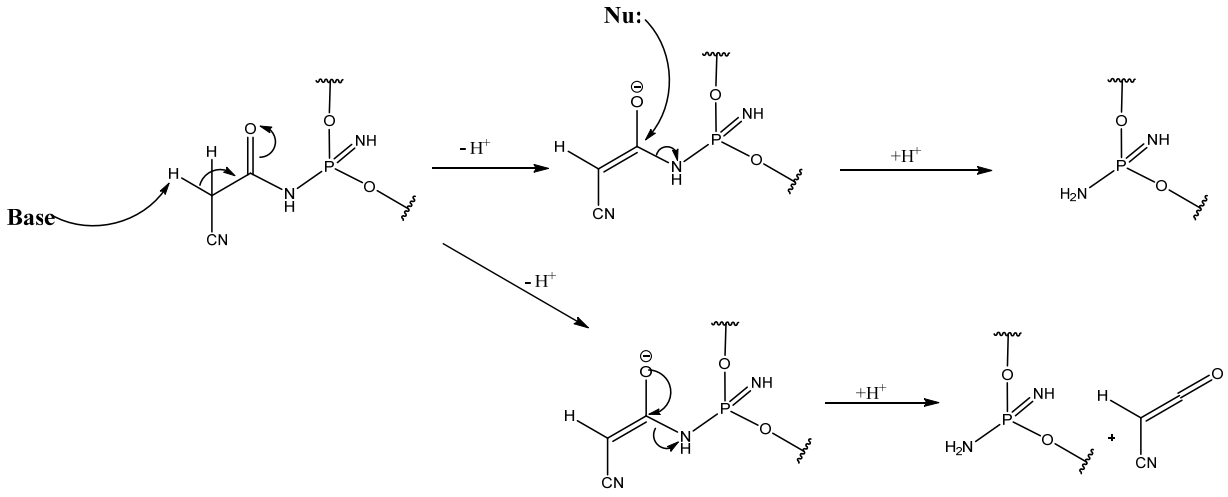


**Figure 4.8: A proposed deprotection strategy with cyanoacetamide**.

## 4.6 Cyanoacetamide Protecting Group Validation

As a first step toward validation of cyanoacetamide protection, thymidine dinucleotides having either a phosphoramidimidate or aminoboranephosphonate linkage were synthesized. The synthesis schemes are outlined in (**figure 4.9**).

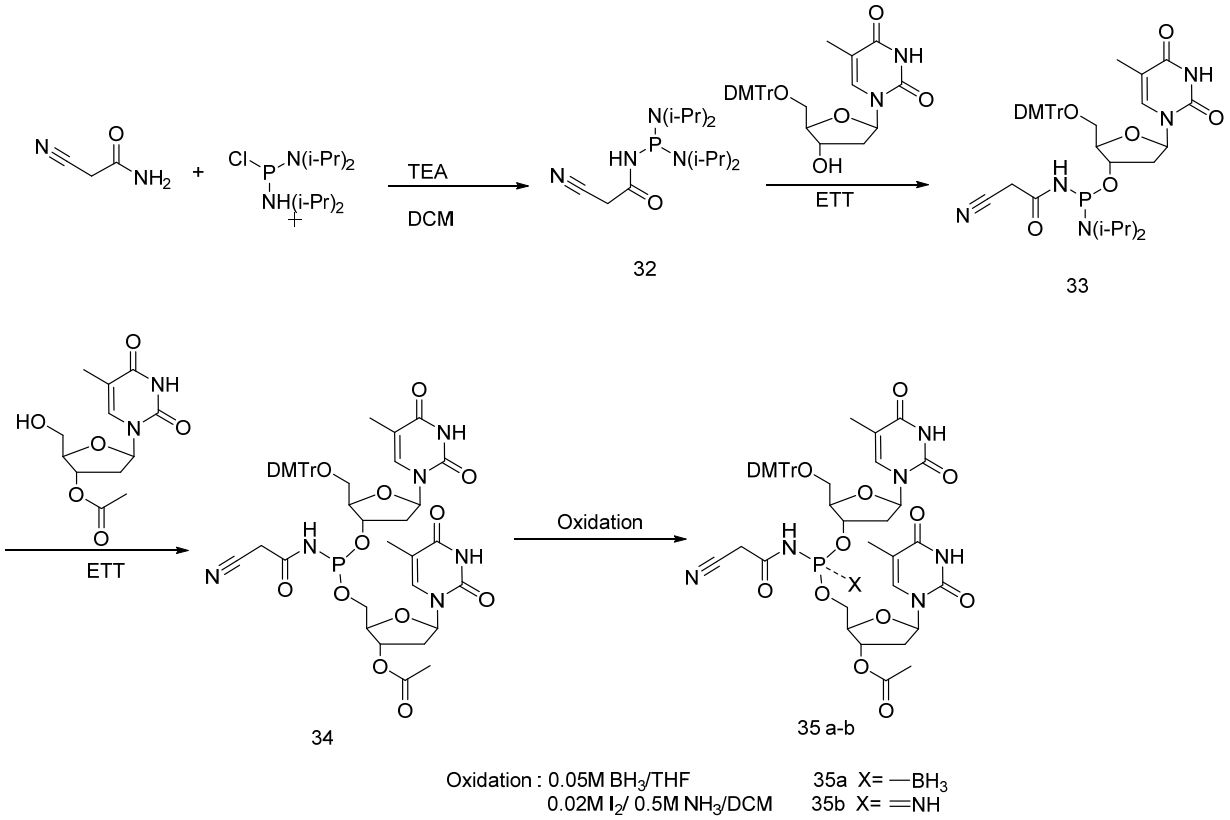


**Figure 4.9 Synthesis scheme used to prepare dithymidine phosphoramidimidate and aminoboranephosphonate DNA**.

Synthesis of bis(diisopropylamino)cyanoacetamidophosphane (**32**) was completed by condensing cyanoacetamide with bis(diisopropylamino) chlorophosphine in 74% yield. Compound (**32**) was then condensed with 5'-O-dimethothytrityl-2'-deoxythymidine in the presence of ETT to yield (**33**) in 86% yield. The next step was condensation of (**33**) with 3'-O-acetylthymidine to yield the dinucleotide (**34**) in 82%

yield. Finally this phosphoramidite was oxidized with either 0.05M $BH_3$/THF or 0.02M $I_2$ / 0.25M $NH_3$ / dioxane to yield the cyanoacetamide protected aminoboranephosphonate (**35a**, 88% yield) or the phosphoramidimidate (**35b**, 92% yield) respectively. In order to test the use of these intermediate linkages relative to the deprotection steps used for oligonucleotide synthesis on solid support, each was exposed to the following reagents:

1. Cap mixture A: 10% Acetic Anhydride, 10% Pyridine, 80% THF.
2. Cap mixture B: 1-Methylimidazole in THF.
3. Tert-butyl peroxide solution: 0.5 M in DCM
4. 3% Trichloroacetic acid in dichloromethane
5. Aqueous ammonium hydroxide.

In each experiment 50 mg of the compound was added to a NMR tube, the reagent was added and $^{31}P$ NMR was carried out over 12 hours in order to examine if there was degradation of starting materials, formation of new product peaks, or if the intensity of the main starting material sample decreased. Cap mixture A, cap mixture B and *tert*-butyl peroxide were satisfactory and did not affect the quality of dinucleotide (either the aminoboranephosphonate (**35a**) or phosphoramidimidate (**35b**)).

The thymidine phosphoramidimidate dimer (**35b**), was also treated with aqueous ammonium hydroxide solution (30%, 16 hours) in order to remove the cyanoacetamide and 3'-O-acetyl protecting groups. Under these conditions, 87% deprotection of the amide was observed despite the low solubility of the 5'-DMT protected dimer (**Figure 4.10**). Thus the amount of deprotection with aqueous ammonia under these conditions exceeds the amount observed with the pivaloyl

derivative (55-70%). The $^{31}P$ NMR in figure 4.10 shows approximately 87% conversion of the protected amide to the phosphoramidimidate. The peak at 21 ppm corresponds to protected phosphoramidimidate and the peak at 17 ppm corresponds to unprotected phosphoramidimidate.

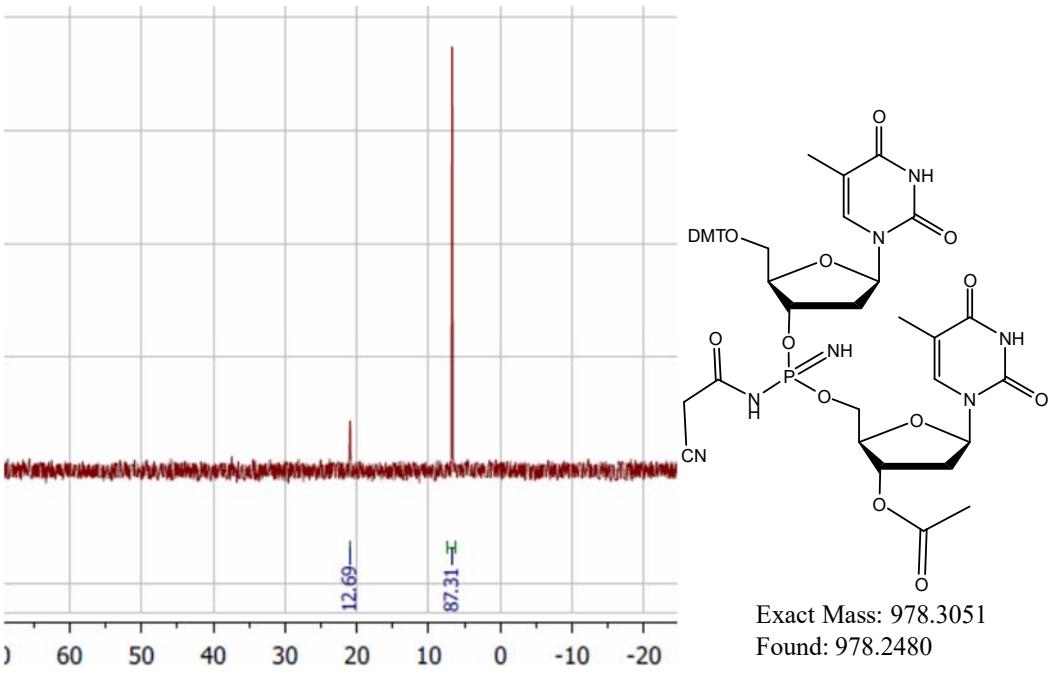


**Figure 4.10: $^{31}P$ NMR showing the deprotection phosphoramidimidate in aqueous ammonium hydroxide solution** (30%, 16 hours). the peak at 21 ppm corresponds to protected phosphoramidimidate, the peak at 17 ppm corresponds to unprotected phosphoramidimidate.

These results encouraged us to examine the acid stability of the cyanoacetamide protected phosphoramidimidate and the deprotected phosphoramidimidate (**Figure 4.11**).

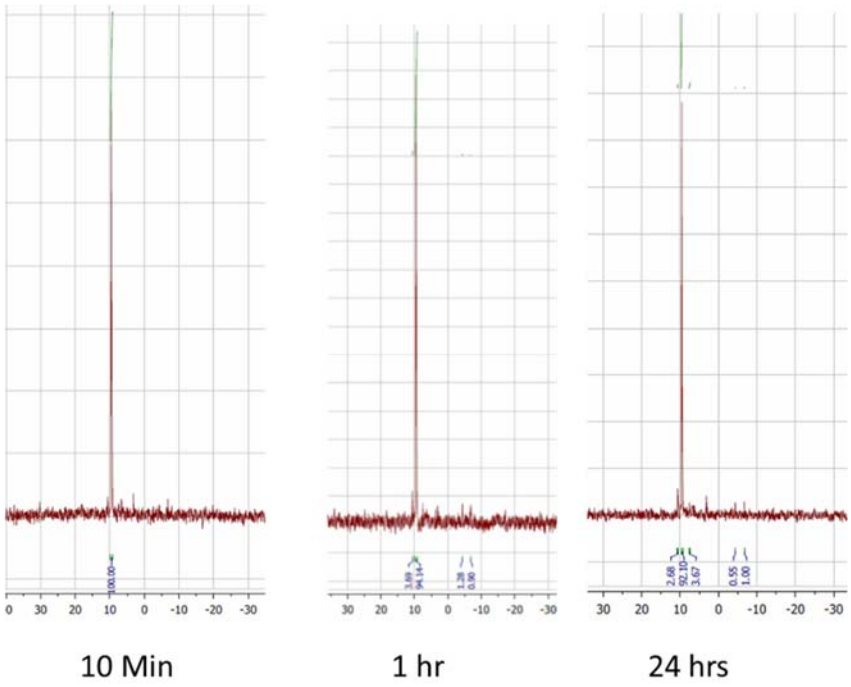


**Figure 4.11: $^{31}$P NMR showing the decomposition of compound 35b** containing the phosphoramidimidate internucleotide linkage protected with the cyanoacetyl group at 10 minutes, 1 hour and 24 hours time points using 3% trichloroacetic acid in dichloromethane. The main peak at 10.1 ppm corresponds to protected phosphoramidimidate and the small peaks that appear at (-7.7, -4.13, 3.3 and 10.93 ppm) represent degradation side products.

The $^{31}$P NMR in figure 4.11 showing the decomposition of compound (**35b**) containing the phosphoramidimidate internucleotide linkage protected with the cyanoacetyl group at 10 minutes, 1 hour and 24 hours time points using 3% trichloroacetic acid in dichloromethane. The main peak at 10.1 ppm corresponds to protected phosphoramidimidate and the small peaks that appear at (-7.7, -4.13, 3.3 and 10.93 ppm) represent degradation side products. Treating the cyanoacetamide protected phosphoramidimidate with 3% trichloroacetic acid in DCM for 24 hours generated less than 10% decomposition. This result is quite encouraging as the cyanoacetamide protected phosphoramidimidate would be the derivative that is present throughout multiple synthesis cycles on a solid support. Moreover and because treatment during

each cycle for removal of the dimethoxytrityl group is 90 seconds, this result means that an oligomer with 21 units in length could be prepared without significant loss of product.

### 4.7 Solid Phase Synthesis of Phosphoramidimidate DNA Using Cyanoacetamide Protection

DNA containing phosphoramidimidate internucleotide linkages at variable positions were synthesized on a solid support. Initially, oligonucleotides 10 in length and containing only thymidine were prepared. One modification was introduced per oligonucleotide and one variable was examined per synthesis (i.e: condensation time, monomer concentration, oxidizing reagent, activator used, detritylation and capping reagents). Initially, the modification was introduced at the 5'-end internucleotide linkage so as to minimize exposure the phosphoramidimidate linkage to the different reagents used during the solid phase synthesis cycle. Additionally, all oligonucleotides were prepared with the 5'-DMT protecting group. In this way the product oligonucleotide can be purified by RP-HPLC from failure sequences. This procedure therefore provides a more complete image of the synthesis and coupling efficiencies. Because these results were encouraging, oligothymidines having two modifications at variable positions were synthesized, purity was checked using RP-HPLC and the products were characterized by $^{31}$P NMR and mass spectrometry.

Based upon the investigation outlined earlier in this chapter, the following modifications were introduced to the standard synthesis cycle:

1) Condensation Step: The concentration of cyanoacetamide synthon (**33**) was increased from 0.1M to 0.15 M in order to increase coupling efficiency and therefore reduce the amount of failure sequences. Further reduction in failure sequences was also observed when ETT was used as activator and the condensation time was extended to 15 minutes.
2) Iodine / Ammonia Oxidation: A 0.5 M anhydrous ammonia solution in dioxane dissolved in DCM (final concentration of 0.2 M $NH_3$) was used in the presence 0.05 g of iodine (final concentration 0.02 M of iodine). In order to convert the cyanoacetamide phosphoramidite internucleotide linkage to the protected phosphoramidimidate, the oxidizing solution was loaded to the column for 15 seconds and then 240 seconds of wait time was used for oxidation. This solution was removed with argon (10 seconds). The column was next exposed to a second cycle of oxidizing solution (120 seconds).

All the remaining synthesis steps for addition of the phosphoramidimidate linkage (capping and detritylation) were unchanged relative to the standard cycle. Similarly, the addition of unmodified nucleotides was completed without modifying the standard cycle. Once a synthesis was completed, the product was cleaved from the solid support and the protecting groups, cyanoethyl and cyanoacetyl, were removed simultaneously using 30% aqueous ammonia and 10% ethylenediamine at 55 °C for 24 hours. Portions of the crude synthesis mixtures were then injected to RP-HPLC in order to evaluate the synthesis. Figure 4.8 shows some of the HPLC profiles for

various successful syntheses of 2'-deoxyoligonuclotides containing variable numbers of phosphoramidimidate internucleotide linkages.

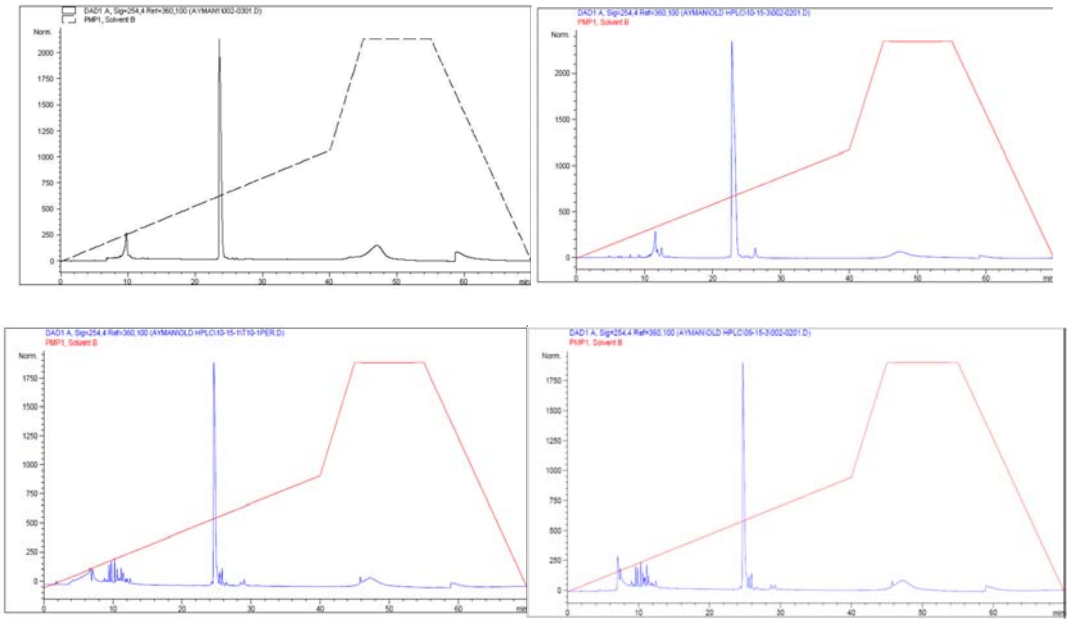

**Figure 4.12: RP-HPLC profiles (B-D) of crude reaction mixtures as obtained from the modified solid phase DNA synthesis cycle outlined in section 4.7**. The profile in A represents the total crude reaction mixture as obtained using the standard synthesis cycle for the preparation of an unmodified 2'-deoxyoligonuclotide. The targeted product peaks appear at retention time 24 and failure sequences at 10-14 minutes. Sequences: A) 5' DMT-TTTTTTTTTTTTTTTTTTTT. B) 5'-DMT-TTTTTTTTTTTTTTTTTTT*T. C) 5'-DMT-TTTTTT*TTTT. D) 5'-DMT-TTTTTT*TTTT. * = phosphoramidimidate.

## 4.8 Limitations of the Cyanoacetamide Protecting Group Approach

The basic deprotection procedure that was used to remove the cyanoacetamide protecting group and also to cleave the oligonucleotides from the solid support was aqueous ammonia containing 10% ethylenediamine at 55 °C for 24 hours. When this procedure was used with oligomers having one or two phosphoramidimidate internucleotide linkages, satisfactory results were obtained; however, when the number of modifications increased beyond two, a noticeable side product was observed where new mass adducts were observed by mass spectrometry. The acquired $^{31}P$ NMR spectrum for the oligomers demonstrated that complete deprotection of the phosphoramidimidate had occurred but the mass spectrometry showed these oligomers retained a cyanoacetamide linkage. This observation suggests that a side reaction occurred during the base deprotection. (**Figure 4.13**). The LCMS profile mass analysis of $T_{15}$ containing three phosphoramidimidate internucleotide linkages and 5'-O protected with DMT showed a mass analysis peak at 1598.9839 which corresponds to the oligonucleotide where all three phosphoramidimidate linkages have been deprotected and in ionization state -3. The peaks at 1627.3311, 1649.6595 and 1671.3365 correspond to 2, 1 and 0 of the phosphoramidimidate linkages having been deprotected respectively and all are in ionization state -3.

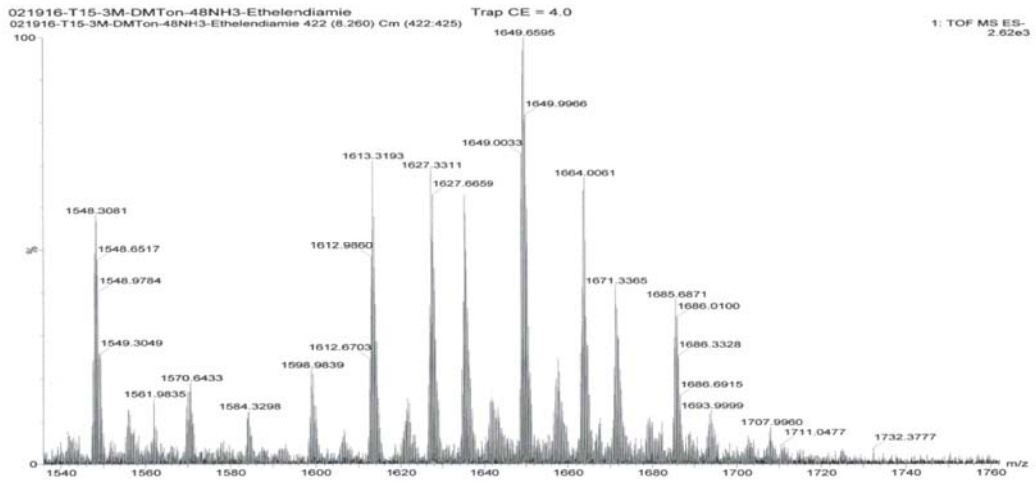


Figure 4.13: LCMS analysis of $T_{15}$ containing three phosphoramidimidate internucleotide linkages and 5'-O protected with DMT. The mass analysis peak at 1598.9839 corresponds to the oligonucleotide where all three phosphoramidimidate linkages have been deprotected and in ionization state -3. The peaks at 1627.3311, 1649.6595 and 1671.3365 correspond to 2,1 and 0 of the phosphoramidimidate linkages have been deprotected respectively and all are in ionization state -3.

One proposed mechanism for generating this unexpected side-product is shown in figure 5-14. Here a ketene, as generated during cleavage of the cyanoacetamide protecting group (see figure 5-8), reacts with the thymidine nucleobase to generate a cyanoacetamide presumably linked to N-3 of the thymidine base. This side product has been reported when cyanoethyl is used to protect a phosphate triester during oligonucleotide synthesis.[43]

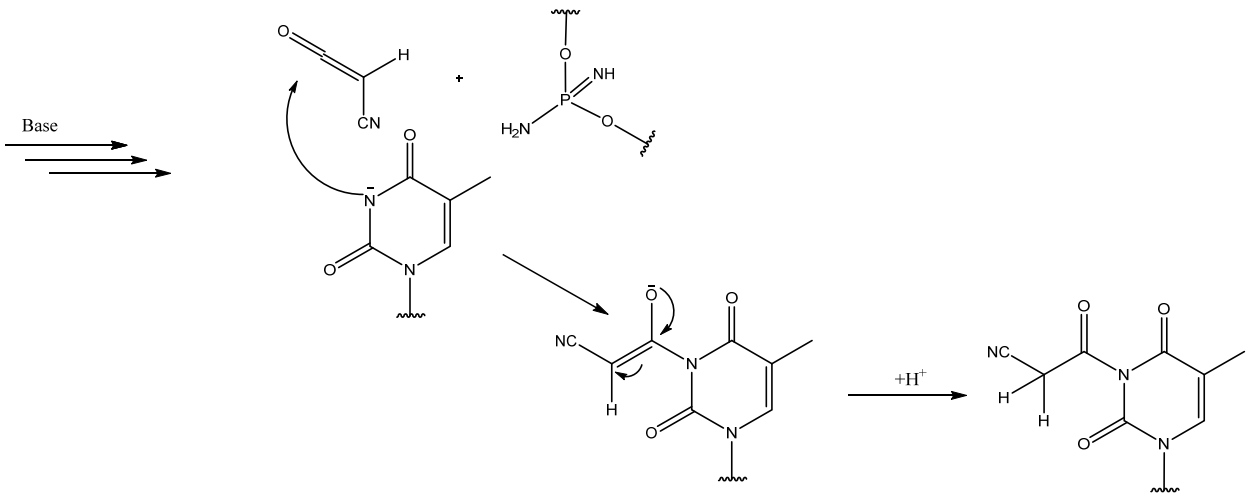


Figure 4.14: Proposed mechanism for the cyanoacetamide side reaction with thymidine during base treatment.

This cyanoacetamide side reaction encouraged us to find an alternative nitrogen protecting group which shares the same deprotecting activation through α-H initiation. Thus, phenoxyacetamide was chosen and studied as outlined in the next chapter.

# CHAPTER 5

# SYNTHESIS AND BIOCHEMICAL ACTIVITY OF PHOSPHORAMIDIMIDATE DNA USING PHENOXYACETYL PROTECTION

## 5.1 Introduction

Despite the formation of adducts when the cyanoacetamide protecting group was used to synthesize phosphoramidimidate DNA, the successful synthesis of this analogue encouraged us to look for alternative protecting groups that utilize the same amide protection principle but generate fewer side products. Initial results with pivaloyl, isopropyl, and acetyl showed that these carbonyls were not electrophilic enough to be deprotected using mild bases without breaking the DNA backbone. Consequently, in order to further develop the approach whereby the amine attached to the phosphorous is protected with an amide, I decided to focus on studying amides that are more electrophilic.

This chapter outlines the successful use of phenoxyacetamide for the synthesis of phosphoramidimidate DNA. Phenoxyacetyl has been used to protect the exocyclic amines of the nucleobases. For this application it showed complete deprotection under mild conditions: 29% ammonia at room temperature in less than four hours.[44] Thus, the ability to remove the phenoxyacetyl protecting group under mild conditions encouraged us to apply it to the synthesis of phosphoramidimidate DNA using an approach outlined previously with the cyanoethyl amide protecting group.

## 5.2 Phenoxyacetyl Protecting Group Validation

As proof of concept, a 2'-deoxythymidine dinucleotide was synthesized where the linking phosphate contained phosphoramidimidate having phenoxyacetamide protection (**figure 5.1**). The usual 5' DMT was replaced with a base labile levulinoyl group (Lev). This was considered necessary so that acid lability studies on the phenoxyacetamide could be completed without interference from the carbocation generated by cleavage of the DMT group. The synthesis begins by condensing bis(diisopropylamino) chlorophosphine with phenoxyacetamide to generate bis(diisopropylamino) phenoxyacetamidophosphane (**36**) in 71% yield. Compound (**36**) was then condensed with 5'-O- levulinoyl-2'-deoxythymidine in the presence of one equivalent of ETT to yield (**37**) in 84% yield. The next step was condensation of (**37**) with 3'-O-acetylthymidine and one equivalent of ETT to yield the dinucleotide (**38**) in 82% yield. Finally, this phosphoramidite was oxidized using an anhydrous solution of 0.02 M $I_2$ / 0.25M $NH_3$ in dioxane to yield the phenoxyacetamide phosphoramidimidate (**39**, 88% yield).

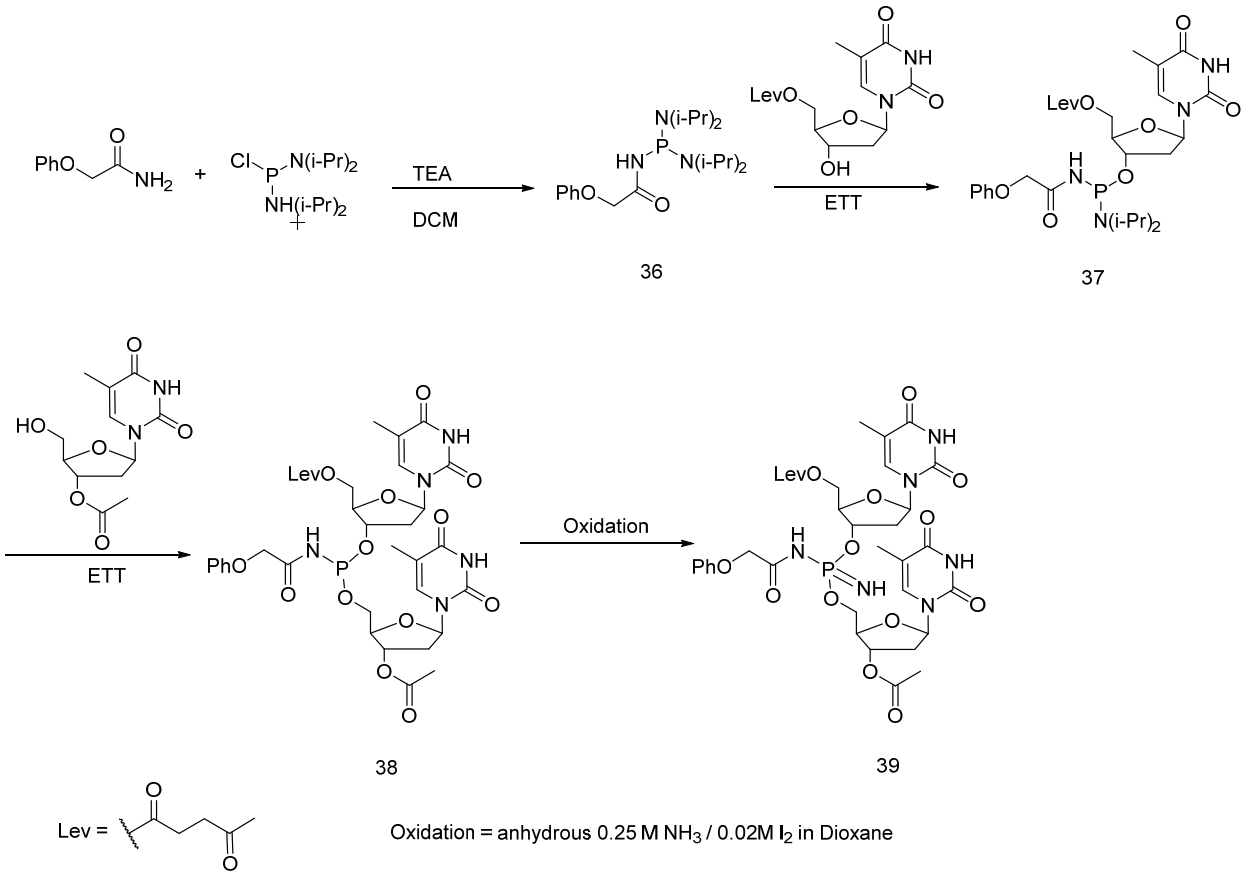


Figure 5.1 Synthesis scheme used to prepare dithymidine containing the phosphoramidimidate internucleotide linkage N-protected with the phenoxyacetyl group.

The stability of the dinucleotide (**39**) was examined with respect to the following reagents used in the solid phase synthesis cycle:

1. 3% Trichloroacetic acid in dichloromethane.
2. Cap mixture A: 10% Acetic Anhydride, 10% Pyridine, 80% THF.
3. Cap mixture B: 1-Methylimidazole in THF.
4. Tert-butyl peroxide solution: 0.5M tert-butyl peroxide solution in DCM.

In each experiment, 50 mg of the dinucleotide and the appropriate reagent were added to a NMR tube. The $^{31}P$ NMR was then monitored in order to test for degradation of the internucleotide linkage due to the formation of new peaks and/or decreased intensity of the starting

material peak. Cap mixture A, cap mixture B and t-butyl peroxide showed no degradation of product within 12 hours. The protected dinucleotide phosphoramidimidate showed 15% degradation after 24 hours (**figure 5.2**) with 3% trichloroacetic acid. This I considered acceptable as acid treatment per cycle (addition of one mononucleotide) was 90 seconds. Thus over 24 hours and 15% total degradation, 2'-deoxyoligonucleotides well over 1000 nucleotide could be synthesized which is longer than the 2'-deoxyoligonucleotides contemplated for this work (20-25 nucleotide in length). Thus, the phosphoramidimidate dinucleotide when protected by phenoxyacetyl is sufficiently acid stable for my research.

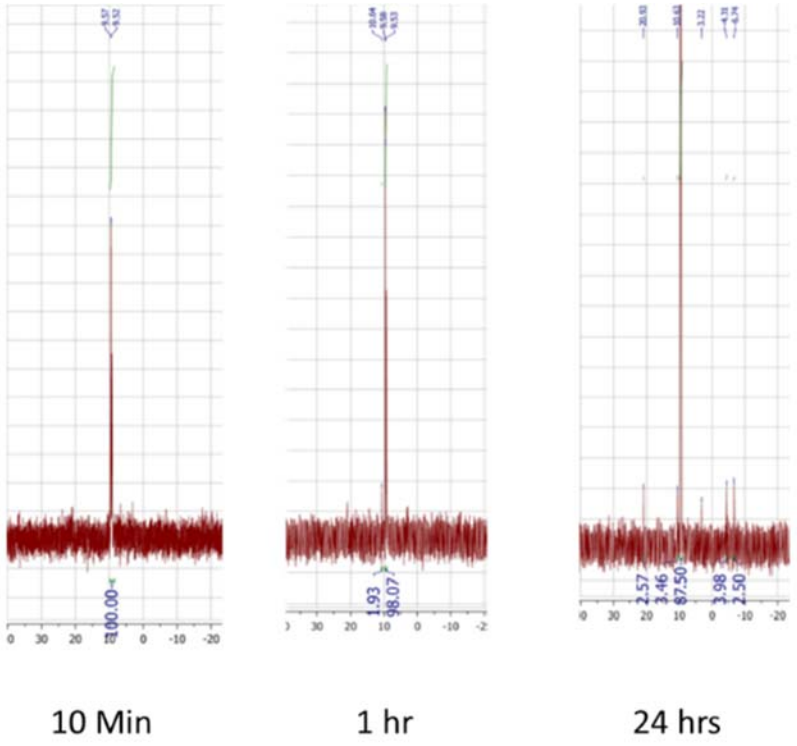


**Figure 5.2: $^{31}$P NMR showing the decomposition of compound 39** containing the phosphoramidimidate internucleotide linkage protected with phenoxyacetyl at 10 minutes, 1 hour and 24 hours time points using 3% trichloroacetic acid in dichloromethane. The small peaks that appear on the $^{31}$P NMR 24 scan at (-6.74, -4.31, 3.2, 10.63 and 20.93 ppm) represent degradation side products.

## 5.3: DNA Solid Phase Phosphoramidimidate Synthesis Using the Phenoxyacetyl Protecting Group

Since cyanoacetamide and phenoxyacetamide have similar reactivity towards reagents used in solid phase DNA synthesis and reactivity towards activation with ETT, the same synthetic procedures as used for the cyanoacetamide protecting group were used with the phenoxyacetamide synthesis approach. Prior to initiating solid phase synthesis of 2'-deoxyoligonucleotides having the phosphoramidimidate linkage, the four synthons (**Figure 5.3, 40 a-d**) used to prepare 2'-deoxyoligonucleotides were prepared. The synthesis started by dissolving phenoxyacetamide in DCM followed by adding 1.1 equivalents of triethylamine. After stirring for 15 minutes bis(diisopropylamino)-chlorophosphine (0.9 equivalents) was added and the reaction monitored by $^{31}P$ NMR. The disappearance of the 141 ppm $^{31}P$ NMR peak indicated complete consumption of the starting material while appearance of a new peak at 112 ppm indicated formation of the desired phosphoramidite. 5'-O-DMT-2'-Deoxythymidine (1.0 equivalents) and ETT (0.9 equivalents) were added and conversion to the product (**40a**) was monitored by TLC (**figure 5.3**). More detailed synthesis procedure and characterization date are included in the experimental chapter.

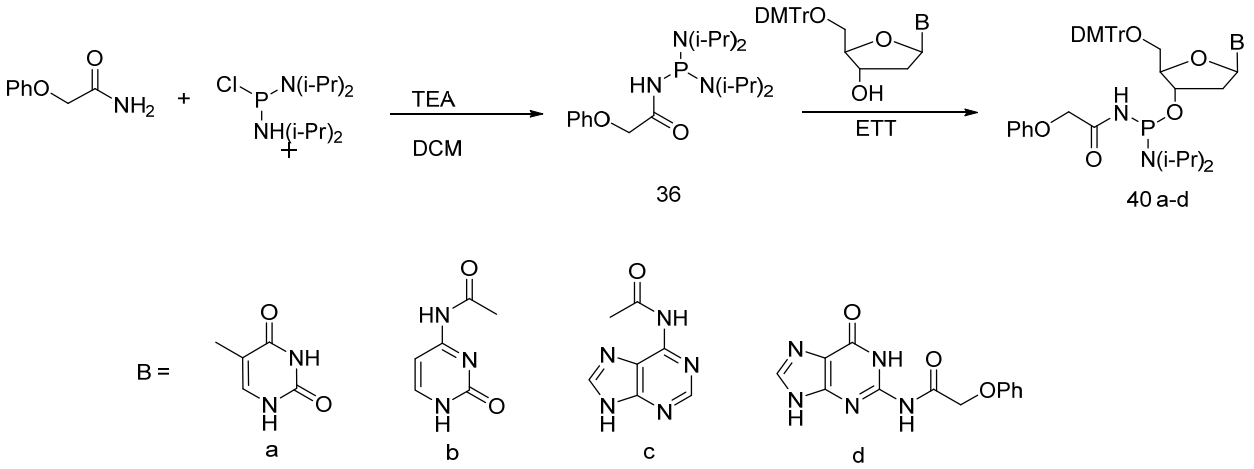


**Figure 5.3: Synthesis scheme for preparation of the synthons (compounds 40 a-d)** used as precursors for preparing phosphoramidimidate DNA.

The same synthetic procedure was used for preparing 5'-O-DMT-N-acetyl-2'-deoxyadenosine (**40c**), 5'-O-DMT-N-acetyl-2'-deoxycytidine(**40b**) and 5'-O-DMT-N-phenoxyacetyl-2'-deoxyguanosine (**40d**). All compounds (**40 a-d**) were confirmed by $^{1}H$ NMR, 2D NMR, $^{13}C$ NMR, $^{31}P$ NMR and mass spectrometry. The preparation of these synthons generated both diastereomers as evidenced by $^{31}P$ and TLC. However, the diastereomers proved inseparable by silica column chromatography under various solvent conditions. More detailed synthesis procedures and characterization date are included in the experimental chapter.

In order to validate compatibility of these synthons (**40 a-d**) with solid phase DNA synthesis, DNAs containing phenoxyacetamide phosphoramidimidate internucleotide linkages at variable positions were synthesized using the standard solid phase synthesis cycle. For simplicity, synthon (**40a**) was chosen initially for preparing 2'-deoxyoligonucleotides having the phosphoramidimidate internucleotide linkage. I first synthesized a $T_{12}$ 2'-deoxyoligonucleotide containing one modification located at

the 5' -end of the 2'-deoxyoligonucleotide (**figure 5.4**). By adding one modification at the 5'-end, exposure of phosphoramidimidate linkage to different reagents during the solid phase cycle was minimized. I left the final 5' DMT protecting group on the 2'-deoxyoligonucleotide because this group shifts the final polynucleotide away from failure sequences and provides a clearer image on the HPLC profile for evaluating the synthesis products and coupling efficiency. After cleavage from the solid support as outlined in figure 5.4, the crude reaction mixture was analyzed by HPLC.

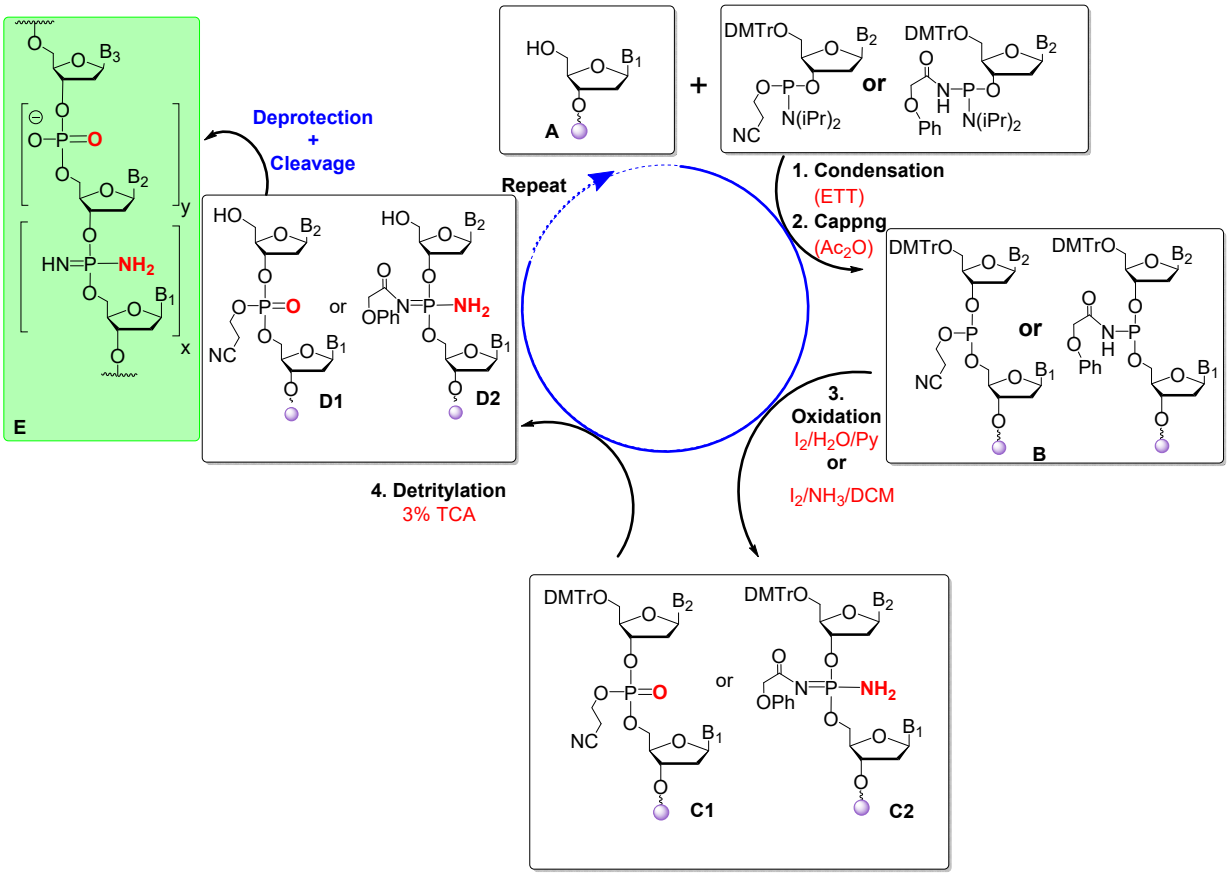


Figure 5.4 Solid-phase DNA synthesis cycle used to synthesize phosphoramidimidate DNA using the phenoxyacetamide protecting group approach; deprotection and cleavage condition: 0.5 mL ethylenediamine at room temperature for 15 minutes followed by adding 0.5 mL of 0.5 M anhydrous ammonia in dioxane and incubation for 24 hours at 45 °C.

Several additional $T_{15}$ oligomers having a phosphoramidimidate linkage at variable positions were prepared and analyzed. Data from these experiments resulted in

the following modifications to the standard solid phase phosphoramidite synthesis protocol:

1) Condensation Step: The concentration of phenoxyacetyl phosphoramidite was increased from 0.1M to 0.15 M. This change increased the product yield and decreased the amount of failure sequences. Using ETT as the activator and extending the condensation time to 15 minutes also increased the product yield and decreased the amount of failure sequences. Introduction of the monomers twice to the reaction column did not change the coupling yield.
2) Oxidation: The standard oxidizing solution consisting of $I_2/H_2O$/pyridine was used to convert the phosphite triester to phosphate when the regular phosphate linkage was introduced. The use of a peroxide oxidizing solution had no beneficial effect.
3) Iodine/ammonia oxidation: A solution of anhydrous ammonia and $I_2$ dissolved in DCM was used to convert the phenoxyacetyl protected phosphoramidite to phosphoramidimidate. This oxidizing solution was initially loaded into the column for 15 seconds which was enough time to fill the column. The reaction was then allowed to proceed for 240 seconds. The column was then flushed with argon for 10 seconds in order to remove the oxidizing reagents. A new oxidation solution was loaded onto the column and a second incubation was carried out for 120 seconds.

In order to further test the synthesis, thymidine containing polynucleotides 12 to 21 nucleotides in length and having two to four modifications at variable positions were next synthesized and the crude reaction mixtures analyzed by HPLC. The purified

product 2'-deoxyoligonucleotides were characterized by mass spectrometry and $^{31}P$ NMR. Figure 5.5 shows HPLC profiles for various 2′-deoxyoligonucleotides containing 2 - 3 phosphoramidimidate modifications.

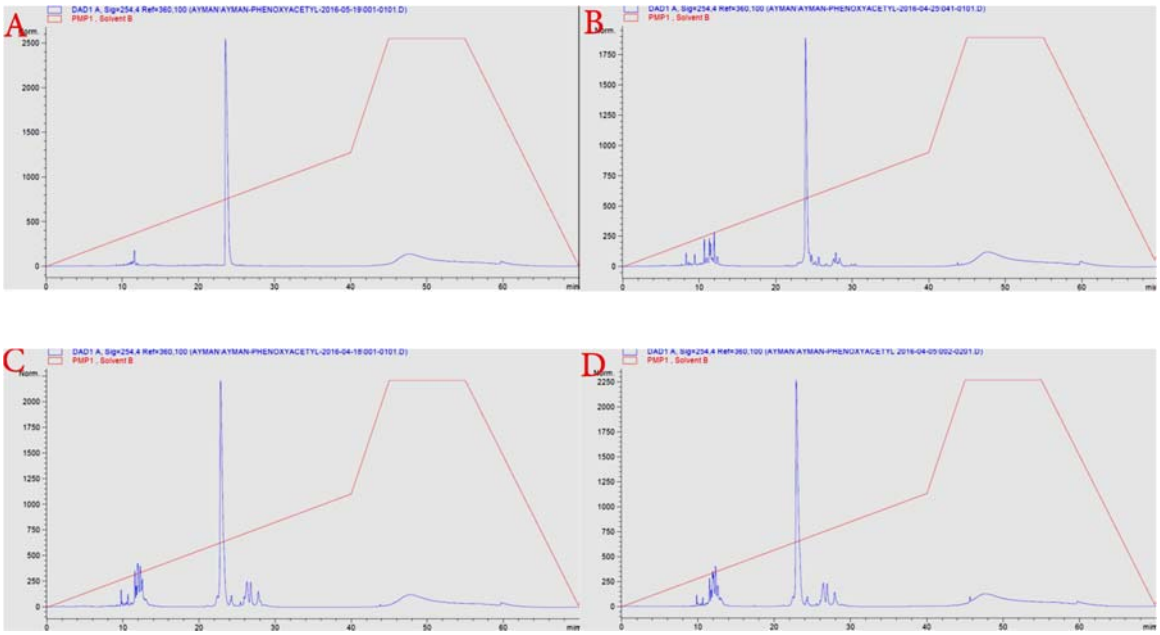


Figure 5.5: HPLC profiles (B-D) of crude reaction mixtures as obtained from the modified solid phase DNA synthesis cycle outlined in figure 5.4. The profile in A represents the total crude reaction mixture as obtained using the standard synthesis cycle for the preparation of unmodified 2'-deoxyoligonuclotide. The targeted product peaks appear at retention time 24 and failure sequences at 10-14 minutes. Sequences: A) 5'-DMT-TTTTTTTTTTTTTTTTTTTT; B) 5'-DMT-TT*TTTT*TTTTT*T; C) 5'-DMT-TT*TTTTTTTTT*TTTTTTTTT*T; D) 5'-DMT-TTTTTTTTTTTTTTTT*TT*TT*T; * = phosphoramidimidate.

As shown in figure 5.5, the targeted product peaks appear at retention time 24 minutes and failure sequences at 10-14 minutes. Minor peaks after the targeted product peak appear at retention time 26-29 minutes and are expected to correspond to incomplete removal of phenoxyacetyl group or the cyanoethyl group.

## 5.4 Phenoxyacetamide Deprotection of Phosphoramidimidate DNA

Although the phenoxyacetamide can be removed in 1 hour with aqueous ammonia when it is used to protect the exocyclic amines of cytosine, adenine and guanine, I found it to be more difficult to remove when it is used as the protecting group on the phosphoramidimidate internucleotide linkages. Several deprotection procedures were evaluated for removal of the phenoxyacetamide from the phosphoramidimidate. These included varying the basic conditions, time, temperature and hydrous verses anhydrous conditions. The specific reagents and conditions included: aqueous ammonia, anhydrous ammonia in dioxane, 1:1 anhydrous ammonia/ toluene, 1:1 anhydrous ammonia/ ethylenediamine, 1:1 ethylenediamine/toluene, aqueous ammonia with 10% ethylene diamine, DBU, aqueous ammonia with 10% 2-pyrrolidone, aqueous ammonia with 10% pyrrolidine and aqueous ammonia with 10% ethylenediamine.

The study was performed on 22 nucleotide oligomers having mixed combinations of nucleobases and 3 phosphoramidimidate internucleotide linkages per oligomer. Each synthesized oligomer while still attached to CPG was divided into two parts; one was cleaved from CPG using 30% aqueous ammonia for 1 hour at room temperature, the ammonia was removed and the oligomer redissolved in water. These conditions did not remove the phenoxyacetamide protecting group. A sample of this aqueous solution was injected to the HPLC in order to evaluate the quality of the total product mixture. The second half was dissolved in the appropriate test solution and the sample subjected to the deprotection procedure. Solvent was removed, the sample was redissolved in water, filtered from CPG and analyzed by HPLC. The HPLC profiles of these two samples were then compared in order to evaluate the deprotection procedure.

Of the various procedures, the best deprotection of phenoxyacetamide occurred with 0.5 mL ethylenediamine at room temperature for 15 minutes followed by 0.5 mL of 0.5 M anhydrous ammonia in dioxane for 24 hours at 45 °C. Increasing the temperature of this reaction mixture to °55 C generated shorter oligomers due to phosphorous bond breakage. This optimized protocol also served to cleave the 2'-deoxyoligonucleotide from the solid support and remove the nucleobase protecting groups from cytosine, guanine and adenine.

All samples were analyzed by mass spectrometry in order to confirm complete deprotection and generation of the desired phosphoramidimidate. $^{31}$P NMR provided further evidence since the protected phosphoramidimidate appears at 10 ppm and the deprotected at 12 ppm when deuterated water is used as solvent. The next section will discuss how to differentiate between protected and unprotected phosphoramidimidate products.

### 5.5 Phenoxyacetamide Base Deprotection Study Using $^{31}$P NMR

Since the chemical shift of the unprotected phosphoramidimidate (12 ppm) was at higher resonance than the phenoxyacetamide protected linkage (10 ppm), an additional study was carried out in order to confirm this assignment. Thus, a 2'-deoxyoligonucleotide containing 22 internucleotide linkages where 3 of these were phenoxyacetamide phosphoramidimidate, was prepared on a support where the oligomer was linked by hydroquinone-O,O′-diacetic acid, (Q-linker)[45] rather than the traditional succinyl linker. With this support (Q-linker), the oligomer could be cleaved from the support in 5 minutes using 1 mL of 0.5 M $K_2CO_3$ in methanol. While the phenoxyacetamide groups remain intact, a small portion were cleaved. Following

removal of methanol by evaporation, the sample was redissolved in 1 mL 2 M ammonium acetate buffer (pH = 7) and 0.1 mL deuterated water. $^{31}P$ NMR was acquired and it confirmed the chemical shifts (**Figure 5.6**). Although ammonium acetate buffer is expected to neutralize the cleavage from the solid support solution (0.5 M $K_2CO_3$), but keeping the sample for 12 hours while acquiring $^{31}P$ showed additional minor removal of phenoxyacetamide group due to the presence of $K_2CO_3$ in the aqueous sample.

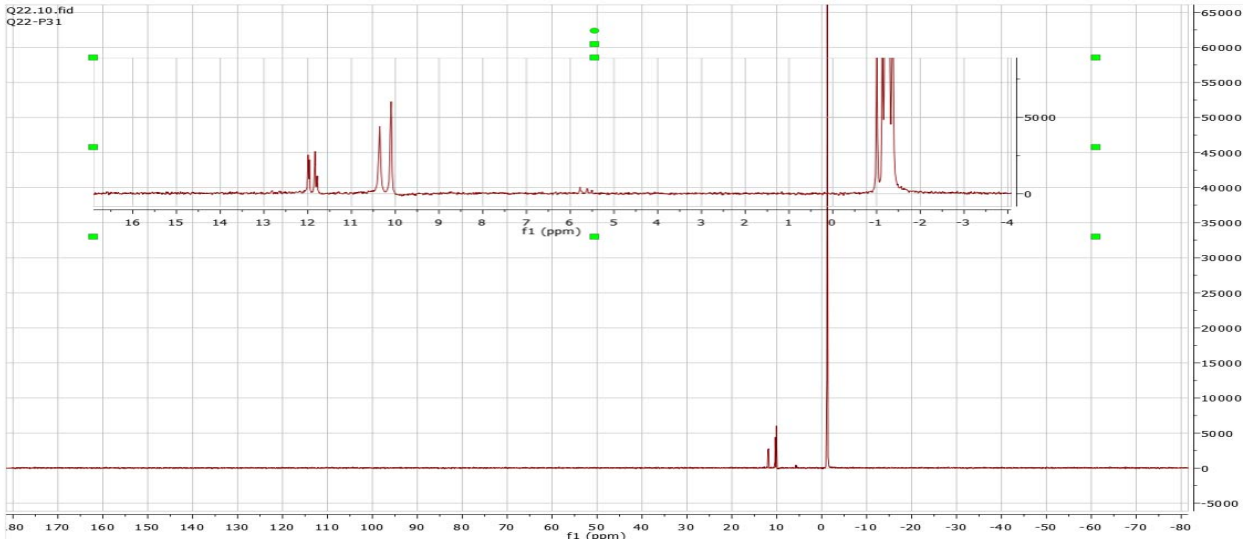


Figure 5.6: $^{31}P$ NMR spectrum for $T_{22}$ containing three phosphoramidimidate internucleotide linkages (**ODN 17**); the peaks at -1 ppm correspond to phosphate, the peaks at 10 and 12 ppm correspond to protected and unprotected phosphoramidimidate respectively.

As shown in figure 5.6 the natural phosphate internucleotide linkage appeared at -1 ppm, and additional peaks appear at 10 and 12 ppm. The major peaks at 10 ppm correspond to the diastereomers of the intact phenoxyacetamide phosphoramidimidate and the smaller peaks at 12 ppm correspond to the diastereomers of the deprotected phosphoramidimidate internucleotide linkage. This result is also confirmed by mass

spectrometry and $^{31}P$ NMR (**Figure 5.7**). Part B of figure 5.7 shows the mass analysis peaks; the peak at 1731.3235 corresponds to the oligonucleotide where all three phosphoramidimidate linkages have been deprotected, the peaks at 1764.8497, 1798.3455 and 1831.8571 correspond to 2′-deoxyoligonucleotides where 2,1 and 0 of the phosphoramidimidate linkages have been deprotected, respectively. The differences between 5.6 and 5.7 likely reflects the different cleavage/deprotection conditions ($K_2CO_3$ vs anhydrous ammonia/ethylenediamine).

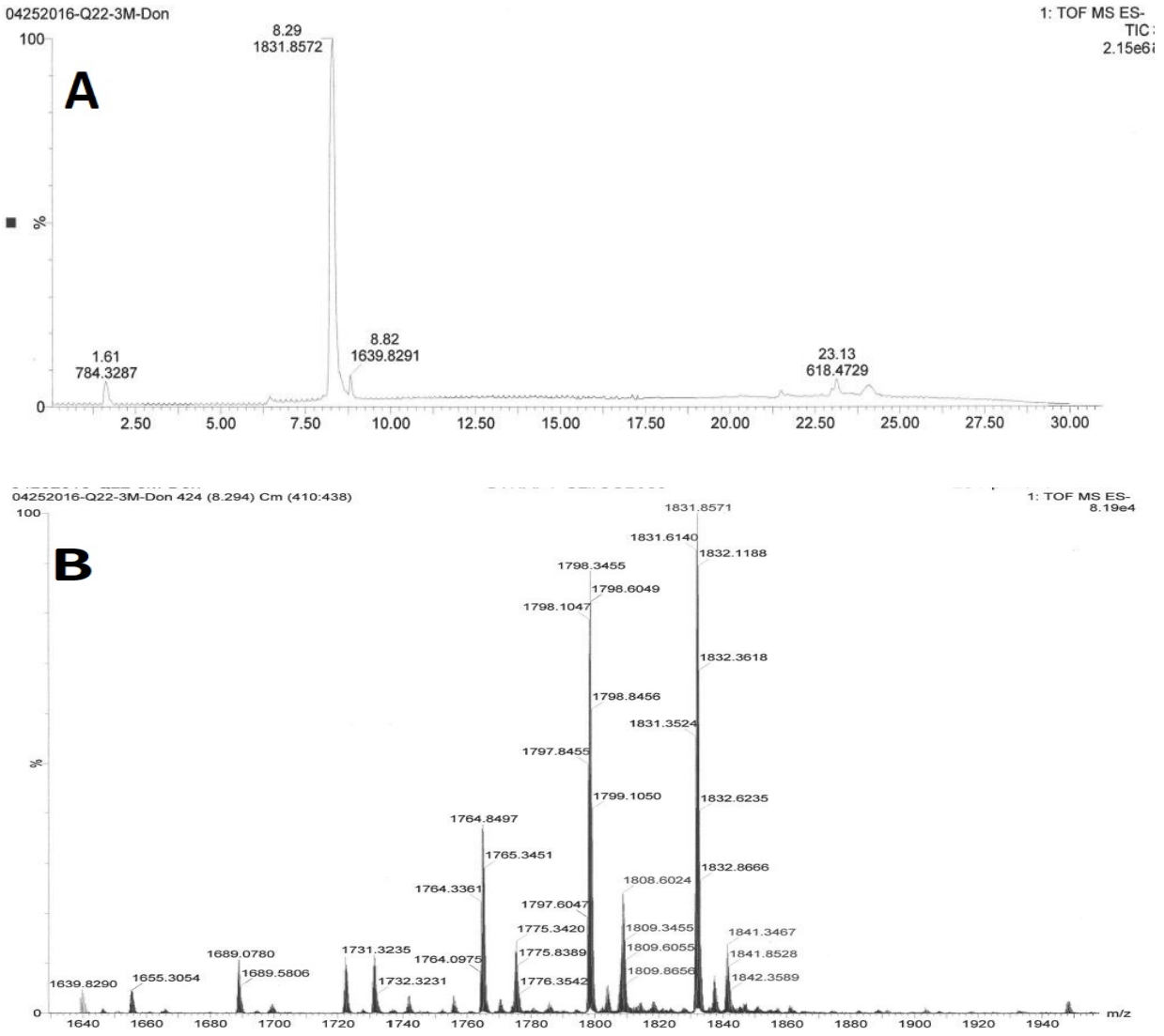


**Figure 5.7: LCMS analysis of $T_{22}$ containing three phosphoramidimidate internucleotide linkages and 5'-O protected with DMT (ODN17)**. Part A shows the total ion chromatogram and part B shows the extracted ion chromatogram for the major peak at 8 minutes showing the mass analysis peaks; the peak at 1731.3235 corresponds to the oligonucleotide where all three phosphoramidimidate linkages have been deprotected and in ionization state -4, the peaks at 1764.8497, 1798.3455 and 1831.8571 correspond to 2,1 and 0 of the phosphoramidimidate linkages have been deprotected respectively and all are in ionization state -4.

Figures 5.8 and 5.9 show an example for the successful deprotection of $T_{21}$ 2'-deoxyoligonucleotide containing three phosphoramidimidate internucleotide linkages (**ODN18**) using 0.5 mL ethylenediamine at room temperature for 15 minutes followed by 0.5 mL of 0.5 M anhydrous ammonia in dioxane for 12 hours. In Figure 5.8 the disappearance of peaks at 10 ppm

indicate the complete deprotection of the phosphoramidimidate linkages. Figure 5.9 shows the LCMS chromatogram for the same $T_{21}$ 2'-deoxyoligonucleotide where all three phosphoramidimidate linkages have been deprotected. A minor peak at 1688.8267 corresponds to a 2'-deoxyoligonuclotide where one of the phosphoramidimidate linkages remains protected. However, this compound was not detected in the $^{31}P$ NMR.

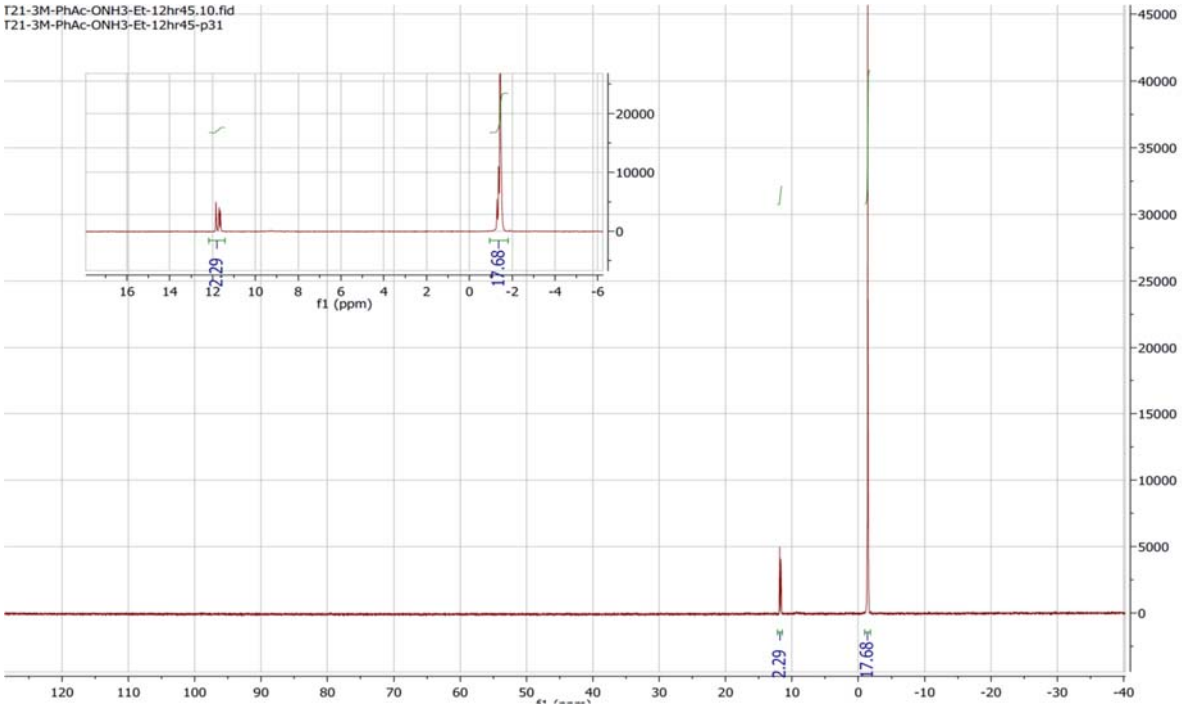


Figure 5.8: $^{31}P$ NMR spectrum for $T_{21}$ containing three phosphoramidimidate internucleotide linkages (**ODN 18**); the peaks at -1 ppm correspond to phosphate, the peaks at 12 ppm corresponds to diastereomers of unprotected phosphoramidimidate. Disappearance of the diastereomer peaks at 10 ppm indicates the complete deprotection of phosphoramidimidate.

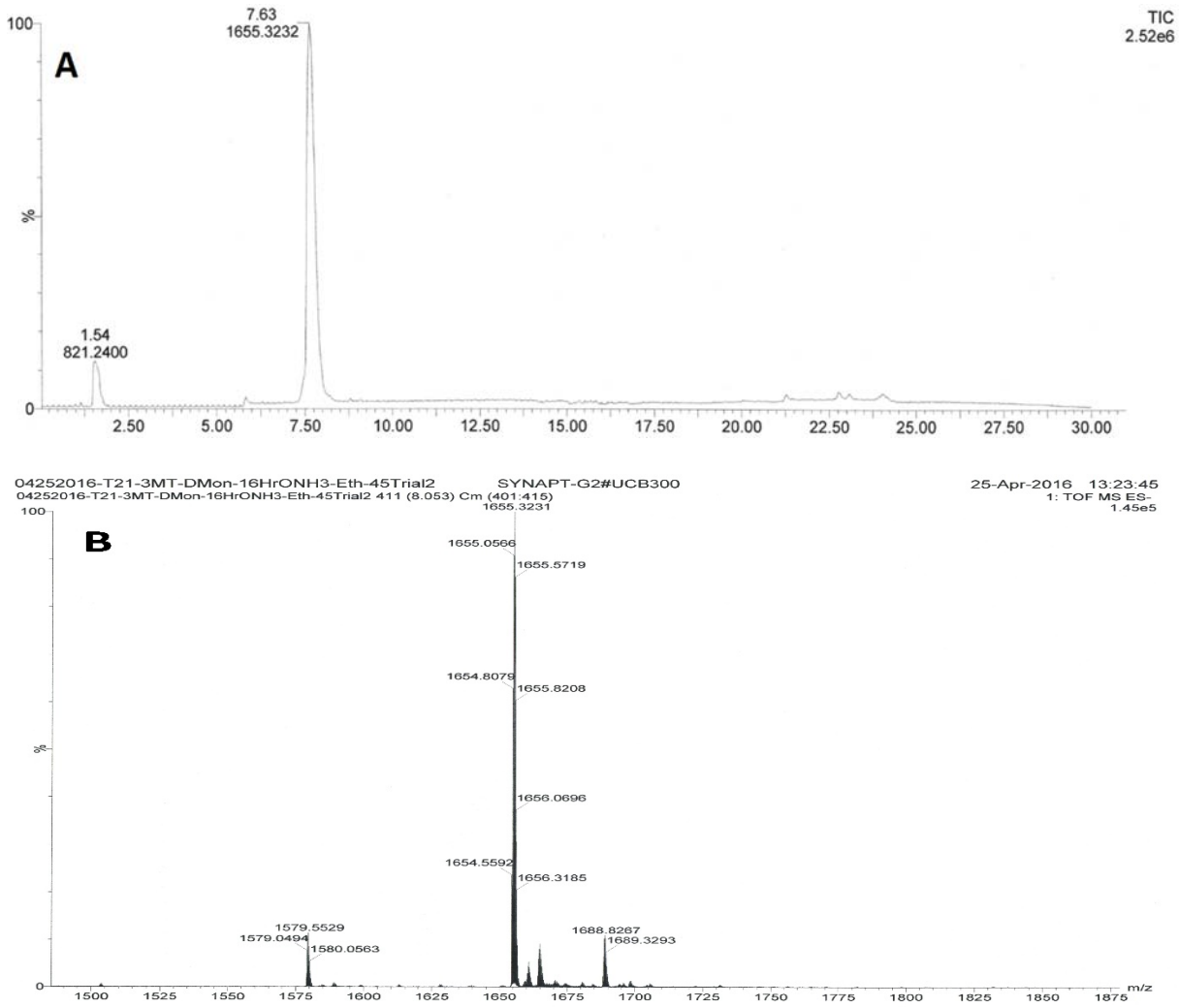


Figure 5.9: LCMS analysis of $T_{21}$ containing three phosphoramidimidate internucleotide linkages and 5'-O protected with DMT (**ODN18**). Part A shows the total ion chromatogram and part B shows the extracted ion chromatogram for the major peak at 7.5 minutes; the peak at 1655.0566 corresponds to the oligonucleotide where all three phosphoramidimidate linkages have been deprotected and in ionization state -4. The peak at 1688.8267, corresponds to a 2'-deoxyoligonuclotide where one of the phosphoramidimidate linkages is still protected with phenoxyacetamide (ionization state -4).

## 5.6 5'-End Additional Modifications of the Deprotection Strategy

As outlined previously in chapter 5, the phosphoramidimidate internucleotide linkage is stable towards acids as long as it is in the amide form but when the amide protecting group is removed, it is acid sensitive at pH lower than 4. Since it is desirable to retain the acid labile and hydrophobic 5'-DMT group during RP-HPLC in order to separate the desired product from failure sequences that are free of the DMT group, another problem had to be solved. This is because removal of the amide protecting group generates an acid labile phosphoramidimidate linkage prior to RP-HPLC and therefore also prior to removal of the 5'-DMT group with acid. Therefore, either a new procedure was necessary for removal of this group as the last synthesis step or I had to identify a new 5' hydrophobic protecting group.

These observations led me to investigate the use of the t-butyldimethylsilyl group in place of the DMT as both are hydrophobic and therefore useful in reverse phase HPLC. Additionally, the silyl protecting group can be removed using a fluoride solution under nonacidic conditions. The commercially available 5'-O-(t-butyldimethylsilyl)- 2'-deoxythymidine was used in order to synthesize the synthon (**41**) for preparation of phosphoramidimidate DNA (**figure 5.10**). The structure of synthon (**41**) was confirmed by $^{31}$P NMR, $^{13}$C NMR, $^{1}$H NMR and mass spectrometry (see experimental section). It was tested in the solid phase cycle, but unfortunately this compound was found to be unacceptable as overall synthesis yields were low and numerous failure sequences were observed.

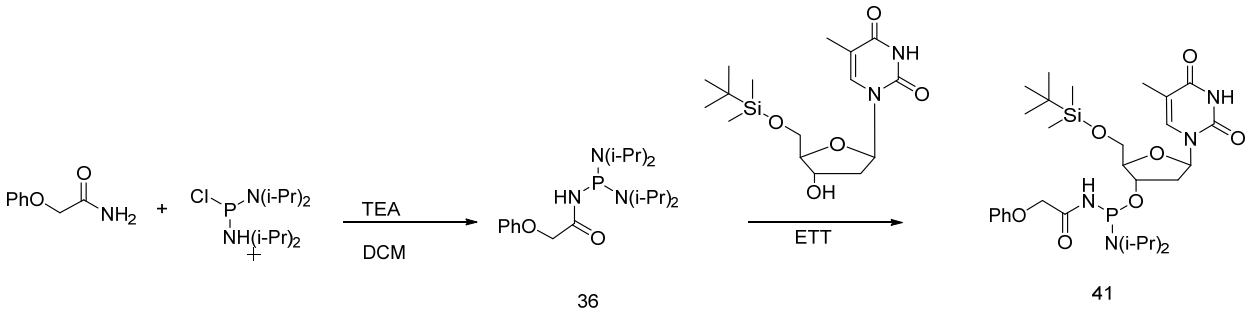


Figure 5.10: Synthesis scheme for compound 40 phosphordiamidite where the 5' hydroxyl is protected with the t-butyldimethylsilyl group.

Studies utilizing the trimethoxytrityl (TMT) as a 5' protecting group proved to be a successful choice. This group has the same protecting functionality and lipophilicity as DMT but is acid labile at a higher pH. These advantages encouraged us to synthesize 2'-deoxyoligonucleotides 5'-protected with TMT and containing the phosphoramidimidate internucleotide linkages. The same synthetic path was used to prepare the synthon for the phosphoramidimidate solid phase cycle except that 5'-O-DMT-2'-deoxythymidine was replaced with 5'-O-TMT-2'-deoxythymidine (**figure 5.11**).

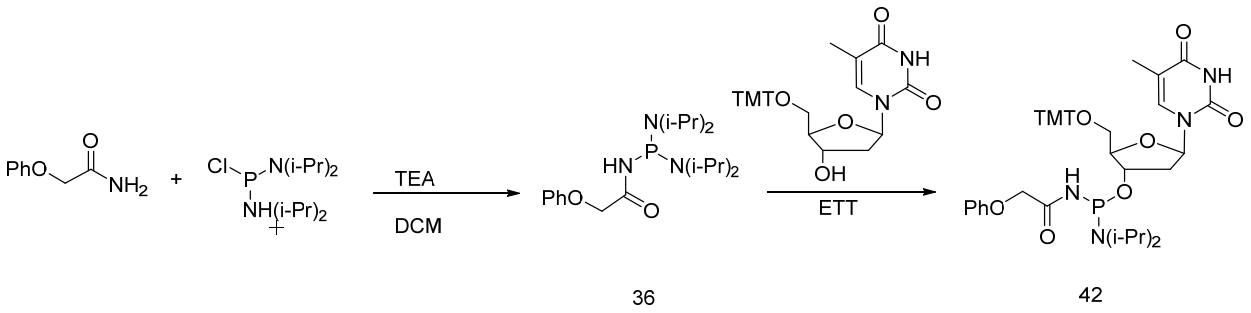


Figure 5.11: Synthesis scheme for compound 42 phosphordiamidite in which the 5' hydroxyl is protected with the trimethoxytrityl (TMT) group.

In order to test the use of synthon (**42**), a 2'-deoxyoligonucleotide containing 6 phosphoramidimidate internucleotide linkages was prepared. The synthesis was completed using the 5'- DMT protected synthons, except for the final deoxynucleotide addition, using synthon (**42**). Thus the final 2'-deoxynuclotide was added as the 5'-TMT-2'-deoxythymidine-3'-phosphoramidite. This 2'-deoxyoligonuclotide was cleaved from the solid support, phenoxyacetyl groups removed, and the product purified using reverse phase preparative HPLC. This 2'-deoxyoligonucleotide was incubated at pH = 5 for 12 hours at room temperature with 1:1:1 water: acetic acid: tetramethylethylenediamine to remove the 5'-TMT group and generate the desired product (Figure 5.12).

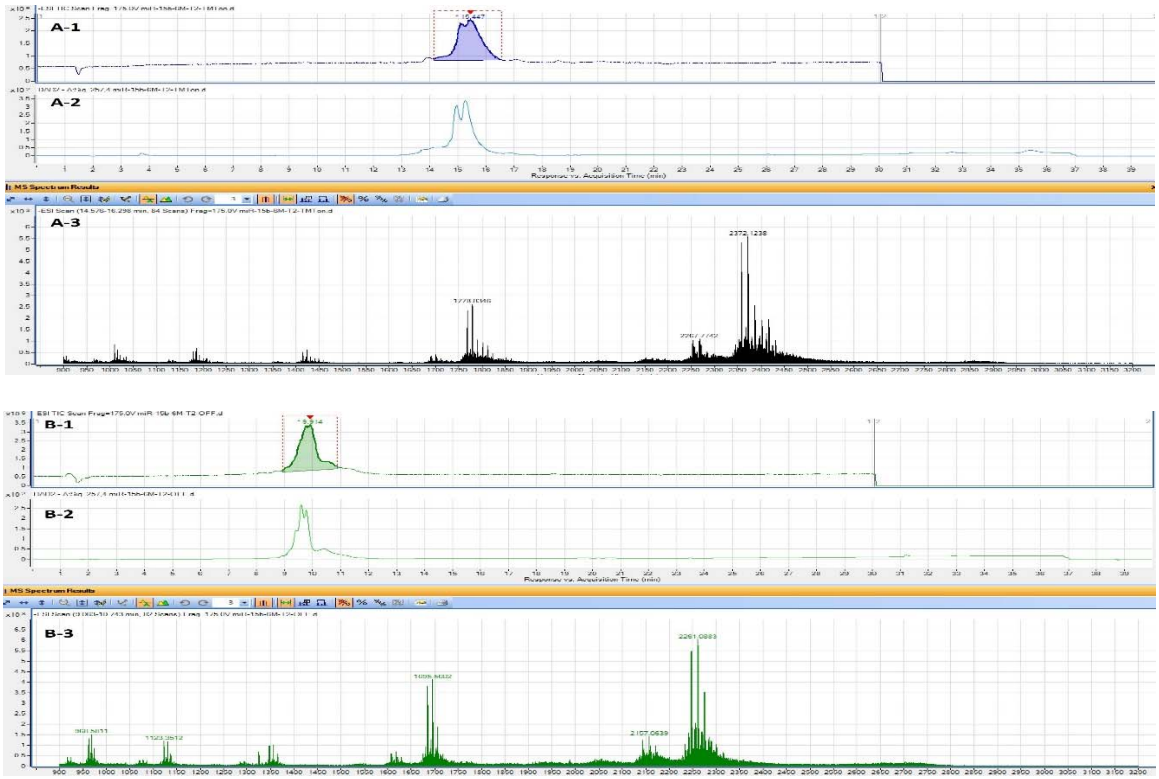


Figure 5.12: LC-UV/MS for the purified 2'-deoxyoligonucleotide 5'-TMT-T*GT*AAA*CCAT*GAT*GTGCTGCT*A $[M+K]^{-3}$ = 2372.1238 (A-1, A-2, A-3) and the same purified 2'-deoxyoligonucleotide after acid treatment to remove the TMT group $[M+K]^{-3}$ = 2261.0883 (B-1, B-2, B-3). A-1/B-1: total ion chromatogram. A-2/B-2: UV absorbance chromatogram. A-3/B-3: extracted ion chromatogram of the main peak in A-1/B-1 at selected time.

As shown in figure 5.12 (A1-A3), a 2'-deoxyoligonuclotide (5'-TMT-T*GT*AAA*CCAT*GAT*GTGCTGCT*A) having the 5'-TMT and 6 phosphoramidimidate internucleotide linkages (*) was characterized using LCMS. The peak at 2372.1238 corresponds to $[M+K]^{-3}$. After removal of the 5'-TMT group the 2'-deoxyoligonuclotide was characterized using LCMS (Figure 5.12 B1-B3), the peak at 2261.0883 corresponds to $[M+K]^{-3}$ of 5'-T*GT*AAA*CCAT*GAT*GTGCTGCT*A.

Using these optimized procedures for synthesizing phosphoramidimidate DNA, 2'-deoxyoligonucleotides 15 to 22 nucleotides in length with 3 to 14 phenoxyacetamide phosphoramidimidate internucleotide linkage were synthesized. The sequential optimized cleavage and purification procedure was as follows:

1) Cleave the 2'-deoxyoligonucleotide from the solid support and simultaneously remove the nucleobase and the phenoxyacetyl protecting groups using 1:1 ethylenediamine: 0.5M $NH_3$ in dioxane (24 hours at 45 °C).
2) Separate the product 2'-deoxyoligonucleotide containing a 5'-TMT from side products using preparative RP-HPLC.
3) Incubate the purified 2'-deoxyoligonucleotide in 1:1:1 water: acetic acid: tetramethylethylenediamine at pH = 5 for 12 hours at room temperature. These conditions remove the TMT group without degrading the 2'-deoxyoligonucleotide.
4) Neutralize the reaction solution using 1M triethylammonium bicarbonate
5) Purify the product 2'-deoxyoligonucleotide using preparative RP-HPLC.

Table 5.1 lists the synthesized 2'-deoxyoligonucleotides. These 2'-deoxyoligonucleotide were used for several experiments including thermal denaturation and biological activity studies.

**Table 5.1: A list of 2'-Deoxyoligonucleotides containing phosphoramidimidate internucleotide linkages that were used for molecular weight analysis, $^{31}$P-NMR, Tm and biological activity studies.**

| No. | Structure |
|---|---|
| **ODN19** | DMT-T*TTTTTTTT*T |
| **ODN20** | DMT-TTT*TTT*TTT*TTT |
| **ODN21** | DMT-TT*TTTTTTTTTTT*T |
| **ODN22** | DMT-TTTTT*TTTTTT*TTTTTT*TTTT |
| **ODN23** | DMT-AAAAT*AAAAAT*AAAAAT*AAAA |
| **ODN24** | DMT-AAAAA*AAAAAA*AAAAAA*AAAA |
| **ODN25** | DMT-TGTA*AA*CCA*TGA*TGTGCTGCTA |
| **ODN26** | DMT-TGT*AAACCAT*GAT*GT*GCTGCTA |
| **ODN27** | DMT-TGT*AAA*CCA*TGAT*GTGCT*GCTA |
| **ODN28** | DMT-T*GTA*AACCA*TGATGTGCTGCT*A |
| **ODN29** | DMT-TG*TAAACCATG*ATGTGC*TGC*TA |
| **ODN30** | DMT-TG*TAAACC*ATG*ATGTGC*TGC*TA |
| **ODN31** | DMT-TG*TAAACC*ATG*ATG*TGC*TGC*TA |
| **ODN31** | DMT-TG*TAA*ACC*ATG*ATG*TGC*TGC*TA |
| **ODN32** | DMT-TGT*AAA*CCA*TGA*TGT*GCT*GCT*A |
| **ODN33** | TGTAAAC*C*ATGATGTGC*TGC*TA |
| **ODN34** | T*GT*AAACC*AT*GAT*GTGCTGCT*A |
| **ODN35** | T*GTA*AA*CCAT*GA*TGTGCTGCT*A |
| **ODN36** | T*GT*AAACC*ATGAT*GTGCTGCT*A |

| | |
|---|---|
| **ODN37** | T*GT*AA*ACCA*TGAT*GTGCTGCT*A |
| **ODN38** | TAGC*AGC*ACATC*ATG*GTTTACA |
| **ODN39** | T*GT*AAA*CCAT*GAT*GTGCTGCT*A |
| **ODN40** | TAGC*AGC*ACAT*CAT*GGTT*TACA |
| **ODN41** | TA*CT*GA*GA*GA*CA*CT*GA*TT*CT*GA*A |
| **ODN42** | TT*CA*GA*AT*CA*GT*GT*CT*CT*CA*GT*A |
| **ODN43** | 6-FAM-P(S)- TG*TA AACC*ATGAT*GTGCTGC T*A |
| **ODN44** | 6-FAM-P(S)- TGT*AAACC*AT*GAT*GTGCTGCT*A |
| **ODN45** | 6-FAM-P(S)- T*GTA*AA*CCAT*GA*TGTGCTGCT*A |
| **ODN46** | 6-FAM-P(S)- T*GTA*AA*CCAT*GA*TGT*GCT GCT*A |
| **ODN47** | 6-FAM-P(S)- T*GT*AAACC*ATG*ATGT*GCTGCT*A |
| **ODN48** | 6-FAM-P(S)- C*TAGCC*ATG*ATGT*GTGCTGCT*A |
| **ODN49** | 6-FAM-P(S)- T*GT*AAACC*ATGAT*GTGCTGCT*A |

(*: phosphoramidimidate); 6-FAM-P(S): 5'-fluorescein thiophosphoramidate.

A 5'-fluorescein thiophosphate tag was introduced on the 5' terminus of certain 2'-deoxyoligonuclotides using the commercially available 5'-fluorescein phosphoramidite. This linkage was then oxidized to thiophosphate instead of standard phosphate because thiophosphate linkages show more resistance towards cell nucleases. Thus, when these 2'-deoxyoligonuclotides are tested in biological systems, this fluorescein tag will remain with the oligomer and not be removed through nuclease hydrolysis. Consequently, a much more accurate determination of biological results was possible.

## 5.7 Phosphoramidimidate Linkages are Positively Charged

During liquid chromatography mass spectrometry (LC-MS) analysis using ammonium acetate buffer (pH = 7), an extra hydrogen atom was added per modification to the 2'-deoxyoligonucleotide exact mass. This indicates that the extra hydrogen came from protonation of the phosphoramidimidate internucleotide linkage. In order to prove that the phosphoramidimidate internucleotide linkage has a positive charge at neutral pH, a gel mobility study was performed to compare three types of DNA internucleotide linkages that have different charge: (1) natural DNA with phosphate that has a negative charge; (2) natural DNA having several phosphoramidate linkage that have no charge; (3) natural DNA having several phosphoramidimidate linkages that were expected to have positive charge. These 2'-deoxyoligonuclotide having 11 internucleotide linkages each (12 mers) were prepared. One contained three phosphoramidate linkages, a second had three phosphoramidimidate linkages and the third was natural DNA. Thus the net charge for the 2'-deoxyoligonucleotide containing all-natural phosphate would be -11 (**ODN52 figure 5.13**). The net charge for 2'-deoxyoligonucleotide containing 3 phosphoramidate linkages would be -8 (**ODN51 figure 5.13**). The net charge for 2'-deoxyoligonucleotide containing 3 phosphoramidimidate linkages would be -5 (**ODN50 figure 5.13**), because three positively charged phosphoramidimidate linkages would neutralize three natural phosphate linkages.

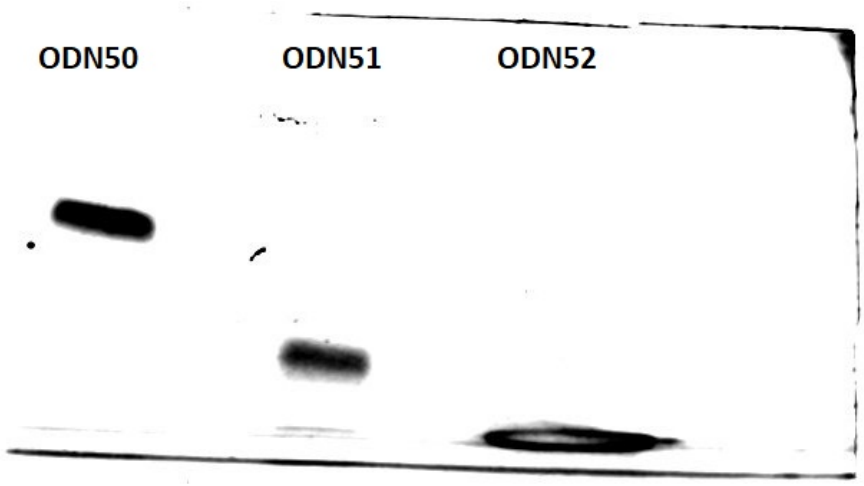


Figure 5.13 Denaturing polyacrylamide gel electrophoresis for **ODN50**: d(T*TTTTT*TTTTT*T), **ODN51**: d(T#TTTTT#TTTTT#T) and **ODN52**: d(TTTTTTTTTTT); These three deoxyoligonucleotides showed different in mobility despite being close in molecular weight due to the difference in the overall charges; (#: phosphoramidate), (*: phosphoramidimidate).

As expected these three 2'-deoxyoligonucleotides showed different mobilities by electrophoresis on a denaturing polyacrylamide gel due to the difference in the overall charge (relative to this study the difference in molecular weights were insignificant ODN50 = 3887.8664, ODN51= 3887.7944 ODN52= 3890.7464 in g/mole). This observation confirms that the phosphoramidimidate internucleotide linkage is positively charged at pH 8 which is consistent with the LC-MS results where an extra hydrogen unit per modification was detected.

## 5.8 Thermal Denaturation Studies

The ability of a 2'-deoxyoligonucleotide to bind to its target is an important parameter for certain biological activities. For example, various modified DNAs may have applications in antisense or antagomir therapy, but their utility is significantly affected by the ability of the oligonucleotides to recognize and bind to target RNA. In order to study the binding ability of the phosphoramidimidate DNAs to complimentary DNA and RNA, thermal denaturation studies were carried out by measuring the Tm values for duplexes in order to observe the effect of phosphoramidimidate modifications on duplex formation and stability. The procedure involved forming duplexes where one strand had phosphoramidimidate DNA and the other strand was natural complementary DNA or RNA. The phosphoramidimidate modification was also introduced in both strands but not opposed to one another. Tm values were then measured as a function of the number of phosphoramidimidate modification in each oligonucleotide.

2'-Deoxyoligonucleotides having phosphoramidimidate linkages (**ODN37-ODN42 table 5.1**) were mixed with the complementary DNA or RNA in a 1:1 ratio (final concentration 1.0 μM of duplex) in solutions of 1.0 M NaCl/0.01 M $Na_2HPO_4$, 0.10 M NaCl/0.01 M $Na_2HPO_4$, or 0.01M NaCl/0.01 M $Na_2HPO_4$ at pH 7.3. The samples were heat denatured at 85 °C for 10 min, cooled to 25 °C at a rate of 1 °C/min, and maintained at this temperature for 10 min. Duplex melting was performed by heating the duplexes from 20 to 85 at 1 °C/min with the absorbance (260 nm) being recorded at one-minute intervals. Melting temperatures were determined at the maximum of first derivative plots. Tm values for unmodified DNA and RNA having the same sequence with complementary DNA were also determined. In order to confirm the stability of duplexes and the effect of the heating/cooling cycles, the melting temperatures were measured four times for each sample (twice during the heating cycle and twice during the cooling cycle).

Tm's were measured for duplexes having variable numbers of phosphoramidimidate modifications and locations within the 2'-deoxyoligonucleotides in order to determine the effect of the modifications on binding. On average, it was found that the Tm depression was 0.5 °C per modification at 100 mM or 10 mM NaCl and 1 °C per modification at 1.0 M NaCl. Figures 5.14 and 5.15 show Tm studies at 100 mM NaCl/10 mM $Na_2HPO_4$ and 10 mM NaCl/10 mM $Na_2HPO_4$ respectively. Figure 5.14 shows melting curves for d(5'-TA*CT*GA*GA*GA*CA*CT*GA*TT*CT*GA*A) with d(5'-TT*CA*GA*AT*CA*GT*GT*CT*CT*CA*GT*A) at 100 mM NaCl/0.01 M $Na_2HPO_4$. Figure 5.15 shows melting curves for d(5'-T*GT*AA*ACCA*TGAT*GTGCTGCT*A) with d(5'-TAGC*AGC*ACATC*ATG*GTTTACA) at 10 mM NaCl/0.01 M $Na_2HPO_4$.

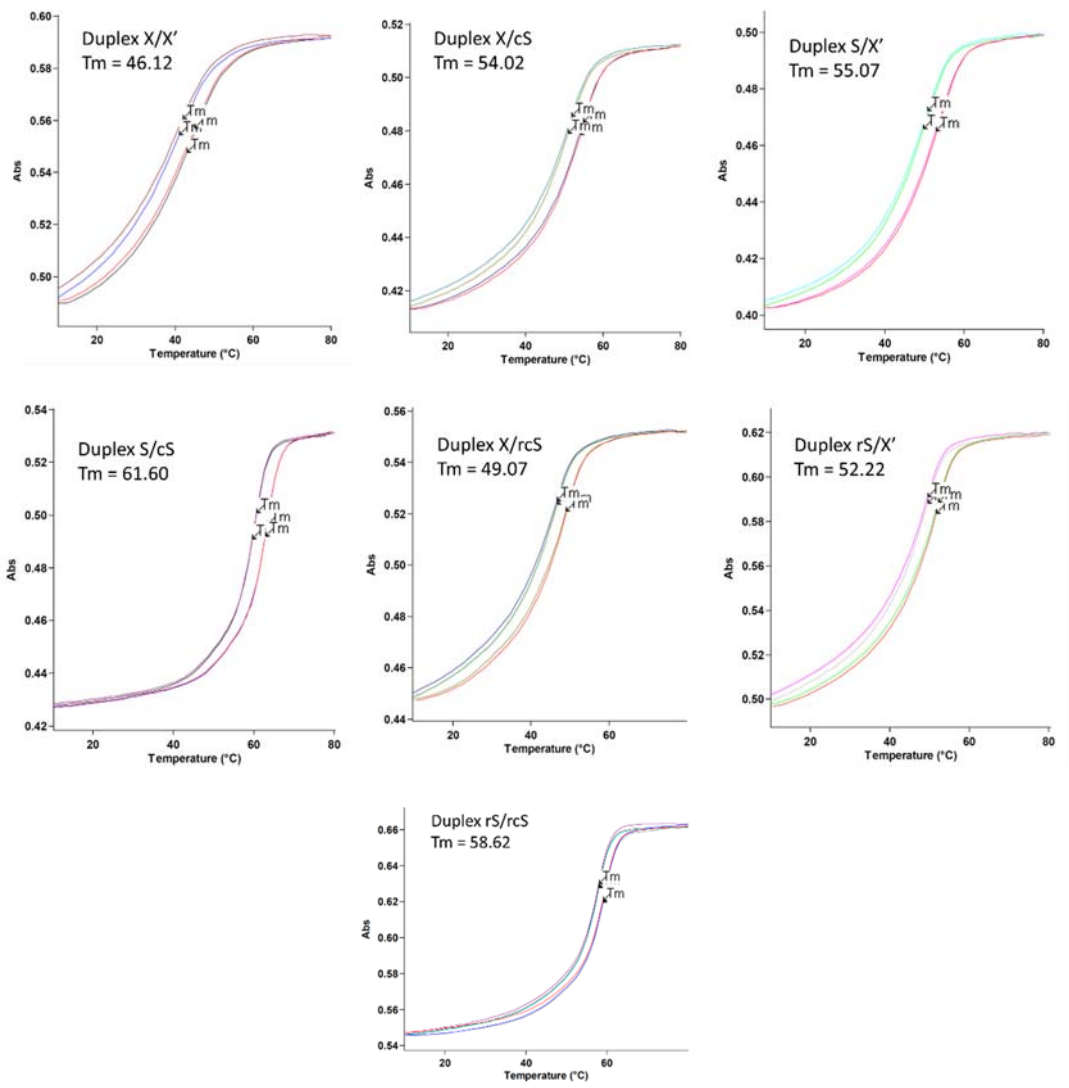


**Figure 5.14: Melting curves of duplex X/X', X/cS, S/X', S/cS, X/rcS, rS/X' and rS/rcS**; X = d(5'-TA*CT*GA*GA*GA*CA*CT*GA*TT*CT*GA*A); X′ = d(5'-TT*CA*GA*AT*CA*GT*GT*CT*CT*CA*GT*A); S = d(5'-TACTGAGAGACACTGATTCTGAA); cS = d(5'-TTCAGAATCAGTGTCTCTCAGTA); rS = r(5'-UACUGAGAGACACUGAUUCUGAA); rcS = r(5'-UUCAGAATCAGUGUCUCUCAGUA) at 100 mM NaCl/10 mM $Na_2HPO_4$; * = phosphoramidimidate.

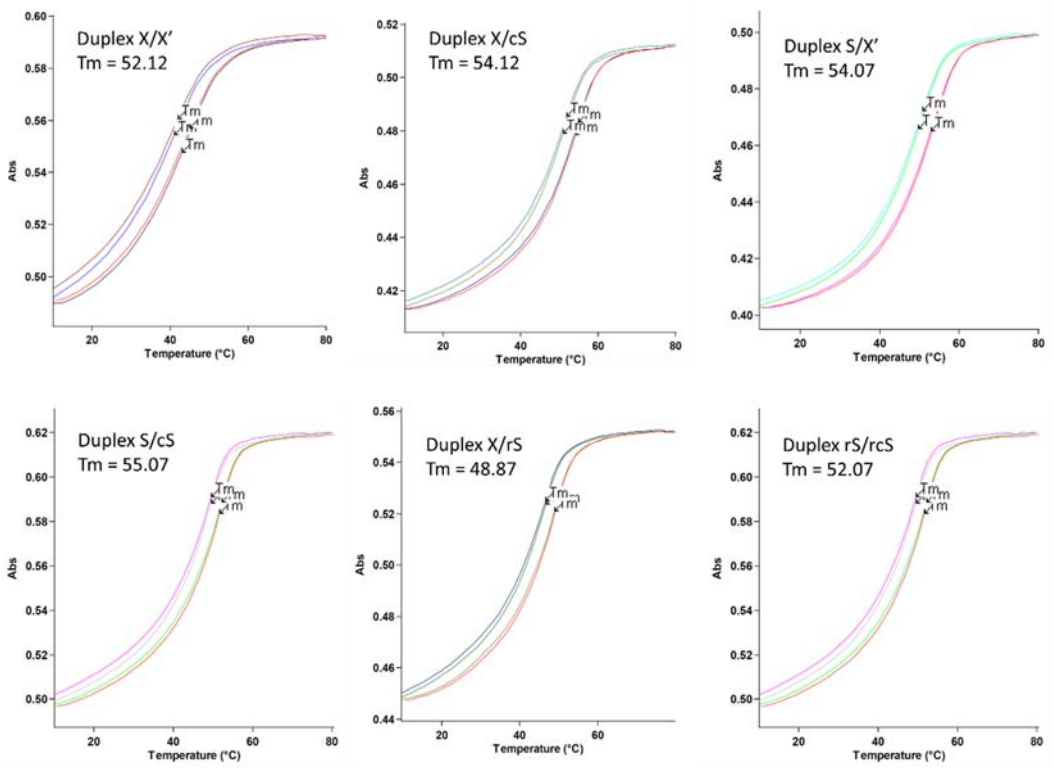


**Figure 5.15: Melting curves of duplex X/X', X/cS, S/X', S/cS, X/rcS and rS/X'**; X = d(5'-T*GT*AA*ACCA*TGAT*GTGCTGCT*A); X′ = d(5'-TAGC*AGC*ACATC*ATG*GTTTACA); S = d(5'-TACTGAGAGACACTGATTCTGAA); cS = d(5'-TTCAGAATCAGTGTCTCTCAGTA); rS = r(5'-TAC TGA GAG ACA CTG ATT CTG AA); rcS = r(5'-TTCAGAATCAGTGTCTCTCAGTA) at 10 mM NaCl/10 mM $Na_2HPO_4$; * = phosphoramidimidate.

Additionally, several Tm measurements were carried out with duplexes having variable number of phosphoramidimidate internucleotide linkage and salt concentrations. The results are summarized in table 5.2 and 5.3.

**Table 5.2: Melting temperature of duplex X/X', X/cS, S/X' and S/cS**

| Duplex | Number of modifications first strand | Number of modifications complementary strand | Tm | ΔTm** | ΔTm/total number of modifications |
|---|---|---|---|---|---|
| X/X' # | 5 | 5 | 52.12 | 2.95 | 0.30 |
| X/cS # | 5 | 0 | 54.12 | 1.0 | 0.20 |
| S/X' # | 0 | 5 | 54.07 | 0.95 | 0.19 |
| S/cS # | 0 | 0 | 55.07 | 0 | 0 |
| X/X' ## | 5 | 5 | 66.22 | 8.9 | 0.89 |
| X/cS ## | 5 | 0 | 71.17 | 3.95 | 0.79 |
| S/X' ## | 0 | 5 | 70.17 | 4.95 | 0.99 |
| S/cS ## | 0 | 0 | 75.12 | 0 | 0 |

X = d(5'-TGT*AA*ACCA*TGAT*GTGCTGCT*A); X′ = d(5'-TAGC*AGC*ACATC*ATG*GTTTAC*A); S = d(5'-TGTAAACCATGATGTGCTGCTA); cS = d(5'-TAGCAGCACATCATGGTTTACA ); #: 10 mM NaCl/10 mM $Na_2HPO_4$; ##: 1 M NaCl/10 mM $Na_2HPO_4$; * = phosphoramidimidate; **: ΔTm = Tm for standard DNA – observed Tm.

**Table 5.3: Melting temperature of duplex X/X', X/cS, S/X' and S/cS**

| Duplex | Number of modifications first strand | Number of modifications complementary strand | Tm (°C) | ΔTm** (°C) | ΔTm/total number of modifications |
|---|---|---|---|---|---|
| X/X' # | 11 | 11 | 36.52 | 15.6 | 0.7 |
| X/cS # | 11 | 0 | 44.52 | 7.6 | 0.69 |
| S/X' # | 0 | 11 | 46.57 | 5.55 | 0.50 |
| S/cS # | 0 | 0 | 52.12 | 0 | 0 |
| X/X' ## | 11 | 11 | 46.12 | 16.9 | 0.77 |
| X/cS ## | 11 | 0 | 54.02 | 7.58 | 0.69 |
| S/X' ## | 0 | 11 | 55.07 | 6.53 | 0.59 |
| S/cS ## | 0 | 0 | 61.60 | 0 | 0 |

X = d(5'-TA*CT*GA*GA*GA*CA*CT*GA*TT*CT*GA*A); X′ = d(5'-TT*CA*GA*AT*CA*GT*GT*CT*CT*CA*GT*A); S = d(5'-TACTGAGAGACACTGATTCTGAA); cS = d(5'-TTCAGAATCAGTGTCTCTCAGTA); #: 10 mM NaCl/10 mM $Na_2HPO_4$; ##: 100 mM NaCl/10 mM $Na_2HPO_4$; * = phosphoramidimidate; **:ΔTm = Tm for standard DNA– observed Tm.

## 5.9: Enzymatic Studies with Snake Venom Phosphodiesterase Exonuclease (SVPDE)

In order to evaluate the relative exonuclease susceptibility of phosphoramidimidate modified DNA, selected 2'-deoxyoligonucleotides were tested for stability against snake venom phosphodiesterase (SVPDE, 3'-exonuclease). A $T_{10}$ was synthesized so as to contain two phosphoramidimidate linkages – one at the 5′- and one at the 3′ ends (**ODN53**). An unmodified $T_{10}$ was used as the control (**ODN54**). A sample of the oligomer (2 OD) was incubated at 37 °C with 150 μL of 100 mM Tris-HCl buffer (pH 9.0), 10mM $MgCl_2$, (2.5 μg) SVPDE in a total volume of 200 μL. Aliquots were removed at different time points, quenched by the addition of 1.0 M EDTA and stored in dry ice until analyzed by analytical RP-HPLC (**Figure 5.16**).

**A**

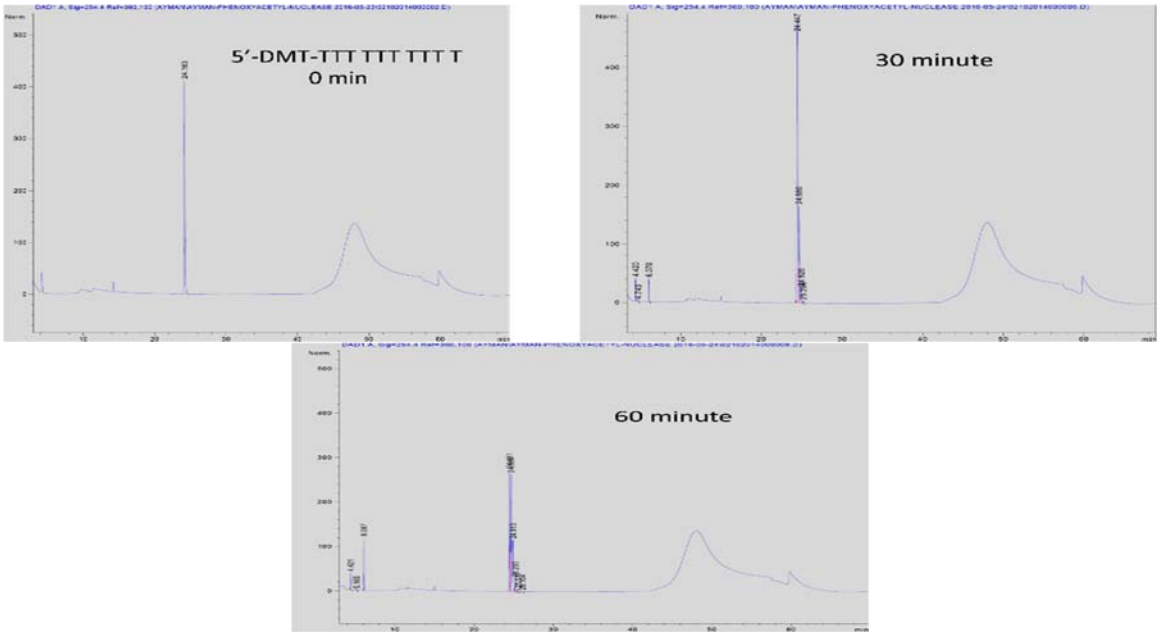


**B**

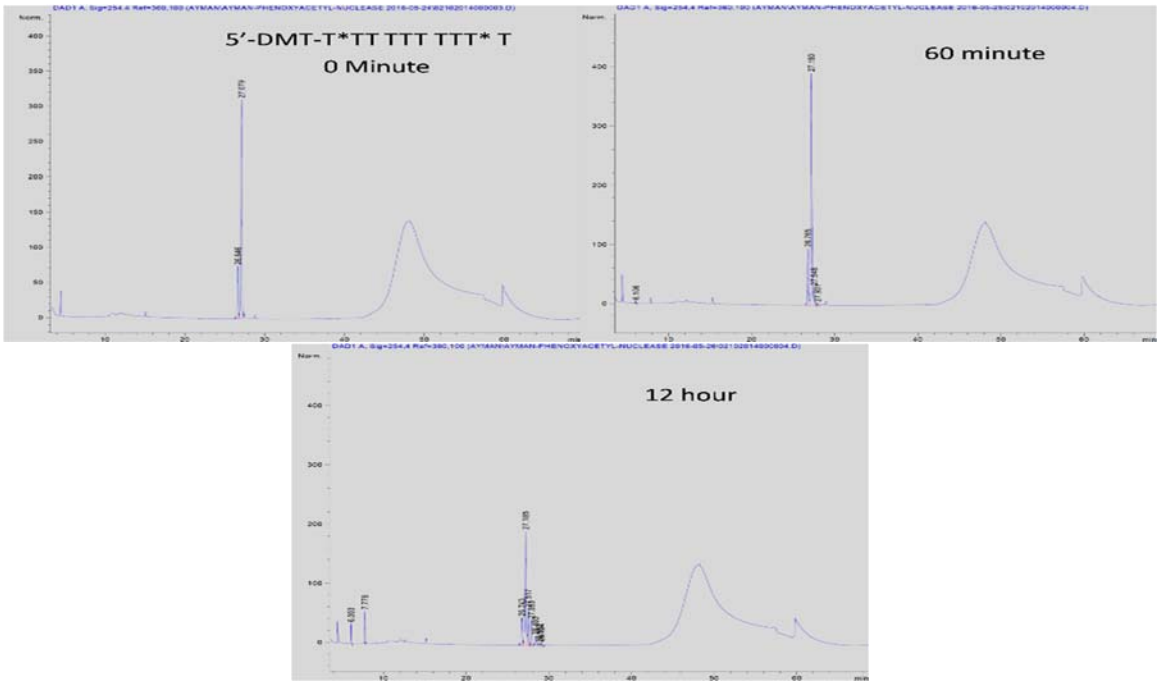


Figure 5.16: Time-dependent enzymatic exonuclease degradation of **ODN54**: 5'-DMT-TTTTTTTTTT and **ODN53**: 5'-DMT-T*TTTTTTTT*T with Snake Venom Phosphodiesterase (SVPDE). ODNs were treated with SVPDE, aliquots of the reaction mixture at different time points were analyzed by RP-HPLC. Panel A: unmodified DNA (**ODN54**) 0, 30, 60 minutes. Panel B: Phosphoramidimidate DNA (**ODN53**) 0, 1, 12 hours. 2'-Deoxyoligonucleotide degradation from the 3' end is indicated by appearance of a mononucleotide peak (retention time 6 minutes) using the reverse phase HPLC (RP-HPLC). *: Phosphoramidimidate.

When a 2'-deoxyoligonucleotide is incubated with SVPDE it degrades from the 3' end and generates mononucleotides which appear by reverse phase HPLC (RP-HPLC) with retention time around 6 minutes. The degradation rate with natural phosphate DNA is more than 90% degradation in 1 hour. Under the same experimental conditions, the 2'-deoxyoligonucleotide (**ODN54**) containing one phosphoramidimidate modification at each end showed more than ten times longer resistance against the 3′ exonuclease SVPDE with less formation of mononucleotides (approximately 10 hours for 90% degradation). The appearance of a new peak at retention time 7.7 minutes corresponds to a dinucleotide. This is explained by SVPDE which is known to jump one nucleotide unit from the 3' end and degrade a natural phosphate linkage.

## 5.10 Biological and Biochemical Activity

Since phosphoramidimidate DNA possesses a positive charge at biological pH (7-7.5), it is possible that the biological activity and cell uptake would be affected by this charge. Previous work[46] showed that the bioactivity with cation conjugated oligonucleotides, relative to negatively charged oligomers, superior cellular uptake properties and facilitate endosomal release via the proton sponge mechanism.

In order to explore the biological activity of phosphoramidimidate DNA, the non-toxic oligonucleotide delivery method known as “passive transfection” was used. This procedure does not require liposomes, electroporation, or microinjection for entry of the oligonucleotide into cells. One simply places the oligonucleotide and appropriate cells in growth media and tests for uptake. A 5'-fluorescein chromophore tag is linked through a thiophosphate linkage to the phosphoramidimidate oligonucleotide. Using a thiophosphate linkage increases resistance toward degradation by nucleases and the fluorescein chromophore can be used to monitor cellular uptake using flow cytometry or microscopy. Phosphoramidimidate modifications were introduced with one at the 3′ end and the remaining distributed near the middle of the DNA. As shown in section 5.9, HPLC studies demonstrated that phosphoramidimidate has resistance against snake venom phosphodiesterase. This observation suggests that these 2′-deoxyoligonucleotides would be resistant towards cellular nucleases. Perhaps as well this positively charged modification would have enhanced binding to cell membranes and cellular uptak.

**FACS Analysis**

Uptake of phosphoramidimidate modified DNA in HeLa cells was measured by taking advantage of the fluorescein tag. The cells were seeded ~$1 \times 10^5$ cells/well (12 well plates) and incubated in DMEM media for 24 hours. The concentration of 5'-fluorescein labeled phosphoramidimidate DNA in HyPure Molecular Biology Grade Water was measured by UV spectroscopy. For transfection, the medium was replaced with Opti-MEM premixed with the ODNs at various concentrations (0.5, 1.0, and 3.0 μM) and the cells were incubated for 24 hours.

Flow cytometric data on at least 10,000 cells per sample was acquired on a Moflow flow-cytometer (BeckmanCoulter) equipped with a single 488 nm argon laser and a 530/40 nm emission filter (Fluorescein). Raw flow cytometry data was visualized using Summit 4.3 software (BeckmanCoulter). Fluorescence intensity of the 5′-fluorescein tag was analyzed for cells presenting higher fluorescence than the background. The background was defined as the auto-fluorescence of cells. Figure 5.17 shows the cell transfection results for **ODN45**. In this figure, it shows that HeLa cells accumulate more fluorescent activity after 24 hours incubation. Part A shows the fluorescent of HeLa cells without oligonucleotide incubation. Part B shows the fluorescent of HeLa cells incubated with 0.5 μM 5'-fluorescein labeled 2'-deoxyoligonucleotide. The Y-axis shows the number of cells and the X-axis shows the intensity of the fluorescein. Shifting the main peak towards the right in the X-axis indicates the increased intensity of the fluorescein which is coming from the fluorescein tag on the nucleotides. Similarly part C and D also show that the main peak is shifted towards the right on the Y-axis.

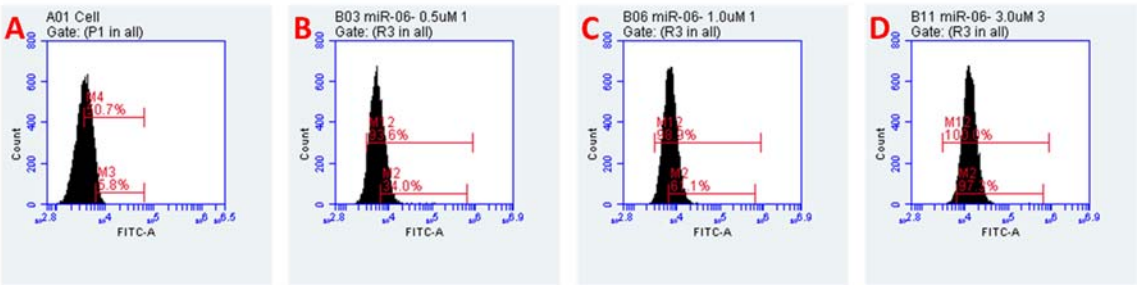


Figure 5.17: FACS analysis of ODN43 5'-fluorescein labeled 6-FAM-P(S)- T*GTA*AA*CCAT*GA*TGTGCTGCT*A. (A)HeLa cells; (B) HeLa cells transfected for 24 h with ODN45 at 0.5 µM; (C) HeLa cells transfected for 24 h with ODN45 at 1.0 µM; (D) HeLa cells transfected for 24 h with ODN45 at 3.0 µM; *: Phosphoramidimidate modification; 6-FAM-P(S): 6-Carboxyfluorescein thioimidate.

Figure 5.18 summarizes the cell uptake results using a bar diagram that shows the percentage of HeLa cells with uptake on the Y-axis, at concentrations 0.5, 1.0 and 3.0 µM of fluorescently labeled single-stranded DNAs **ODNs 43−46** after 24h of transfection in Opti-MEM in absence of lipid transfecting agent.

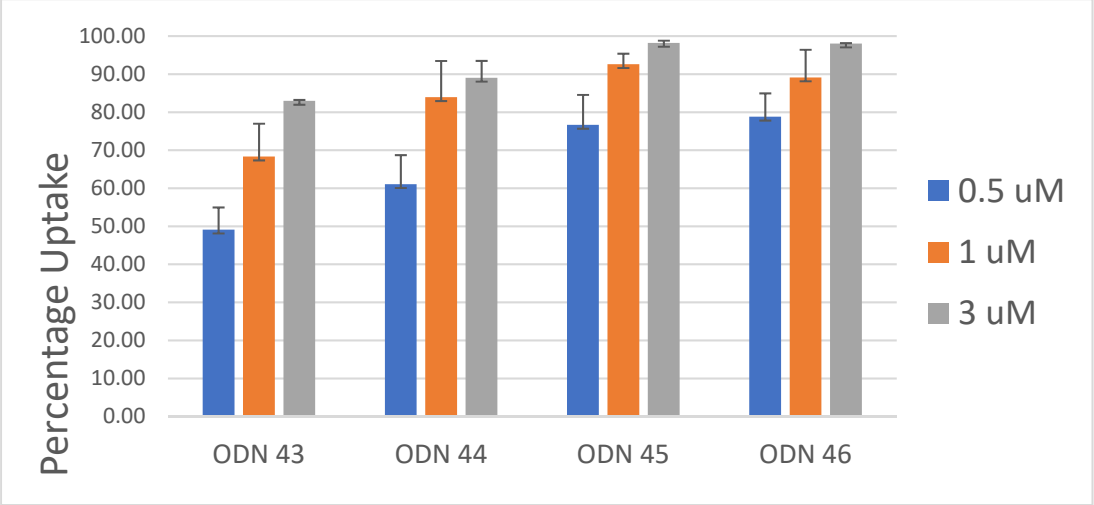


Figure 5.18: Bar diagram showing the percentage of HeLa cells with uptake, at various concentrations 0.5, 1.0 and 3.0 µM, of fluorescently labeled single-stranded DNAs ODNs 1−4 after 24h of transfection in Opti-MEM in absence of lipid transfecting agent. **ODN43**: 6-FAM-P(S)- T*GT AAA* CCA TGA T*GT GCT GCT*A; **ODN44**: 6-FAM-P(S)-TGT*AAACC*AT*GAT*GTGCTGCT*A; **ODN45**: 6-FAM-P(S)-T*GTA*AA*CCAT*GA*TGTGCTGCT*A; **ODN46**: 6-FAM-P(S)- T*GT* AA*A C*CA TG*A T*GT GCT GCT* A; *: Phosphoramidimidate modification; 6-FAM-P(S): 6-Carboxyfluorescein thioimidate.

As shown in figure 5.18, 50% of cells showed cell uptake when **ODN43** containing 4 modifications was used at 0.5 μM concentration. When the concentration was increased to 1.0 μM and 3.0 μM for the same ODN, the uptake increased to 68% and 80% respectively. With 2′-deoxyoligonucleotides having 5, 6 and 7 phosphoramidimidate modifications (**ODNs 44-46**) the uptake increased with saturation at 3 μM for **ODN45** and **ODN46**. This suggests oligomers having 6 and 7 phosphoramidimidate modifications are maximally transfected at 3 μM. Additionally, even at 0.5 μM these ODNs were taken up by 80% of the HeLa cells. Also, of interest was the observation that **ODN43** with only four modifications transfects 50% of the HeLa cells even at 0.5 μM.

**Microscope Imaging**

The transfection experiments showed a significant uptake of phosphoramidimidate DNA. This could be explained by the presence of cationic phosphate that interacts with phospholipids on cell surfaces and thus facilitates transfection. However, an alternative explanation is that these oligomers were only on the surface of the cell membrane and never actually transfected. FACS analysis could simply demonstrate an ionic interaction of these ODNs with phospholipids on cell surfaces and that they do not undergo transfection. This question was addressed using a confocal microscope to examine the location of the fluorescein tag on the 2′-deoxyoligonucleotides.

Initially, HeLa cells were seeded at $0.1 \times 10^6$ cells/well in 10 mL glass bottom dishes (CELLview™ Cell Culture Dishes, Glass Bottom, Sterile, Greiner Bio One). After 24 hours at 60% confluency, 250 µL of stock solution of **ODN45** diluted in OptiMEM was added to each well making the final concentration of 3 µM and cells were then incubated at 37 °C for 24 hours. Cells were stained with Hoechst 33258 to visualize nuclei. To show the cell membrane boundaries the same procedure was used staining with Hoechst 33258 then cells being stained with 1 x of CellMask™ Orange Plasma Membrane Stain. Cells were analyzed in OptiMEM using a confocal microscope.

Figure 5.19 shows laser scanning confocal images (40× magnification) of live HeLa cells treated with 3 µM **ODN45** of fluorescently labeled single-stranded DNA containing 5 phosphoramidimidate modification was efficiently taken up into Hela cells for 24 hours transfection in the absence of a lipid transfecting reagent. Part A is a phase contrast image that shows the cells boundaries and in part B the nucleus appears in blue due to staining with Hoechst 33258 dye. The fluorescein signal is shown in green and represents the 5'-fluorescein labeled modified DNA as it appears part C. Part D shows the superimposed image for the three channels

used to visualize cells. Figure 5.20 is similar to 5.19, except the cell membranes are red due to using CellMask™ Orange Plasma Membrane Stain.

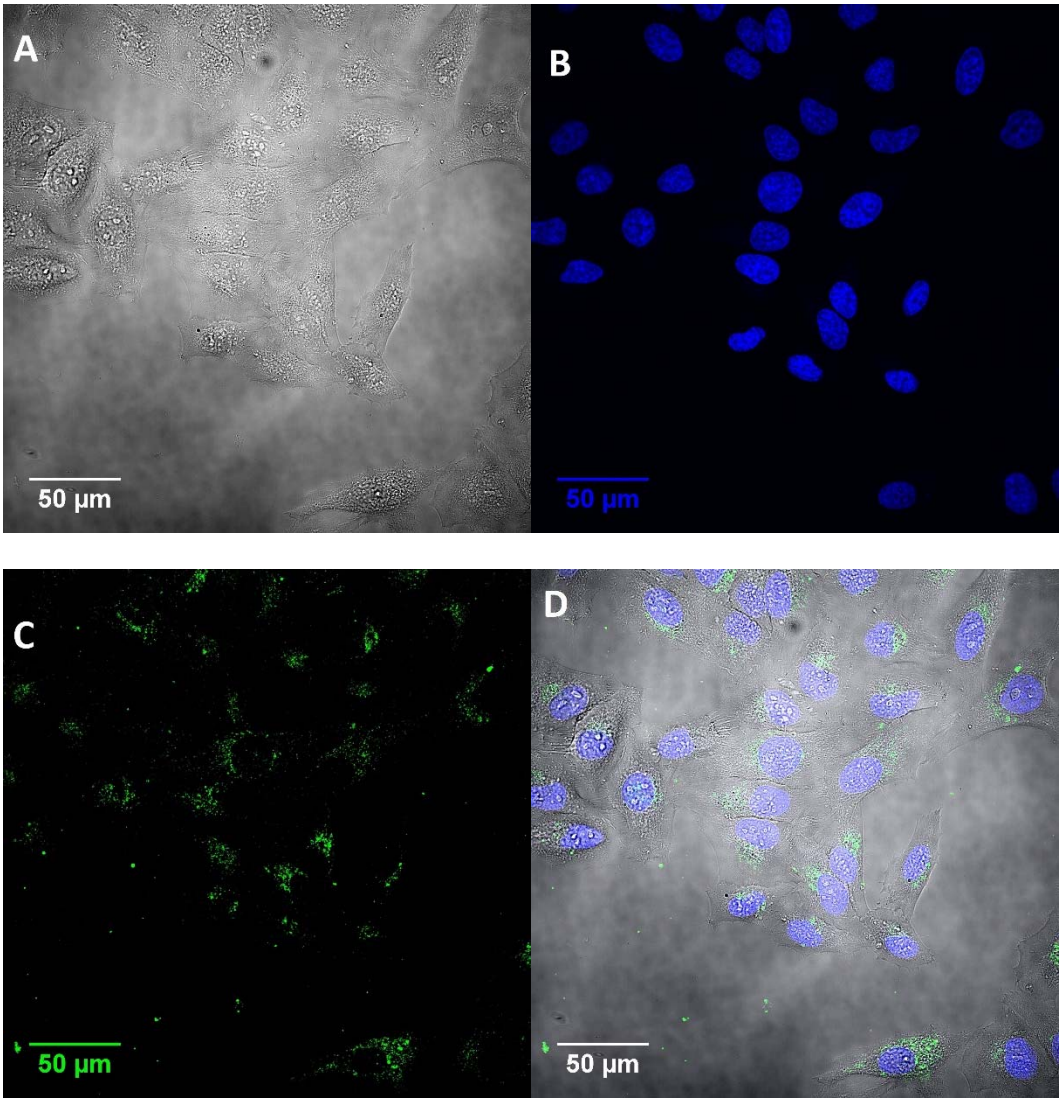


Figure 5.19: Fluorescence microscopy image (40× magnification) of live HeLa cells treated with 3 µM of ODN**45**, a fluorescently labeled single-stranded DNA which were efficiently taken up into Hela cells for 24 hours transfection in absence of lipid transfecting. A) Phase contrast image to show the cells boundaries; B) Nucleus staining with Hoechst 33258 dye and shown in blue; C) The fluorescein signal is shown in green representing the 5'-fluorescein labeled modified DNA; D) Superimposed image for the three channels used to visualize cells.

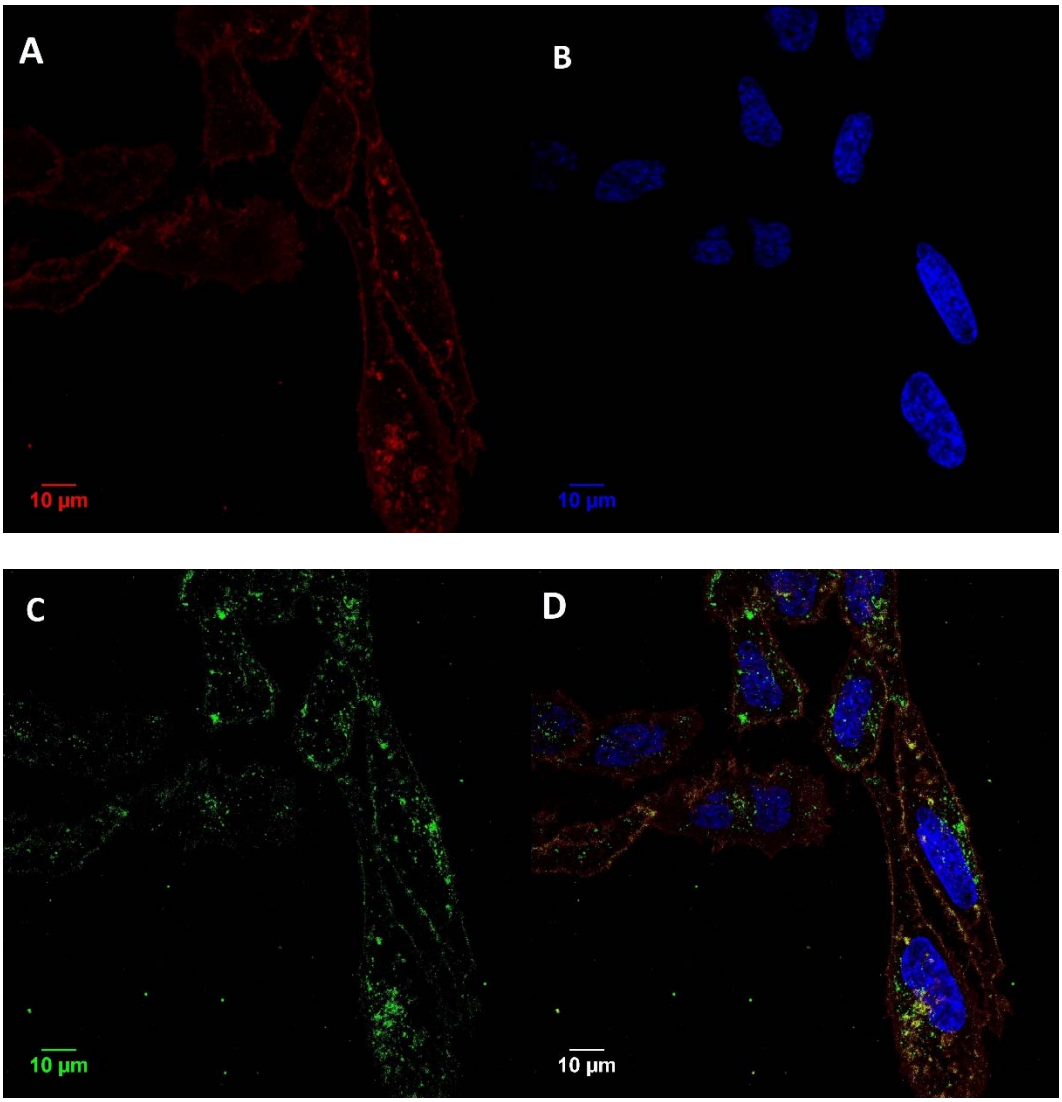


Figure 5.20: Fluorescence microscopy image (40× magnification) of live HeLa cells treated with 3 µM of **ODN45**, a fluorescently labeled single-stranded DNA which was efficiently taken up into Hela cells for 24 hours transfection in absence of lipid. A) Superimposed image for the three channels used to visualize cells; B) Nucleus staining with Hoechst 33258 dye and shown in blue. C) The fluorescein signal is shown in green representing the 5'-fluorescein labeled modified DNA; D) cell membrane is stained with CellMask™ Orange Plasma Membrane shows it boundaries in red;

Figure 5.21 shows z stack confocal image where the Z-axis was used to generate z slices that stack to encompass the entirety of the cells within each field of view and generate a 3D image, thus ensuring the complete detection of any green fluorescein signal, which represents the 5`-fluorescein labeled DNA, present around the nucleus which appears in blue.

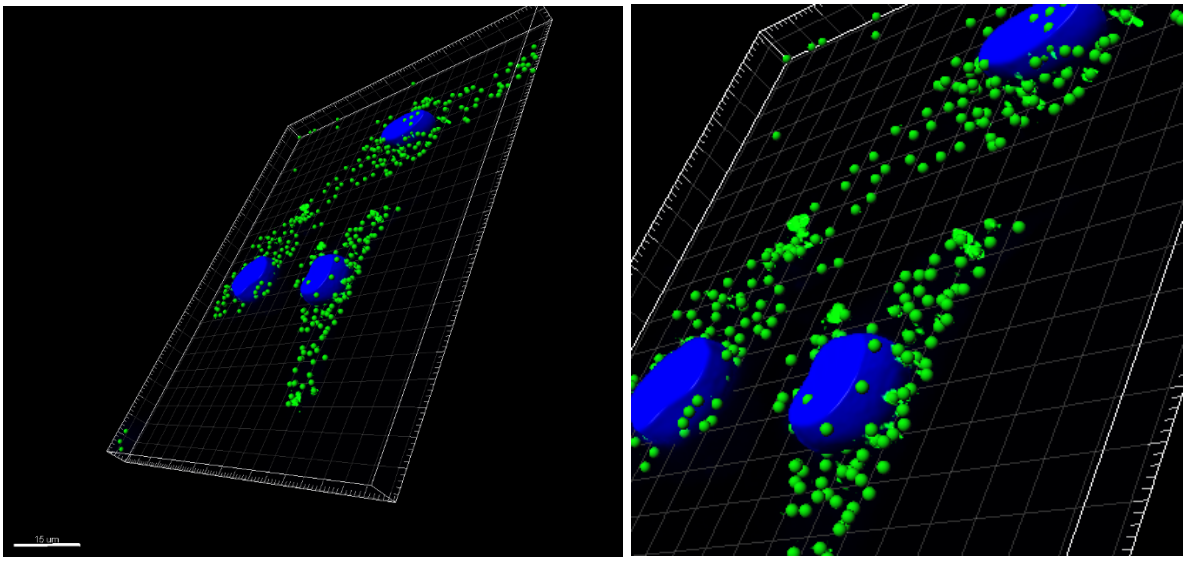


Figure 5.21: Confocal microscope Z-stack images (40× magnification) of live HeLa cells treated with 3 µM **ODN45**, a fluorescently labeled single-stranded DNA which was efficiently taken up into Hela cells for 24 hours transfection in absence of lipid. A) Z-stack image, nucleus staining with Hoechst 33258 dye and shown in blue. The fluorescein signal is shown in green representing the 5'-fluorescein labeled modified DNA; B) Zoomed and inclined view confirmation of image A. scale bar in image A is 15 µm.

## 5.11 Hydrolysis of RNA Heteroduplexes with E. coli RNase H1

The search for antisense and diagnostic DNA analogs has led to a wide range of DNA modifications but few possess the three necessary properties for antisense activity: an ability to form sequence-specific duplexes with complimentary oligoribonucleotides, activation of RNase H and resistance towards nucleases. These observations prompted me to investigate whether phosphoramidimidate DNA could activate RNase H1 and potentially function in antisense therapeutic activity.

Phosphoramidimidate derivatives were tested for their ability to stimulate RNase H1 activity. Thus a 5'-fluorescein labeled RNA and a complementary natural DNA, 2'-O-methyl RNA or phosphoramidimidate ODN (**ODN 55, 56 and 57**) were treated with RNase H1. The positive control was natural DNA complementary to the same RNA that should activate RNA degradation. A negative control was the 2'-O-methyl RNA in duplex with the same RNA as this analogue does not stimulate RNase H1 activity.[47] Two samples of each duplex were incubated in 35 μL of the assay buffer. E. coli RNase H1 (3 units) was added to each sample and the assay was kept at 25 °C for 8 hours. The reaction mixtures were analyzed by polyacrylamide gel electrophoresis and visualized using a Molecular Dynamics Typhoon Phosphorimager.

As shown in figure 5.22, the natural DNA strongly activated RNaseH (**Figure 6.22, lane 6**) while the 2'-O-Methyl oligonucleotides gave minimal activations (Lane 2). Importantly, the phosphoramidimidate 2'-deoxyoligonucleotide (**Lane 5**) also strongly activated RNaseH. Thus, unlike 2'-O-Methyl containing oligonucleotides, the phosphoramidimidate 2'-deoxyoligonucleotides are potentially useful for RNaseH mediated antisense applications. The absence of enzyme (**Lanes 1, 4, 6**) or the absence of complementary DNA (**Lane 3**) kept the RNA intact.

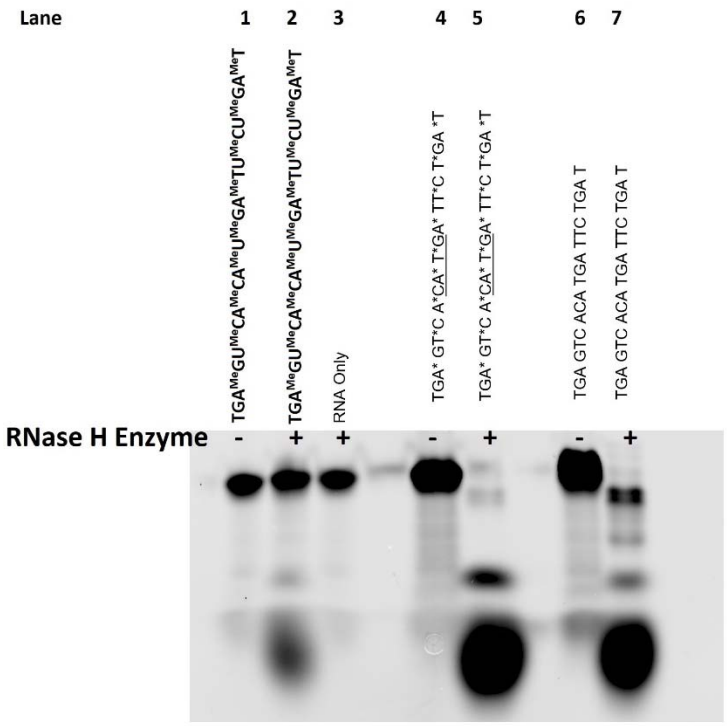


Figure 5.22: E. coli RNase H1 degradation of RNA. 5`-fluorescein labeled RNA was allowed to form duplexes with complementary ODNs (1-3), which were then treated with E. coli RNase H1 for 8 h and analyzed by PAGE.

Lane 1: 2'-O-methyl RNA ODN(1)/RNA; Lane 2: 2'-O-methyl RNA ODN(1), RNA, enzyme;

Lane 3: RNA, enzyme;

Lane 4: ODN (2)/RNA; Lane 5: ODN (2), RNA, enzyme;

Lane 6: ODN (3)/RNA; Lane 7: ODN (3), RNA, enzyme;

ODN 55: TGA$^{Me}$ GU$^{Me}$C A$^{Me}$CA$^{Me}$ U$^{Me}$GA$^{Me}$ TU$^{Me}$C U$^{Me}$GA$^{Me}$T

ODN 56: TGA* GT*C A*CA* T*GA* TT*C T*GA *T

ODN 57: TGA GTC ACA TGA TTC TGA T.

# CHAPTER 6

# A NOVEL SYNTHESIS OF PHOSPHORAMIDATE INTERNUCLEOTIDE LINKAGES

## 6.1: Introduction

Although phosphoramidate mononucleotides have been made as prodrugs,[48,49] there are only a few examples where phosphoramidate oligonucleotides have been investigated for various therapeutic applications.[50] This is primarily due to limitations in the synthesis chemistry for these compounds. The previous successful synthesis strategy developed to date proceeds by first preparing H-phosphonate oligonucleotides that are then oxidized with ammonia in order to generate the phosphoramidate internucleotide linkages (**figure 6.1**).[51] However, this method is limited to low overall yield and quality of the product oligonucleotides.

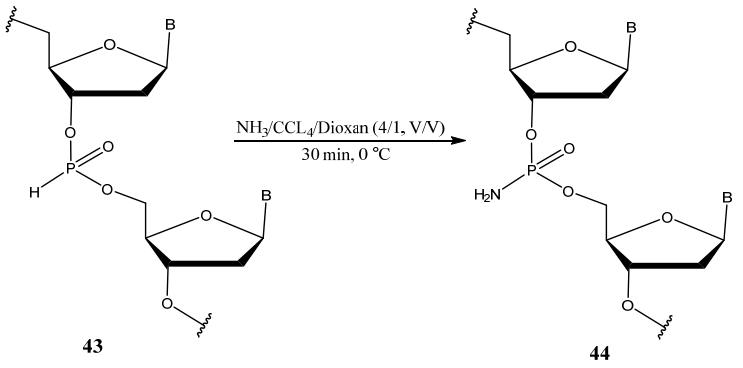


Figure 6.1: Oxidation conversion of H-phosphonate linkage (43) to phosphoramidate (44).

This chapter outlines a new approach for synthesizing phosphoramidate DNA. This method is based upon the successful strategy for preparing phosphoramidimidate DNA as outlined in chapter VI.

## 6.2 DNA Solid Phase Phosphoramidate Synthesis Using the Phenoxyacetyl Protecting Group.

The solid phase DNA synthetic cycle for preparing phosphoramidate DNA is shown in figure 6.2. As can be seen by comparing this strategy to the procedure used for preparing phosphoramidimidate DNA (**figure 5.4**) both are similar. The main difference is the oxidation step.

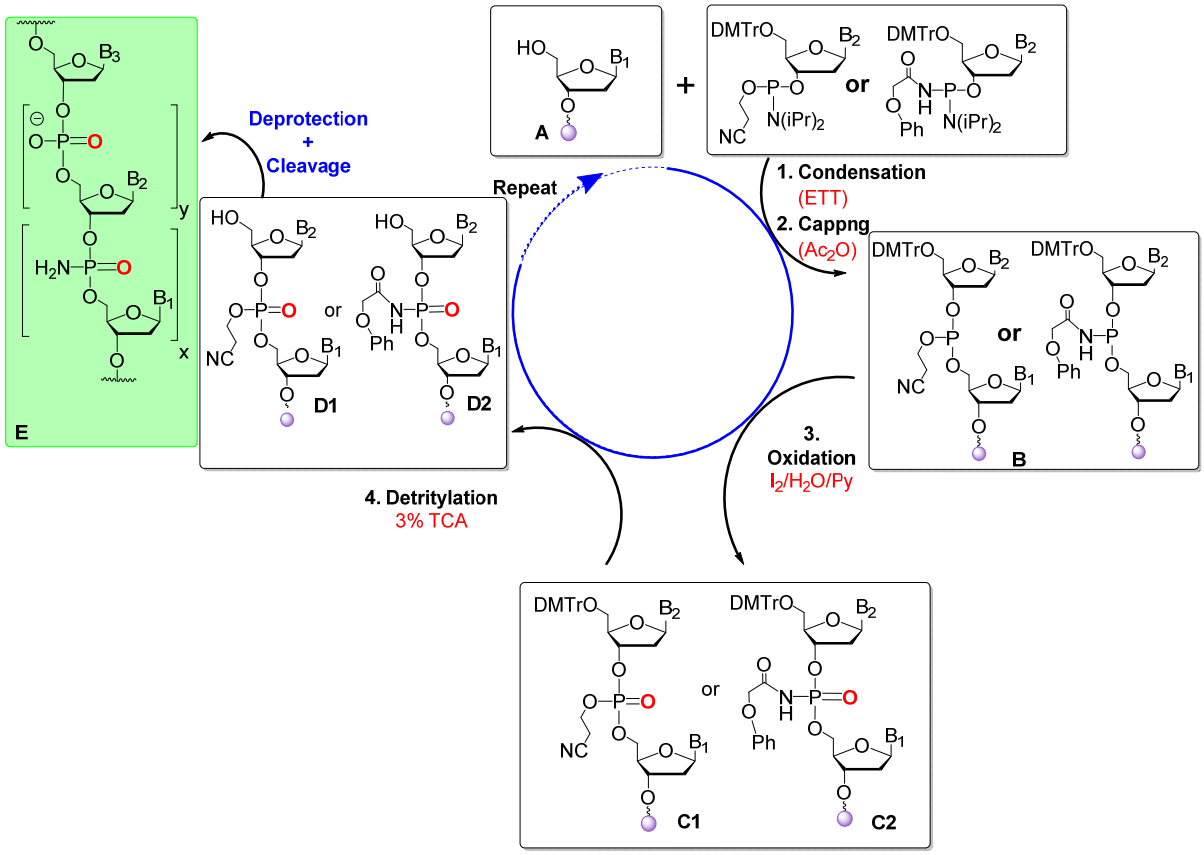


Figure 6.2 Solid-phase DNA synthesis cycle as used to synthesize phosphoramidate DNA.

In order to validate compatibility of synthons (**40 a-d**) with the solid phase DNA synthesis cycle shown in figure 6.2, DNAs containing phenoxyacetamide phosphoramidate internucleotide linkages at variable positions were synthesized. For simplicity, synthon (**40a**) was chosen initially for preparing 2'-deoxyoligonucleotides having the phosphoramidate internucleotide linkage. I first synthesized a $T_{12}$ 2'-deoxyoligonucleotide containing one modification located at the 5'-end of the DNA. In this synthesis scheme exposure of the modified linkage to different reagents as used during the solid phase cycle was minimized. I left the final 5' DMT protecting group on the 2'-deoxyooligonucleotide since this group shifts the polynucleotide away from failure sequences and provides a clearer image on the HPLC profile for evaluating the synthesis products and coupling efficiency. The crude reaction mixture was analyzed by HPLC after cleavage from the solid support. Several additional $T_{15}$ oligomers having one phosphoramidate linkage per 2'-deoxyoligonucleotide at variable positions were prepared and analyzed. As a result, in order to accommodate synthesis of 2'-deoxyoligonucleotides having phosphoramidate linkage the following modifications to the standard solid phase phosphoramidite synthesis protocol have been introduced:

1) Condensation Step: The concentration of phenoxyacetyl phosphoramidite was increased from 0.1M to 0.15 M. This change increased the product yield and decreased the amount of failure sequences. Using ETT as the activator and extending the condensation time to 15 minutes also increased the product yield and decreased the amount of failure sequences. Introduction of the monomers twice to the reaction column did not change the coupling yield.

2) Oxidation: The standard oxidizing solution consisting of $I_2/H_2O$/pyridine was used throughout the solid phase synthesis cycle in order to convert both the phenoxyacetyl protected phosphoramidite to phosphoramidate and the phosphite triester to phosphate.

In order to further test the synthesis, polynucleotides 12 to 21 in length and having two to four modifications at variable positions were next synthesized using all four nucleobases and the crude reaction mixtures were analyzed by HPLC. The purified product 2'-deoxyoligonucleotides were characterized by mass spectrometry and $^{31}P$ NMR. Figure 6.3 shows HPLC profiles for various 2'-deoxyoligonucleotides containing 2-4 phosphoramidate internucleotide linkages per 2'-deoxyoligonucleotide.

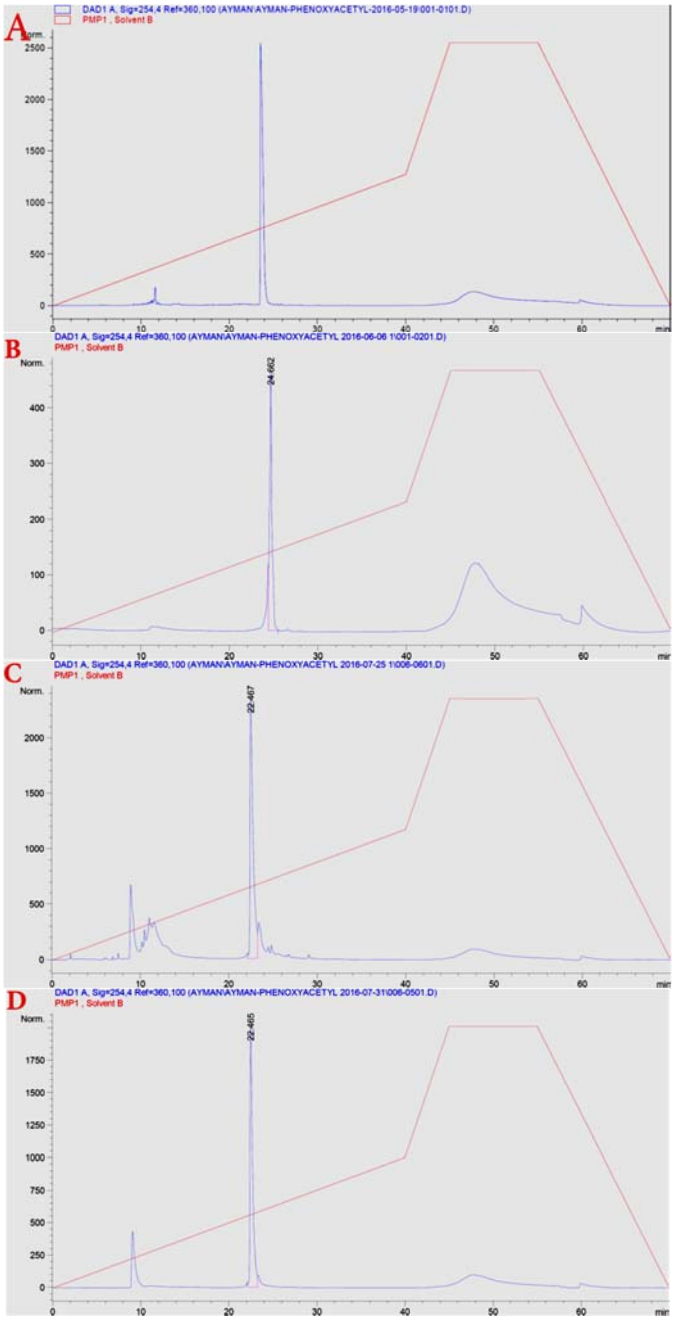


Figure 6.3: HPLC profiles (B-D) of crude reaction mixtures as obtained from the modified solid phase DNA synthesis cycle outlined in figure 6.2. The profile in A represents the total crude reaction mixture as obtained using the standard synthesis cycle. The targeted product peaks appear at retention time approximately 24 minutes for unmodified and modified DNA and failure sequences are at 10-14 minutes. Sequences: A) 5'-DMT-TTTTTTTTTTTTTTTTTTTT; B) 5'-DMT-TT*TTTT*TTTTT*T; C) 5'-DMT- TGT* AAA CCA T*GA TGT GCT GCT* A; D) 5'-DMT- TGT* AAA CCA TGA T*GT* GCT GCT* A; * = phosphoramidate.

## 6.3 Phenoxyacetamide Deprotection of Phosphoramidate DNA

Although the phenoxyacetamide can be removed in 1 hour with aqueous ammonia when used to protect the exocyclic amines of cytosine, adenine and guanine, I found it to be more difficult to remove when it is used as the phenoxyacetyl protecting group on the phosphoramidate internucleotide linkages. Moreover, previous research reported the instability of using 30% aqueous ammonia at 55 °C in order to deprotect 2'-deoxyoligonucleotides containing phosphoramidate internucleotide linkages.[51]

As a result of these observations, several deprotection procedures were evaluated for removal of the phenoxyacetamide from the phosphoramidate internucleotide linkage. These included varying the basic conditions, time, temperature and hydrous verses anhydrous conditions. The specific reagents and conditions included: aqueous ammonia, anhydrous ammonia in dioxane, 1:1 anhydrous ammonia/ toluene, 1:1 anhydrous ammonia/ ethylenediamine, 1:1 ethylenediamine/toluene, aqueous ammonia with 10% ethylene diamine and aqueous ammonia with 10% ethylenediamine.

The study was performed on 2'-deoxyoligonucleotide 22 nucleotides in length having combinations of all four nucleobases with 3 phosphoramidate internucleotide linkage per oligomer. Each synthesized oligomer while still attached to CPG was divided into two parts; one was cleaved from CPG using 30% aqueous ammonia for 1 hour at room temperature, the ammonia was removed and the oligomers redissolved in water. These conditions (30% aqueous ammonia for 1 hour at room) did not remove the phenoxyacetamide protecting group. A sample of this aqueous solution was

analyzed by HPLC in order to evaluate the quality of the total product mixture. The second half was dissolved in the appropriate test solution and deprotection studied under the appropriate procedure. Solvent was removed, the sample was redissolved in water, filtered from CPG and injected into the HPLC. The HPLC profiles of these two samples were then compared in order to evaluate the deprotection procedure.

Of the various conditions studied, it was found that either 1) 30% aqueous ammonia at 45 °C for 24 hours or 2) 0.5 mL ethylenediamine at room temperature for 15 minutes followed by 0.5 mL of 0.5 M anhydrous ammonia in dioxane and incubate for 24 hours at 45 °C were the best cleaving conditions since they simultaneously cleaved the products from the solid support and removed the phenoxyacetyl and nucleobase protecting groups simultaneously. The purity and compatibility of these two methods was confirmed by $^{31}$P NMR and mass spectrometry. Using aqueous ammonia did not show any difference with the second deprotection conditions.

All 2'-deoxyoligonucleotide samples were purified by preparative RP-HPLC and analyzed by mass spectrometry in order to confirm complete deprotection and generation of the desired phosphoramidate internucleotide linkage. $^{31}$P NMR provided further evidence that the chemical shifts were consistent with literature and the ratio of the phosphoramidate to phosphate was as expected of each oligonucleotide.

Using these optimized procedures for synthesizing phosphoramidate DNA, 2'-deoxyoligonucleotides 15 to 22 nucleotides in length with 3 to 14 phenoxyacetamide phosphoramidate internucleotide linkage were synthesized. The optimized cleavage and purification procedure was as follow:

1) Cleave the 2'-deoxyoligonucleotide from the solid support and simultaneously remove the nucleobase and the phenoxyacetyl protecting groups using 1:1 ethylenediamine: 0.5M $NH_3$ in dioxane (24 hours at 45 °C) or aqueous ammonia (24 hours at 45 °C).
2) Using prep-HPLC the product 2'-deoxyoligonucleotides containing a 5'-DMT were separated from side products. This was possible because the hydrophobic product has a longer retention time than side-products lacking the DMT group.
3) Incubate the purified oligo in 80% aqueous acetic acid for 1 hour at room temperature. These conditions remove the DMT group without generating 2'-deoxyoligonucleotide degradation products.
4) Evaporate the acidic solution using vacuum and reconstitute the sample in 1 mL of 0.05 M triethylammonium bicarbonate solution.
5) Purify the product 2'-deoxyoligonucleotide using preparative RP-HPLC.

Table 6.1 shows the sequences of the various synthesized 2'-deoxyoligonucleotides containing 3 - 14 phosphoramidate modification at various positions. These 2'-deoxyoligonucleotides have been used for several experiments including biological activity studies. A 5'-fluorescein thiophosphate tag was introduced at the 5' terminus of certain 2'-deoxyoligonucleotides. This was carried out using the commercially available 5'-fluorescein phosphoramidite followed by oxidation to thiophosphate. Joining fluorescein to DNA through phosphorothioate linkages enhance resistance to cellular nucleases and therefore enhance the

probability that imaging experiments with this tag reflects DNA and not simply fluorescein.

**Table 6.1: 2'-Deoxyoligonucleotide sequences containing phosphoramidate modifications.**

| No. | Structure |
|---|---|
| **ODN58** | DMT-T*GTAAAC*CATGAT*GTGCTGCT*A |
| **ODN59** | DMT-T*GTA*AA*CCAT*GA*TGTGCTGCT*A |
| **ODN60** | DMT-TGT*AAA*CCA*T*GAT*GTGCTGCT*A |
| **ODN61** | DMT-TGTA*AA*CCA*TGA*TGTGCTGCTA |
| **ODN62** | DMT-T*GTAAAC*CATGAT*GTGCTGCT*A |
| **ODN63** | T*GTA*AA*CCAT*GA*TGTGCTGCT*A |
| **ODN64** | TGT*AAA*CCA*T*GAT*GTGCTGCT*A |
| **ODN65** | TGTA*AA*CCA*TGA*TGTGCTGCTA |
| **ODN66** | TGT*AAACCAT*GAT*GT*GCT*GCTA |
| **ODN67** | DMT-TG*TAAACCATG*ATGTGC*TGC*TA |
| **ODN68** | DMT-TG*TAAACC*ATG*ATGTGC*TGC*TA |
| **ODN69** | DMT-TG*TAAACC*ATG*ATG*TGC*TGC*TA |
| **ODN70** | DMT-TG*TAA*ACC*ATG*ATG*TGC*TGC*TA |
| **ODN71** | DMT-TGT*AAA*CCA*TGA*TGT*GCT*GCT*A |
| **ODN72** | TGTAAAC*C*ATGATGTGC*TGC*TA |
| **ODN73** | T*GT*AAACC*AT*GAT*GTGCTGCT*A |
| **ODN74** | T*GTA*AA*CCAT*GA*TGTGCTGCT*A |
| **ODN75** | T*GT*AAACC*ATGAT*GTGCTGCT*A |
| **ODN76** | 6-FAM-P(S)- TGT*AAACC*AT*GAT*GTGCTGCT*A |
| **ODN77** | 6-FAM-P(S)- T*GTA*AA*CCAT*GA*TGTGCTGCT*A |
| **ODN78** | 6-FAM-P(S)- C*TAGCC*ATG*ATGT*GTGCTGCT*A |
| **ODN79** | 6-FAM-P(S)- T*GT*AAACC*ATGAT*GTGCTGCT*A |

*: phosphoramidate; 6-FAM-P(S): 5'-fluorescein thiophosphoramidate.

## 6.4 Biological and Biochemical Activity

In order to explore the biological activity of phosphoramidate DNA, the non-toxic oligonucleotide delivery method known as “passive transfection” was used. This procedure does not require liposomes, electroporation, or microinjection for entry of the oligonucleotide into cells. One simply places the oligonucleotide and appropriate cells in growth media and tests for uptake using the 5'-fluorescein tag. Phosphoramidate modifications were introduced with one at the 3′-end and the remaining distributed near the middle of the DNA. Previous work has showed that the phosphoramidate linkage has resistance against various nucleases.[52] Thus having phosphoramidate at the 3'-end and thiophosphate at 5'-end should decrease the rate of 2′-deoxyoligonucleotide degradation by cellular exonucleases.

### FACS Analysis

Uptake of phosphoramidate modified DNA in HeLa cells was measured by taking advantage of the fluorescein tag. The cells were seeded ~$1 \times 10^5$ cells/well (12 well plates) and incubated in DMEM media for 24 hours. The concentration of 5'-fluorescein labeled phosphoramidate DNA in HyPure Molecular Biology Grade Water was measured by UV spectroscopy. For transfection, the medium was replaced with Opti-MEM premixed with the ODNs at various concentrations (0.5, 1.0, and 3.0 μM) and the cells were incubated for 24 hours. Fluorescence intensity was analyzed for cells presenting higher fluorescence than background. The background was defined as the auto fluorescence of cells. Figure 6.4 show the cell transfection results for **ODN77**. In this figure, it shows that HeLa cells accumulate more fluorescent activity after 24 hours incubation. Part A shows the fluorescent of HeLa cells without oligonucleotide

incubation. Part B shows the fluorescent of HeLa cells incubated with 0.5 µM 5'-fluorescein labeled 2'-deoxyoligonucleotide. The Y-axis shows the number of cells and the X-axis shows the intensity of the fluorescein. Shifting the main peak towards the right in the X-axis indicates the increased intensity of the fluorescein which is coming from the fluorescein tag on the nucleotides. Similarly part C and D show that the main peak is shifted towards the right on the Y-axis.

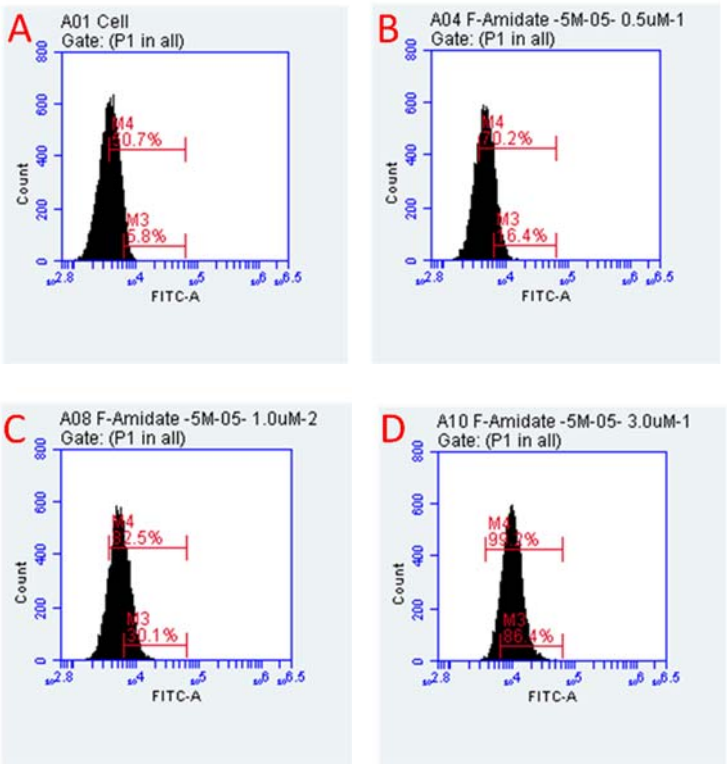


Figure 6.4: FACS analysis of **ODN77** 6-FAM-P(S)- T*GT AAA CCA TG*A T*GT GCT GCT* A. HeLa cells, auto fluorescence of cells is considered as the zero point. The percentile shifting of the cells represent the percent uptake; A) Shows the auto fluorescence of cells which is considered as zero point; (B) HeLa cells transfected for 24 h with **ODN77** at 0.5 µM; (C) HeLa cells transfected for 24 h with **ODN77** at 1.0 µM; (D) HeLa cells transfected for 24 h with **ODN77** at 3.0 µM; *: Phosphoramidate modification; 6-FAM-P(S): 6-Carboxyfluorescein thioimidate.

Figure 6.5 summarizes the cell uptake results using a bar diagram showing the percentage of HeLa cells with uptake on the Y-axis, at various concentrations 0.5, 1.0 and 3.0 µM of

fluorescently labeled single-stranded DNAs **ODNs 76−79** after 24h of transfection in Opti-MEM in absence of lipid transfecting agent.

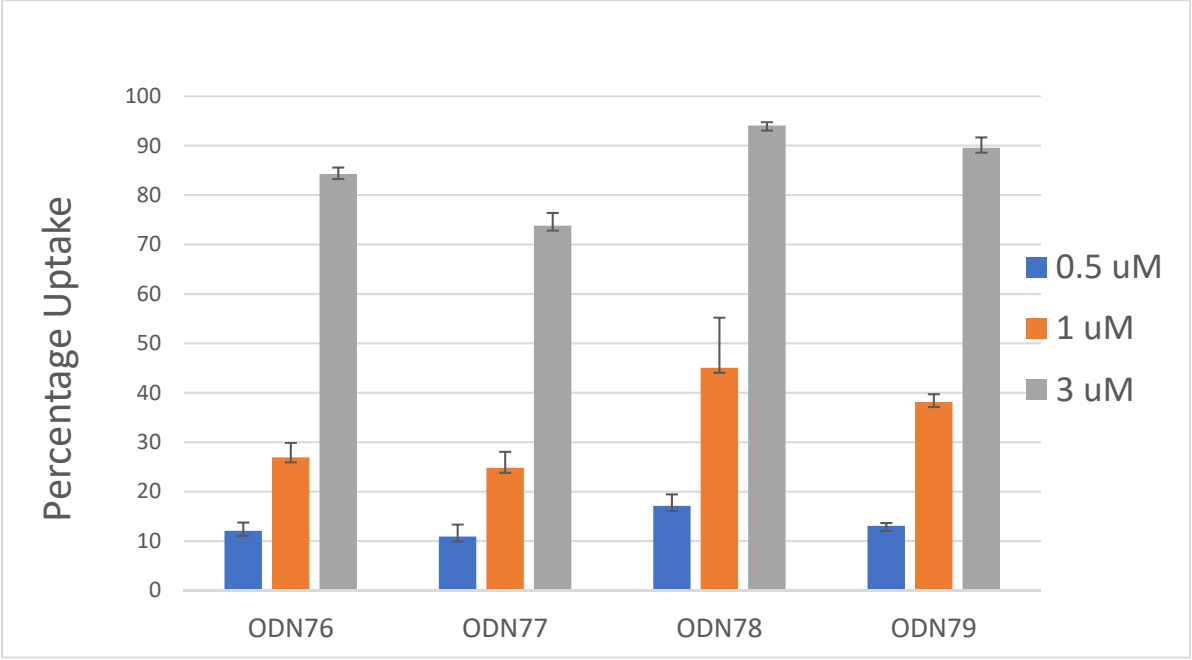


Figure 6.5: Fluorescently labeled single-stranded DNA were efficiently taken up into Hela cells following 24-hour transfection in the absence of a lipid transfecting agent. **ODN76**: 6-FAM-P(S)- TG*TAAACC*ATGAT*GTGCTGCT*A; **ODN77**: 6-FAM-P(S)-TGT*AAACC*AT*GAT*GTGCTGCT*A; **ODN78**: 6-FAM-P(S)-T*GTA*AA*CCAT*GA*TGTGCTGCT*A; **ODN79**: 6-FAM-P(S)-T*GTA*AA*CCAT*GA*TGT*GCTGCT*A; *: Phosphoramidate modification; 6-FAM-P(S): 6-Carboxyfluorescein thioimidate.

Following the observation that ODN 1-4 were successfully taken up by cells in the absence of lipid, 2'-deoxyoligonucleotide having 4-7 phosphoramidates were examined for cell uptake and the result summarized in figure 6.5. 50% of cells showed cell uptake when **ODN76** with 4 modifications was used at 0.5 µM concentration. When the concentration was increased to 1.0 µM and 3.0 µM for the same ODN, the uptake increased to 68% and 80% respectively. With oligonucleotides having 5, 6 and 7 phosphoramidate modifications the uptake increased, however,

saturation was obtained at 3 μM with **ODN78** and **ODN79**. This suggests oligomers having 6 and 7 phosphoramidate modifications are maximally transfected at 3 μM. Additionally, even at 0.5 μM these ODNs are taken up by 80% of the HeLa cells. Also, of interest was the observation that **ODN76** with only four modifications transfects 50% of the HeLa cells even at 0.5 μM, thereby indicating the efficiency of this modification for allowing cell uptake.

**Microscope Imaging**

The transfection experiments showed a significant uptake of phosphoramidate DNA. One probability is that these oligomers are located on the cell membrane and never actually transfected. Therefore FACS analysis could simply demonstrate an ionic interaction with phospholipids on cell surfaces. This question was addressed using a confocal microscope in order to examine the location of the fluorescein tag and therefore the attached oligonucleotides. Initially HeLa cells were seeded at $0.1 \times 10^6$ cells/well in 10 mL glass bottom dishes (CELLview™ Cell Culture Dishes, Glass Bottom, Sterile, Greiner Bio One). After 24 hours at 60% confluency, 250 μL of stock solution of **ODN77** diluted in OptiMEM was added to each well making the final concentration of 3 μM and cells were then incubated at 37 °C for 24 hours. Cells were stained with Hoechst 33258 to visualize nuclei (Figure 6.6). To show the cell membrane boundaries the same procedure was used and after staining with Hoechst 33258 the cells were stained with 1 x of CellMask™ Orange Plasma Membrane Stain (Figure 6.7). Cells were analyzed in OptiMEM using a confocal microscope.

Figure 6.6 shows laser scanning confocal images (40× magnification) of live HeLa cells treated with 3 μM **ODN77** of fluorescently labeled single-stranded DNA containing 5 phosphoramidimidate modification which were efficiently taken up into Hela cells after 24 hours

transfection in absence of lipid. Part A is a phase contrast image to show the cell boundaries and in part B the nucleus appears in blue due to staining with Hoechst 33258 dye. The fluorescein signal is shown in green representing the 5'-fluorescein labeled modified DNA as it appears in part C. Part D shows the superimposed image for the three channels used to visualize cells. Similarly, in figure 6.7 however the cell membrane boundaries appear in red in part C due to CellMask™ Orange Plasma Membrane Stain.

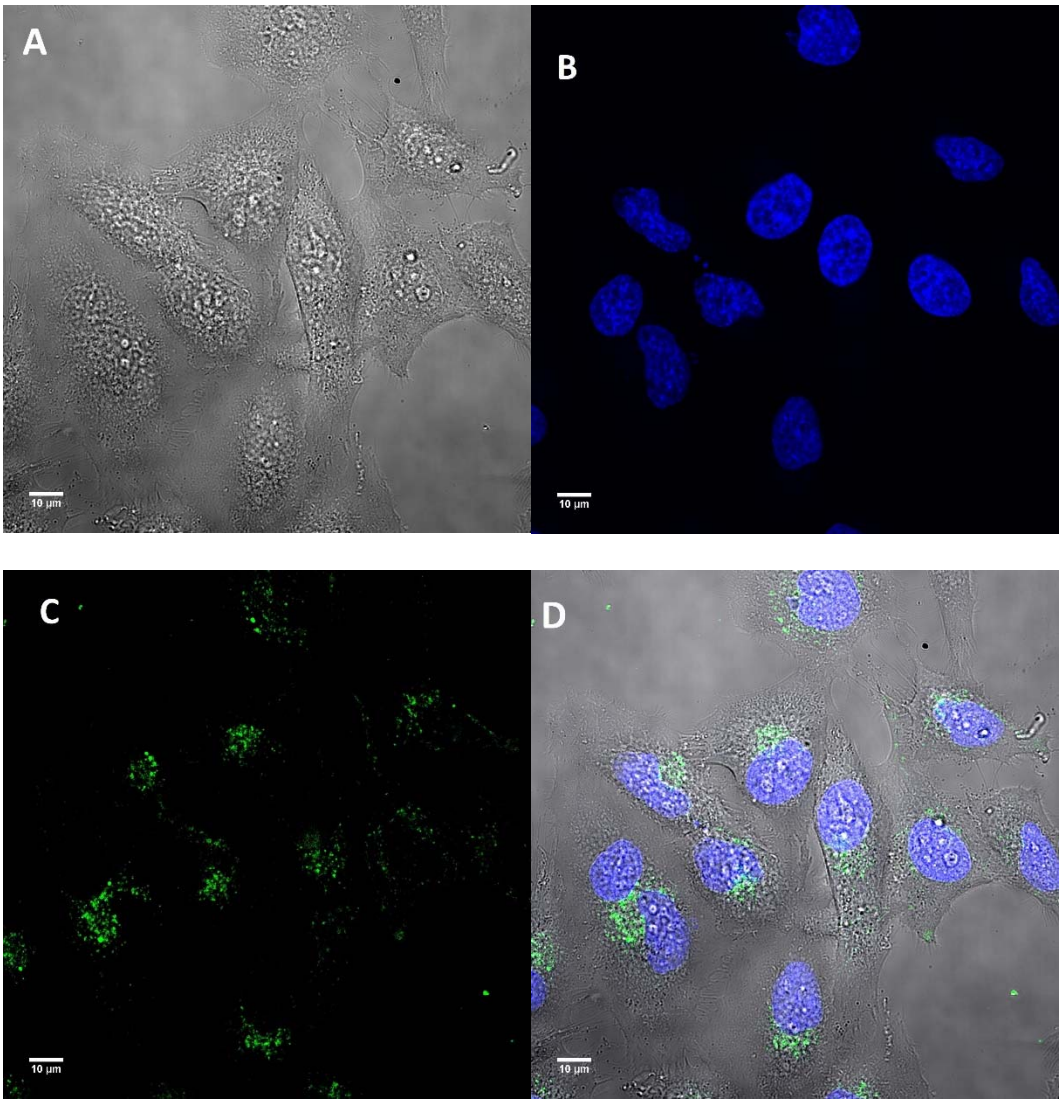


**Figure 6.6: Fluorescence microscopy image (40× magnification) of live HeLa cells treated with 3 µM of ODN77**, a fluorescently labeled single-stranded DNA which were efficiently taken up into Hela cells for 24 hours transfection in absence of lipid transfecting. A) Phase contrast image to show the cells boundaries; B) Nucleus is stained with Hoechst 33258 dye and shown in blue; C) The fluorescein signal is shown in green representing the 5'-fluorescein labeled modified DNA; D) Superimposed image for the three channels used to visualize cells.

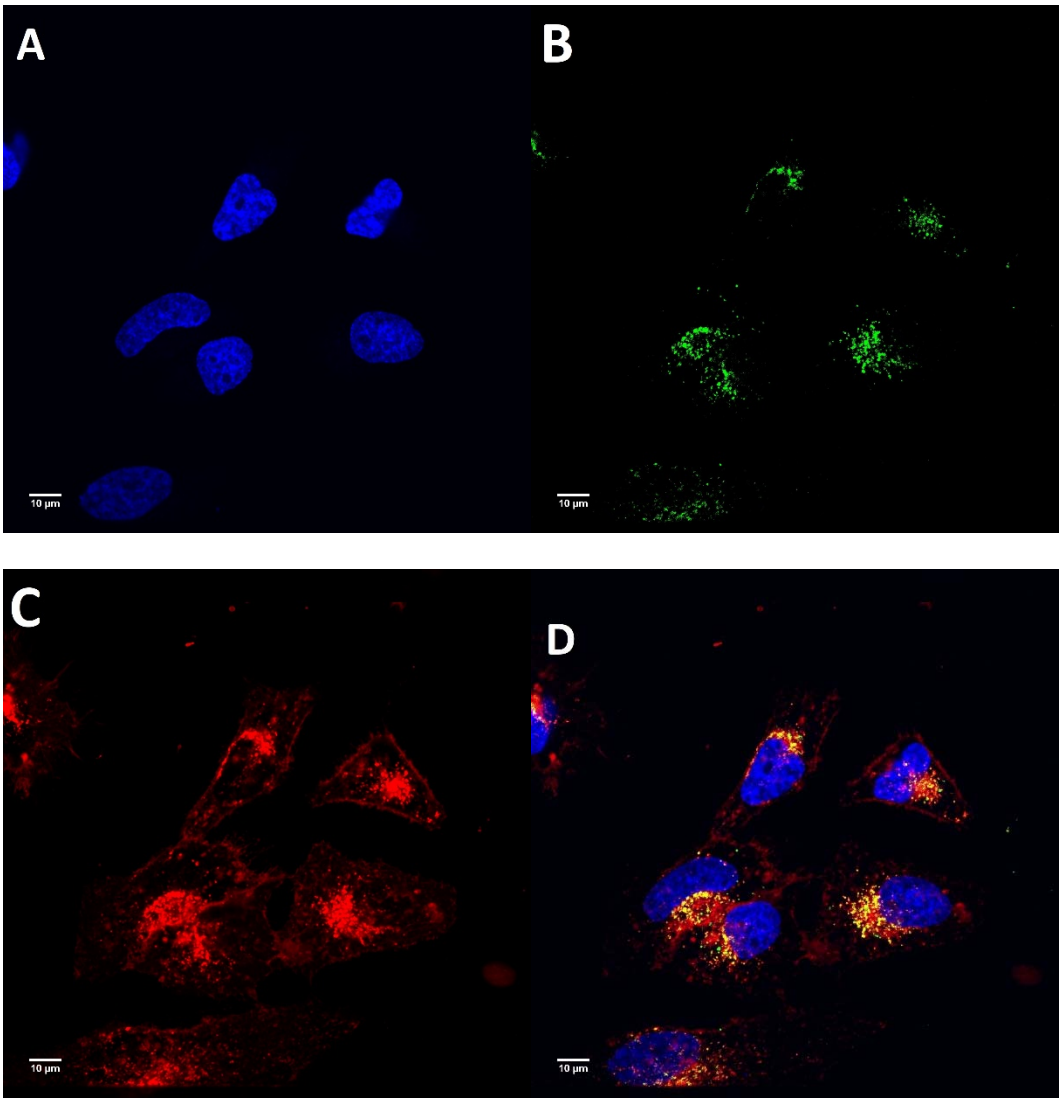


**Figure 6.7: Fluorescence microscopy image (40× magnification) of live HeLa cells treated with 3 µM of ODN77**, a fluorescently labeled single-stranded DNA which were efficiently taken up into Hela cells for 24 hours transfection in absence of lipid transfecting. A) Nucleus is stained with Hoechst 33258 dye and shown in blue; B) The fluorescein signal is shown in green representing the 5'-fluorescein labeled modified DNA; C) cell membrane is stained with CellMask™ Orange Plasma Membrane to show it boundaries in red; D) Superimposed image for the three channels used to visualize cells.

## 6.5 Hydrolysis of RNA Heteroduplexes with E. coli RNase H1

The search for antisense and diagnostic DNA analogs has led to a wide range of DNA modifications but few possess the three necessary properties for antisense activity: an ability to form sequence-specific duplexes with complimentary oligoribonucleotides, activation of RNase H1 and resistance towards nucleases. These observations prompted me to investigate whether phosphoramidate DNA could activate RNase H1 and potentially function in antisense therapeutic activity.

Phosphoramidate derivatives were tested for their ability to stimulate RNase H1 activity. Thus, a 5'-fluorescein labeled RNA and complementary phosphoramidate ODNs (**ODN 83, 84 and 85**) were combined and treated with RNase H1. A positive control was natural DNA complementary to the same RNA that should activate RNA degradation. A negative control was 2'-O-methyl RNA in duplex with the same RNA and that does not stimulate RNase H1 activity.[47] Two samples of each duplex were incubated in 35 μL of the assay buffer. E. coli RNase H1 (3 units) was added to one of them and the assay kept at 25 °C for 8 hours. The reaction mixtures were analyzed by polyacrylamide gel electrophoresis and visualized using a Molecular Dynamics Typhoon Phosphorimager.

As shown in figure 6.8, the natural DNA strongly activated RNase H1 (Figure 6.8, lane 6) while the 2'-O-Methyl oligonucleotides gave minimal activations (Lane 2). Importantly, the phosphoramidate oligonucleotides (Lane 5) also strongly activated RNase H1. Thus, unlike 2'-O-Methyl containing oligonucleotides, the phosphoramidate containing oligonucleotides are potentially useful for RNase H1 mediated antisense applications. The absence of enzyme (Lanes 1, 4, 6) or the absence complementary DNA strand (Lane 3) kept the RNA intact.

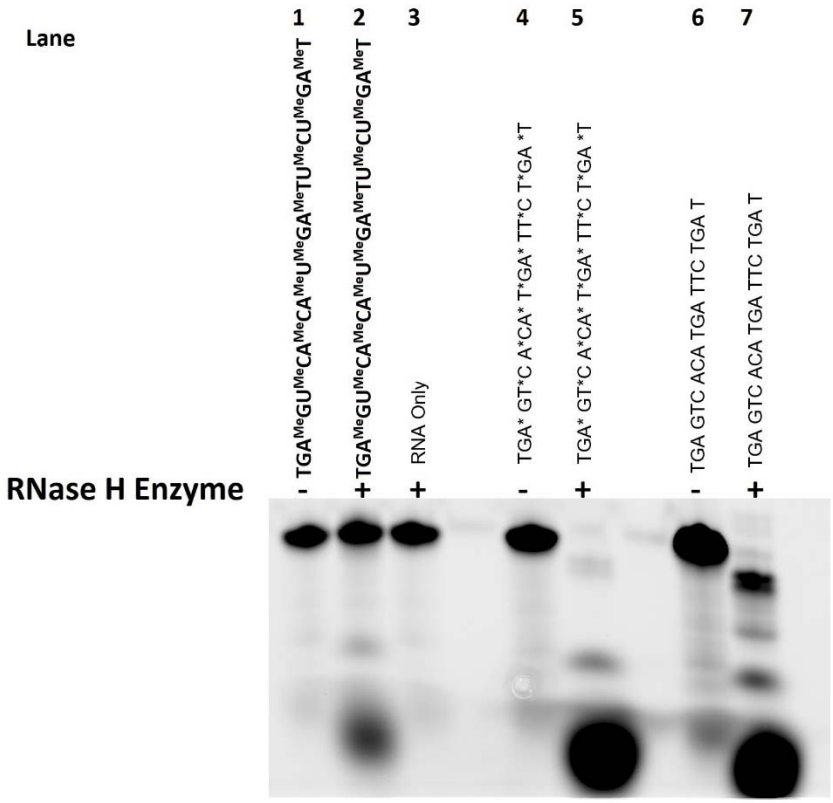


Figure 6.8: E. coli RNase H1 degradation of RNA. 5`-Fluorescein labeled RNA was allowed to form duplexes with complementary ODNs (83-85), which were then treated with E. coli RNase H1 for 8 h and analyzed by PAGE.

Lane 1: 2'-O-methyl RNA ODN (1)/RNA; Lane 2: 2'-O-methyl RNA ODN (1), RNA, enzyme;

Lane 3: RNA, enzyme;

Lane 4: ODN (2)/RNA; Lane 5: ODN (2), RNA, enzyme;

Lane 6: ODN (3)/RNA; Lane 7: ODN (3), RNA, enzyme;

ODN83: TGA$^{Me}$ GU$^{Me}$C A$^{Me}$CA$^{Me}$ U$^{Me}$GA$^{Me}$ TU$^{Me}$C U$^{Me}$GA$^{Me}$T;

ODN84: TGA* GT*C A*CA* T*GA* TT*C T*GA *T;

ODN85: TGA GTC ACA TGA TTC TGA T.

# CHAPTER 7

# CONCLUSIONS AND OUTLOOK

## 7.1 Summary of results

We developed a method to synthesize novel modified 2'-deoxyoligonucleotides containing aminoboranephosphonate DNA. This modification, where the two non-bridging oxygens of the phosphodiester backbone were replaced with borane and amine, was introduced into several 2'-deoxythymidine oligonucleotides using phosphoramidite chemistry. A key enabling feature of the synthesis was using a pivaloyl protecting group for the nitrogens. Using a pivaloyl group helped not only protecting the nitrogen attached on the phosphorous but also prevented any carbonyl reduction by the boronating reagent $BH_3$ solution when pivaloyl is used as protecting group for the exocyclic amines on the aromatic bases. The final 2'-deoxythymidine oligonucleotides products were readily purified by RP-HPLC and characterized by $^{31}P$ NMR and mass spectrometry.

This modification imparted to the oligonucleotides several potentially advantageous biochemical properties. Thermal denaturation studies showed this modification has only a small effect on its binding to the complementary DNA and RNA oligonucleotide. Placing the aminoboranephosphonate on the 3'-end of 2'-deoxythymidine reduced the sensitivity of the DNA to exonuclease activity by 20-fold compared to natural DNA. Additionally, this modification significantly enhanced the cell uptake of 5'-fluorescein labeled 2'-deoxythymidine oligonucleotides into HeLa cells and did not require using transfecting lipids for uptake. Together, these features suggest this modification could help solve the longstanding problem of obtaining efficient uptake of oligonucleotides by cells.

In chapter 4, I synthesized and examined several phosphordiamidites having a wild variety of amide based protecting groups on the phosphorus amine. Their compatibility with solid phase DNA synthesis cycle were tested and the ability of deprotecting the 2'-deoxyoligonucleotieds

having these amino protecting led to the development of two novel protecting groups for DNA synthesis, cyanoethylamide and phenoxyacetamide. Importantly, this enabled us to synthesize oligonucleotides with this new DNA modifications. Of these two, phenoxyacetamide became the group of choice for the ease of its removal and its compatibility with a modified solid phase DNA synthesis cycle. All four nucleobase phosphordiamidites containing phenoxyacetamide nitrogen protecting were synthesized and characterized by $^{1}$H NMR, $^{13}$C NMR, 2D NMR, $^{31}$P NMR and mass spectrometry. Importantly, these modified and protected phosphordiamidites facilitated the synthesis in outstanding yield of DNA containing multiple phosphoramidimidate linkages.

Phosphoramidimidates, novel phosphate analogs in which the two nonbridging oxygens of a phosphodiester are replaced by nitrogen, were synthesized using the aforementioned phosphordiamidites. The key discovery that allowed their synthesis was the new phenoxyacetyl protecting group. As well as protecting the nitrogens from unwanted reactions, it was easily removed by base. Furthermore, since we could prepare all phosphordiamidites with all four natural bases, we could readily synthesize 2'-deoxyoligonucleotides of mixed synthesis using phosphoramidite solid phase synthesis and readily obtain the desired product in reasonable yield.

We tested various chemical and biological properties of oligonucleotides containing the phhosphoramidimidate linkage. Oligonucleotides containing these linkages are completely stable at neutral or basic pH. Under acidic conditions, it showed less than 10% decomposition at pH =1 for the protected phosphoramidimidate, while it undergoes rapid hydrolysis under acidic conditions once it is deprotected. The main target of synthesizing this DNA modification was to minimize the overall negative charge coming from the natural phosphate and consequent electrostatic repulsion when incorporated into duplex DNA. Phosphoramidimidate is expected to have a positive charge coming from the introduced two nitrogen atoms, and this was confirmed by mass spectrometry and gel electrophoresis. Although we were expecting an increase of the melting temperature of the duplexes having phosphoramidimidate internucleotide linkage

due to the elimination of electrostatic repulsion between phosphates, thermal denaturation studies showed that this modification actually caused minor depression in Tm values (0.5 °C/ modification) when the phosphoramidimidate oligonucleotide was bound to either the complementary RNA or DNA oligonucleotide. Phosphoramidimidate also greatly enhanced the cellular uptake of 5'-fluorescein labeled 2'-deoxythymidine oligonucleotides into HeLa cells without using transfecting lipids. Treating HeLa cells with oligonucleotides having 6 and 7 phosphoramidimidate modifications resulted in transfection of virtually all cells at 3 μM, and even at 0.5 μM these oligonucleotides were taken up by 80% of the HeLa cells. Imaging of live HeLa cells showed that these 5'-fluorescein labeled oligonucleotides were actually up taken by cells and crossed the cell membrane as opposed to remaining bound to the surface of the cells (By, potentially, an electrostatic interaction). Introduction of the phosphoramidimidate on the 3'-end of an oligonucleotide resulted in a 12-fold decrease in sensitivity to exonuclease compared to the natural DNA. Phosphoramidimidate derivatives were tested for their ability to stimulate E. coli RNase H1 activity. Incubating a phosphoramidimidate ODN, complementary 5'-fluorescein labeled RNA and E. coli RNase H1 did give activation and cleavage of the target RNA. Since all of these properties – stability at neutral pH, cellular uptake, exonuclease resistance and RNaseH activation – are ideal for various therapeutic applications of oligonucleotides, this modification is clearly worthy of further study.

I also developed a novel and high yield for synthesizing DNA containing phosphoramidate linkages. The only reported method for synthesizing phosphoramidate DNA was through H-phosphonate chemistry. Significantly, the yields for synthesizing phosphoramidate 2'-deoxyoligonucleotides were low and the monomers for H-phosphonate synthesis were not optimal. A novel method for synthesizing this derivative was developed using solid phase phosphoramidite

chemistry. Not only were the nucleosides obtained in better yields than for H-phosphonate chemistry, but the synthesized 2'-deoxyoligonucleotides using these monomers were obtained in higher yield and purity. The high quality of these synthesized phosphoramidate 2'-deoxyoligonucleotides enabled us to perform biostudies. Oligomers having 4-7 phosphoramidate modifications were transfected into HeLa cells without using transfecting lipids and showed more than 70% percent of HeLa were transfected with the 5'-fluorescein labeled phosphoramidate DNA. Imaging of live HeLa cells confirmed that they were actually up taken by cells and crossed the cell membrane. Phosphoramidate derivatives were tested for their ability to stimulate E. coli RNase H1 activity. Incubating a phosphoramidate ODN, complementary 5'-fluorescein labeled RNA and E. coli RNase H1 did show an activation and cleavage of the target RNA.

## 7.2 Conclusion and Future Work

The synthetic methods outlined in this thesis provide the basis for the synthesis of a variety of biologically important molecules. The initial studies on the aminoboranephosphonate and phosphoramidimidate analogs showed they have the appropriate chemical and biochemical properties for their use in whole cells, and clearly studies of this sort are warranted. The novel application of phosphoramidite chemistry for synthesizing phosphoramidate DNA likewise holds promise with respect to improvements of scale-up and product quality. The studies described here is expanded to the synthesis of sequences containing all four nucleosides. Lastly, the chemistries I developed for synthesizing these modified phosphodiester linkages may be useful for other aspects of DNA synthesis and synthesizing DNA containing unnatural bases and sugars.

# CHAPTER 8

# EXPERIMENTAL SECTION

## 8.1 General

Unless otherwise noted, all materials were obtained from commercial suppliers and used without further purification. Phenoxy acetamide was purchased from Oakwood Chemicals and used without further purification. All reactions were carried out under argon in round bottom flasks that were dried overnight in the oven before used. Dichloromethane (DCM) was distilled over $CaH_2$. DNA grade acetonitrile (ACN) was purchased from Sigmaldrich and was used for all synthetic steps without further purification. ACN diluent was bought from Glen Research and used to dissolve the monomers. Commercially available DNA synthesis reagents and 2'-deoxyoligonucleotide-3'-phosphoramidites were purchased from Glen Research. Medium-pressure, preparative column chromatography was performed using 60 Å standard grade silica gel from Sorbent Technologies (Atlanta, GA). The silica gel was dried overnight in an oven before being used for chromatography. Thin-layer chromatography was performed on aluminum-backed silica 60 F254 plates from EMD Chemicals, USA.

## NMR

$^{1}H$, $^{31}P$, $^{13}C$ NMR spectra were carried out on a Bruker Avance-III 300 ($^{1}H$ = 300.13 MHz., and/or a Bruker Avance-III 400 ($^{1}H$=400.13 MHz). TMS was used as an internal reference Chemical shifts are given in ppm with positive shifts downfield. $^{31}P$ Chemical shifts are referenced to 0.0 ppm in the $^{1}H$ NMR spectrum according to the standard IUPAC method.

**LC-MS**

Analyses were carried out on an Agilent 6530 series Q-TOF LC/MS spectrometer. A waters ACQUITY UPLC BEH C18, 1.7 μm, 2.1 X 100 nm column was used with a gradient of 0-100% of buffer B in 50 min with a flow rate of 0.2 mL/min at 25 °C (buffer A was a 1:80:9.5:0.5 solution of 500 mM dibutylammonium acetate:water: isopropanol:acetonitrile respectively and buffer B was a 1:10:44.5:44.5 solution of 500 mM dibutylammonium acetate: water: isopropanol:acetonitrile). Or analyses were carried out on Waters Synapt G2 HDMS Q-TOF LC/MS spectrometer. A waters ACQUITY UPLC BEH C18, 1.7 μm, 2.1 X 100 nm column was used with a gradient of 0-95% of buffer B in 22 minutes with a flow rate of 0.2 mL/min at 40 °C (buffer A was 50 mM triethylammonium acetate buffer and mobile B was acetonitrile).

**HPLC methods**

Analytical HPLC injections were carried out using an Agilent Hypersil ODS 5 μm column, 4.0 mm i.d. × 250 mm, eluting at 1.5mL/min with a gradient of acetonitrile/50 mM triethylammonium bicarbonate buffer, pH 8.5. Preparative HPLC (Agilent Zorbax SB-C18, 5 μm column 9.4 mm i.d. × 250 mm) was performed on an Agilent Technologies Model HPLC 1100, eluting at 1.5mL/min with a gradient of acetonitrile/50 mM triethylammonium bicarbonate buffer. The eluent was monitored for absorption at 280 nm. The same mobile phases and flow rate were applied on both systems; the following gradient: 0 - 30 minutes, 0-50 % B, 30 – 50 minutes, 50 – 100 % B, 50 – 60 minutes, 100 –0 % B, 60 – 70 minutes, 0 % B.

**Thermal Melting Experiments**

Duplex melting experiments were performed on a Cary 100 Bio UV-visible spectrophotometer (Varian, Santa Clara, CA) equipped with a thermoelectrically controlled multicell holder. Samples containing 1μM and complementary DNA or RNA in solutions of 1.0 M NaCl/0.01 M $Na_2HPO_4$, 0.10 M NaCl/0.01 M $Na_2HPO_4$, or 0.01M NaCl/0.01 M $Na_2HPO_4$ at pH 7.3. The samples were heat denatured at 85 °C for 10 min, cooled to 25 °C at a rate of 1 °C/min, and maintained at this temperature for 10 min. Duplex melting was performed by heating the duplexes from 20 to 85 at 1 °C/min with the absorbance (260 nm) being recorded at one-minute intervals. Melting temperatures were determined at the maximum of first derivative plots. In order to confirm the stability of duplexes and the effect of the heating/cooling cycles, the melting temperatures were measured four times for each sample (twice during the heating cycle and twice during the cooling cycle).

## 8.2 Solid-phase Synthesis

Low Volume controlled pore glass (CPG) columns (1 μmol synthesis scale) were purchased from Glen Research. DNA synthesis was carried out on an Applied Biosystems Model 394 automated DNA synthesizer (Applied Biosystems) using the standard DNA synthesis cycle when regular phosphate linkage with synthesized. Other reagents were: Activator (0.25 M ETT), Cap A (THF/Pyridine/$Ac_2O$), Cap B (16% 1-methylimidazole in THF) were purchased from Glen Research. Modifications were introduced to the standard DNA synthesis cycle when morpholinoboranephosphonate, aminoboranephosphonate, phosphoramidimidate and phosphoramidate DNA were synthesized. More details for each synthesis cycle explained separately.

### Solid-phase Synthesis for Morpholinoboranephosphonate and Aminoboranephosphonate

Monomer amidites (**15**, **20**) were dissolved in anhydrous acetonitrile at 0.15M concentration, it was delivered to the column using ports 5-7 with 0.25M 5-(Ethylthio)-1H-tetrazole (ETT) in acetonitrile. Coupling time was 15 minutes. The oxidation step was replaced by boronation using solution of 0.05 M $BH_3$ dissolved in THF. This boronating solution was prepared right before each synthesis and installed on the synthesizer on port 8. The boronation time was 60 seconds. The oxidation of the standard phosphoramidites from phosphite triester to phosphate with more commonly used iodine is replaced by with 1.0 M tert-butyl peroxide in DCM. This peroxide solution was prepared right before each synthesis by dissolving in 27 mL of DCM 6 mL of 5-6 M tert-butyl peroxide solution in decane. The solution installed on the synthesizer on port 9. Deblocking solution was prepared by dissolving 1 mL of TFA in 180 mL DCM followed by adding

20 mL of TMPB. The solution installed on the synthesizer on port 14. Table 8.1 summarizes the solid phase synthesis conditions.

**Table 8.1: Solid phase synthesis cycle for morpholinoboranephosphonate and aminoboranephosphonate**

| *Step* | *Reaction Step* | *Reagent/Conditions* | *Time* |
|---|---|---|---|
| 1 | Detritylation | 10% TMPB + 0.5% TFA in DCM | Flow 95s |
| 2 | Wash | Methanol | Flow 60 s, wait 10 s, flow 20 s. |
| | Wash | Acetonitrile | Flow 30s |
| 3 | Condensation | 0.15 M phosphoramidte in acetonitrile with 0.25 ETT in acetonitrile | 900s wait |
| 4 | Capping | Cap A (THF/Pyridine/$Ac_2O$), and Cap B (16% 1-methylimidazole in THF) | Flow 10 s, wait 5 s |
| 5 | Oxidatiation or Boronation | 1.0 M tert-butyl hydroperoxide in DCM<br>0.05 M BH3-THF in THF | Flow 15 s wait 240s<br>flow 10s wait 120 s |
| 6 | Wash | Anhydrous acetonitrile | Flow 60 s |
| 7 | Wash | DCM | Flow 35 s |

After completion of solid-phase synthesis, oligonucleotides were cleaved from the CPG solid support and the heterocyclic bases deprotected using aqueous ammonia at 55 °C for 16 hours. The solution was evaporated to dryness and the crude oligonucleotides were dissolved in 1.0 ml water where the CPG was removed by filtration and the remaining oligonucleotide applied to analytical HPLC to check purity or semi-preparative RP-HPLC column for purification.

**Solid-phase Synthesis for Phosphoramidimidate**

Monomer amidites (**40a-d**) were dissolved in anhydrous acetonitrile at 0.15M concentration, it was delivered to the column using ports 5-7 with 0.25M 5-(Ethylthio)-1H-tetrazole (ETT) in acetonitrile. Coupling time was 15 minutes. The oxidation step was replaced by oxidation using mixture of 0.2 M anhydrous ammonia and 0.02 M iodine dissolved in DCM. This oxidizing solution was prepared right before each synthesis by dissolving 0.05 g of iodine in 6 ml of freshly distilled DCM, the mixture was shacked well until complete dissolve. 4 ml of 0.5 M anhydrous ammonia in dioxane was added to the mixture and installed on the synthesizer on port 8. The oxidation time was extended to 360 seconds. Table 8.2 summarizes the solid phase synthesis conditions.

**Table 8.2: Solid phase synthesis cycle for phosphoramidimidate.**

| Step | Reaction Step | Reagent/Conditions | Time |
|---|---|---|---|
| *1* | Detritylation | 3% Trichloroacetic acid in DCM | Flow 95s |
| *2* | Wash | Acetonitrile | Flow 30s |
| *3* | Condensation | 0.15 M phosphoramidte in acetonitrile with 0.25 ETT in acetonitrile | 900s wait |
| *4* | Capping | Cap A (THF/Pyridine/$Ac_2O$), and Cap B (16% 1-methylimidazole in THF) | Flow 10 s, wait 5 s |
| *5* | Oxidatiation | 0.2 M anhydrous ammonia and 0.02 M iodine dissolved in DCM. or<br>0.02 M Iodine in THF/Water/Pyridine | Flow 15 s wait 240s flow 10s wait 120s.<br>Or 20s |
| *6* | Wash | Anhydrous acetonitrile | Flow 60 s |
| *7* | Wash | DCM | Flow 35 s |

After completion of solid-phase synthesis, oligonucleotides were cleaved from the CPG solid support and the heterocyclic bases deprotected using (1:1) of ethylene diamine and 0.5 M

anhydrous ammonia in dioxane at 45 °C for 24 hours. The solution was evaporated to dryness and the crude oligonucleotides were dissolved in 1.0 ml water where the CPG was removed by filtration and the remaining oligonucleotide applied to analytical HPLC to check purity or semi-preparative RP-HPLC column for purification.

**Solid-phase Synthesis for Phosphoramidate**

Monomer amidites (**40a-d**) were dissolved in anhydrous acetonitrile at 0.15M concentration, it was delivered to the column using ports 5-7 with 0.25M 5-(Ethylthio)-1H-tetrazole (ETT) in acetonitrile. Coupling time was 15 minutes. Table 8.3 summarizes the solid phase synthesis conditions.

**Table 8.3: Solid phase synthesis cycle for phosphoramidate.**

| Step | Reaction Step | Reagent/Conditions | Time |
|---|---|---|---|
| *1* | Detritylation | 3% Trichloroacetic acid in DCM | Flow 95s |
| *2* | Wash | Acetonitrile | Flow 30s |
| *3* | Condensation | 0.15 M phosphoramidte in acetonitrile with 0.25 ETT in acetonitrile | 900s wait |
| *4* | Capping | Cap A (THF/Pyridine/$Ac_2O$), and Cap B (16% 1-methylimidazole in THF) | Flow 10 s, wait 5 s |
| *5* | Oxidatiation | 0.02 M Iodine in THF/Water/Pyridine | 20s |
| *6* | Wash | Anhydrous acetonitrile | Flow 60 s |
| *7* | Wash | DCM | Flow 35 s |

After completion of solid-phase synthesis, oligonucleotides were cleaved from the CPG solid support and the heterocyclic bases deprotected using (1:1) of ethylene diamine and 0.5 M

anhydrous ammonia in dioxane at 45 °C for 24 hours. The solution was evaporated to dryness and the crude oligonucleotides were dissolved in 1.0 ml water where the CPG was removed by filtration and the remaining oligonucleotide applied to analytical HPLC to check purity or semi-preparative RP-HPLC column for purification.

## 8.3 Biological Studies

### HeLa Cells

HeLa cells were purchased from ATCC and maintained as monolayer cultures in Dulbecco's Modified Eagle Medium (DMEM) containing 10% fetal bovine serum (FBS), penicillin and streptomycin (Pen-Strep, 100 U/mL). Cells were grown in a humidified atmosphere of 5% carbon dioxide at 37 °C. They were counted and adjusted to the appropriate density, seeded onto plates or chambers, and incubated for 24 hours prior to transfection.

### Cellular Uptake Studies using FACS analysis

HeLa cells were seeded at $8 \times 10^4$ cells/well in 12-well plates in DMEM medium containing 10% FBS and Pen-Strep (100 U/mL). The concentration of a 5'-fluorescein labeled TP ODN in HyPure Molecular Biology Grade Water (Thermo Scientific) was measured by UV spectroscopy. After 24 hours, the cells were transfected with the appropriate TP ODN in DMEM to give the required final concentration. The cells were then incubated at 37 °C for 24 hours. After incubation, the medium was removed from wells and the cells were washed three times with Dulbecco's phosphate buffered saline (D-PBS). Cells were then treated for 3 min at 37 °C with a pre-warmed solution of trypsin-EDTA (1×) until all cells became detached from the plates. The cells from each plate were placed in 1 mL D-PBS and pelleted by centrifugation at 1000 rpm for 5 min. The pellets were washed and resuspended in D-PBS and kept at 0 °C in the dark until analyzed by flow cytometry.

Flow cytometric data on at least 10,000 cells per sample was acquired on a Moflow flow-cytometer (BeckmanCoulter) equipped with a single 488 nm argon laser and a 530/40 nm emission

filter (Fluorescein). Raw flow cytometry data was manipulated and visualized using Summit 4.3 software (BeckmanCoulter). Fluorescence intensity of the 5′-fluorescein tag was analyzed for cells presenting higher fluorescence than the background. The background was defined as the auto fluorescence of cells.

**Passive Transfection as Observed by Microscope Imaging**

All fluorescence images were acquired on a Nikon A1R Laser Scanning Confocal (Nikon, Japan) equipped with Nikon elements software. The normalized aperture 0.95 and magnification was 40x. DAPI (405 excitation, 450/50 emission), GFP (488 excitation, 525/50 emission) and red (561 excitation, 600/50 emission) filter sets. Live cells were maintained at 37°C and 5% $CO_2$ in a LiveCell environment chamber (CELLview™ Cell Culture Dishes, Glass Bottom, Sterile, Greiner Bio One/ VWR) during the experiments. Hoechst® 33342 nucleic acid (nuclear) stain was purchased from ThermoFisher as 10 mg/mL solution and was diluted 2000 times in D-PBS. CellMask™ Orange Plasma Membrane Stain was purchased from ThermoFisher and was diluted 2000 times in D-PBS.

Hela cells were seeded in DMEM medium containing 10% FBS at $1 \times 10^5$ cells/well in (CELLview™ Cell Culture Dishes, Glass Bottom, Sterile, Greiner Bio One/ VWR). After 24 hours, the cells were transfected with the appropriate 5'-fluorescein labeled DNA in DMEM to give the required final concentration. The cells were then incubated at 37 °C for 24 hours. After incubation, the medium was removed from wells and the cells were washed three times with D-PBS. A freshly prepared solution of Hoechst sufficiently to cover the cells was added and incubated for 10 min at 37 °C. The medium was removed from wells and the cells were washed three times with D-PBS. If needed, freshly prepared solution of CellMask sufficiently to cover the

cells was addend incubated for 10 min at 37 °C. The medium was removed from wells and the cells were washed three times with D-PBS. The cells were kept in phenol red free DMEM containing 10% FBS and kept until the images was taken using a confocal microscope.

**Nuclease Stability Experiments:**

Snake Venom Phosphodiesterase I (Crotalus adamanteus) was purchased from Sigma (St. Louis, MO). While performing enzymatic hydrolysis experiments, the oligodeoxynucleotide (1 OD) was incubated at 37 °C in 150 μL of 100 mM Tris-HCl buffer (pH 9.0), 10 mM $MgCl_2$ (5 μg), Snake Venom Phosphodiesterase I, and the total volume made up to 200 μL. 20 μL aliquots of the reaction mixtures were removed at the indicated time points, quenched by the addition of 1.0 M EDTA and stored in dry ice until analyzed by analytical RP-HPLC.

**Hydrolysis of RNA Heteroduplexes with E. coli RNase H1**

RNase H1 experiments were performed with E. coli RNase H1 using the conditions described by Hogrefe et al.[53] The reactions were carried out using an assay buffer of 50 mM tris-HCl (pH 8.0), 20 mM KCl, 9 mM $MgCl_2$, 1 mM β-mercaptoethanol, and 250 μg/mL bovine serum albumin. An oligodeoxynucleotide or modified oligodeoxynucleotide (200 pmol) and 5'-fluorescein labeled complementary oligoribonucleotide were added to the assay buffer (35 μL). Following addition of E. coli RNase H1 (3 units), reaction mixtures were placed in water bath at 25 °C for 8 hours. The reaction mixtures were then diluted with an equal volume of 80% formamide gel loading buffer containing tracking dyes and analyzed by polyacrylamide gel electrophoresis (20%, 19:1 crosslinking, 7 M urea). The developed gels were analyzed using a Molecular Dynamics Typhoon Phosphorimager.

**8.4 Synthesis:**

**Synthesis of (10 b)**

In a round bottom flask bis(dimethylamino)chlorophosphine (1.0 g, 6.5 mmol) was added and the flask was repeatedly flushed with argon. 50 mL of dichloromethane followed by freshly distilled Hunig Base (1.0 g, 7.8 mmol) were added via syringe. 5'-O-DMT-thymidine (3.2 g, 5.8 mmol) was added to the flask and the mixture was stirred at 25 °C for 30 minutes. At this time TLC (96:4; $CHCl_3$:$CH_3OH$) indicated all starting material had disappeared. The crude reaction mixture was evaporated to dryness, diluted with ethylacetate (100 mL) and poured into 75 mL of saturated $NaHCO_3$. The organic layer was extracted twice with 75 mL of saturated $NaHCO_3$ and once with 50 mL brine. The ethylacetate layer was dried over magnesium sulfate, filtered and evaporated to dryness. The product mixture was purified by flash chromatography on a silica gel column. The silica gel slurry was initially prepared in a mixture of ethlyacetate:hexanes:triethylamine (47.5:47.5:5 ) and poured into the column. The column was washed with two column volumes of an ethylacetate-hexanes (1:1) mixture before loading the reaction mixture on to the column. The desired product was eluted using a gradient of 1:1 ethylacetate hexanes to 100% ethylacetate and isolated as a white foam (2.6 g, 67 % yield). $^{31}$P NMR (121 MHz, $CDCl_3$): δ 138.7; $^{1}$H NMR (300 MHz, $CDCl_3$) δ 10.08 (s, 1H), 7.64 (d, *J* = 1.2 Hz, 1H), 7.45 – 7.38 (m, 2H), 7.35 – 7.21 (m, 8H), 6.88 – 6.81 (m, 4H), 6.42 (dd, *J* = 7.6, 5.9 Hz, 1H), 4.74 – 4.45 (m, 1H), 4.20 – 4.12 (m, 1H), 3.80 (s, 6H), 3.53 – 3.29 (m, 2H), 2.71 – 2.60 (m, 2H), 2.55 (d, *J* = 9.2 Hz, 6H), 2.45 (d, *J* = 9.3 Hz, 6H), 2.29 (ddd, *J* = 13.8, 7.8, 6.5 Hz, 1H), 1.45 (d, *J* = 1.2 Hz, 3H). ESI-MS (*m/z*): 663.3 $(M+H)^+$.

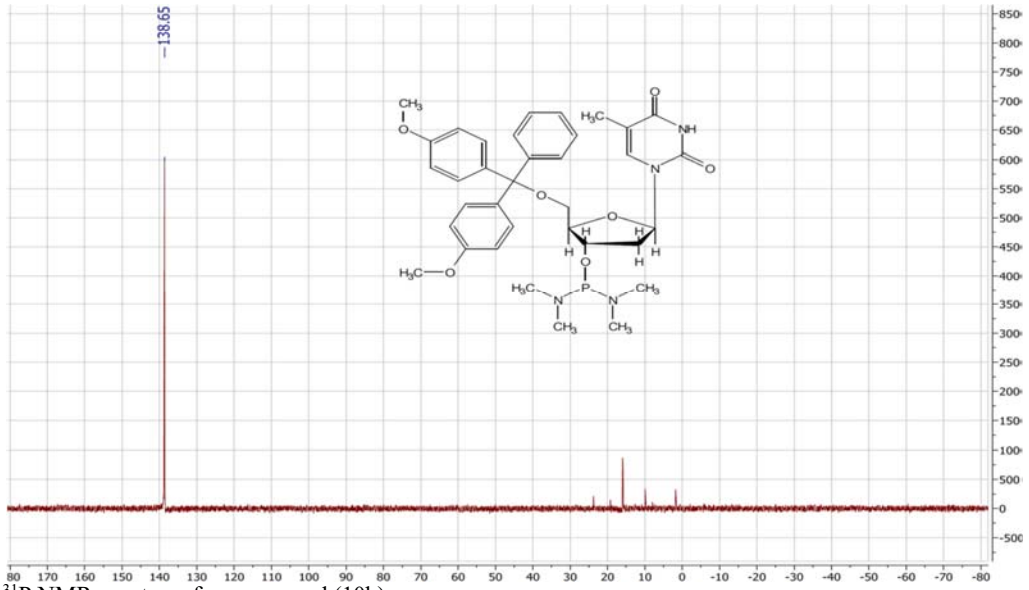


Figure 8.1: $^{31}P$ NMR spectrum for compound (10b).

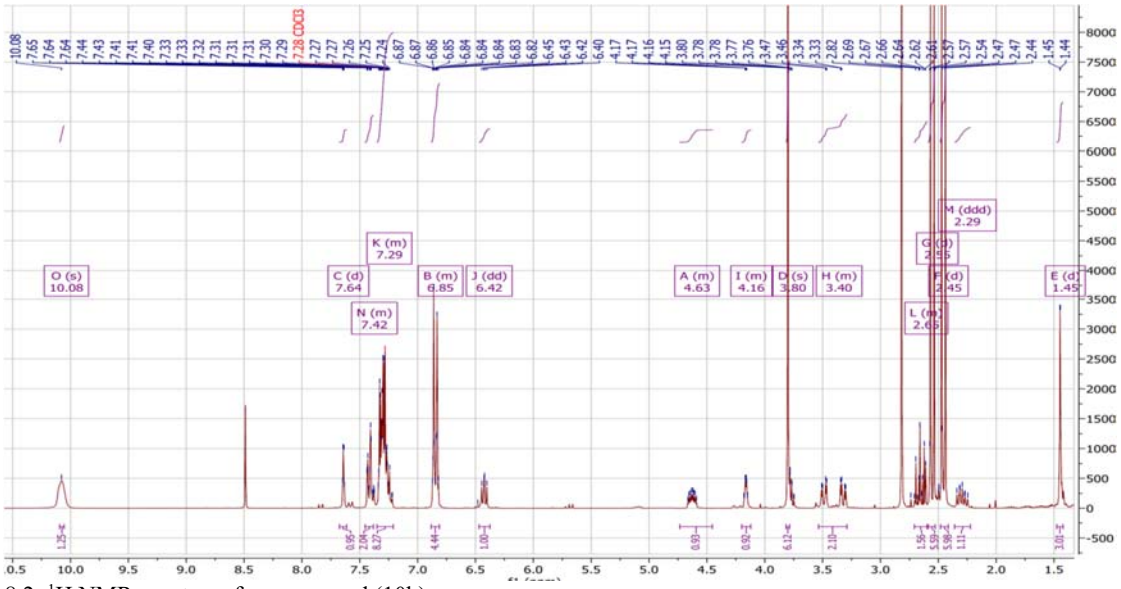


Figure 8.2: $^{1}H$ NMR spectrum for compound (10b).

**Synthesis of (11 b)**

Compound (10 b) (1.0 g, 1.6 mmol) was dried overnight under vacuum in round bottomed flasks. The flask was flushed repeatedly with argon. Anhydrous dichloromethane (50 mL) and 3'-O-acetylthymidine (0.5 g, 1.8 mmol) were added to the flask. This was followed by dropwise addition of 5.4 mL of ETT (0.25 M in acetonitrile; Glen Research) to the reaction flask. After stirring for 3

hours at room temperature, TLC (9.5:0.5; $CHCl_3$:$CH_3OH$) showed complete disappearance of starting material. The crude reaction mixture was evaporated to dryness, diluted with ethylacetate (100 mL), and then washed with saturated $NaHCO_3$ (10 mL) and brine (10 mL). The ethylacetate layer was dried over magnesium sulfate, filtered and evaporated to dryness. The crude mixture was dissolved in ethylacetate and purified by flash chromatography on a silica column. The desired product was eluted using a gradient of 1:1 ethylacetate hexanes to 100% ethylacetate and isolated as a white foam (1.2 g, 87 % yield). $^{31}P$ NMR ($CDCl_3$): 147.5, 146.3 (diastereomers); $^{1}H$ NMR (300 MHz, $CDCl_3$) δ 8.80 (s, 2H), 7.69 – 7.36 (m, 4H), 7.36 – 7.20 (m, 8H), 6.91 – 6.78 (m, 4H), 6.52 – 6.24 (m, 2H), 5.42 – 5.13 (m, 1H), 5.04 – 4.55 (m, 1H), 3.81 (d, $J$ = 0.9 Hz, 6H), 3.44 – 3.19 (m, 1H), 2.51 – 2.16 (m, 4H), 2.11 (q, $J$ = 2.3 Hz, 3H), 2.06 (s, 3H), 1.96 – 1.87 (m, 3H), 1.53 – 1.40 (m, 3H). ESI-MS (m/z): 900.3 $[M-H]^-$.

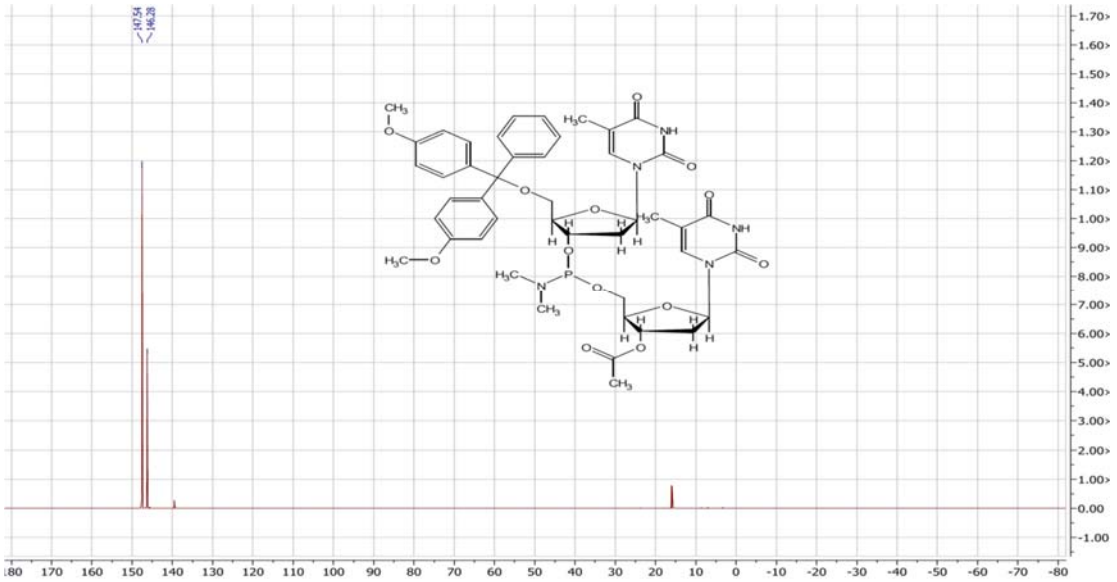

Figure 8.3: $^{31}P$ NMR spectrum for compound (11b).

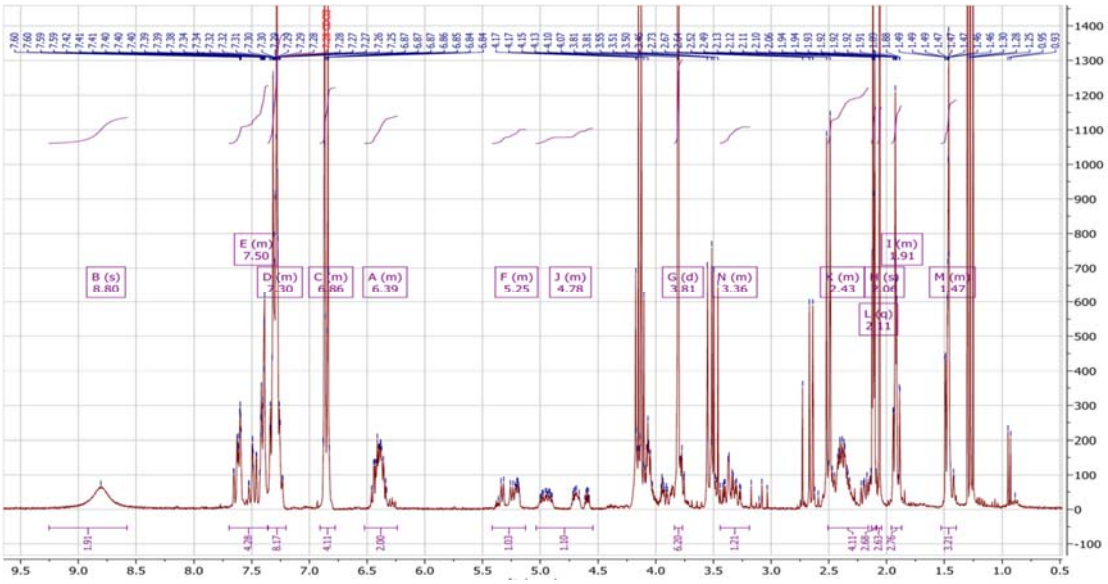

Figure 8.4: $^{1}$H NMR spectrum for compound (11b).

**Synthesis (12 b)**

In round bottomed flasks (1.0 g, 1.1 mmol) of compound (11 b) was dissolved in anhydrous dichloromethane (50 ml) followed by dropwise addition of $BH_3.Me_2S$ (0.2 mL, 10.0-10.2 M $BH_3$) to the starting material solutions. The reaction mixture was stirred at room temperature and monitored by $^{31}$P NMR. After 15 minutes, the $^{31}$P NMR spectra showed complete conversion of starting materials to the broad product peak at 121.8 ppm. Excess $BH_3$-$Me_2S$ in the reaction mixtures was quenched by addition of a few drops of methanol and the solvent removed under reduced pressure in a rotary evaporator. The products were further dried overnight under high vacuum. The crude mixture was dissolved in ethylacetate and purified by flash chromatography on a silica column. The desired product was eluted using ethylacetate and isolated as a white foam (1.0 g, 88 % yield). $^{31}$P NMR ($CDCl_3$): 121.8 (broad); $^{1}$H NMR (300 MHz, $CDCl_3$) δ 9.09 (d, 2H), 7.74 – 7.51 (m, 1H), 7.39 (dt, *J* = 7.2, 1.4 Hz, 3H), 7.35 – 7.20 (m, 9H), 6.91 – 6.78 (m, 5H), 6.49 – 6.24 (m, 2H), 5.37 – 4.97 (m, 2H), 4.38 – 4.15 (m, 3H), 3.81 (d, *J* = 0.7 Hz, 6H), 3.52 – 3.34 (m,

2H), 2.56 – 2.31 (m, 3H), 2.16 – 2.09 (m, 3H), 1.98 – 1.88 (m, 3H), 1.51 – 1.42 (m, 3H), 0.71 (d, $J$ = 100.3 Hz, 3H). ESI-MS (m/z): 914.4 $[M-H]^-$.

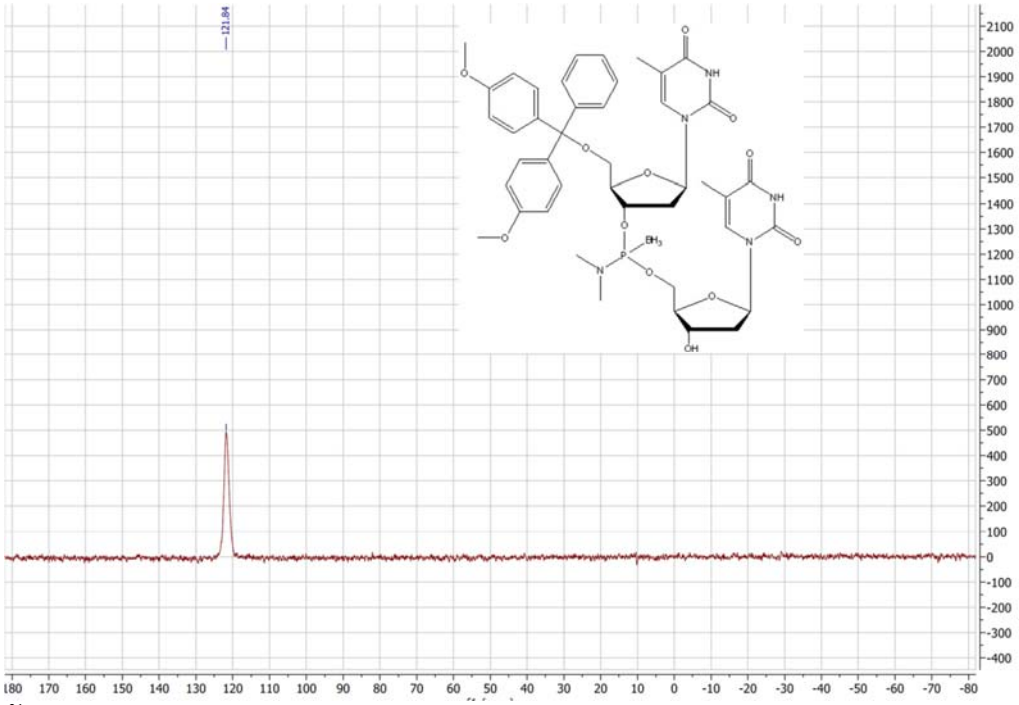

Figure 8.5: $^{31}P$ NMR spectrum for compound (12b).

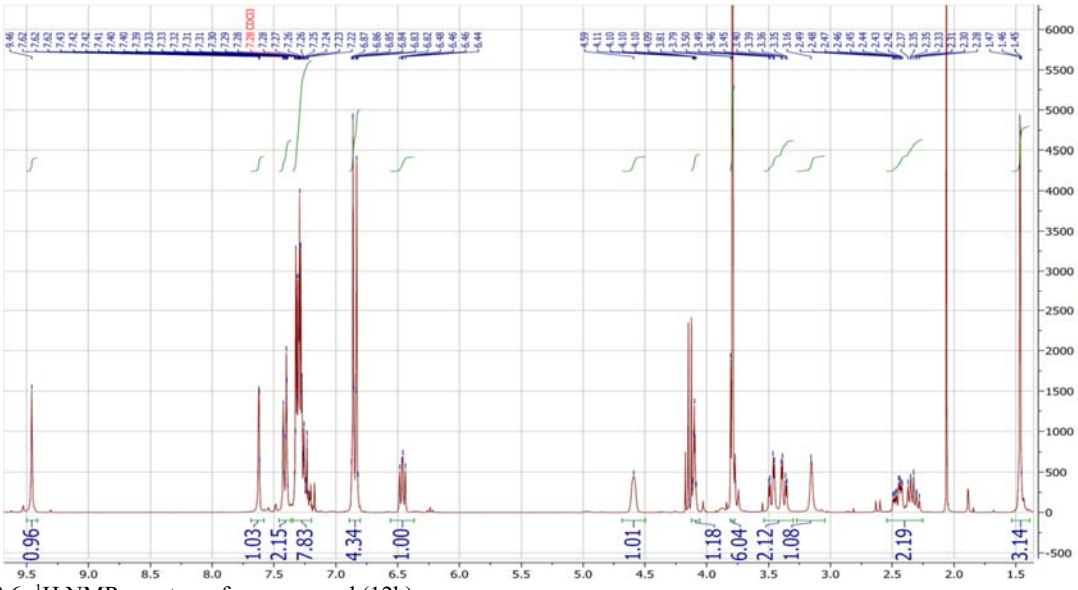

Figure 8.6: $^{1}H$ NMR spectrum for compound (12b).

**Synthesis of (17)**

In round bottomed flasks (1.0 g, 1.1 mmol) of compound (16) was dissolved in anhydrous dichloromethane (50 ml) followed by dropwise addition of $BH_3.Me_2S$ (0.2 mL, 10.0-10.2 M $BH_3$) to the starting material solutions. The reaction mixture was stirred at room temperature and monitored by $^{31}P$ NMR. After 15 minutes, the $^{31}P$ NMR spectra showed complete conversion of starting materials to the broad product peak at 119.3 ppm. Excess $BH_3$-$Me_2S$ in the reaction mixtures was quenched by addition of a few drops of methanol and the solvent removed under reduced pressure in a rotary evaporator. The products were further dried overnight under high vacuum. The crude mixture was suspended in 50 mL concentrated aqueous ammonia (30%) and stirred for 4 hours until all solid had dissolved. The solvent removed under reduced pressure in a rotary evaporator and redissolved in ethylacetate and purified by flash chromatography on a silica column. The desired product was eluted using ethylacetate and isolated as a white foam (0.76 g, 78 % yield). $^{31}P$ NMR (162 MHz, $CDCl_3$) δ 119.3 (broad); $^{1}H$ NMR (400 MHz, $CDCl_3$) δ 9.59 (s, 2H), 7.60 (dd, *J* = 10.1, 1.4 Hz, 1H), 7.44 – 7.37 (m, 2H), 7.37 – 7.23 (m, 9H), 6.92 – 6.82 (m, 4H), 6.40 (ddd, *J* = 14.2, 8.9, 5.4 Hz, 1H), 6.22 (dt, *J* = 14.0, 6.7 Hz, 1H), 5.13 – 4.95 (m, 1H), 4.74 – 4.26 (m, 2H), 4.05 (d, *J* = 4.6 Hz, 1H), 3.81 (s, 6H), 3.75 – 3.36 (m, 9H), 3.27 – 3.02 (m, 5H), 2.66 – 2.09 (m, 5H), 1.92 (dd, *J* = 4.7, 1.2 Hz, 3H), 1.50 (dd, *J* = 7.5, 1.2 Hz, 3H), 0.49 (s, 3H). ESI-MS (m/z): 938.4 $[M+Na]^+$.

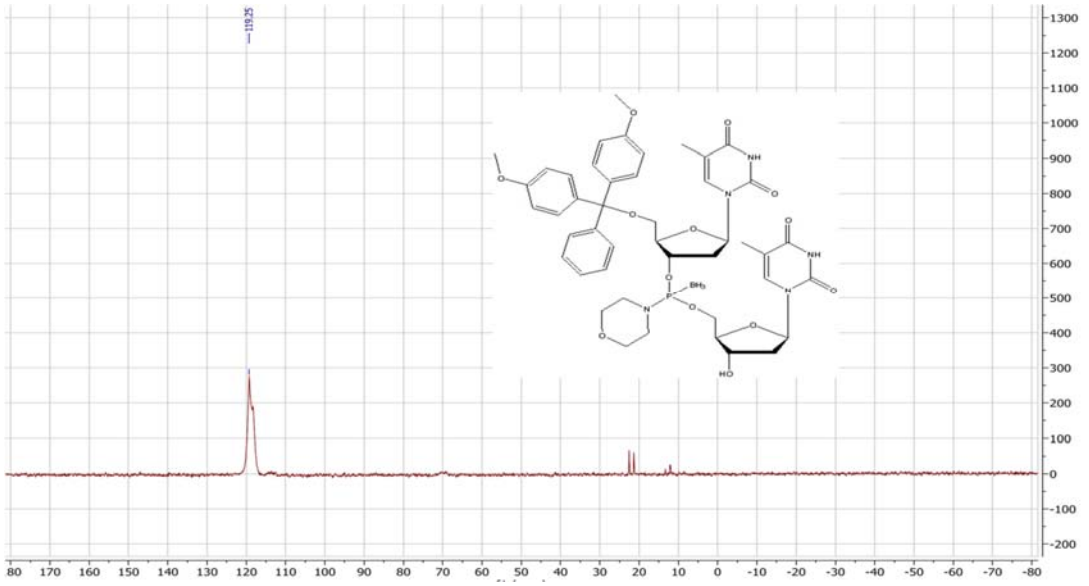

Figure 8.7: $^{31}P$ NMR spectrum for compound (17).

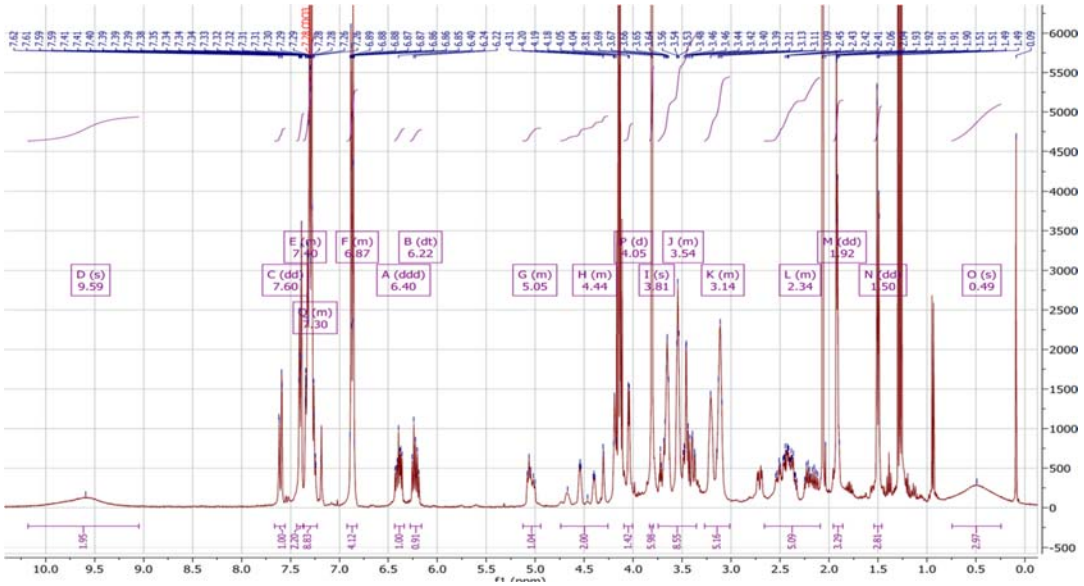


Figure 8.8: $^{1}H$ NMR spectrum for compound (17).

**Synthesis of (18)**

(5.0 g, 5.4 mmol) was dissolved in dichloromethane (50 ml) and 4,5-dicyanoimidazole (637 mg, 5.4 mmol) and 2-cyanoethyl-N,N,N',N'-tetraisopropyl phosphane (2.4 g, 8.1 mmol) were added. The reaction was stirred for 2 hours before the solvent was removed under reduced pressure and the residue purified by flash column with EtOAc. $^{31}$P NMR (162 MHz, $CDCl_3$) δ 149.3, 149.2, 149.0 (diastereomers), 119.1(broad); $^{1}$H NMR (400 MHz, $CDCl_3$) δ 8.67 (s, 2H), 7.67 – 7.52 (m, 2H), 7.40 (dt, *J* = 8.4, 1.4 Hz, 3H), 7.36 – 7.24 (m, 9H), 6.95 – 6.82 (m, 4H), 6.44 (dd, *J* = 9.0, 5.5 Hz, 1H), 6.28 – 6.13 (m, 1H), 5.10 (t, *J* = 7.1 Hz, 1H), 4.69 – 4.42 (m, 1H), 4.34 – 4.06 (m, 4H), 3.89 (ddt, *J* = 10.3, 7.7, 6.4 Hz, 2H), 3.81 (d, *J* = 1.1 Hz, 6H), 3.77 – 3.70 (m, 2H), 3.70 – 3.57 (m, 5H), 3.55 – 3.33 (m, 6H), 3.29 – 3.03 (m, 5H), 2.74 – 2.61 (m, 3H), 2.57 – 2.11 (m, 4H), 1.47 (td, *J* = 4.3, 1.9 Hz, 3H), 1.25 – 1.14 (m, 12H), 0.52 (s, 3H). ESI-MS (m/z): 1116.5 $[M+H]^+$.

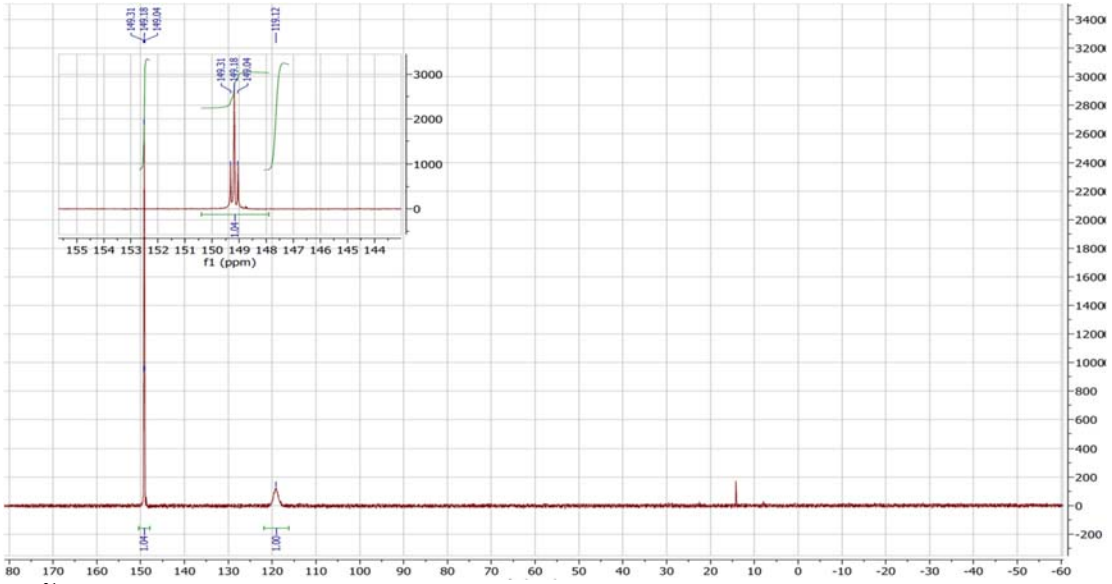


Figure 8.9: $^{31}$P NMR spectrum for compound (18).

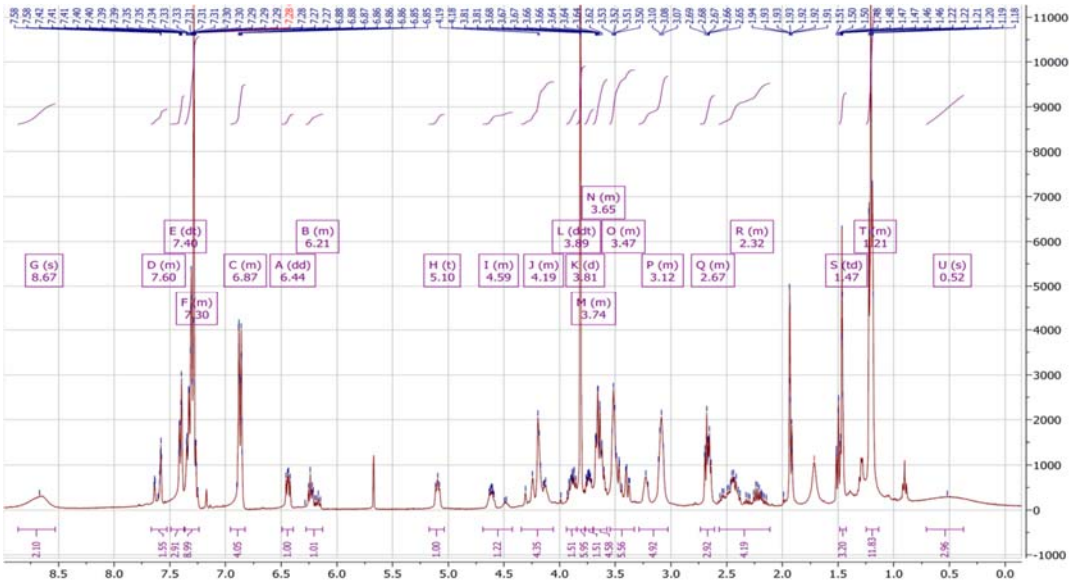

Figure 8.10: $^{1}$H NMR spectrum for compound (18).

**Synthesis of (20)**

In a round bottom flask bis(diisopropylamino)chlorophosphine (2.5 g, 9.4 mmol) was added and the flask was repeatedly flushed with argon. 50 mL of dichloromethane followed by Hunig base (1.45 g, 11 mmol) were added via syringe and stirred for 5 minutes under argon. Pivalamide (1.1 g, 11 mmol) was add in two portions separated in 5 minutes and stirred for 15 min. The reaction was monitored by $^{31}$P NMR to confirm the complete reaction of bis(diisopropylamino)chlorophosphine and used for the next step without purification. ETT (0.9 equivalents) was added to the solution followed by 1 equivalent 5`-DMT thymidine (calculated from the $^{31}$P NMR data). The reaction was stirred for 3 hours and monitored by TLC using ethylacetate ($R_f$ product = 0.6). The crude reaction mixture was evaporated to dryness using rotary evaporator and redissolved in ethylacetate (200 mL) and poured into 100 mL of saturated $NaHCO_3$. The organic layer was extracted twice with 100 mL of saturated $NaHCO_3$ and once with 50 mL brine. The ethylacetate layer was dried over magnesium sulfate, filtered and evaporated to dryness and kept under argon at -20 °C until purification. The product mixture was purified by

flash chromatography on a silica gel column. The silica gel slurry was initially prepared in a mixture of DCM:hexanes:triethylamine (47.5:47.5:5 ) and poured into the column. The column was washed with two column volumes of ethylacetate before loading the reaction mixture on to the column. The desired product was eluted using ethylacetate and isolated as a white foam. Yield (6.0 g, 83%). $^{31}$P NMR (162 MHz, $CDCl_3$) δ 115.7, 114.3 (diastereomers); $^{1}$H NMR (400 MHz, $CDCl_3$) δ 8.83 (s, 1H), 7.72 – 7.57 (m, 1H), 7.46 – 7.34 (m, 2H), 7.35 – 7.17 (m, 7H), 6.95 – 6.78 (m, 4H), 6.48 (dd, *J* = 8.9, 5.5 Hz, 1H), 5.99 – 5.80 (m, 1H), 4.79 – 4.60 (m, 1H), 4.37 – 4.14 (m, 1H), 3.81 (s, 6H), 3.65 – 3.26 (m, 4H), 2.59 – 2.29 (m, 2H), 2.06 (s, 1H), 1.41 (s, 3H), 1.23 (d, *J* = 1.5 Hz, 6H), 1.21 – 1.14 (m, 11H), 1.05 (d, *J* = 6.7 Hz, 3H). $^{13}$C NMR (101 MHz, $CDCl_3$) δ 181.13, 181.03, 180.95, 163.69, 163.65, 158.77, 158.75, 158.73, 150.48, 150.43, 144.27, 144.12, 135.65, 135.61, 135.34, 135.26, 135.22, 135.13, 130.10, 128.16, 128.14, 128.06, 128.01, 127.19, 127.16, 113.29, 113.27, 111.51, 111.43, 87.07, 87.02, 86.21, 86.16, 85.71, 85.65, 84.83, 84.55, 84.37, 77.36, 77.04, 76.73, 75.88, 75.63, 75.30, 75.07, 63.86, 63.59, 60.40, 55.26, 55.25, 44.24, 44.14, 44.11, 44.01, 40.06, 39.89, 39.85, 39.25, 27.54, 26.80, 26.77, 24.63, 24.56, 24.48, 24.40, 24.17, 24.13, 24.10, 24.06, 21.06, 14.21, 11.66, 11.64. ESI-MS (m/z): 775.4 $[M+H]^+$.

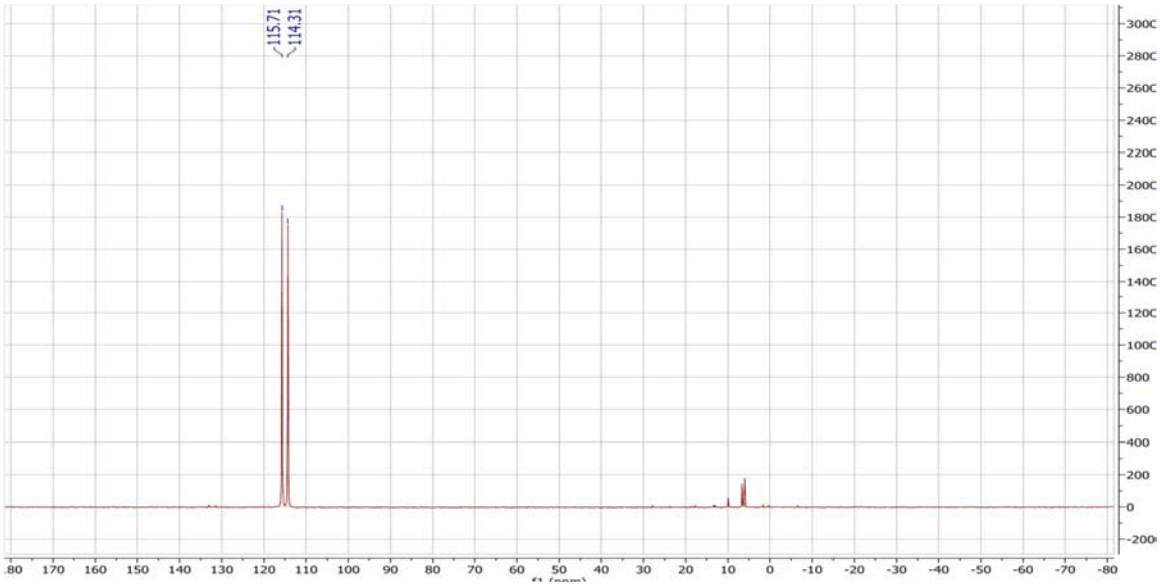


Figure 8.11: $^{31}P$ NMR spectrum for compound (20).

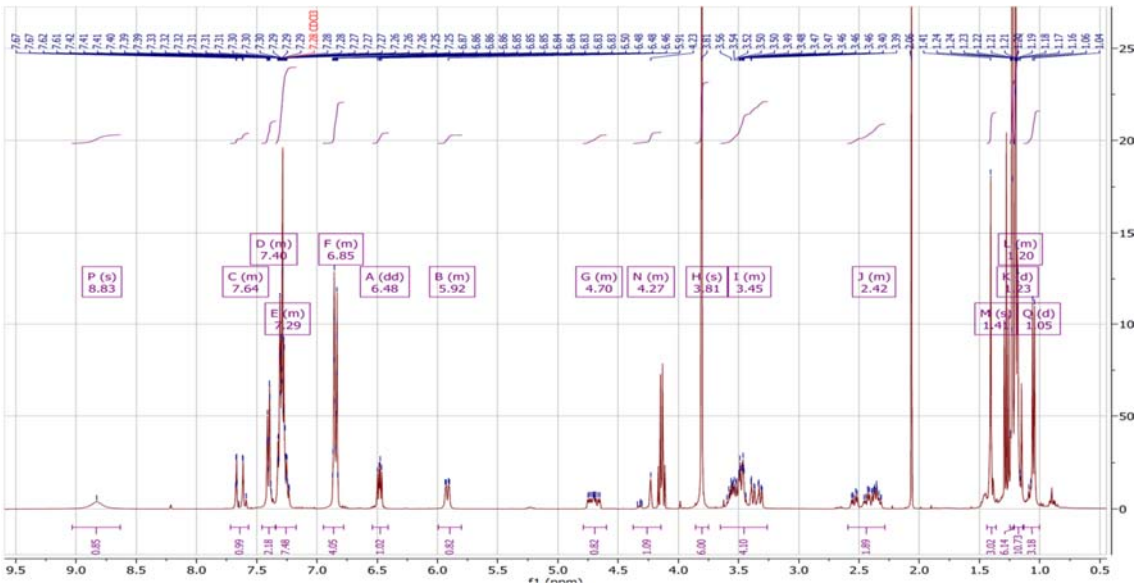


Figure 8.12: $^{1}H$ NMR spectrum for compound (20).

**General procedure for synthesis of compounds** (**22a-c**). This procedure is based on Jones' method[40] for protecting nucleosides.

To 2.5 g (10 mmol) of 2'-deoxynucleoside (**21a-c**) dried three times by evaporation of pyridine and suspended in 50 mL of dry pyridine was added 6.4 mL (50 mmol) of trimethyl chlorosilane. After the mixture was stirred for 30 min 2.4 mL (20 mmol) of pivaloyl chloride was added and the reaction was maintained at room temperature for 3 hours. The mixture was then cooled in an ice bath and 10 mL of water was added. After 5 min 20 mL of 29% aqueous ammonia was added and the mixture was stirred at room temperature for 1 hour. The reaction was then evaporated to near dryness and the residue was dissolved in 150 mL of water. The solution was washed once with a 50 mL portion of ethyl acetate. Crystallization began immediately after separation of the layers. After the solution was cooled, filtration gave the desired product. Yield (76% -84%).

**(22a)** yield (84%). $^{1}$H NMR (400 MHz, $CDCl_3$) δ 8.70 (s, 1H), 8.59 (s, 1H), 8.14 (s, 1H), 6.41 (dd, *J* = 8.9, 5.6 Hz, 1H), 5.81 (s, 1H), 4.87 – 4.70 (m, 1H), 4.22 (q, *J* = 1.9 Hz, 1H), 3.95 (dd, *J* = 12.7, 2.0 Hz, 1H), 3.81 (d, *J* = 12.8 Hz, 1H), 3.54 (s, 1H), 2.98 (ddd, *J* = 13.1, 8.9, 5.3 Hz, 1H), 2.39 (ddd, *J* = 13.4, 5.7, 1.8 Hz, 1H), 1.39 (s, 9H). $^{13}$C NMR (101 MHz, $CDCl_3$) δ 175.86, 152.00, 150.58, 150.08, 142.48, 124.22, 89.45, 87.42, 77.35, 77.03, 76.71, 72.79, 63.14, 60.40, 40.83, 40.58, 27.37, 23.98, 19.72, 14.18, 13.61. ESI-MS (m/z): 336.2 $[M+H]^+$.

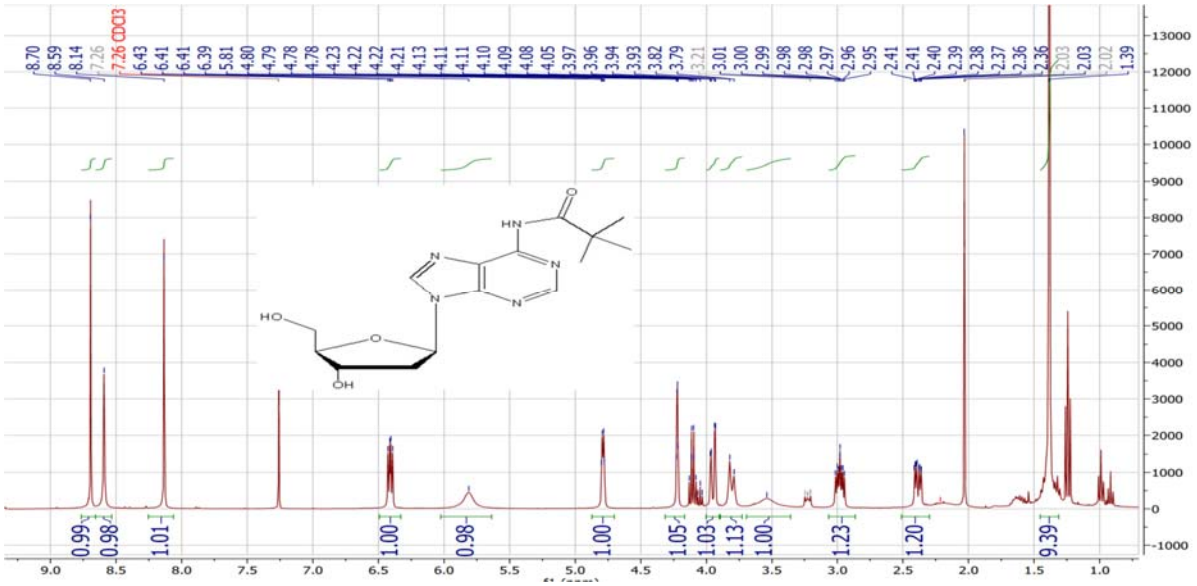

Figure 8.13: $^{1}$H NMR spectrum for compound **(22 a)**.

**(22b)** Yield 76%. $^{1}$H NMR (400 MHz, DMSO) δ 12.19 (s, 1H), 11.13 (s, 1H), 8.26 (d, *J* = 1.0 Hz, 1H), 6.29 (dd, *J* = 7.8, 5.9 Hz, 1H), 5.52 – 5.17 (m, 1H), 4.98 (s, 1H), 4.37 (dt, *J* = 5.8, 2.9 Hz, 1H), 3.83 (td, *J* = 4.6, 2.7 Hz, 1H), 3.54 (qd, *J* = 11.7, 4.6 Hz, 2H), 2.64 – 2.52 (m, 1H), 2.27 (ddd, *J* = 13.2, 5.9, 3.0 Hz, 1H), 1.25 (d, *J* = 1.3 Hz, 9H). ESI-MS (m/z): 352.2 $[M+H]^{+}$.

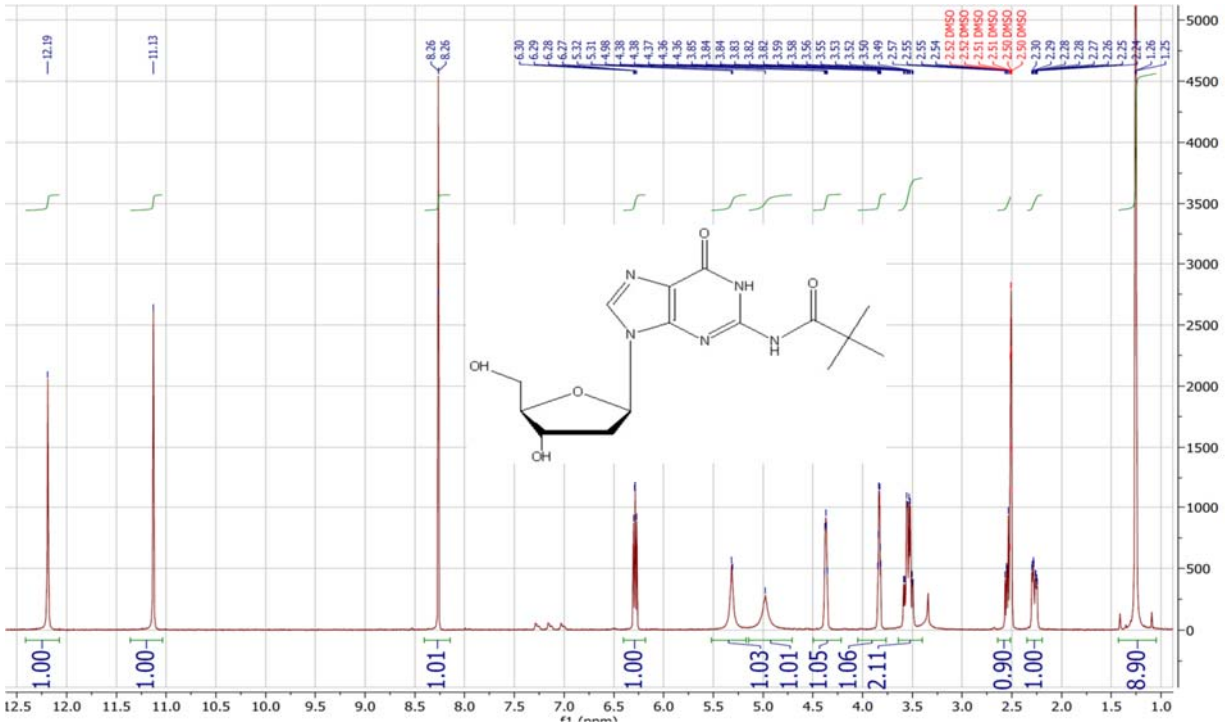

Figure 8.14: $^{1}$H NMR spectrum for compound **(22 b)**.

**(22c)** Yield 80%. $^{1}$H NMR (400 MHz, MeOD) δ 8.51 (d, *J* = 7.5 Hz, 1H), 7.50 (d, *J* = 7.5 Hz, 1H), 6.24 (t, *J* = 6.2 Hz, 1H), 4.43 – 4.36 (m, 1H), 4.03 (q, *J* = 3.6 Hz, 1H), 3.90 – 3.73 (m, 2H), 2.52 (ddd, *J* = 13.7, 6.2, 4.2 Hz, 1H), 2.20 (dt, *J* = 13.7, 6.2 Hz, 1H), 1.30 (s, 9H). $^{13}$C NMR (101 MHz, MeOD) δ 179.08, 163.22, 156.40, 144.96, 96.59, 88.08, 87.28, 70.21, 61.01, 48.24, 48.03, 47.81, 41.10, 25.69.

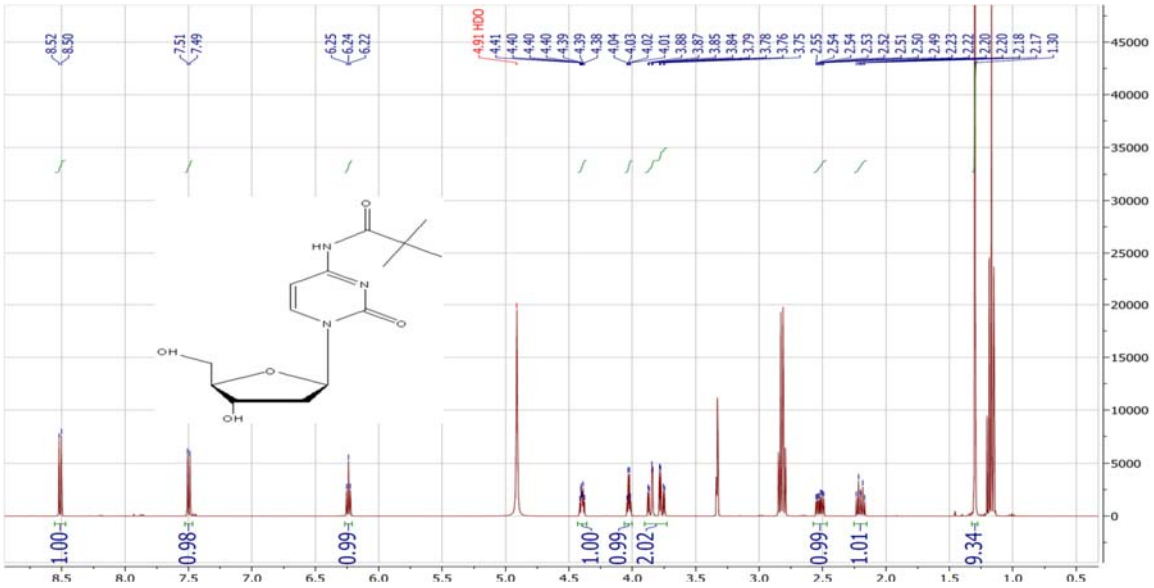

Figure 8.15: $^{1}$H NMR spectrum for compound **(22 c)**.

**General procedure for synthesis of compounds (23a-c)**.

This procedure is based on Jones' method[40] for protecting nucleosides.

To 2.5 g (10 mmol) of (**22a-c)** dried three times by evaporation of pyridine and suspended in 50 mL of dry pyridine was added 5 g (15 mmol) of 4,4',4''-trimethoxytritylchloride, 2.1 mL (15 mmol) of triethylamine. After 4 h TLC using ethylacetate as mobile phase showed complete reaction. The mixture was then poured into 250 mL of cold, saturated NaHCO, and the solution was extracted three times with 150-mL portions of ethylacetate. The combined organic layers were evaporated to dryness and purified by flash chromatography on a silica column. The desired product was eluted using ethylacetate and isolated as a white foam. (Yield 86% - 93%)

**(23a)** Yield 93%. $^{1}$H NMR (400 MHz, $CDCl_3$) δ 8.13 (s, 1H), 8.04 (d, *J* = 7.5 Hz, 1H), 7.46 – 7.37 (m, 2H), 7.35 – 7.21 (m, 13H), 7.19 – 7.07 (m, 5H), 6.79 (ddd, *J* = 8.5, 5.1, 3.1 Hz, 8H), 6.40 (dd, *J* = 7.7, 5.6 Hz, 1H), 4.35 (d, *J* = 5.5 Hz, 1H), 3.93 (s, 1H), 3.81 (s, 9H), 3.22 (dd, *J* = 10.7, 2.4

Hz, 1H), 3.00 (dd, *J* = 10.6, 3.8 Hz, 1H), 2.46 (ddd, *J* = 13.7, 5.7, 2.0 Hz, 1H), 1.86 (ddd, *J* = 13.6, 7.7, 5.9 Hz, 1H), 1.29 (s, 9H). $^{13}$C NMR (101 MHz, $CDCl_3$) δ 177.82, 161.86, 158.68, 158.64, 158.58, 154.92, 145.05, 144.94, 144.11, 136.19, 136.07, 135.37, 135.25, 130.26, 130.18, 129.97, 129.93, 129.15, 128.25, 128.10, 127.98, 127.92, 127.85, 127.79, 127.03, 113.31, 113.23, 113.17, 95.75, 87.81, 87.22, 86.75, 86.00, 77.39, 77.07, 76.75, 74.66, 63.30, 55.21, 41.35, 27.12. ESI-MS (m/z): 668.3 $[M+H]^+$.

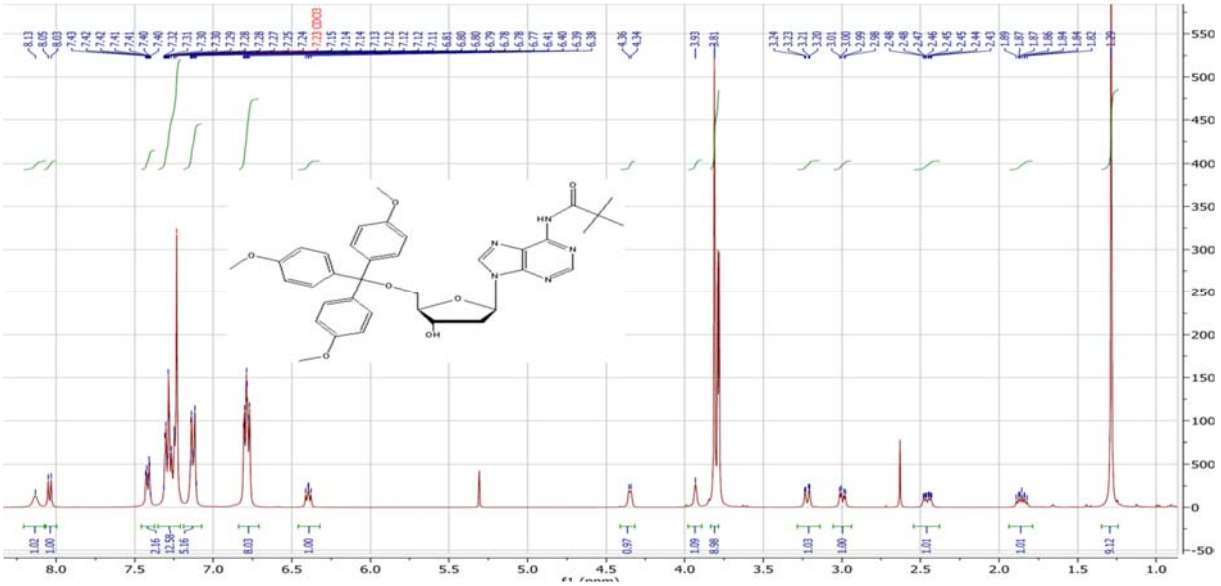

Figure 8.16: $^1$H NMR spectrum for compound **(23 a)**.

**(23b)** Yield 86%. $^1$H NMR (400 MHz, DMSO) δ 12.23 (s, 1H), 11.14 (s, 1H), 8.13 (s, 1H), 7.21 (d, *J* = 8.9 Hz, 6H), 6.81 (d, *J* = 8.9 Hz, 6H), 6.33 (t, *J* = 6.4 Hz, 1H), 5.38 (s, 1H), 4.40 (q, *J* = 4.8 Hz, 1H), 3.96 (dt, *J* = 6.2, 3.8 Hz, 1H), 3.72 (s, 9H), 3.27 – 3.03 (m, 2H), 2.68 (ddt, *J* = 21.1, 14.4, 6.8 Hz, 1H), 2.35 (ddd, *J* = 13.2, 6.4, 4.4 Hz, 1H), 1.26 (s, 9H). $^{13}$C NMR (101 MHz, DMSO) δ 181.68, 170.77, 158.36, 155.41, 149.04, 148.90, 137.74, 136.60, 129.84, 120.86, 113.48, 86.42, 85.64, 83.11, 70.90, 64.53, 63.94, 60.21, 55.42, 40.61, 40.48, 40.40, 40.19, 39.98, 39.77, 39.56, 39.53, 39.36, 26.75. ESI-MS (m/z): 684.4 $[M+H]^+$.

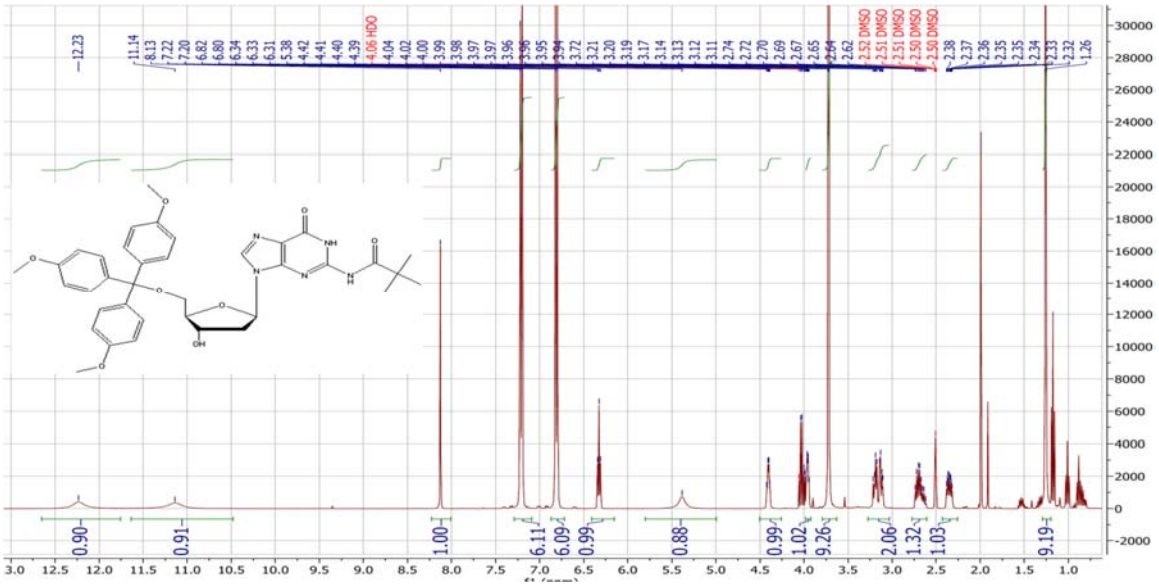

Figure 8.17: $^{1}$H NMR spectrum for compound **(23 b)**.

**(23c)** Yield 89%. $^{1}$H NMR (400 MHz, $CDCl_3$) δ 8.31 (d, *J* = 7.4 Hz, 1H), 8.18 (s, 1H), 7.36 – 7.26 (m, 6H), 7.21 – 7.15 (m, 1H), 6.91 – 6.80 (m, 6H), 6.36 – 6.16 (m, 1H), 4.56 (dq, *J* = 15.8, 5.8, 5.4 Hz, 1H), 3.82 (s, 9H), 3.48 (ddd, *J* = 38.2, 10.8, 3.4 Hz, 2H), 3.17 – 2.98 (m, 1H), 2.79 – 2.58 (m, 1H), 2.40 – 2.20 (m, 1H), 1.28 (s, 9H). $^{13}$C NMR (101 MHz, $CDCl_3$) δ 177.85, 162.13, 158.57, 158.53, 158.47, 155.08, 145.95, 144.92, 139.71, 136.62, 135.84, 135.76, 129.92, 129.76, 129.70, 129.05, 113.31, 113.26, 113.19, 113.12, 96.16, 96.09, 87.77, 87.52, 87.15, 86.76, 86.47, 86.43, 85.99, 77.35, 77.03, 76.71, 70.72, 62.43, 55.25, 55.23, 55.19, 27.08, 27.06. ESI-MS (m/z): 644.4 $[M+H]^+$.

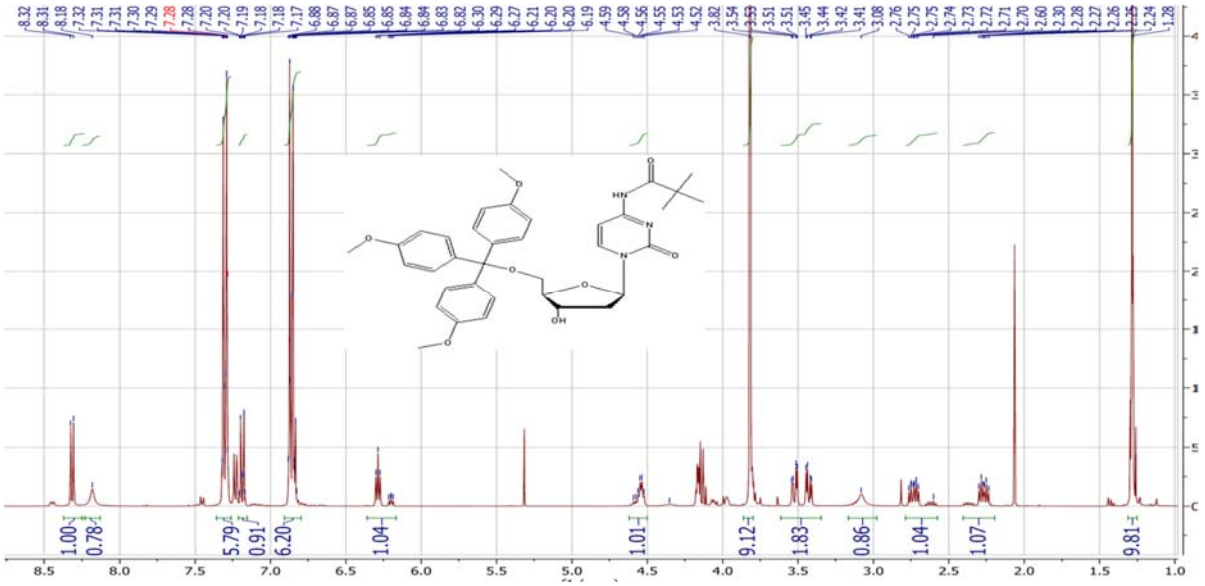

Figure 8.18: $^{1}$H NMR spectrum for compound **(23 c)**.

**Synthesis of (33):**

In a round bottom flask bis(diisopropylamino)chlorophosphine (2.5 g, 9.4 mmol) was added and the flask was repeatedly flushed with argon. 50 mL of dichloromethane followed by freshly distilled triethylamine (1.1 g, 11 mmol) were added via syringe and stirred for 5 minutes under argon. Cyanoacetamide (1.0 g, 12 mmol) was add in two portions separated in 5 minutes and stirred for 15 min. The reaction was monitored by $^{31}$P NMR to confirm the complete reaction of bis(diisopropylamino)chlorophosphine and used for the next step without purification. ETT (0.9 equivalents) was added to the solution followed by 1 equivalent 5`-DMT thymidine (calculated from the $^{31}$P NMR data). The reaction was stirred for 3 hours and monitored by TLC using acetonitrile: DCM ($R_f$ product = 0.7). The crude reaction mixture was evaporated to dryness using rotary evaporator and redissolved in ethylacetate (200 mL) and poured into 100 mL of saturated $NaHCO_3$. The organic layer was extracted twice with 100 mL of saturated $NaHCO_3$ and once with 50 mL brine. The ethylacetate layer was dried over magnesium sulfate, filtered and evaporated to

dryness and kept under argon at -20 °C until purification. The product mixture was purified by flash chromatography on a silica gel column. The silica gel slurry was initially prepared in a mixture of DCM:hexanes:triethylamine (47.5:47.5:5 ) and poured into the column. The column was washed with two column volumes of DCM before loading the reaction mixture on to the column. The desired product was eluted using a gradient of 100% DCM to 1:1 DCM acetonitrile and isolated as a white foam. Yield (5.2 g, 74%). $^{31}$P NMR (162 MHz, $CDCl_3$) δ 117.0, 115.5 (diastereomers). $^{1}$H NMR (400 MHz, $CDCl_3$) δ 9.49 (s, 1H), 7.71 – 7.57 (m, 1H), 7.45 – 7.34 (m, 2H), 7.36 – 7.19 (m, 8H), 6.93 – 6.76 (m, 5H), 6.41 (q, *J* = 6.3 Hz, 1H), 4.78 – 4.58 (m, 1H), 4.18 (d, *J* = 45.2 Hz, 1H), 3.80 (s, 6H), 3.68 – 3.26 (m, 4H), 2.62 – 2.30 (m, 2H), 1.42 (s, 3H), 1.21 (ddd, *J* = 10.5, 7.1, 3.3 Hz, 12H). $^{13}$C NMR (101 MHz, $CDCl_3$) δ 158.77, 158.75, 158.73, 144.22, 144.07, 135.57, 135.18, 135.14, 135.06, 130.18, 130.07, 130.06, 128.09, 128.07, 128.03, 127.21, 113.33, 113.31, 113.29, 113.23, 111.61, 111.51, 87.14, 87.08, 85.62, 84.73, 84.56, 77.36, 77.04, 76.72, 63.74, 63.51, 55.27, 55.25, 45.99, 39.80, 27.04, 26.93, 25.54, 24.44, 24.35, 23.69, 23.66, 22.63, 22.61. ESI-MS (m/z): 756.8 $[M-H]^-$.

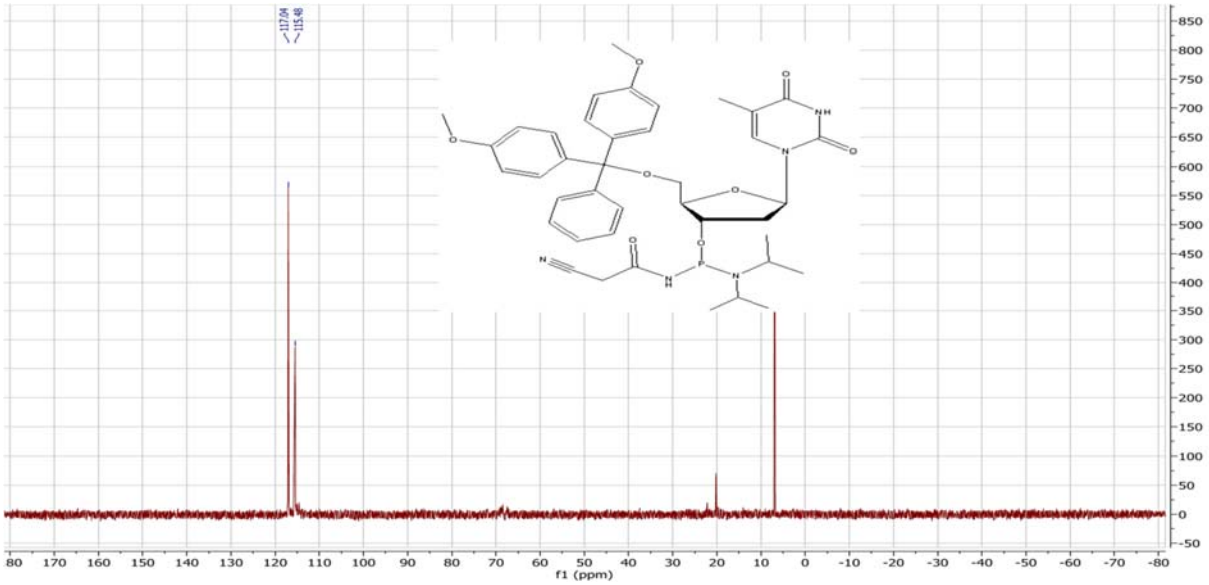


Figure 8.19: $^{31}$P NMR spectrum for compound **(33)**.

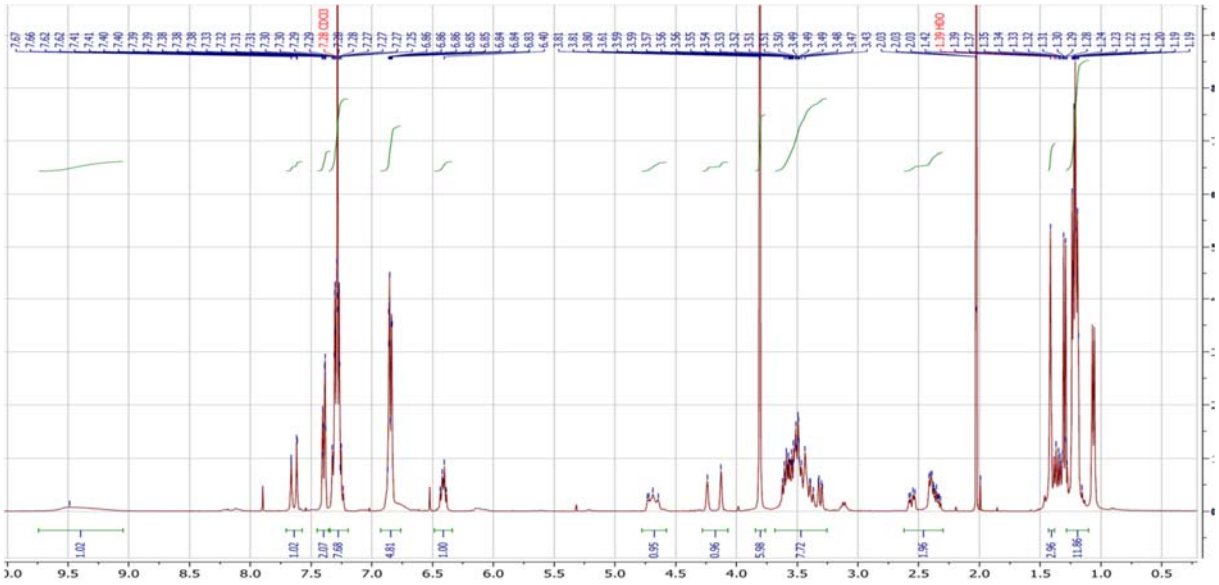

Figure 8.20: $^{1}$H NMR spectrum for compound **(33)**.

## Synthesis of (34):

Compound (33) (2.0 g, 2.6 mmol) was dried overnight under vacuum in round bottomed flasks. The flask was flushed repeatedly with argon. Anhydrous dichloromethane (100 mL) and 3'-O-acetylthymidine (0.83 g, 2.9 mmol) were added to the flask. This was followed by dropwise addition of 9.5 mL of ETT (0.25 M in acetonitrile; Glen Research) to the reaction flask. After stirring for 3 hours at room temperature, TLC (1:1; DCM:acetonitrile) showed complete disappearance of starting material. The crude reaction mixture was evaporated to dryness using rotary evaporator and redissolved in ethylacetate (200 mL) and poured into 100 mL of saturated $NaHCO_3$. The organic layer was extracted twice with 100 mL of saturated $NaHCO_3$ and once with 50 mL brine. The ethylacetate layer was dried over magnesium sulfate, filtered and evaporated to dryness and kept under argon at -20 °C until purification. The product mixture was purified by flash chromatography on a silica gel column. The silica gel slurry

was initially prepared in a mixture of DCM:hexanes:triethylamine (47.5:47.5:5 ) and poured into the column. The column was washed with two column volumes of DCM before loading the reaction mixture on to the column. The desired product was eluted using a gradient of 100% DCM to 1:1 DCM acetonitrile and isolated as a white foam. Yield (1.9 g, 84%). $^{31}$P NMR (162 MHz, $CDCl_3$) δ 130.2, 129.0 (diasteriomers). $^{1}$H NMR (400 MHz, $CDCl_3$) δ 9.77 (s, 1H), 8.13 (s, 1H), 7.56 (dd, *J* = 10.8, 1.3 Hz, 1H), 7.43 – 7.31 (m, 3H), 7.31 – 7.21 (m, 8H), 6.89 – 6.79 (m, 4H), 6.31 (dq, *J* = 7.2, 4.2, 3.5 Hz, 1H), 6.24 – 6.02 (m, 1H), 5.28 – 5.07 (m, 1H), 4.91 (d, *J* = 8.0 Hz, 1H), 4.15 – 4.07 (m, 2H), 3.80 (d, *J* = 1.2 Hz, 6H), 3.68 – 3.25 (m, 6H), 2.52 – 2.32 (m, 3H), 2.07 (s, 2H), 1.96 – 1.83 (m, 3H), 1.49 – 1.40 (m, 3H), 1.33 – 1.25 (m, 7H). $^{13}$C NMR (101 MHz, $CDCl_3$) δ 164.04, 158.78, 151.03, 150.64, 144.11, 135.12, 135.07, 135.02, 130.11, 128.08, 128.06, 127.27, 113.34, 111.93, 111.41, 87.22, 77.35, 77.04, 76.72, 60.41, 55.29, 46.78, 46.73, 44.52, 44.47, 23.69, 23.66, 23.21, 23.14, 22.63, 22.61, 21.08, 20.92. ESI-MS (m/z): 939.2 $[M-H]^-$.

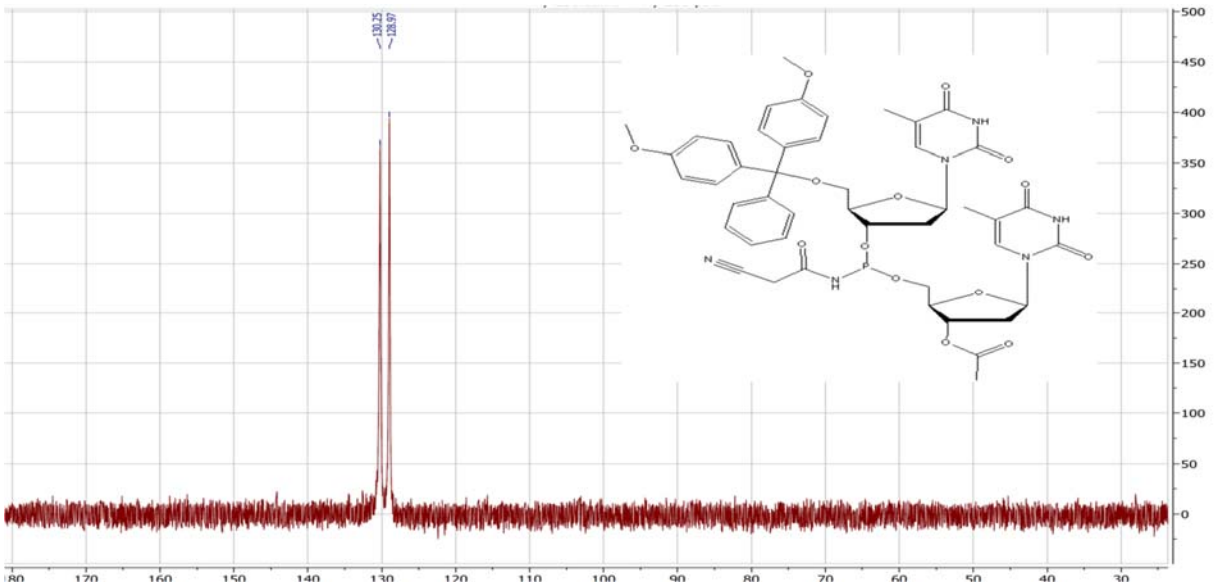


Figure 8.21: $^{31}$P NMR spectrum for compound **(34)**.

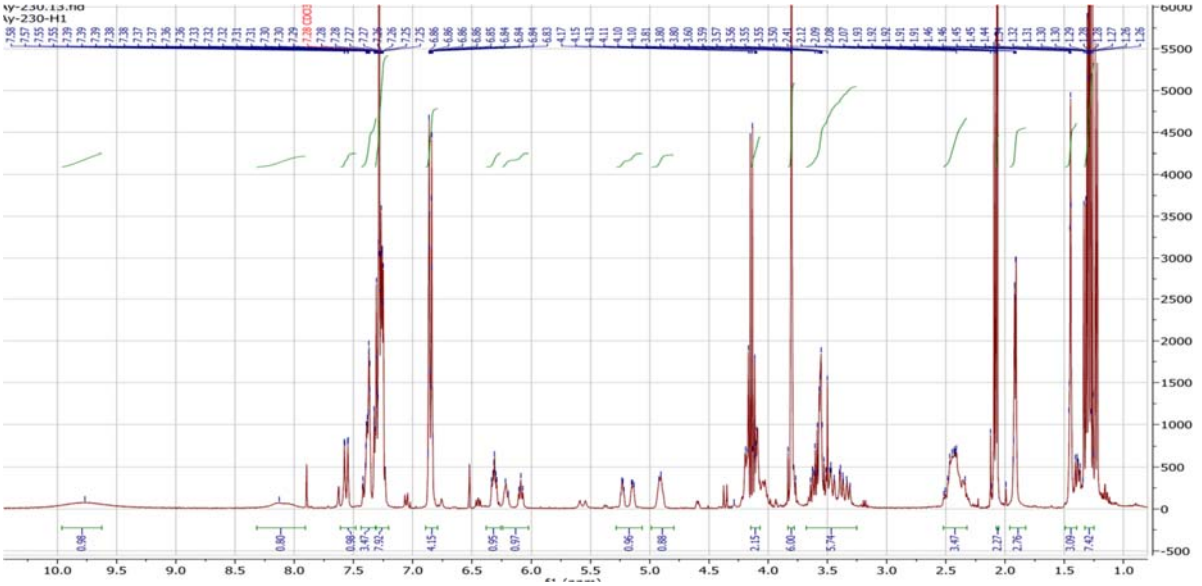

Figure 8.22: $^{1}$H NMR spectrum for compound **(34)**.

**Synthesis of (35a)**

Compound (**34**) (0.24 g, 0.26 mmol) was dissolved in anhydrous tetrahydrofuran (20.0 mL) followed by dropwise addition of 1 M $BH_3$ in THF (0.5 mL, 0.5 mmol) to the starting material solutions. The reaction mixture was stirred at room temperature and monitored by $^{31}$P NMR. After 15 minutes, the $^{31}$P NMR spectra showed complete conversion of starting materials to the broad product peak at 116.0 ppm. Excess $BH_3$ in the reaction mixtures was quenched by addition of a few drops of methanol and the solvent removed under reduced pressure using rotary evaporator. The crude product was purified by flash chromatography on a silica column. The product mixture was purified by flash chromatography on a silica gel column. The silica gel slurry was initially prepared in a mixture of DCM:hexanes:triethylamine (47.5:47.5:5 ) and poured into the column. The column was washed with two column volumes of DCM before loading the reaction mixture on to the column. The desired product was eluted using a gradient of 100% DCM to 1:1 DCM

acetonitrile and isolated as a white foam. Yield (0.19 g, 88%). $^{31}$P NMR (162 MHz, $CDCl_3$) δ 116.00 (broad). ESI-MS (m/z): 952.3 $[M-H]^-$.

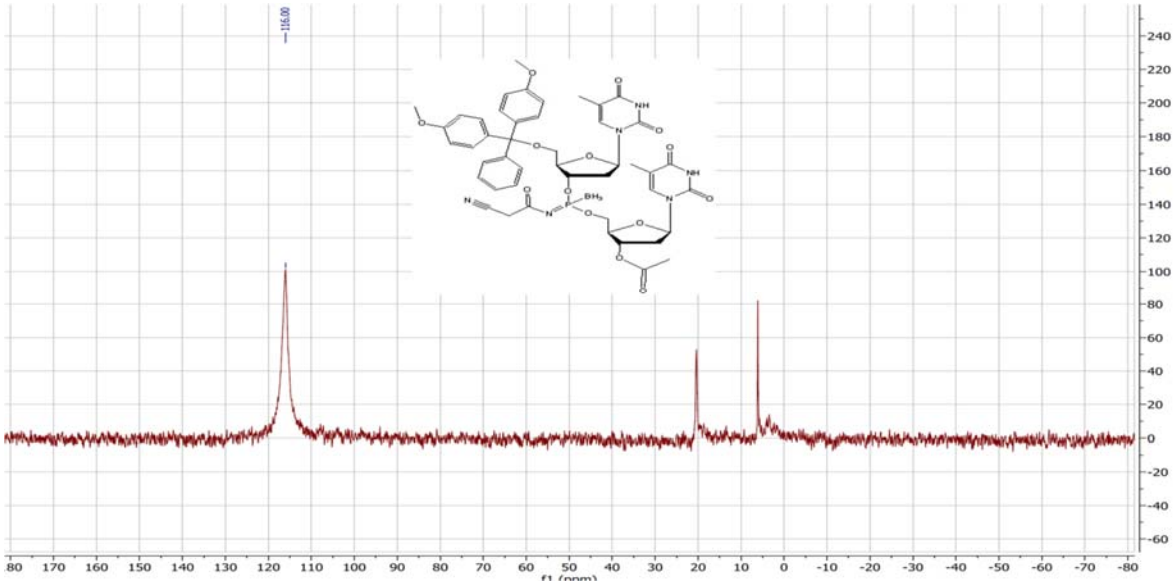


Figure 8.23: $^{31}$P NMR spectrum for compound **(35 a)**.

**Synthesis of (35b)**

Compound (**34**) (0.24 g, 0.26 mmol) was dissolved in anhydrous tetrahydrofuran (10.0 mL). Iodine (0.22 g, 0.87 mmol) immediately followed by anhydrous amine (2.6 mL, 0.5 M in dioxane, 1.3 mmol) was added to the reaction mixture. The reaction mixture was stirred at room temperature under argon and monitored using TLC (1:1; DCM:acetonitrile) and $^{31}$P NMR. After completion (1 hour) the reaction mixture was concentrated to minimum volume, diluted with ethylacetate (50 mL) and washed with saturated sodium thiosulfate (25 mL) and brine (25 mL). The ethylacetate layers were dried over $Na_2SO_4$, filtered and evaporated to dryness. The crude product was purified by flash chromatography on a silica column. The product mixture was purified by flash chromatography on a silica gel column. The silica gel slurry was initially prepared in a mixture of DCM:hexanes:triethylamine (47.5:47.5:5 ) and poured into the column. The column was washed

with two column volumes of DCM before loading the reaction mixture on to the column. The desired product was eluted using a gradient of 100% DCM to 1:1 DCM acetonitrile and isolated as a white foam. Yield (0.22 g, 92%). $^{31}$P NMR (162 MHz, $CDCl_3$) δ 23.63, 23.14 (diastereomers). ESI-MS (m/z): 956.3 $[M+H]^+$, 978.2 $[M+Na]^+$

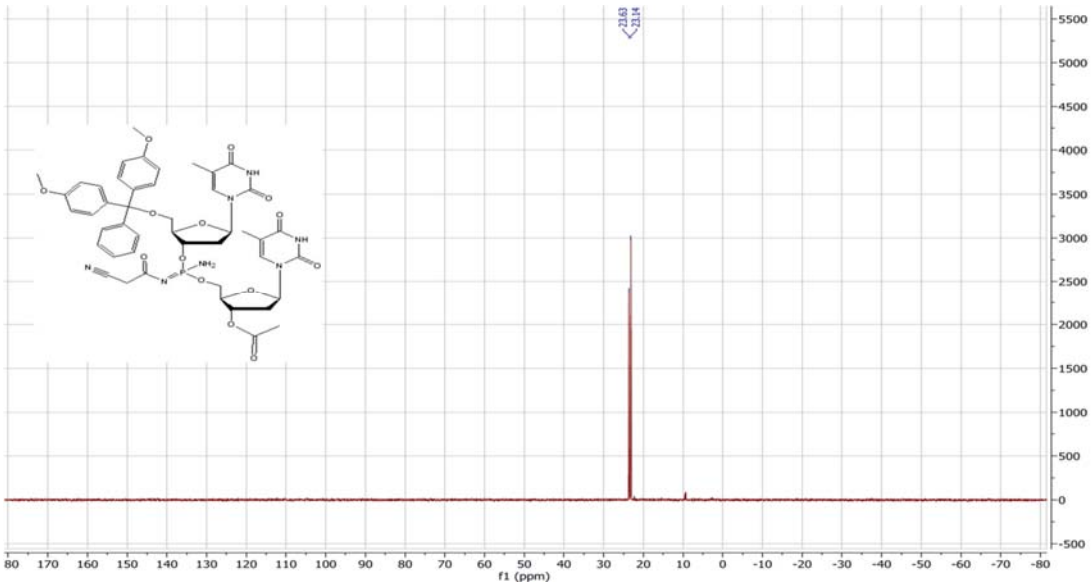


Figure 8.24: $^{31}$P NMR spectrum for compound **(35 b)**.

**General procedure for synthesis ofcompounds (40a-d)**

In a round bottom flask bis(diisopropylamino)chlorophosphine (2.5 g, 9.4 mmol) was added and the flask was repeatedly flushed with argon. 50 mL of dichloromethane followed by freshly distilled triethylamine (1.1 g, 11 mmol) were added via syringe and stirred for 5 minutes under argon. Phenoxyacetamide (1.8 g, 12 mmol) was add in two portions separated in 5 minutes and stirred for 15 min. The reaction was monitored by $^{31}$P NMR to confirm the complete reaction of bis(diisopropylamino)chlorophosphine and used for the next step without purification. ETT (0.9 equivalents) was added to the solution followed by 1 equivalent 5'-DMT deoxynucleoside, 5'-

TMT-deoxythymidine or 5'-O-(tert-Butyldimethylsilyl)thymidine (calculated from the $^{31}P$ NMR data). The reaction was stirred for 3 hours and monitored by TLC using acetonitrile: DCM ($R_f$ product = 0.7). The crude reaction mixture was evaporated to dryness using rotary evaporator and redissolved in ethylacetate (200 mL) and poured into 100 mL of saturated $NaHCO_3$. The organic layer was extracted twice with 100 mL of saturated $NaHCO_3$ and once with 50 mL brine. The ethylacetate layer was dried over magnesium sulfate, filtered and evaporated to dryness and kept under argon at -20 °C until purification. The product mixture was purified by flash chromatography on a silica gel column. The silica gel slurry was initially prepared in a mixture of DCM:hexanes:triethylamine (47.5:47.5:5 ) and poured into the column. The column was washed with two column volumes of DCM before loading the reaction mixture on to the column. The desired product was eluted using a gradient of 100% DCM to 1:1 DCM acetonitrile and isolated as a white foam. Yield (75%-85%).

**Synthesis of (40a):**

$^{31}P$ NMR (162 MHz, $CDCl_3$) δ 115.34, 114.40. $^{1}H$ NMR ($CDCl_3$, 400 MHz) δ 8.65 (s, 1H, Thy-NH), 7.64 (d, *J* = 30.6 Hz, 1H, H-6), 7.44 – 7.38 (m, 2H, DMTr), 7.39 – 7.21 (m, 10H, DMT & *Ph*O), 7.07 – 6.99 (m, 1H, *Ph*O), 6.99 – 6.88 (m, 3H, PhO & *H*N-P), 6.89 – 6.79 (m, 4H, DMTr), 6.46 (m, 1H, H-1`), 4.87 – 4.71 (m, 1H, H-3`), 4.53 – 4.38 (d, 2H, C*H*$_2$OPh), 4.25 – 4.09 (m, 1H, H-4`), 3.81 (s, 6H, 2x C*H*$_3$-O), 3.64 – 3.44 (m, 3H, 2x HN$^{i}$Pr$_2$ & H-5`), 3.36 (m, 1H, H-5`), 2.62 – 2.27 (m, 2H, H-2`), 1.42 (s, 3H, C*H*$_3$-Thy), 1.22 – 1.01 (m, 12H, 2x *i*Pr$_2$NH). $^{13}C$ NMR (101 MHz, $CDCl_3$) δ 171.31, 171.14, 171.02, 170.90, 163.95, 163.86, 158.74, 158.72, 158.71, 158.69, 157.16, 157.05, 157.01, 150.47, 144.34, 144.16, 135.62, 135.38, 135.29, 135.16, 130.10, 129.80, 129.78,

128.15, 128.11, 128.01, 127.17, 127.13, 122.16, 114.69, 114.66, 114.64, 113.29, 113.27, 111.42, 111.30, 87.04, 86.98, 85.97, 85.92, 85.55, 85.50, 84.74, 84.55, 77.39, 77.07, 76.76, 76.14, 75.88, 75.69, 75.45, 67.44, 67.38, 67.09, 63.70, 63.48, 55.26, 55.25, 44.62, 44.59, 44.51, 44.49, 44.46, 40.16, 40.12, 39.83, 39.78, 24.40, 24.32, 24.28, 24.24, 24.20, 24.17, 23.69, 23.66, 22.65, 22.63, 11.73, 11.71. ESI-MS (m/z): Calculated: 823.3472 $(M-H)^-$ Found: 823.3521 $(M-H)^-$.

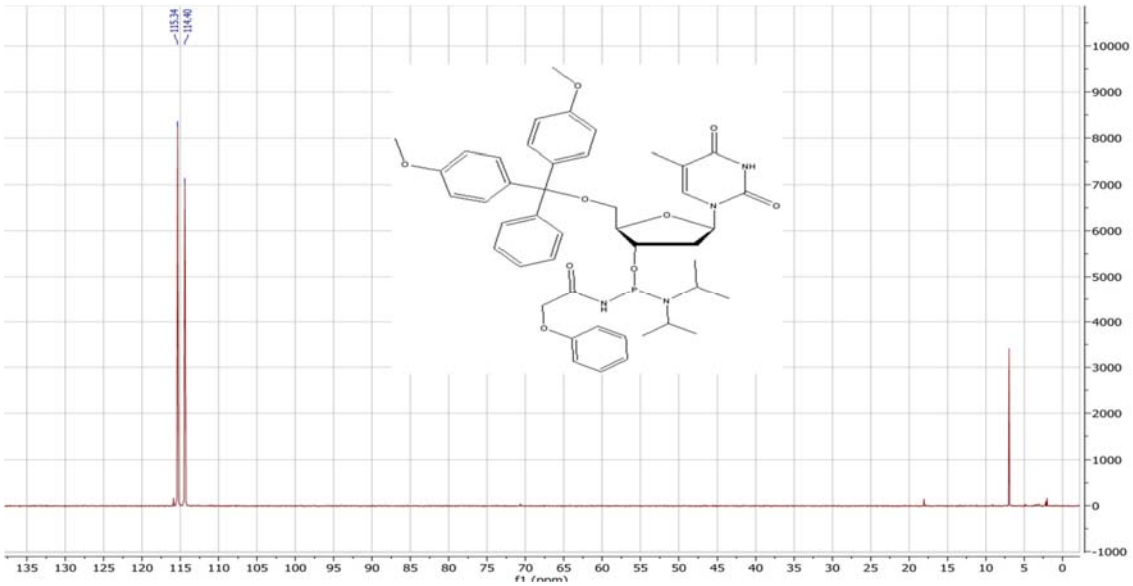


Figure 8.25: $^{31}P$ NMR spectrum for compound **(40a)**.

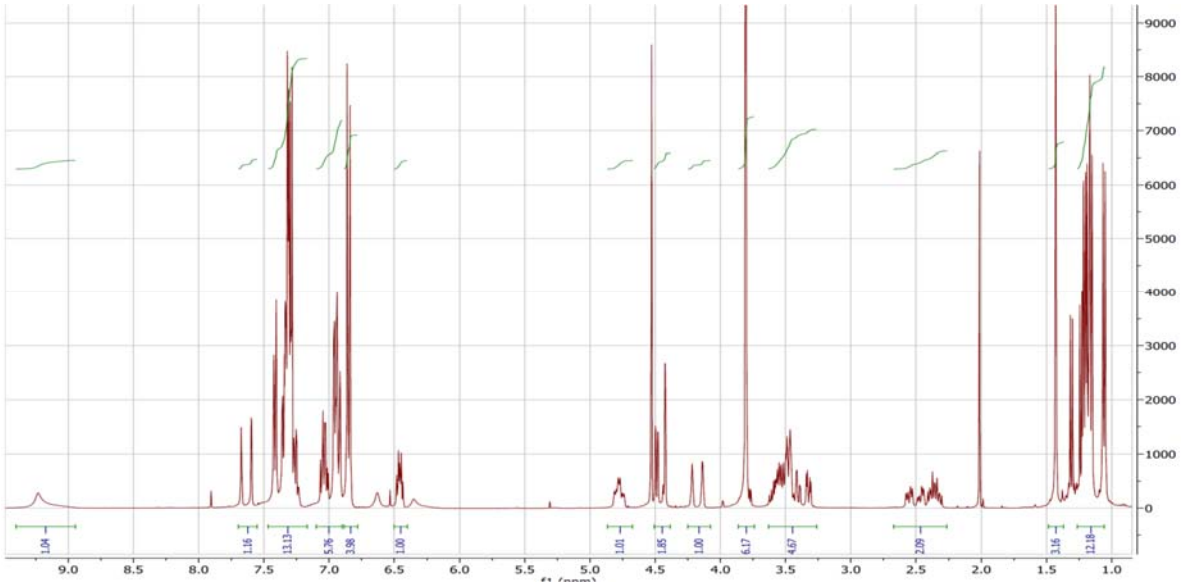

Figure 8.26: $^{1}$H NMR spectrum for compound **(40a)**.

## Synthesis of (40b)

$^{31}$P NMR (162 MHz, $CDCl_3$) δ 115.81, 115.19. $^{1}$H NMR (400 MHz, $CDCl_3$) δ 8.15 (dd, *J* = 23.9, 7.3 Hz, 1H, H-6), 7.42 – 7.25 (m, 12H, DMTr), 7.15 (dd, *J* = 13.2, 7.3 Hz, 1H, H-5), 7.09 – 7.00 (m, 2H, DMTr), 6.98 – 6.82 (m, 7H, DMTr & PhO), 6.67 (s, 1H, *H*N-P), 6.29 (dt, *J* = 23.4, 6.2 Hz, 1H, H-1`), 4.72 (m, 1H, H-3`), 4.51 – 4.39 (m, 2H, C*H*$_2$OPh), 4.32 – 4.21 (m, 1H, H-4`), 3.86 – 3.77 (2s, 6H, 2x C*H*$_3$-O), 3.66 – 3.33 (m, 4H, 2x HN*i*Pr$_2$ & 2x H-5`), 2.82 – 2.66 (m, 1H, H-2`), 2.36 – 2.15 (m, 4H, h-2` & $CH_3$(CO)), 1.28 – 1.11 (m, 12H, 2x $^{i}$Pr$_2$NH). $^{13}$C NMR (101 MHz, $CDCl_3$) δ 171.45, 171.09, 170.97, 170.92, 170.80, 158.69, 158.64, 157.15, 157.05, 157.01, 144.58, 144.43, 144.24, 144.08, 135.34, 135.24, 135.15, 135.08, 130.12, 130.08, 130.06, 129.82, 129.78, 128.13, 128.06, 128.00, 127.14, 127.07, 122.15, 114.69, 114.65, 114.61, 113.28, 87.24, 87.05, 86.97, 86.94, 86.29, 85.97, 77.35, 77.03, 76.72, 75.17, 74.92, 74.42, 74.42, 67.46, 67.40, 67.05, 62.90, 62.74, 55.25, 55.23, 44.72, 44.60, 44.51, 44.46, 41.30, 41.12, 24.90, 24.49, 24.41, 24.34,

24.27, 24.20, 24.13, 23.69, 23.66, 22.65, 22.63. ESI-MS (m/z): Calculated: 850.3581 $(M-H)^-$ Found: 850.3514 $(M-H)^-$.

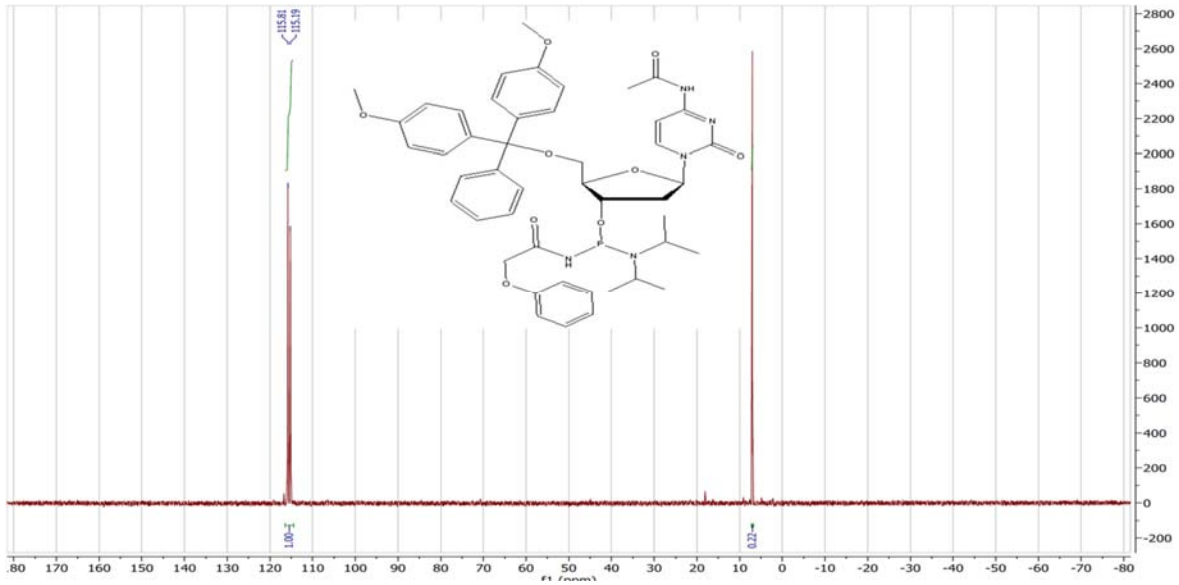

Figure 8.27: $^{31}P$ NMR spectrum for compound **(40b)**.

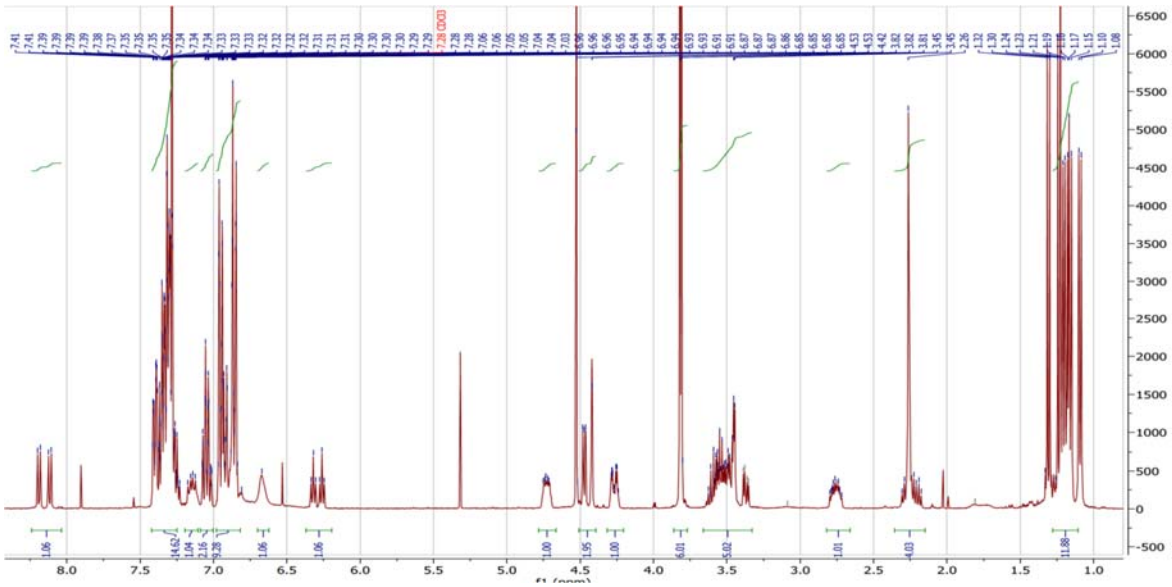

Figure 8.28: $^{1}H$ NMR spectrum for compound **(40b)**.

**Synthesis of (40c)**

$^{31}$P NMR (162 MHz, $CDCl_3$) δ 114.94, 114.501. $^{1}$H NMR (400 MHz, $CDCl_3$) δ 8.63 (d, *J* = 12.6 Hz, 1H, H-2), 8.51 (s, 1H, Ade-NH), 8.14 (d, *J* = 26.7 Hz, 1H, H-2), 7.46 – 7.14 (m, 12H, DMT & *Ph*O), 7.10 – 7.00 (m, 2H, *Ph*O), 6.95 (m, 4H, PhO & *H*N-P), 6.85 – 6.72 (m, 4H, DMTr), 6.53 – 6.43 (m, 1H, H-1`), 4.87 (m, 1H, H-3`), 4.51 – 4.42 (m, 2H, C*H*$_2$OPh), 4.38 – 4.26 (m, 1H, H-4`), 3.85 – 3.72 (s, 6H, 2x C*H*$_3$-O), 3.65 – 3.48 (m, 2H, 2x HN*i*Pr$_2$), 3.48 – 3.29 (m, 2H, H-5`), 3.03 – 2.66 (m, 2H, H-2`), 2.64 (s, 3H, $CH_3$(CO)), 1.31 – 1.14 (m, 12H, 2x $^{i}$Pr$_2$NH). $^{13}$C NMR (101 MHz, $CDCl_3$) δ 171.13, 171.10, 170.98, 170.90, 170.35, 170.30, 158.55, 158.53, 157.15, 157.07, 152.23, 152.21, 149.09, 144.47, 144.39, 141.37, 141.29, 135.55, 135.51, 130.03, 130.01, 129.82, 129.80, 128.10, 128.08, 127.86, 127.84, 126.92, 122.22, 122.18, 114.69, 114.64, 114.63, 113.15, 113.13, 86.61, 86.58, 86.02, 85.96, 84.73, 77.34, 77.03, 76.71, 75.89, 75.65, 67.47, 67.14, 63.56, 63.51, 55.21, 44.68, 44.63, 44.51, 44.46, 38.99, 25.64, 24.47, 24.37, 24.33, 24.26, 23.68, 23.66, 22.65, 22.62. ESI-MS (m/z): Calculated: 874.3693 $(M-H)^-$ Found: 874.3649 $(M-H)^-$.

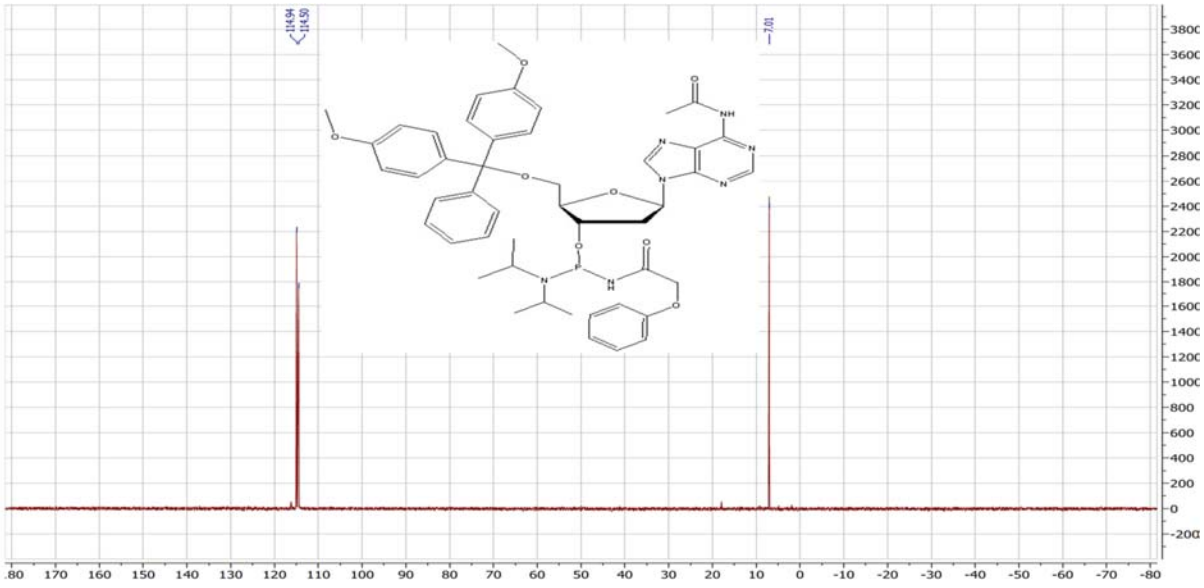


Figure 8.29: $^{31}$P NMR spectrum for compound **(40c)**.

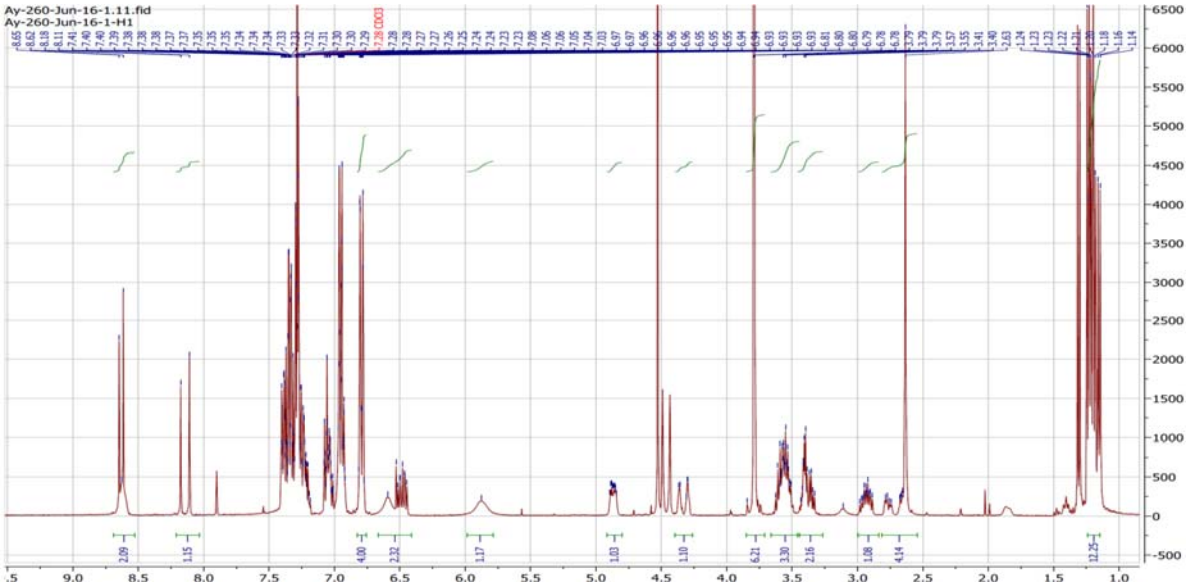


Figure 8.30: $^{1}$H NMR spectrum for compound **(40c)**.

## Synthesis of (40d)

$^{31}$P NMR (162 MHz, $CDCl_3$) δ 115.01, 114.68. $^{1}$H NMR (400 MHz, $CDCl_3$) δ 11.82 (s, 1H), 9.45 (s, 1H), 7.83 (d, *J* = 7.1 Hz, 1H, H-8), 7.41 – 7.14 (m, 14H, PhO), 7.13 – 6.94 (m, 5H, DMTr & PhO), 6.93 – 6.82 (m, 2H, DMTr), 6.82 – 6.72 (m, 4H, DMTr), 6.26 (q, *J* = 6.5 Hz, 1H, H-1`), 5.10 – 4.90 (m, 1H, H-3`), 4.69 (d, *J* = 2.8 Hz, 2H, C*H*$_2$OPh on the base), 4.54 – 4.29 (m, 2H, C*H*$_2$OPh), 4.28 – 4.19 (m, 1H, H-4`), 3.83 – 3.69 (m, 6H, 2x C*H*$_3$-O), 3.54 (m, 2H, 2x HN*i*Pr$_2$), 3.44 – 3.25 (m, 2H, 2x H-5`), 2.92 – 2.50 (m, 2H, H-2`), 1.29 – 1.03 (m, 12H, 2x $^{i}$Pr$_2$NH). $^{13}$C NMR (101 MHz, $CDCl_3$) δ 171.33, 171.27, 171.21, 171.16, 169.63, 169.56, 158.53, 158.50, 156.93, 156.90, 156.58, 156.53, 155.39, 147.59, 147.50, 146.18, 144.51, 144.38, 137.66, 137.56, 135.58, 135.53, 135.42, 130.03, 130.01, 129.97, 129.83, 129.81, 128.08, 128.06, 127.85, 126.92, 126.88, 122.93, 122.35, 122.27, 122.25, 114.93, 114.85, 114.60, 114.56, 113.13, 113.12, 86.52, 86.50, 85.83, 85.78, 85.71, 85.66, 84.00, 83.95, 77.38, 77.06, 76.74, 75.49, 75.24, 74.79, 74.57,

67.36, 67.30, 67.15, 67.08, 63.56, 63.52, 55.24, 55.21, 53.47, 44.84, 44.82, 44.71, 44.68, 39.56, 39.52, 38.96, 38.92, 24.39, 24.32, 24.28, 24.20. ESI-MS (m/z): Calculated: 982.3904 $(M-H)^-$ Found: 982.3862 $(M-H)^-$.

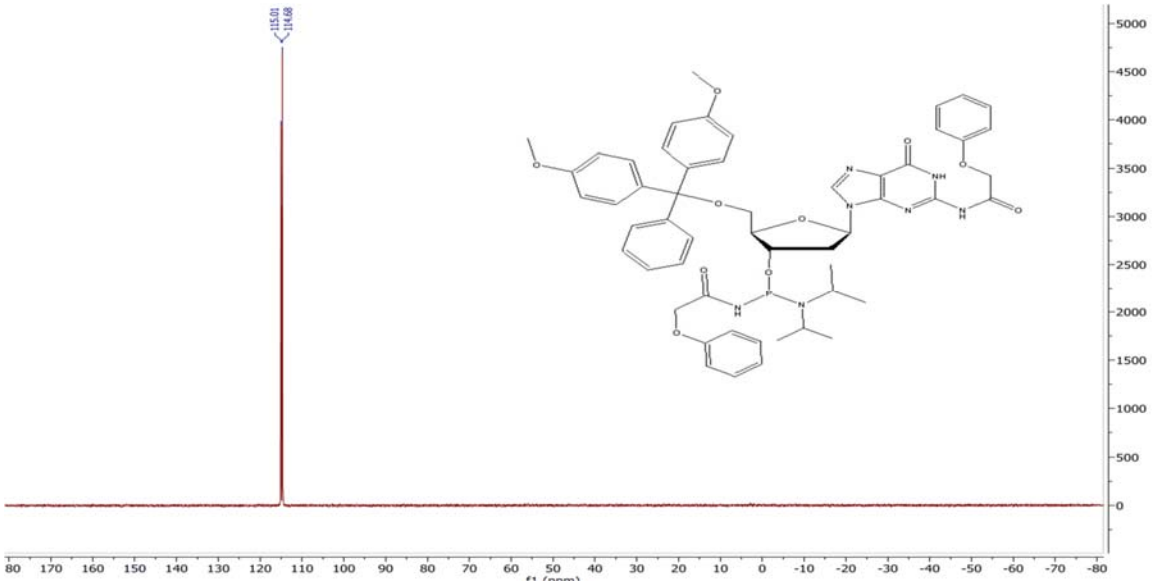

Figure 8.31: $^{31}P$ NMR spectrum for compound **(40d)**.

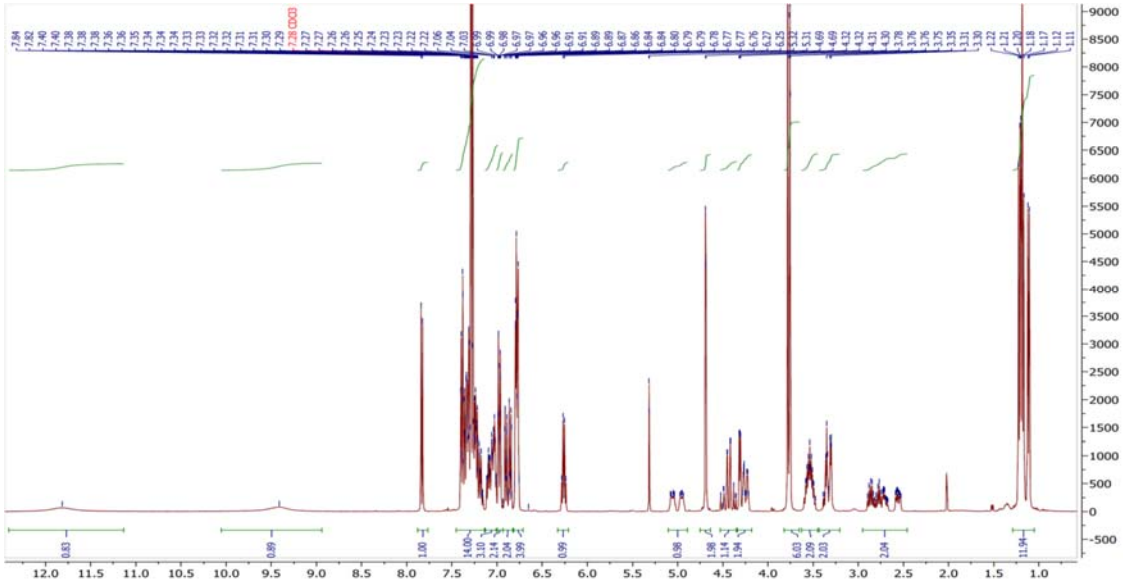

Figure 8.32: $^{1}H$ NMR spectrum for compound **(40d)**.

**Synthesis of (41):**

$^{31}$P NMR (162 MHz, $CDCl_3$) δ 117.0, 115.7 (diastereomers). $^{1}$H NMR (400 MHz, $CDCl_3$) δ 8.62 (s, 1H), 7.54 (dq, *J* = 34.7, 1.2 Hz, 1H), 7.34 (dddd, *J* = 9.6, 5.9, 3.0, 1.6 Hz, 4H), 7.05 (dddd, *J* = 7.3, 6.4, 4.2, 1.1 Hz, 2H), 6.96 (dddd, *J* = 8.7, 2.9, 2.1, 1.0 Hz, 4H), 6.38 (ddd, *J* = 9.0, 5.4, 2.1 Hz, 1H), 4.69 – 4.59 (m, 1H), 4.49 (dt, *J* = 7.7, 1.6 Hz, 2H), 4.16 (dp, *J* = 30.0, 2.0 Hz, 1H), 3.99 – 3.71 (m, 2H), 3.70 – 3.46 (m, 3H), 2.57 – 2.29 (m, 1H), 2.07 (ddt, *J* = 13.5, 8.9, 5.5 Hz, 1H), 1.94 (t, *J* = 1.0 Hz, 3H), 1.24 – 1.18 (m, 12H), 0.96 – 0.91 (m, 9H), 0.14 (dd, *J* = 4.4, 2.2 Hz, 6H). $^{13}$C NMR (101 MHz, $CDCl_3$) δ 171.17, 171.05, 163.68, 163.58, 157.12, 157.00, 150.22, 135.37, 129.82, 129.81, 129.78, 122.20, 122.17, 114.74, 114.67, 114.64, 114.61, 111.04, 110.87, 87.15, 87.10, 86.52, 86.47, 85.02, 84.73, 77.35, 77.04, 76.72, 75.99, 75.97, 75.73, 67.57, 67.42, 67.39, 67.08, 63.70, 63.45, 46.61, 46.48, 44.68, 44.65, 44.55, 44.52, 44.45, 40.45, 39.82, 39.78, 25.94, 24.33, 24.29, 24.26, 24.22, 24.19, 24.05, 23.98, 23.69, 22.65, 22.63, 18.37, 18.34, 12.54, -5.34, -5.37, -5.46. ESI-MS (m/z): Calculated: 635.3035 $(M-H)^-$ Found: 635.3968 $(M-H)^-$.

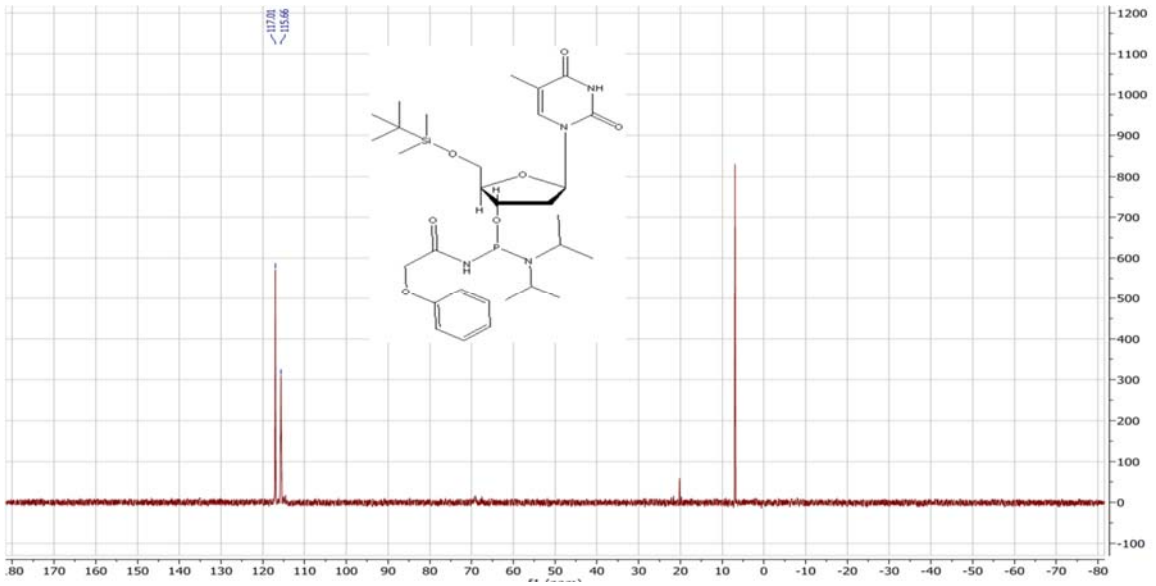


Figure 8.33: $^{31}$P NMR spectrum for compound **(41)**.

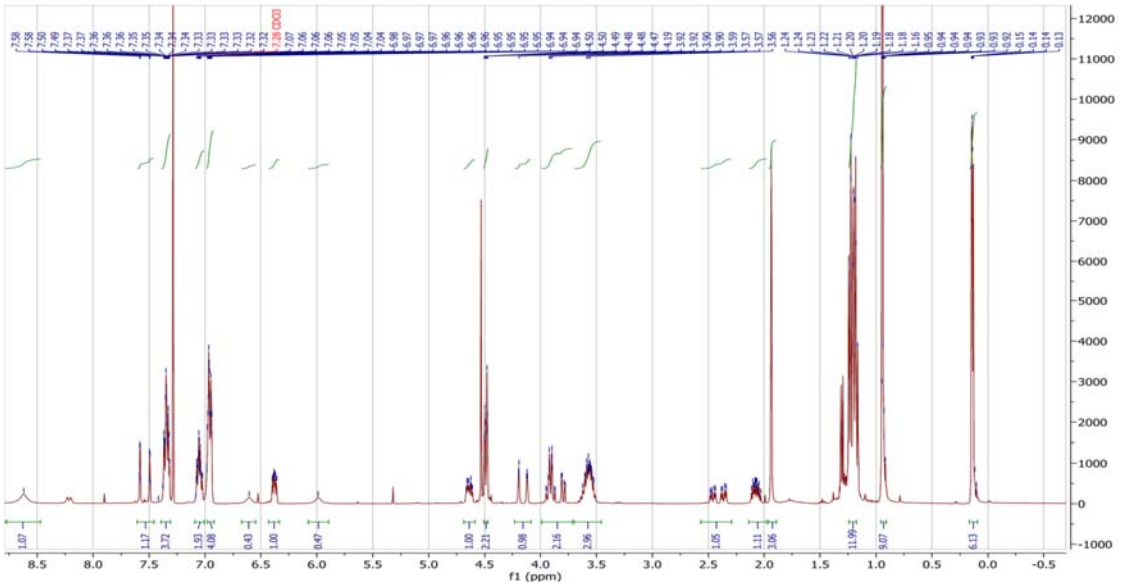


Figure 8.34: $^{1}$H NMR spectrum for compound **(41)**.

## Synthesis of (42)

$^{31}$P NMR (162 MHz, $CDCl_3$) δ 115.26, 114.34. $^{1}$H NMR (400 MHz, $CDCl_3$) δ 8.63 (s, 1H, Thy-NH), 7.65 (dq, *J* = 28.0, 1.1 Hz, 1H, H-6), 7.39 – 7.26 (m, 10H, TMT & *Ph*O), 7.11 – 6.89 (m, 4H, *Ph*O), 6.89 – 6.79 (m, 6H, TMT), 6.45 (m, 1H, H-1`), 4.76 (m, 1H, H-3`), 4.51 – 4.39 (m, 2H, C$H_2$OPh), 4.26 – 4.09 (m, 1H, H-4`), 3.80 (s, 9H, 3x C$H_3$-O), 3.64 – 3.25 (m, 4H, 2x HN$^{i}$Pr$_2$ & 2x H-5`), 2.60 – 2.28 (m, 2H, H-2`), 1.42 (dd, *J* = 2.5, 1.2 Hz, 3H, C$H_3$-Thy), 1.22 – 1.01 (m, 12H, 2x $^{i}$Pr$_2$NH). $^{13}$C NMR (101 MHz, $CDCl_3$) δ 171.13, 171.06, 171.01, 170.89, 163.68, 163.61, 158.63, 158.60, 157.12, 157.02, 156.99, 150.30, 150.28, 135.83, 135.69, 129.83, 129.81, 129.79, 122.17, 114.67, 114.65, 114.61, 113.27, 113.25, 111.41, 111.30, 86.79, 86.74, 86.04, 85.99, 85.62, 85.57, 84.75, 84.56, 77.37, 77.05, 76.73, 76.19, 75.93, 75.77, 75.53, 67.42, 67.36, 67.08, 63.62, 63.37, 55.27, 55.26, 44.60, 44.58, 44.47, 44.45, 40.12, 39.81, 24.39, 24.31, 24.29, 24.26, 24.23, 24.18, 11.70, 11.68. ESI-MS (m/z): Calculated: 853.3577 $(M-H)^-$ Found: 853.3642 $(M-H)^-$.

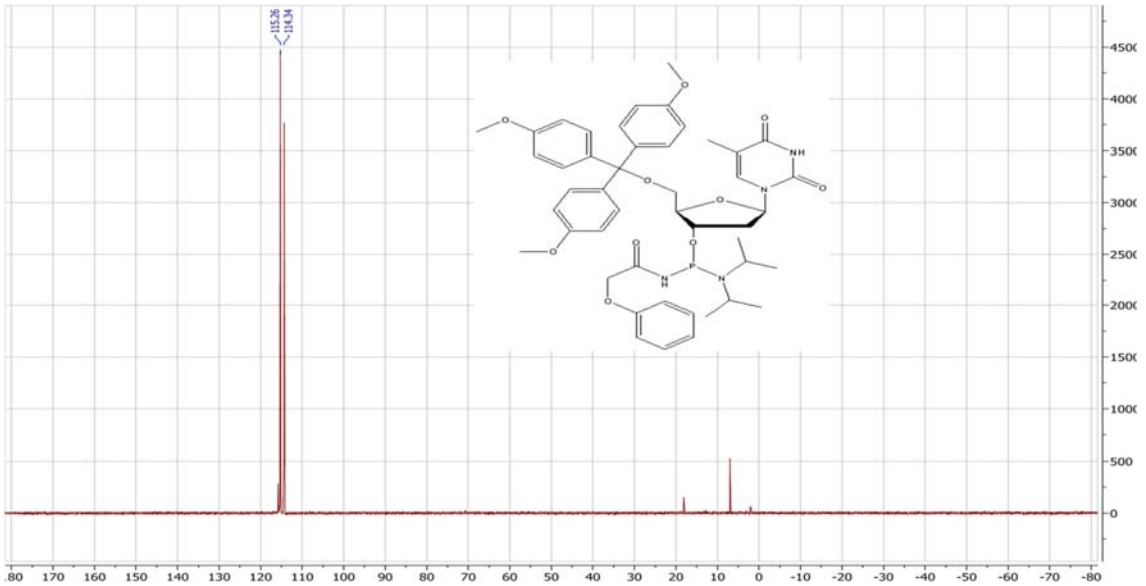

Figure 8.35: $^{31}$P NMR spectrum for compound **(42)**.

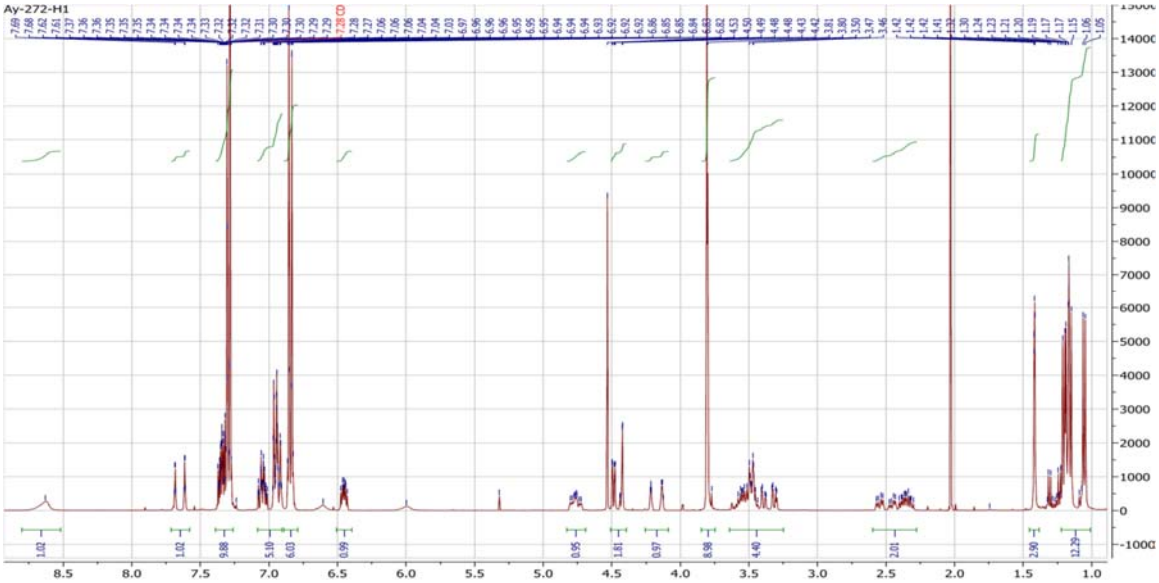

Figure 8.36: $^{1}$H NMR spectrum for compound **(42)**.

## 8.5 Summary of the synthesized 2`-Deoxyoligonucleotides containing Phosphoramidimidate and Phosphoramidate Modifications

Several 2`-deoxyoligonucleotides containing phosphoramidimidate have been synthesized and used in different studies. Table 8.4 list these oligonucleotides.

**Table 8.4: Synthesized Sequences containing phosphoramidimidate internucleotide linkages:**

| No. | Structure | Exact Mass $[M-XH]^{x-}$ | |
|---|---|---|---|
| | | Calculated | Observed |
| **ODN19** | DMT-T*TTTTTTTT*T [-2] | 1638.3496 | 1638.3438 |
| **ODN20** | DMT-TTT*TTT*TTT*TTT[-3] | 1294.2744 | 1294.2686 |
| **ODN21** | DMT-TT*TTTTTTTTTTT*T[-3] | 1599.3092 | 1599.3331 |
| **ODN22** | DMT-TTTTT*TTTTTT*TTTTTT*TTTT [-4] | 1654.5575 | 1654.5769 |
| **ODN23** | DMT-AAAAT*AAAAAT*AAAAAT*AAAA [-4] | 1695.1095 | 1695.1145 |
| **ODN24** | DMT-AAAAA*AAAAAA*AAAAAA*AAAA [-3] | 2269.4934 | 2269.5139 |
| **ODN25** | DMT-TGTA*AA*CCA*TGA*TGTGCTGCTA[-3] | 2347.1427 | 2347.1070 |
| **ODN26** | DMT-TGT*AAACCAT*GAT*GT*GCTGCTA[-3] | 2346.8227 | 2346.7766 |
| **ODN27** | DMT-TGT*AAA*CCA*TGAT*GTGCT*GCTA[-3] | 2346.8227 | 2346.8017 |
| **ODN28** | DMT-T*GTA*AACCA*TGATGTGCTGCT*A[-3] | 2347.1427 | 2347.1133 |
| **ODN29** | DMT-TG*TAAACCATG*ATGTGC*TGC*TA[-3] | 2347.1427 | 2347.1343 |
| **ODN30** | DMT-TG*TAAACC*ATG*ATGTGC*TGC*TA[-3] | 2346.8227 | 2346.8166 |
| **ODN31** | DMT-TG*TAAACC*ATG*ATG*TGC*TGC*TA[-3] | 2346.5026 | 2346.4947 |
| **ODN31** | DMT-TG*TAA*ACC*ATG*ATG*TGC*TGC*TA[-3] | 2346.1825 | 2346.1706 |
| **ODN32** | DMT-TGT*AAA*CCA*TGA*TGT*GCT*GCT*A[-3] | 2346.1825 | 2346.1714 |
| **ODN33** | TGTAAAC*C*ATGATGTGC*TGC*TA[-3] | 2246.4325 | 2246.4195 |
| **ODN34** | T*GT*AAACC*AT*GAT*GTGCTGCT*A[-4] | 1684.0919 | 1684.0005 |
| **ODN35** | T*GTA*AA*CCAT*GA*TGTGCTGCT*A[-4] | 1684.0919 | 1684.0184 |
| **ODN36** | T*GT*AAACC*ATGAT*GTGCTGCT*A[-4] | 1684.3022 | 1684.2515 |

| | | | |
|---|---|---|---|
| **ODN37** | T*GT*AA*ACCA*TGAT*GTGCTGCT*A[-4] | 1684.0919 | 1684.0879 |
| **ODN38** | TAGC*AGC*ACATC*ATG*GTTTACA[-4] | 1676.8234 | 1676.8140 |
| **ODN39** | T*GT*AAA*CCAT*GAT*GTGCTGCT*A[-4] | 1684.0919 | 1684.0969 |
| **ODN40** | TAGC*AGC*ACAT*CAT*GGTT*TACA[-4] | 1676.5834 | 1676.5797 |
| **ODN43** | 6-FAM-P(S)- TG*TA AACC*ATGAT*GTGCTGC T*A[-4] | 1822.8466 | 1822.8046 |
| **ODN44** | 6-FAM-P(S)- TGT*AAACC*AT*GAT*GTGCTGCT*A[-4] | 1822.8572 | 1822.8113 |
| **ODN45** | 6-FAM-P(S)- T*GTA*AA*CCAT*GA*TGTGCTGCT*A[-4] | 1822.6171 | 1822.6103 |
| **ODN46** | 6-FAM-P(S)- T*GTA*AA*CCAT*GA*TGT*GCT GCT*A[-4] | 1822.3771 | 1822.3558 |
| **ODN47** | 6-FAM-P(S)- T*GT*AAACC*ATG*ATGT*GCTGCT*A[-4] | 1822.3665 | 1822.3072 |
| **ODN48** | 6-FAM-P(S)- C*TAGCC*ATG*ATGT*GTGCTGCT*A[-4] | 1820.8531 | 1820.8061 |
| **ODN49** | 6-FAM-P(S)- T*GT*AAACC*ATGAT*GTGCTGCT*A[-4] | 1822.8572 | 1822.8114 |

***: phosphoramidimidate; [X]: X= ionization state**

Several 2`-deoxyoligonucleotides containing phosphoramidate have been synthesized and used in different studies. Table 8.5 list these oligonucleotides.

**Table 8.5: Synthesized Sequences containing phosphoramidate internucleotide linkages:**

| No. | Structure | Exact Mass [M-XH]$^{x-}$ | |
|---|---|---|---|
| | | Calculated | Observed |
| **ODN58** | DMT-T*GTAAAC*CATGAT*GTGCTGCT*A[-3] | 2347.1110 | 2347.0882 |
| **ODN59** | DMT-T*GTA*AA*CCAT*GA*TGTGCTGCT*A[-3] | 2346.455 | 2346.4595 |
| **ODN60** | DMT-TGT*AAA*CCA*T*GAT*GTGCTGCT*A[-3] | 2346.455 | 2346.4529 |
| **ODN61** | DMT-TGTA*AA*CCA*TGA*TGTGCTGCTA[-3] | 2347.1110 | 2347.1066 |
| **ODN62** | DMT-T*GTAAAC*CATGAT*GTGCTGCT*A[-3] | 2347.1110 | 2347.0954 |
| **ODN63** | T*GTA*AA*CCAT*GA*TGTGCTGCT*A[-3] | 2245.7448 | 2245.7535 |
| **ODN64** | TGT*AAA*CCA*T*GAT*GTGCTGCT*A[-3] | 2245.7448 | 2245.7177 |
| **ODN65** | TGTA*AA*CCA*TGA*TGTGCTGCTA[-3] | 2246.4325 | 2246.3996 |
| **ODN66** | TGT*AAACCAT*GAT*GT*GCT*GCTA[-3] | 2246.0728 | 2246.0661 |
| **ODN67** | DMT-TG*TAAACCATG*ATGTGC*TGC*TA[-3] | 2347.1110 | 2347.1899 |
| **ODN68** | DMT-TG*TAAACC*ATG*ATGTGC*TGC*TA[-3] | 2346.7830 | 2346.7713 |
| **ODN69** | DMT-TG*TAAACC*ATG*ATG*TGC*TGC*TA[-3] | 2346.4550 | 2346.4621 |
| **ODN70** | DMT-TG*TAA*ACC*ATG*ATG*TGC*TGC*TA[-3] | 2346.1270 | 2346.0782 |
| **ODN71** | DMT-TGT*AAA*CCA*TGA*TGT*GCT*GCT*A[-3] | 2346.1270 | 2346.1307 |
| **ODN72** | TGTAAAC*C*ATGATGTGC*TGC*TA | 2246.4325 | 2246.4218 |
| **ODN73** | T*GT*AAACC*AT*GAT*GTGCTGCT*A[-4] | 1684.0562 | 1684.0005 |
| **ODN74** | T*GTA*AA*CCAT*GA*TGTGCTGCT*A[-4] | 1684.0562 | 1684.0005 |
| **ODN75** | T*GT*AAACC*ATGAT*GTGCTGCT*A[-4] | 1684.3022 | 1684.2515 |
| **ODN76** | 6-FAM-P(S)-TGT*AAACC*AT*GAT*GTGCTGCT*A[-4] | 1822.5768 | 1822.5722 |
| **ODN77** | 6-FAM-P(S)-T*GTA*AA*CCAT*GA*TGTGCTGCT*A[-4] | 1822.3308 | 1822.2908 |
| **ODN79** | 6-FAM-P(S)-T*GT*AAACC*ATGAT*GTGCTGCT*A[-4] | 1822.5768 | 1822.6008 |

***: phosphoramidate; [X]: X= ionization state**

## 8.6 $^{31}$P NMR for some Synthesized 2`-deoxyoligonucleotides

The synthesized 2`-deoxyoligonucleotides have been also confirmed by $^{31}$P NMR. This section shows $^{31}$P NMR spectrum as an example

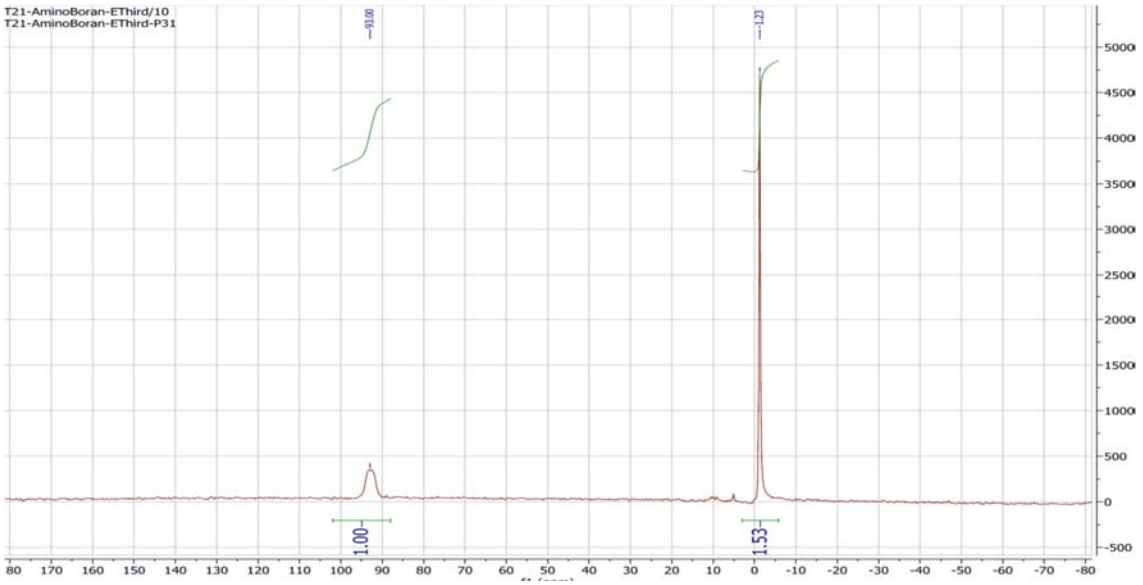


Figure 8.37: $^{31}$P NMR spectrum for ODN **(9)**.

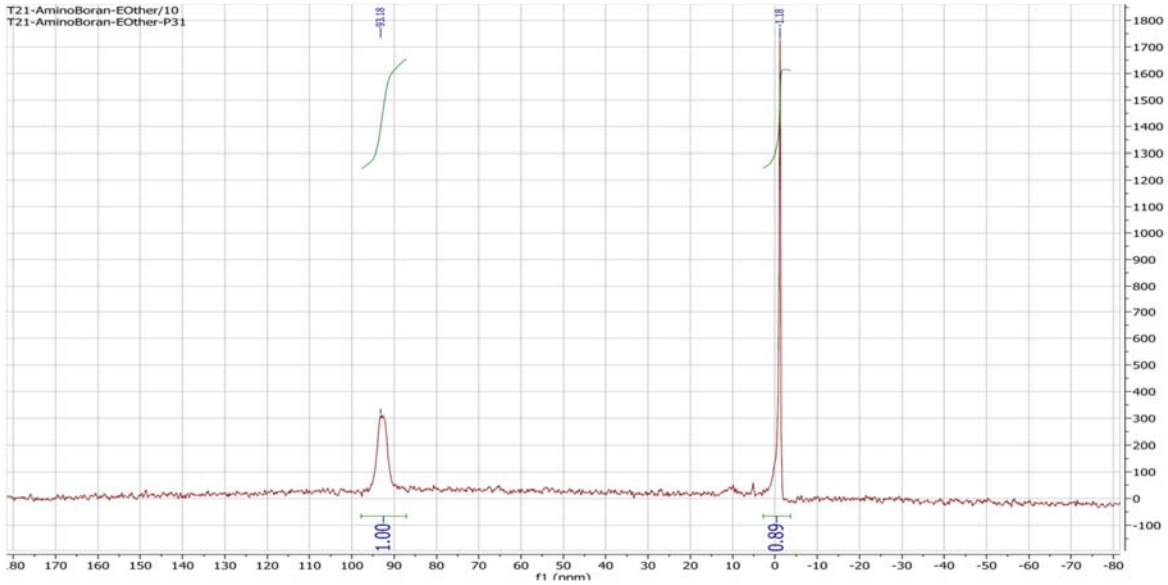


Figure 8.38: $^{31}$P NMR spectrum for ODN **(10)**.

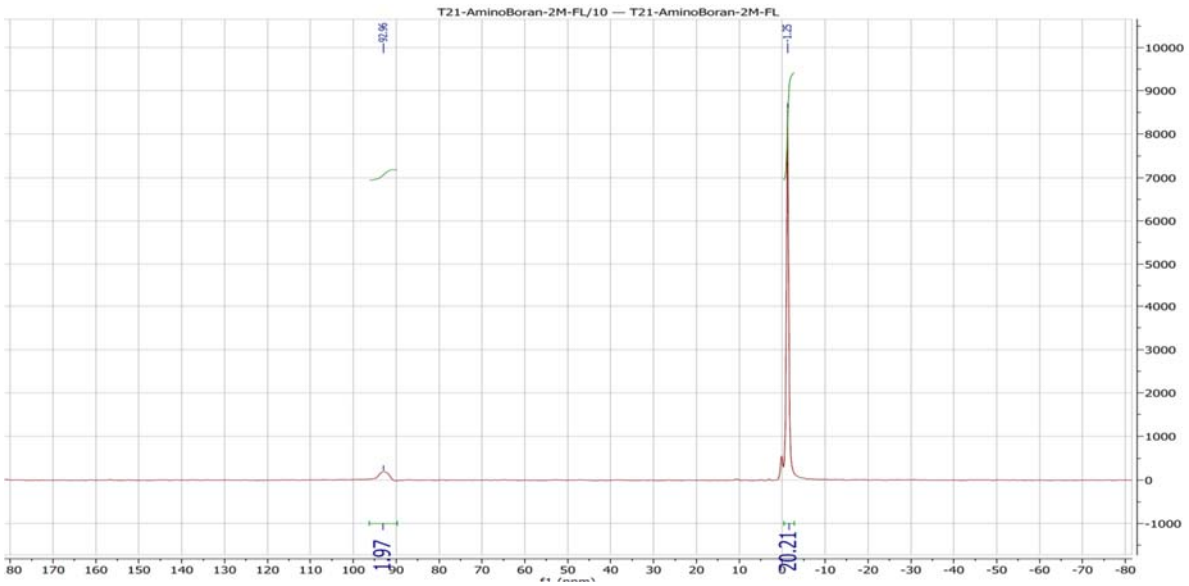


Figure 8.39: $^{31}$P NMR spectrum for ODN **(11)**.

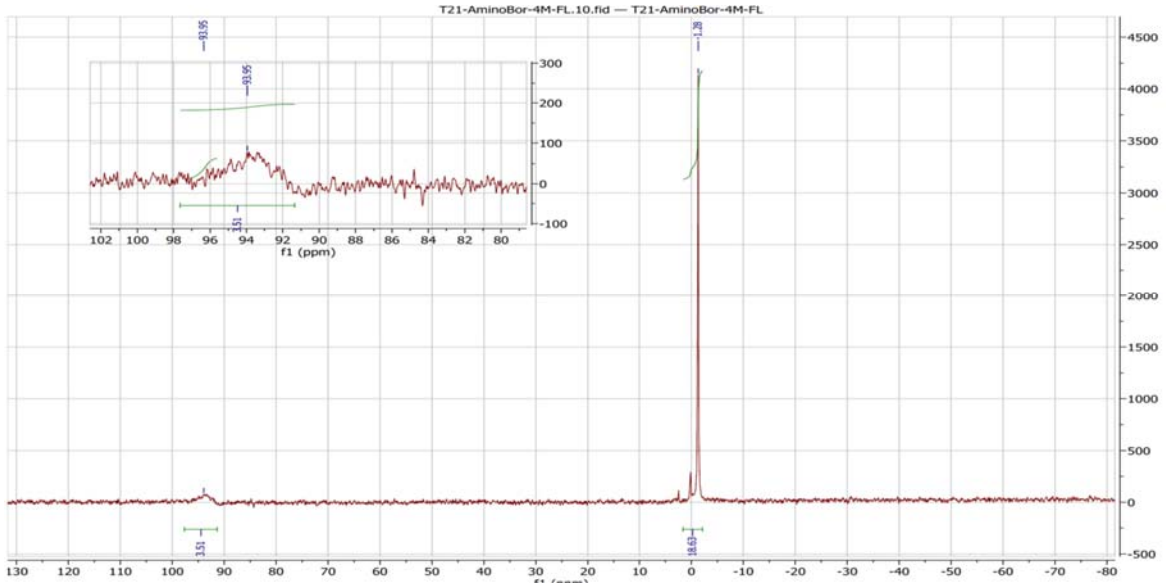


Figure 8.40: $^{31}$P NMR spectrum for ODN **(12)**.

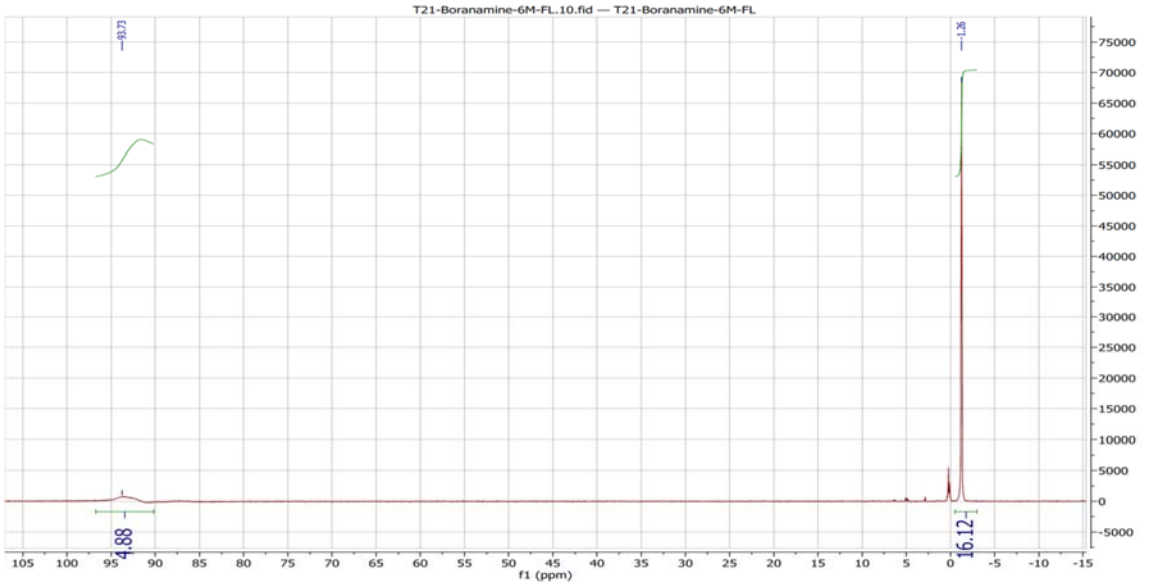


Figure 8.41: $^{31}$P NMR spectrum for ODN **(13)**.

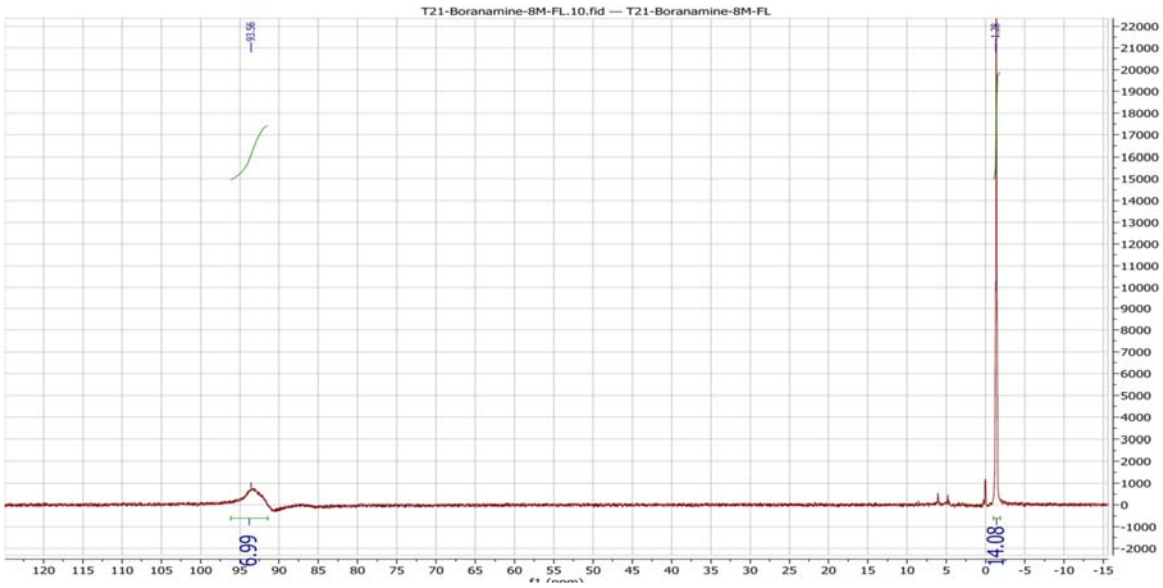


Figure 8.42: $^{31}$P NMR spectrum for ODN **(14)**.

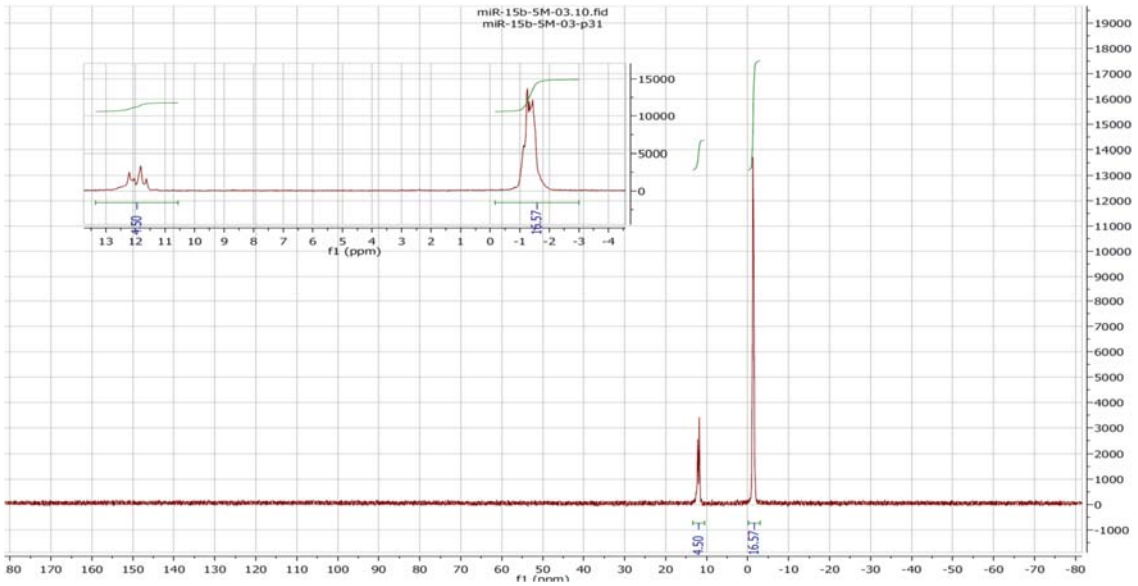


Figure 8.43: $^{31}$P NMR spectrum for ODN **(27)**.

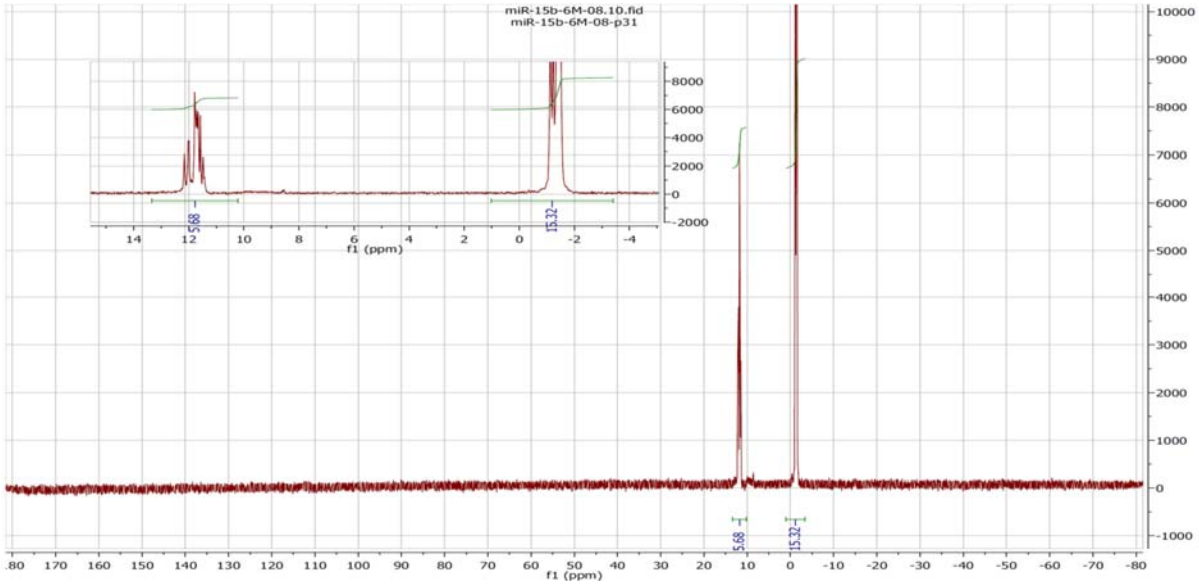


Figure 8.44: $^{31}$P NMR spectrum for ODN **(30)**.

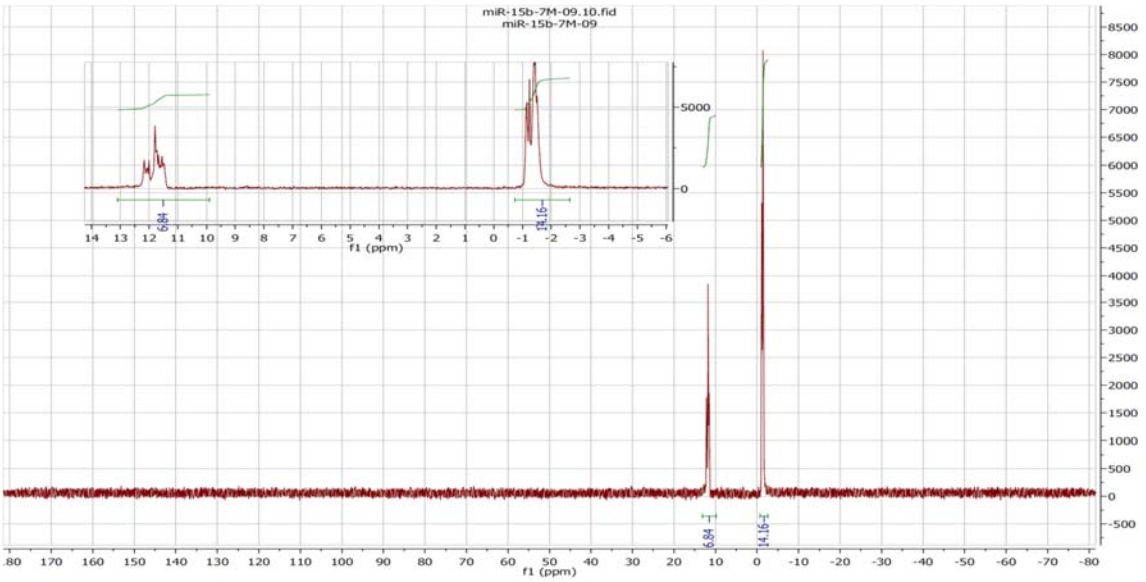


Figure 8.45: $^{31}$P NMR spectrum for ODN **(31)**.

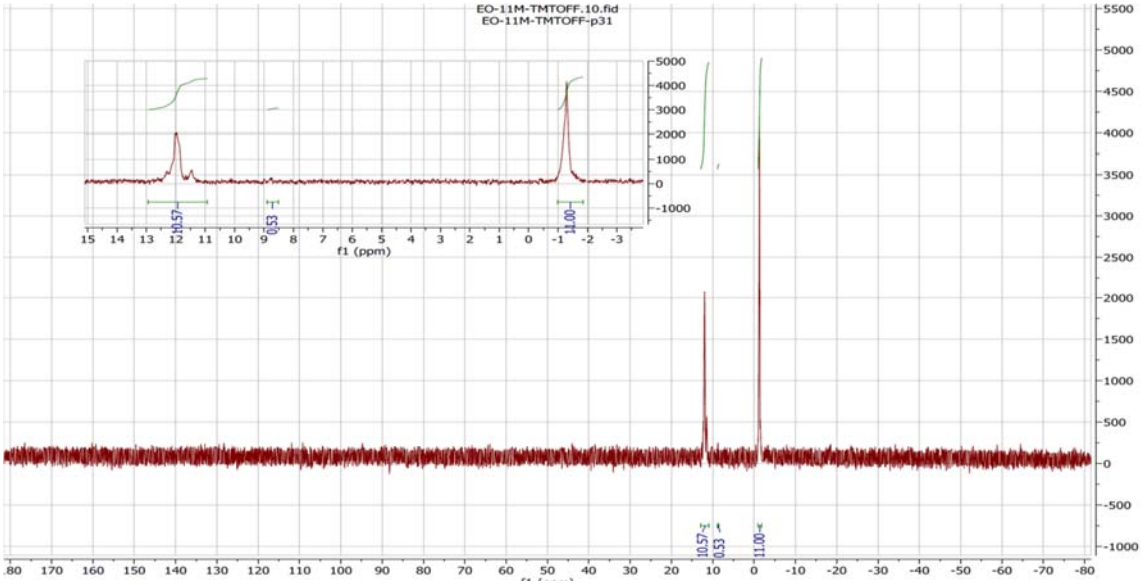


Figure 8.46: $^{31}$P NMR spectrum for ODN **(41)**.

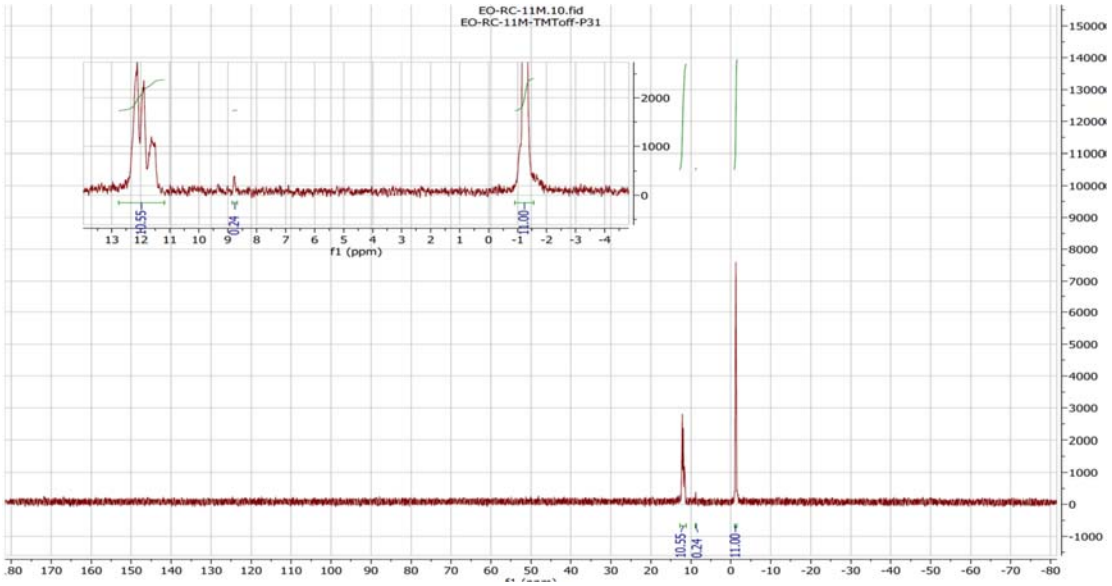


Figure 8.47: $^{31}$P NMR spectrum for ODN **(42)**.

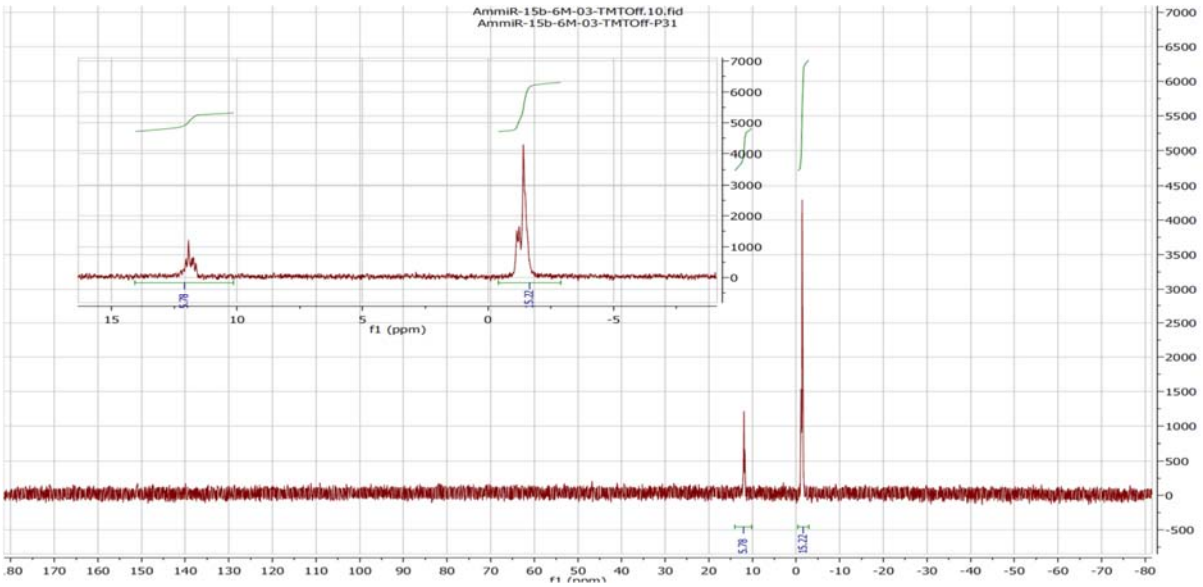


Figure 8.48: $^{31}$P NMR spectrum for ODN **(64)**.

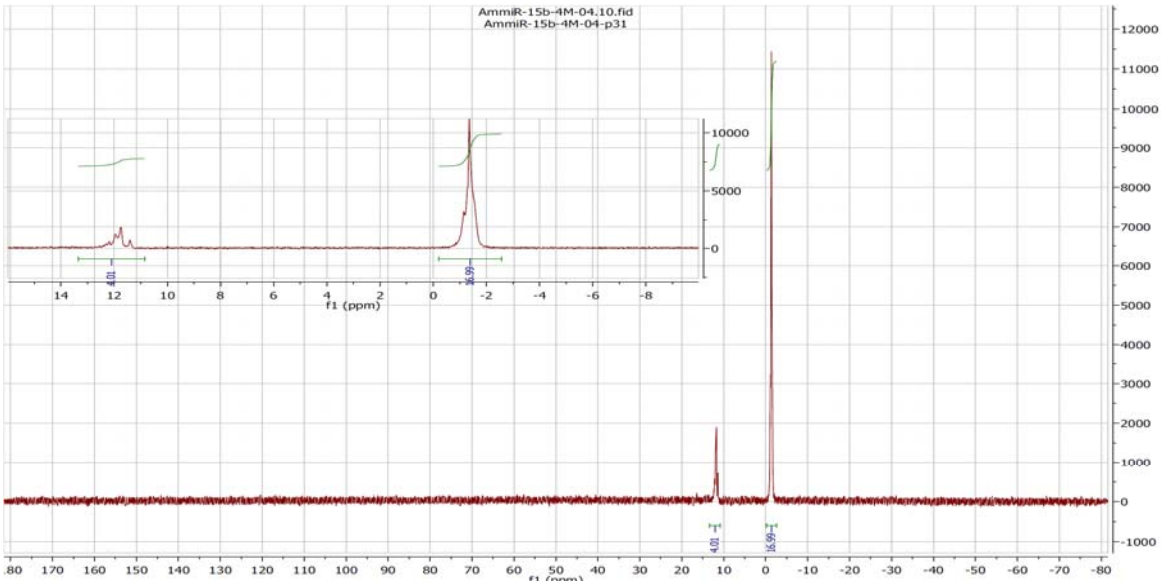


Figure 8.49: $^{31}$P NMR spectrum for ODN **(65)**.

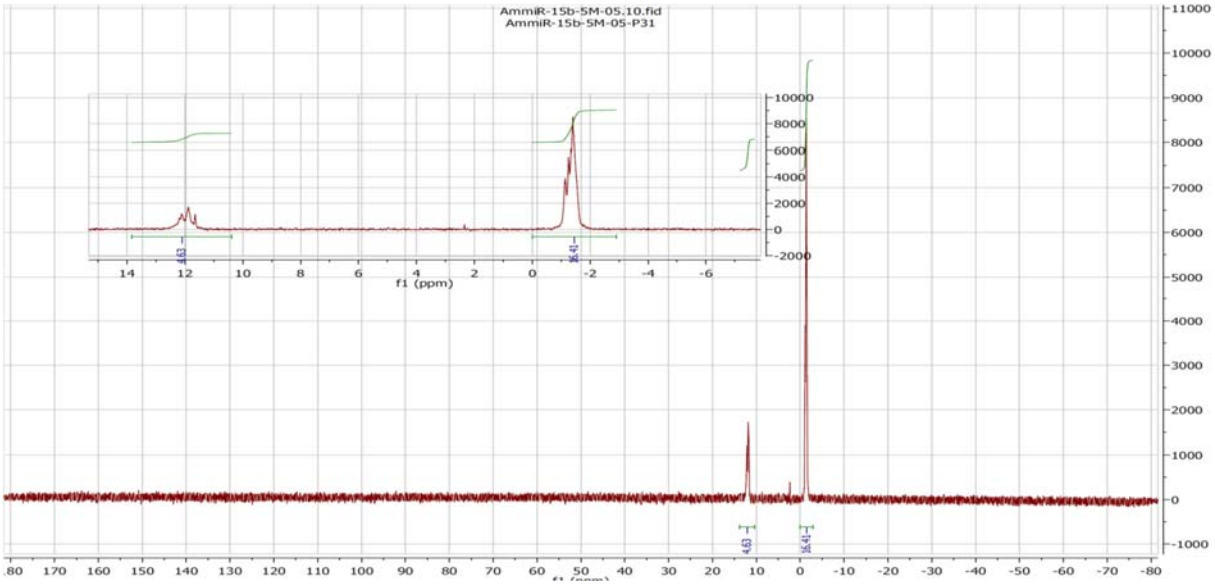


Figure 8.50: $^{31}$P NMR spectrum for ODN **(66)**.

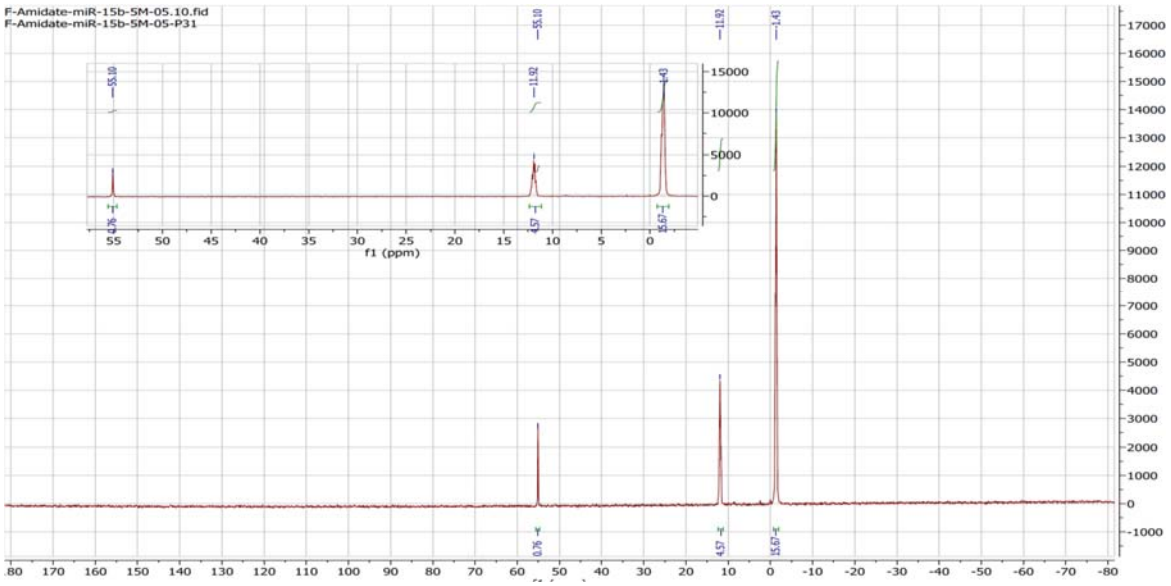


Figure 8.51: $^{31}$P NMR spectrum for ODN **(76)**.

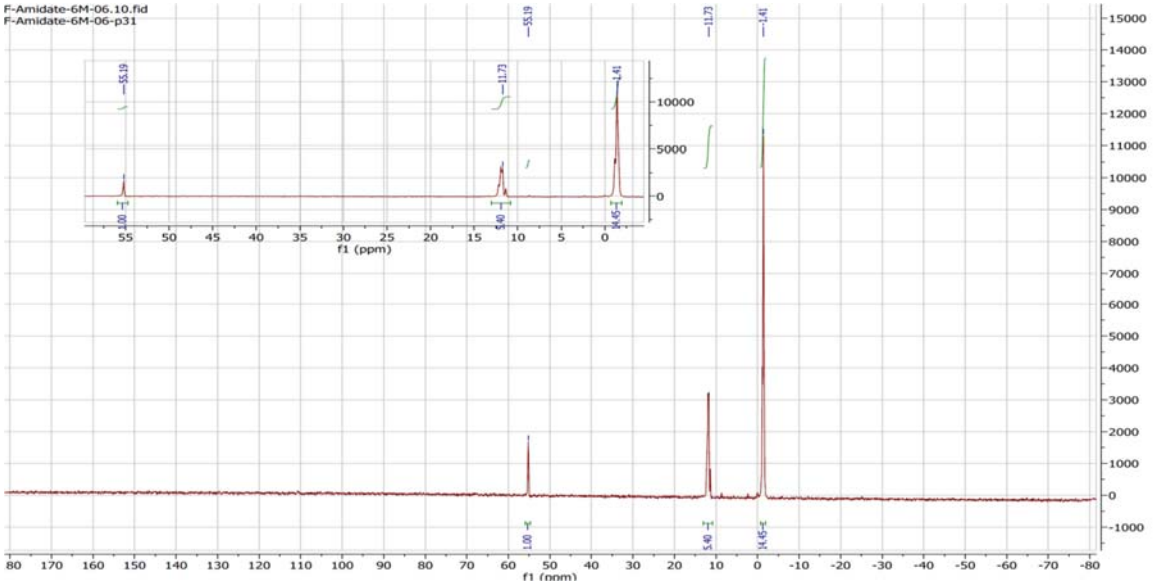


Figure 8.52: $^{31}$P NMR spectrum for ODN **(77)**.

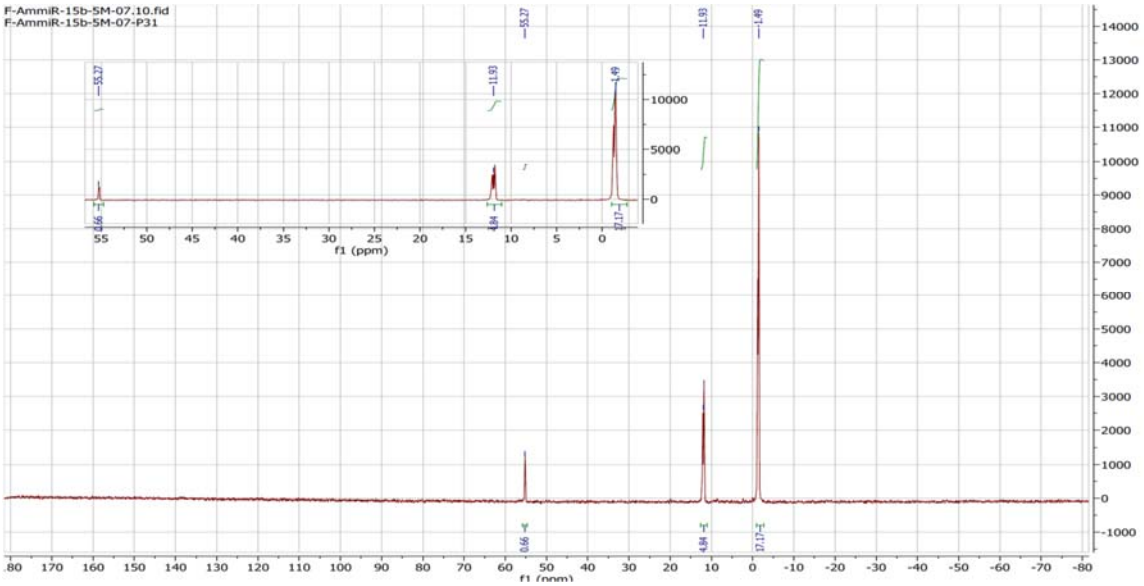


Figure 8.53: $^{31}$P NMR spectrum for ODN **(79)**.

## References


(1) Avery, O. T., MacLeod, C. M., and McCarty, M. (1944) Studies on the Chemical Nature of the Substance Inducing Transformation of Pneumococcal Types - Induction of Transformation by a Desoxyribonucleic Acid Fraction Isolated from Pneumococcus Type III. *J. Exp. Med. 79*, 137–158.(Page 1)

(2) Watson, J. D., and Crick, F. C. H. (1953) Molecular structure of nucleic acid. A structure for deoxyribose nucleic acid. *Nature 171*, 737–738. (Page 1)

(3) Beaucage, S. L., and Caruthers, M. H. (1981) Deoxynucleoside phosphoramidites—A new class of key intermediates for deoxypolynucleotide synthesis. *Tetrahedron Lett. 22*, 1859–1862. (Page 2)

(4) Kurreck, J. (2003) Antisense technologies. *Eur. J. Biochem. 270*, 1628–1644. (Page 5)

(5) Miller, P. S., Yano, J., Yano, E., Carroll, C., Jayaraman, K., and Ts'o, P. O. P. (1979) Nonionic nucleic acid analogs. Synthesis and characterization of dideoxyribonucleoside methylphosphonates. *Biochemistry 18*, 5134–5143. (Page 5)

(6) Miller, P. S., Yano, J., Yano, E., Carroll, C., Jayaraman, K., and Ts'o, P. O. P. (1979) Nonionic nucleic acid analogs. Synthesis and characterization of dideoxyribonucleoside methylphosphonates. *Biochemistry 18*, 5134–5143. (Page 6)

(7) Eckstein, F. (2002) Developments in RNA chemistry, a personal view. *Biochimie 84*, 841–848. (Page 7)

(8) Kibler-Herzog, L., Zon, G., Uznanski, B., Whittier, G., and Wilson, W. D. (1991) Duplex stabilities of phosphorothioate, methylphosphonate, and RNA analogs of two DNA 14-mers. *Nucleic Acids Res. 19*, 2979–2986. (Page 7)

(9) de Smet, M. D., Meenken, C., and van den Horn, G. J. (1999) Fomivirsen – a phosphorothioate oligonucleotide for the treatment of CMV retinitis. *Ocul. Immunol. Inflamm. 7*, 189–198. (Page 7)

(10) Wan, W. B., Migawa, M. T., Vasquez, G., Murray, H. M., Nichols, J. G., Gaus, H., Berdeja, A., Lee, S., Hart, C. E., Lima, W. F., Swayze, E. E., and Seth, P. P. (2014) Synthesis, biophysical properties and biological activity of second generation antisense oligonucleotides containing chiral phosphorothioate linkages. *Nucleic Acids Res. 42*, 13456–68. (Page 7)

(11) Froehler, B. C. (1986) Deoxynucleoside H-Phosphonate diester intermediates in the synthesis of internucleotide phosphate analogues. *Tetrahedron Lett. 27*, 5575–5578. (Page 7)

(12) Gryaznov, S. M., Lloyd, D. H., Chen, J. K., Schultz, R. G., DeDionisio, L. A., Ratmeyer, L., and Wilson, W. D. (1995) Oligonucleotide N3'→P5' phosphoramidates. *Proc. Natl. Acad. Sci. 92*, 5798–5802. (Page 7)

(13) Bannwarth, W. (1988) Solid-Phase Synthesis of Oligodeoxynucleotides containing phosphoramidate internucleotide linkages and their specific chemical cleavage. *Helv. Chim. Acta 71*, 1517–1527. (Page 7)

(14) Gryaznov, S. M. (2010) Oligonucleotide N3′→P5′ Phosphoramidates and *Thio* - Phoshoramidates as Potential Therapeutic Agents. *Chem. Biodivers. 7*, 477–493. (Page 8)

(15) Ito, K. R., Kodama, T., Makimura, F., Hosoki, N., Osaki, T., Orita, A., Imanishi, T., and Obika, S. (2011) Cleavage of oligonucleotides containing a P3'→N5' phosphoramidate linkage mediated by single-stranded oligonucleotide templates. *Molecules 16*, 10695–10708. (Page 8)

(16) Gryaznov, S. M. (2010) Oligonucleotide N3' → P5' phosphoramidates and thio-phoshoramidates as potential therapeutic agents. *Chem. Biodivers. 7*, 477–493. (Page 8)

(17) Sood, A., Shaw, B. R., and Spielvogel, B. F. (1990) Boron-containing nucleic acids. 2. Synthesis of oligodeoxynucleoside boranophosphates. *J. Am. Chem. Soc. 112*, 9000–9001. (Page 8)

(18) Huang, F. Q., Sood, A., Spielvogel, B. F., and Shaw, B. R. (1993) Nuclease resistance and hydrolytic stability of oligodeoxynucleotide boranophosphate stereoisomers. *J. Biomol. Struct. Dyn. 10*, a078. (Page 8)

(19) RAIT, V. K., and SHAW, B. R. (1999) Boranophosphates Support the RNase H Cleavage of Polyribonucleotides. *Antisense Nucleic Acid Drug Dev. 9*, 53–60. (Page 9)

(20) Shaw, B. R., Sergueev, D., He, K., Porter, K., Summers, J., Sergueeva, Z., and Rait, V. B. T.-M. in E. (2000) Boranophosphate backbone: a mimic of phosphodiesters, phosphorothioates, and methyl phosphonates, in *Antisense Technology Part A: General Methods, Methods of Delivery, and RNA Studies*, pp 226–257. Academic Press. (Page 9)

(21) Kibler-Herzog, L., Zon, G., Uznanski, B., Whittier, G., and Wilson, W. D. (1991) Duplex stabilities of phosphorothioate, methylphosphonate, and RNA analogs of two DNA 14-mers. *Nucleic Acids Res. 19*, 2979–2986. (Page 9)

(22) Ferlini, A., Goemans, N., Tulinius, M., Niks, E. H., Dorricott, S., Morgan, A., Lourbakos, A., Kimpe, S., Wilson, R., Armaroli, A., van Deutekom, J., and Campion, G. (2013) T.I.2 Exon skipping and PRO044 in Duchenne muscular dystrophy: Extending the program. *Neuromuscul. Disord. 23*, 847. (Page 9)

(23) Koo, T., and Wood, M. J. (2013) Clinical Trials Using Antisense Oligonucleotides in Duchenne Muscular Dystrophy. *Hum. Gene Ther. 24*, 479–488. (Page 9)

(24) Shen, X., and Corey, D. R. (2018) Chemistry, mechanism and clinical status of antisense oligonucleotides and duplex RNAs. *Nucleic Acids Res. 46*, 1584–1600. (Page 9)

(25) Braasch, D. A., and Corey, D. R. (2001) Locked nucleic acid (LNA): fine-tuning the recognition of DNA and RNA. *Chem. Biol. 8*, 1–7. (Page 10)

(26) Wada, T., Shimizu, M., Oka, N., and Saigo, K. (2002) A new boranophosphorylation reaction for the synthesis of deoxyribonucleoside boranophosphates. *Tetrahedron Lett. 43*, 4137–4140. (Page 15)

(27) Uznański, B., Wilk, A., and Stec, W. J. (1987) Deoxyribonucleoside 3′-phosphordiamidites as substrates for solidsupported synthesis of oligodeoxyribonucleotides and their phosphorothioate and dna-triester analogues. *Tetrahedron Lett. 28*, 3401–3404. (Page 19)

(28) (1987) Evaluating and Isolating Synthetic Oligonucleotides The Complete Guide. (Page 22)

(29) Paul, S., Roy, S., Monfregola, L., Shang, S., Shoemaker, R., and Caruthers, M. H. (2015) Oxidative Substitutions of Boranephosphonate Diesters as a Route to Post Synthetically Modified DNA. *J. Am. Chem. Soc.* 150213155405008. (Page 25)

(30) Sergueeva, Z. A., Sergueev, D. S., and Shaw, B. R. (2001) BORANE-AMINE COMPLEXES - VERSATILE REAGENTS IN THE CHEMISTRY OF NUCLEIC ACIDS AND THEIR ANALOGS. *Nucleosides, Nucleotides and Nucleic Acids 20*, 941–945. (Page 25)

(31) Higson, A. P., Sierzchala, A., Brummel, H., Zhao, Z., and Caruthers, M. H. (1998) Synthesis of an oligothymidylate containing boranophosphate linkages. *Tetrahedron Lett. 39*, 3899–3902. (Page 25)

(32) Roy, S., Olesiak, M., Shang, S., and Caruthers, M. H. (2013) Silver nanoassemblies constructed from boranephosphonate DNA. *J. Am. Chem. Soc. 135*, 6234–6241. (Page 25)

(33) Paul, C. H., and Royappa, a T. (1996) Acid binding and detritylation during oligonucleotide synthesis. *Nucleic Acids Res. 24*, 3048–52. (Page 26)

(34) Sergueeva, Z. A., Sergueev, D. S., and Shaw, B. R. (2000) Rapid and selective reduction of amide group by borane-amine complexes in acyl protected nucleosides. *Nucleosides, Nucleotides and Nucleic Acids 19*, 275–282. (Page 26)

(35) Sergueeva, Z. A., Sergueev, D. S., and Shaw, B. R. (2001) BORANE-AMINE COMPLEXES - VERSATILE REAGENTS IN THE CHEMISTRY OF NUCLEIC ACIDS AND THEIR ANALOGS. *Nucleosides, Nucleotides and Nucleic Acids 20*, 941–945. (Page 26)

(36) Sergueeva, Z. A., Sergueev, D. S., and Shaw, B. R. (2001) Borane-amine complexes - Versatile reagents in the chemistry of nucleic acids and their analogs. *Nucleosides, Nucleotides and Nucleic Acids 20*, 941–945. (Page 38)

(37) Higson, A. P., Sierzchala, A., Brummel, H., Zhao, Z., and Caruthers, M. H. (1998) Synthesis of an oligothymidylate containing boranophosphate linkages. *Tetrahedron Lett. 39*, 3899–3902. (Page 40)

(38) Miller, P. S., Annan, N. D., McFarland, K. B., and Pulford, S. M. (1982) Oligothymidylate Analogues Having Stereoregular, Alternating Methylphosphonate/Phosphodiester Backbones as Primers for DNA Polymerase. *Biochemistry 21*, 2507–2512. (Page 48)

(39) Chen, Y. Q., Qu, F. C., and Zhang, Y. B. (1995) Diuridine 3′,5′-boranophosphate: Preparation and properties. *Tetrahedron Lett. 36*, 745–748. (Page 48)

(40) Ti, S., Gaffney, B. L., and Jones, R. a. (1982) Transient Protection: Efficient One-Flask Syntheses of Protected Deoxynucleosides. *J. Am. Chem. Soc. 39*, 1316–1319. (Page 51)

(41) Bjergrde, K., Dahl, O., and Caruthers, M. H. (1994) Synthesis of dinucleoside phosphoramidimidates. *Tetrahedron Lett. 35*, 2941–2944. (Page 58)

(42) Fischer, R. W., and Caruthers, M. H. (1995) Synthesis of a dinucleotide phosphoramidimidate. *Tetrahedron Lett. 36*, 6807–6810. (Page 58)

(43) Capaldi, D. C., Ravikumar, V. T., Gaus, H., Krotz, A. H., Arnold, J., Carty, R. L., Moore, M. N., Scozzari, A. N., Lowery, K., and Cole, D. L. (2003) Synthesis of High-Quality Antisense Drugs. Addition of Acrylonitrile to Phosphorothioate Oligonucleotides: Adduct Characterization and Avoidance. *Org. Process Res. Dev. 7*, 832–838. (Page 77)

(44) Schulhof, J. C., Molko, D., and Teoule, R. (1987) The final deprotection step in oligonucleotide synthesis is reduced to a mild and rapid ammonia treatment by using labile base-protecting groups. *Nucleic Acids Res. 15*, 397–416. (Page 80)

(45) Pon, R. T., and Yu, S. (1997) Hydroquinone-O,O'-diacetic acid ('Q-linker') as a replacement for succinyl and oxalyl linker arms in solid phase oligonucleotide synthesis. *Nucleic Acids Res. 25*, 3629–3635. (Page 90)

(46) Karver, M. R., Weissleder, R., and Hilderbrand, S. A. (2011) Synthesis and evaluation of a series of 1,2,4,5-tetrazines for bioorthogonal conjugation. *Bioconjug. Chem. 22*, 2263–2270. (Page 112)

(47) Inoue, H., Hayase, Y., Iwai, S., and Ohtsuka, E. (1987) Sequence-dependent hydrolysis of RNA using modified oligonucleotide splints and RNase H. *FEBS Lett. 215*, 327–330. (Page 120)

(48) Settanni, G., Zhou, J., Suo, T., Schöttler, S., Landfester, K., Schmid, F., and Mailänder, V. (2016) Protein corona composition of PEGylated nanoparticles correlates strongly with amino acid composition of protein surface. (Page 123)

(49) Serpi, M., Madela, K., Pertusati, F., and Slusarczyk, M. (2013) Synthesis of phosphoramidate prodrugs: ProTide approach. *Curr. Protoc. Nucleic Acid Chem. Chapter 15*, 1–15. (Page 123)

(50) Siegel, D., Hui, H. C., Doerffler, E., Clarke, M. O., Chun, K., Zhang, L., Neville, S., Carra, E., Lew, W., Ross, B., Wang, Q., Wolfe, L., Jordan, R., Soloveva, V., Knox, J., Perry, J., Perron, M., Stray, K. M., Barauskas, O., Feng, J. Y., Xu, Y., Lee, G., Rheingold, A. L., Ray, A. S., Bannister, R., Strickley, R., Swaminathan, S., Lee, W. A., Bavari, S., Cihlar, T., Lo, M. K., Warren, T. K., and Mackman, R. L. (2017) Discovery and Synthesis of a Phosphoramidate Prodrug of a Pyrrolo[2,1-f][triazin-4-amino] Adenine C-Nucleoside (GS-5734) for the Treatment of Ebola and Emerging Viruses. *J. Med. Chem. 60*, 1648–1661. (Page 123)

(51) Froehler, B. C. (1986) Deoxynucleoside H-Phosphonate diester intermediates in the synthesis of internucleotide phosphate analogues. *Tetrahedron Lett. 27*, 5575–5578. (Page )

(52) Peyrottes, S., Vasseur, J. J., Imbach, J. L., and Rayner, B. (1996) Oligodeoxynucleoside phosphoramidates (P-NH2): Synthesis and thermal stability of duplexes with DNA and RNA targets. *Nucleic Acids Res. 24*, 1841–1848. (Page 123)

(53) Hogrefes, H. H., Hogrefeq, I., Walderso, Y., and Technologies, D. N. a. (1990) Kinetic Analysis of Escherichia coli RNase H Using DNA-RNA-DNA / DNA Substrates *. *J. Biol. Chem. 265*, 5561–5566. (Page )